Anaerobic digestion of selenium-rich wastewater for simultaneous methane and volatile fatty acid production and selenium bioremediation

Mohanakrishnan Logan

Supervisor: Prof. Piet N. L. Lens

A thesis submitted to the National University of Ireland Galway (NUI Galway) as fulfilment of the requirements for the degree of Doctor of Philosophy (PhD)

School of Natural Sciences

September 2022

Declaration

I, Mohanakrishnan Logan, declare that this thesis or any part thereof has not been, or not currently being, submitted for any degree at the National University of Ireland, or any other University. I further declare that the work embodied is my own.

Mohanakrishnan Logan

Summary

This research aimed at investigating the anaerobic digestion (AD) of selenium (Se)-rich and lipid-rich wastewaters via evaluating the operational parameters in sequential and continuous bioreactors. In the first part of the study, batch AD of dissolved air floatation (DAF) slurry derived from dairy wastewater showed methane yield was improved up to 177% after up to three folds dilution. Similarly, adjustment of the initial pH to 6.0 resulted in a higher methane yield, which was 23% higher than the control without pH adjustment. Following this, the potential of granular activated carbon (GAC) supplementation to enhance the AD of dairy wastewater was studied in sequential batch reactors (SBR). The methane production increased by up to 500% in the GAC-amended SBR when compared to the Control SBR. GAC addition led to faster lipid degradation and promoted the activity of syntrophic and electroactive microorganisms such as *Geobacter*, *Synergistes*, *Methanolinea* and *Methanosaeta*.

The second part of the study evaluated the effect of Se oxyanions on AD of different model substrates and real waste/wastewater. AD of dairy wastewater based DAF slurry supplemented with 0.05 and 0.10 mM Se oxyanions achieved a similar cumulative methane yield of 180 mL/g COD as that of digestion of Se free DAF slurry after 65 days of incubation. The IC_{50} was 0.08 mM for selenate (SeO_4^{2-}) and 0.07 mM for selenite (SeO_3^{2-}). Following this, the influence of pH, heat treatment (HT) of inoculum and Se oxyanions on volatile fatty acids (VFA) production from food waste was studied. The highest VFA yield (0.516 g COD/g VS) was achieved at pH 10, which was 45% higher than that at pH 5. The VFA composition was dominated by acetic and propionic acids at pH 10 with non-heat treated inoculum, which diversified at other test conditions. HT and Se resulted in VFA accumulation in alkaline pH, but HT was detrimental for SeO_4^{2-} reduction (< 15 % Se removal after 20 days). Finally, a long term, continuous and simultaneous methane production and Se bioremediation was demonstrated in up-flow anaerobic sludge blanket reactors. About 150 mL/g COD daily methane yield was achieved which was comparable with that of the control until 400 µM SeO_4^{2-}. Simultaneously, more than 90% Se removal was accomplished. Biosynthesis of Se nanoparticles and metal selenides were observed, supported by X-ray diffraction, scanning and transmission electron microscopy. However, methane production deteriorated when SeO_4^{2-} was increased to 500 µM, due to inhibition in the activity of *Methanosaeta*. Remarkably, Se facilitated sludge granulation. The SeO_4^{2-} concentration, but not the COD/SeO_4^{2-} ratio, was found to govern the AD of selenate rich wastewaters.

Acknowledgement

This PhD thesis is the output of the effort and support of several people to whom I am eternally grateful. I would like to thank the Science Foundation Ireland Research Professorship PhD scholarship for providing the financial support to carry out this thesis.

First and foremost, I thank my supervisor Professor Piet N. L. Lens for your kindness, patience, encouragement and constant supervision of the progress of my research. Thank you for your scientific suggestions and constructive comments on the work which was critical to achieve success. The best thing that happened in my professional life is to meet you and I am privileged to receive my PhD under you.

I thank Assoc. Prof. Zeynep Cetecioglu Gurol (KTH Royal Institute of Technology, Sweden) for your supervision during my research placement. I am grateful to Prof. C. Visvanathan (Asian Institute of Technology, Thailand) for your training and support. I cannot be more thankful to Prof. Kurian Joseph (Anna University, Chennai, India) for awakening the researcher in me during my masters in engineering. I acknowledge the mentorship of Dr. Lea Chua Tan, your critical insights helped to improve the quality of this thesis.

Thanks to Dr. Michael Joseph Gormally, Dr. Terry Morley and Dr. Ronan Sulpice for the annual Graduate Research Committee meetings that boosted my morale to finish my PhD thesis and defense. Special thanks to my PhD thesis examiners Prof. Mohammad Taherzadeh (University of Borås) and Prof. Xinmin Zhan (NUI Galway) for your critical review comments.

Thank you Borja for patiently responding to my requests in the lab. Thanks also to Manu and Leah for your technical assistance. Éadaoin and Emma, thank you for your assistance in SEM, TEM and EDX. Thank you Juan for your help with the reactor setup. Ciarán, thank you for your support in XRD. Thank you Corine for your help with the microbial community analyses. Thank you Mike and Ann for being helpful with the administrative requests in our department.

This section is incomplete without acknowledging my colleagues in the IETSBIO^3 and Bioconversion group including the PhDs, Postdocs, Research Assistants and visiting researchers for your support and friendship. I am grateful to my family and friends back in India for your love.

I dedicate this work to my beloved father Mr. Logan Balakrishnan who departed to heaven immediately after seeing me commence my doctoral program. I thank my mother Mrs. Prabhavathy Thiruvenkadam who is behind every success.

Table of Contents

List of figures

List of tables

List of publications and chapter contributions

The work contained in this thesis consists of the following publications in international peer-reviewed journals:

Publication	Author contributions
Chapter 3 Logan, M., Ravishankar, H., Tan, L.C., Lawrence, J., Fitzgerald, D., Lens, P.N.L., 2021. Anaerobic digestion of dissolved air floatation slurries: Effect of substrate concentration and pH. Environmental Technology and Innovation 21, 101352. https://doi.org/10.1016/j.eti.2020.101352	**Logan, M.**: Conceptualization, Data curation, Writing - Original Draft. **Ravishankar, H.**: Conceptualization, Methodology, Writing - review & editing. **Tan, L.C.**: Conceptualization, Methodology, Writing - review & editing. **Lawrence, J.**: Investigation. **Fitzgerald, D.**: Investigation. **Lens, P.N.L.**: Supervision, Funding acquisition, Writing - Review & Editing.
Chapter 4 Logan, M., Tan, L.C., Nzeteu, C.O., Lens, P.N.L., 2022. Enhanced anaerobic digestion of dairy wastewater in a granular activated carbon amended sequential batch reactor. GCB Bioenergy 14(7), 840-857. https://doi.org/10.1111/gcbb.12947	**Logan, M.**: Investigation, Writing - Original Draft. **Tan, L.C.**: Conceptualization, Methodology, Investigation, Writing - review & editing. **Nzeteu, C.O.**: Investigation, Writing - review & editing. **Lens, P.N.L.**: Project administration, Resources, Supervision, Funding acquisition, Writing - Review & Editing.
Chapter 5 Logan, M., Tan, L.C., Lens, P.N.L., 2022. Anaerobic co-digestion of dissolved air floatation slurry and selenium rich wastewater for simultaneous methane production and selenium bioremediation. International Biodeterioration and Biodegradation 172, 105425. https://doi. org/10.1016/j.ibiod.2022.105425	**Logan, M.**: Conceptualization, Investigation, Formal analysis, Data curation, Visualization, Writing - Original Draft. **Tan, L.C.**: Conceptualization, Methodology, Validation, Writing - Review & Editing. **Lens, P.N.L.**: Project administration, Resources, Supervision, Funding acquisition, Writing - Review & Editing.

The work contained in this thesis consists of the following manuscripts under review for publication in international peer-reviewed journals:

Manuscript	Author contributions
Chapter 6 Logan, M., Zhu, F., Lens, P.N.L., Cetecioglu, Z., 2022. Influence of pH, heat treatment of inoculum and selenium oxyanions on concomitant selenium bio-remediation and volatile fatty acids production from food waste. ACS Sustainable Chemistry and Engineering (Under Review)	**Logan, M.**: Conceptualization, Methodology, Investigation, Formal analysis, Data curation, Visualization, Writing - Original Draft. **Zhu, F.**: Investigation, Writing - Review & Editing. **Lens, P.N.L.**: Project administration, Resources, Funding acquisition, Writing - Review & Editing. **Cetecioglu, Z.**: Conceptualization, Methodology, Project administration, Validation, Supervision, Resources, Funding acquisition, Writing - Review & Editing.
Chapter 7 Logan, M., Tan, L.C., Nzeteu, C.O., Lens, P.N.L., 2022. Effect of selenate on treatment of glycerol containing wastewater in UASB reactors. Renewable Energy (Under Review)	**Logan, M.**: Conceptualization, Methodology, Investigation, Formal analysis, Data curation, Visualization, Writing - Original Draft. **Tan, L.C.**: Conceptualization, Writing - Review & Editing. **Nzeteu, C.O.**: Investigation, Writing - Review & Editing. **Lens, P.N.L.**: Conceptualization, Project administration, Resources, Supervision, Funding acquisition, Writing - Review & Editing.

Funding

This PhD thesis was supported by the Science Foundation Ireland (SFI) through the SFI Research Professorship Program entitled *Innovative Energy Technologies for Biofuels, Bioenergy and a Sustainable Irish Bioeconomy* (IETSBIO^3; Grant Number 15/RP/2763), the Research Infrastructure research grant *Platform for Biofuel Analysis* (Grant Number 16/RI/3401) and the COST Action fellowship CA18113 – EuroMicropH (*Understanding and exploiting the impacts of low pH on micro-organisms*).

Nomenclature

AD	Anaerobic digestion
AGS	Anaerobic granular sludge
APHA	American public health association
BMP	Biomethane potential
cDNA	Complementary deoxyribonucleic acid
CM	Conductive material
COD	Chemical oxygen demand
DAF	Dissolved air floatation
DIET	Direct interspecies electron transfer
DNA	Deoxyribonucleic acid
EDX	Energy-dispersive X-ray spectroscopy
EPS	Extracellular polymeric substances
FEEM	Fluorescence Excitation Emission Matrix
FOG	Fats, oils and grease
GAC	Granular activated carbon
GHG	Green House Gas
HRT	Hydraulic retention time
IC_{50}	Half maximal inhibitory concentration
λ	Lag-phase time
LCFA	Long chain fatty acids
M_o	Maximum methane yield
MPA	Methane producing archaea
OLR	Organic loading rate
R_m	Maximum methane production rate
RA	Relative abundance
RNA	Ribonucleic acid
SEM	Scanning electron microscopy
SBR	Sequential batch reactor
SeRB	Selenium reducing bacteria
SRB	Sulfate reducing bacteria
Se^0	Elemental selenium
SeO_4^{2-}	Selenate
SeO_3^{2-}	Selenite
SMA	Specific methanogenic activity
TEM	Transmission electron microscopy
T_m	Peak time of biomethane production
TS	Total solid
UASB	Up-flow anaerobic sludge bed
VFA	Volatile fatty acids
VS	Volatile solid
WAS	Waste activated sludge
XRD	X-ray diffraction

Chapter 1 General Introduction

1.1 Background and problem statement

1.1.1 Regulations and policies in Europe to adopt renewable energy

The European Union (EU) has aimed by 2030 to replace 32% of its energy consumption by renewable energy with the Renewable Energy Directive 2 or RED II (directive 2018/2001/EC). Recently, the EU launched the global methane pledge to cut methane emissions (including from untreated waste) by at least 30% by 2030, compared to 2020 levels at the Conference of the Parties (CoP26) to the 2021 UNFCC summit (European Commission, 2021). On the other hand, over the years, favourable support schemes are being unveiled in several EU member states for renewable energy, especially for electricity, heat and transport (Scarlat et al., 2018). Further technology development and the use of renewables will lead to carbon-neutrality targeted by the European Green Deal by 2050 (Potrč et al., 2021).

1.1.2 Waste as a resource

A bio-based circular economy regards organic wastes as potential resources that can be utilized to supply fuels, nutrients and chemicals (Wainaina et al., 2020). This helps to achieve net-zero carbon emissions as well as the United Nations Sustainable Development Goals (Leong et al., 2021). In 2021, Ireland generated about a million tonnes of food waste from both households and commercial establishments which were not managed properly (EPA, 2021). Industries such as dairy and brewery have a strong presence in Ireland and therefore the treatment and management of the wastewaters generated are also imperative. Though the availability of these wastewaters is in abundance, their energy potential is vastly underutilised. Furthermore, units such as dissolved air floatation (DAF) are employed in these industries, especially those that generate lipid-rich wastewater, as a pre-treatment for biological processes. There is a need to demonstrate that the generated DAF slurry can be a valuable resource to produce energy and other valuable bioproducts.

1.1.3 Bioenergy and bioproducts from AD

Anaerobic digestion (AD) is described as the technology for refining waste into bioenergy and bio-products (Harirchi et al., 2022). AD reduces global methane emissions through proper management of organic wastes. AD is conducted through four steps (Caiardi et al., 2022), viz. hydrolysis (break down of large polymers to smaller molecules), acidogenesis (volatile fatty

acids production), acetogenesis (acetic acid production) and methanogenesis (methane generation). The biogas that is produced during AD could be upgraded for high-end applications such as vehicular fuel and power generation. The volatile fatty acids produced before the final step in AD could be used as a platform for biological nutrient removal and production of bioplastics, biodiesel and single cell protein (Khatami et al., 2021). In addition to the biogas, AD allows the possibility to recover resources such as nitrogen, phosphorous, potassium and selenium from domestic or industrial wastewaters (Logan and Visvanathan, 2019).

1.1.4 Selenium pollution and remediation

Selenium is a non-metal or chalcogen (16th group of the periodic table) which is both an essential nutrient as well as a toxic element to living organisms with a narrow range between these two concentrations (Sakr et al. 2018). Selenium laden wastewaters are generated in acid mine drainage, flue gas desulfurisation, petrochemical activities, agricultural drainage and leachate from seleniferous soils (Sinharoy and Lens, 2020). Selenium discharge into water bodies leads to bioaccumulation resulting in human health hazards, and therefore a minimum threshold limit of 5 µg/L is set for effluent discharge by the United States Environmental Protection Agency (Tan et al., 2016).

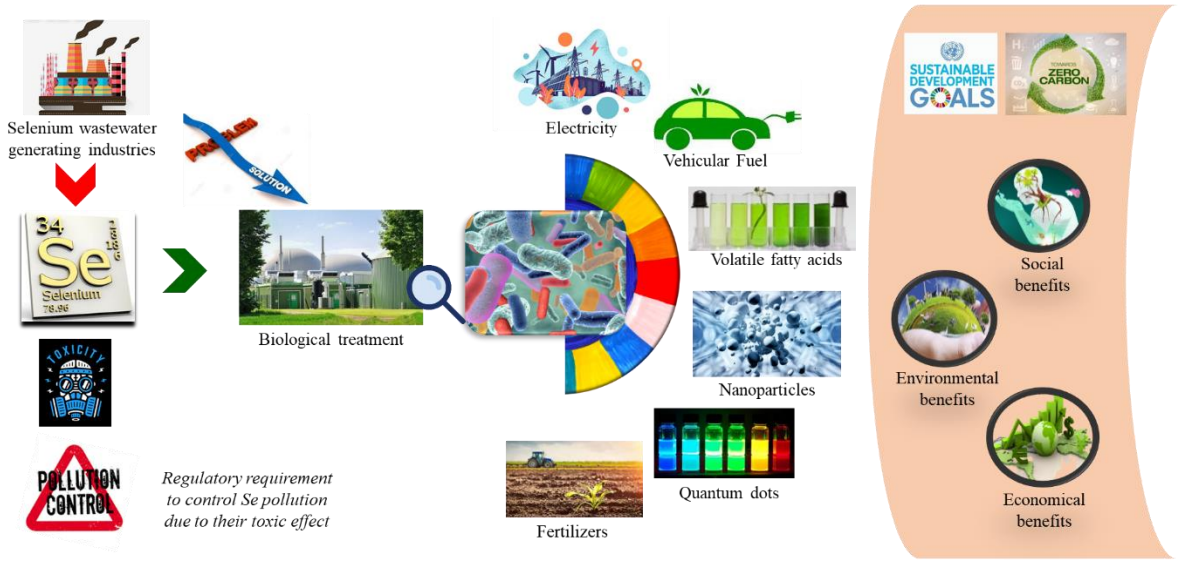

Figure 1.1 Benefits from biological treatment of Se rich wastewater

Selenium exists in several oxidation states (+6, +4, 0, -2) which influences toxicity levels, bioavailability and success of the treatment methods. Bioremediation of soluble selenium oxyanions, viz. selenate (+6) and selenite (+4) to insoluble, less toxic elemental selenium (0) has been gaining momentum as an environment friendly and cost effective green alternative to physical and chemical methods (Eswayah et al., 2016). Several concomitant benefits such as selenium removal, methane recovery, and biogenic synthesis of elemental selenium or metal selenides could be realised during AD of selenium rich waste stream. However, there has been no study to demonstrate this wide range of benefits illustrated in Figure 1.1. Selenium that could be recovered finds applications in metallurgy, agriculture, electronics, glass manufacturing, chemicals and pigments (Nanchariah et al., 2015). Several studies have been conducted in the last three decades on biological selenium reduction using different substrates. Though supplementing selenium as a trace element in AD is well established for enhancing biomethane production, wastewaters with elevated selenium concentrations are generally not considered as a suitable feedstock for AD owing to their toxic effect on process performance and microbial communities (Ariunbaatar et al., 2016, Lenz et al., 2008). Therefore, there is a need to investigate AD of selenium rich wastewater and establish its toxicity limit on methanogenesis.

1.2 Objectives and scope of this PhD study

This research investigated on the production of methane, volatile fatty acids and selenium nanoparticles from selenium-rich and lipid-rich wastewaters. The specific objectives of this research are:

1. Improvement of methane production from DAF slurry through substrate dilution and initial pH adjustment.
2. Enhancement of dairy wastewater AD through conductive material (granular activated carbon) supplementation in a mesophilic sequential batch reactor. Study of the enrichment of microbial communities and physiological changes to link with the process performance.
3. Investigation of the toxicity of selenate and selenite to methane production from DAF slurry with (anaerobic granular sludge and waste activated sludge) and without inoculum.
4. Demonstration of continuous and long-term methane recovery from glycerol containing wastewater at elevated selenate concentrations in an upflow anaerobic sludge bed reactor, including characterisation of the microbial community dynamics.

5. Influence of pH, heat treatment of inoculum and selenium oxyanion supplementation on the concomitant VFA production and selenium removal using food waste as the substrate.
6. Evaluation of reduction of selenium oxyanions to elemental selenium or metal selenides using a model substrate (glycerol) and real waste (food waste and DAF slurry) as the electron donors with different inoculum, pH, heat treatment of inoculum, COD/selenium ratio in batch and continuous reactors.

1.3 Structure and layout

The PhD thesis is divided into 8 chapters (Figure 1.2).

Chapter 1 presents an overview of this research including background, problem description, research objectives and thesis outline. AD of DAF slurry, sulfate- and selenate-rich wastewaters was reviewed in chapter 2. Chapters 3 and 4 focused on mesophilic AD of lipid-rich wastewaters, viz. DAF slurry and dairy wastewater. Chapters 5, 6 and 7 investigated mesophilic anaerobic digestion of model substrates and real waste/wastewater supplemented with Se oxyanions.

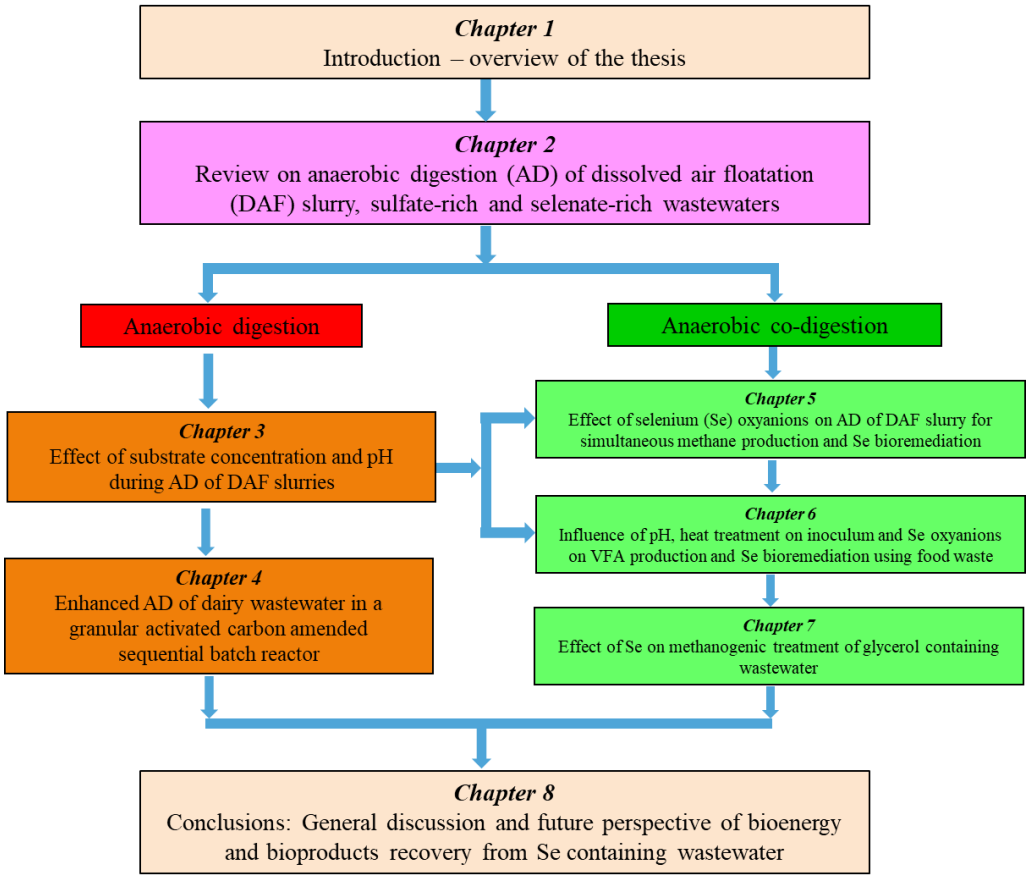

Figure 1.2 Structure of this PhD thesis

Chapter 2 provides a literature review on anaerobic treatment of DAF slurry and wastewaters with high sulfate and selenate content. The working principle of DAF systems and the characteristics of DAF slurry are presented. Pre-treatment technologies and co-digestion options for DAF slurry are explored. Literature on anaerobic treatment of sulfate- and selenate-rich wastewaters are reviewed. Bio-refinery approaches for these substrates are also discussed.

In chapter 3, the effect of substrate dilutions with mineral salt media (1:0, 1:1, 1:2 and 1:3) and initial pH (4.5, 5.0, 5.5, 6.0 and 7.0) on the biomethane potential of DAF slurry using two inocula (anaerobic granular sludge and waste activated sludge) was studied in manual and automated BMP tests, respectively.

Chapter 4 investigated the enhancement of AD of dairy wastewater due to granular activated carbon supplementation in a sequential batch reactor. The enriched and functional microbial community for conductive material induced enhanced process performance was also investigated. Besides, the physiological observation on the presence of e-pili structures was carried out with scanning electron microscopy.

Chapter 5 studied the effect of Se oxyanions on anaerobic digestion of DAF slurry for simultaneous methane production and selenium remediation. The biomethane potential tests were carried out with and without inocula, viz. anaerobic granular sludge and waste activated sludge. The IC_{50} values were determined for different Se species and inoculum conditions. Transmission electron microscopic imaging was carried out to investigate the biogenic synthesis of elemental Se nanoparticles.

Chapter 6 evaluated VFA production and selenium remediation using food waste in batch reactors. It was hypothesized that VFA production could be enhanced by three strategies, viz. pH adjustment (10 and 5), heat treatment of the inoculum (85 ^{o}C for 1 hour) and selenium oxyanion supplementation (up to 500 µM). The microbial communities in the fermentation and selenium reducing environment were also studied. The selenium nanoparticles synthesised were studied using transmission and scanning electron microscopy as well as energy dispersive X-ray analysis.

Based on the proof of concepts established in chapters 5 and 6, chapter 7 investigated long term and continuous methane production from selenate and glycerol containing wastewater in an upflow anaerobic sludge bed reactor. The study aimed to establish the methanogenesis threshold concentration for selenate. The chapter also addressed the research

question whether it was the selenate concentration or the COD/selenate ratio that governs the process performance of AD of selenate rich wastewater. The dynamics in microbial communities, especially in methanogenic archaeal communities, with increment of the selenate concentrations were examined. Se nanoparticles and metal selenides were studied using transmission and scanning electron microscopy, energy dispersive X-ray analysis, and X-ray diffraction.

Chapter 8 provides a general discussion based on the research objectives and findings from this thesis and further explores strategies on future prospects for bioenergy and bioproducts recovery from selenium rich wastewater.

1.4 References

Ariunbaatar, J., Esposito, G., Yeh, D.H., Lens, P.N.L., 2016. Enhanced anaerobic digestion of food waste by supplementing trace elements: role of Selenium (VI) and Iron (II). Frontiers in Environmental Science 4(8). https://doi.org/10.3389/fenvs.2016.00008

Caiardi, F., Belaud, J-P., Vialle, C., Monlau, F., Tayibi, S., Barakat, A., Oukarroum, A., Zeroual, Y., Sablayrolles, C., 2022. Waste-to-energy innovative system: Assessment of integrating anaerobic digestion and pyrolysis technologies. Sustainable Production and Consumption 31, 657-669. https://doi.org/10.1016/j.spc.2022.03.021

EPA, 2021. How much food do we waste in Ireland? Ireland Environmental Protection Agency. https://www.epa.ie/publications/circular-economy/resources/NWPP-Food-Waste-Report.pdf

Eswayah, A.S., Smith, T.J., Gardiner, P.H.E., 2016. Microbial transformations of selenium species of relevance to bioremediation. Applied and Environmental Microbiology 82, 16. https://doi.org/10.1128/AEM.00877-16

European Commission, 2021. Launch by United States, the European Union, and partners of the global methane pledge to keep 1.5 ºC within reach. https://ec.europa.eu/commission/presscorner/detail/en/statement_21_5766

Harirchi, S., Wainaina, S., Sar, T., Nojoumi, S.A., Parchami, M., Parchami, M., Varjani, S., Khanal, S.K., Wong, J., Awasthi, M.K., Taherzadeh, 2022. Microbiological insights into anaerobic digestion for biogas, hydrogen or volatile fatty acids (VFAs): a review. Bioengineered 13. https://doi.org/10.1080/21655979.2022.2035986

Lenz, M., Janzen, N., Lens, P.N.L., 2008. Selenium oxyanion inhibition of hydrogenotrophic and acetoclastic methanogenesis. Chemosphere 73(3), 383-388. https://doi.org/10.1016/j.chemosphere.2008.05.059

Leong, H.Y., Chang, CK., Khoo, K.S., Chew, K.W., Chia, S.R., Lim, J.W., Chang, J-S., Show, P.L., 2021. Waste biorefinery towards a sustainable circular bioeconomy: a solution to global issues. Biotechnology for Biofuels 14, 87. https://doi.org/10.1186/s13068-021-01939-5

Logan, M., Visvanathan, C., 2019. Management strategies for anaerobic digestate of organic fraction of municipal solid waste: Current status and future prospects. Waste Management and research 37, 27-39. https://doi.org/10.1177/0734242X18816793

Nancharaiah, Y.V., Lens, P.N.L., 2015. Selenium biomineralization for biotechnological applications. Trends in Biotechnology 33(6), 323-330. https://doi.org/10.1016/j.tibtech.2015.03.004

Potrč, S., Čuček, L., Martin, M., Kravanja, Z., 2021. Sustainable renewable energy supply networks optimization – the gradual transition to a renewable energy system within the European Union by 2050. Renewable and Sustainable Energy Reviews 146, 111186. https://doi.org/10.1016/j.rser.2021.111186

Sakr, T.M., Korany M., Katti, K.V., 2018. Selenium nanomaterials in biomedicine – An overview of new opportunities in nanomedicine of selenium. Journal of Drug Delivery Science and Technology 46: 223–233

Scarlat, N., Dallemand, J., Fahl, F., 2018. Biogas: Developments and perspectives in Europe. Renewable Energy 129, 457-472. https://doi.org/10.1016/j.renene.2018.03.006

Sinharoy, A., Lens, P.N.L., 2020. Biological removal of selenate and selenite from wastewater: options for selenium recovery as nanomaterials. Current Pollution Reports 6, 230-249. https://doi.org/10.1007/s40726-020-00146-4

Tan, L.C., Nancharaiah, Y.V., van Hullebusch, E.D., Lens, P.N.L., 2016. Selenium: Environmental significance, pollution, and biological treatment technologies. Biotechnology Advances 34(5), 886-907. https://doi.org/10.1016/j.biotechadv.2016.05.005

Wainaina, S., Awasthi, M.K., Sarsaiya, S., Chen, H., Singh, E., Kumar, A., Ravindran, B., Awasthi, S.K., Liu, T., Duan, Y., Kumar, S., Zhang, Z., Taherzadeh, M.J., 2020. Resource

recovery and circular economy from organic solid waste using aerobic and anaerobic digestion technologies. Bioresource Technology 301, 122778. https://doi.org/10.1016/j.biortech.2020.122778

Chapter 2 Unravelling the potential of dissolved air floatation slurry, sulfate-rich and selenate-rich wastewaters for anaerobic digestion

2.1 Introduction

Anaerobic digestion (AD) is a well-established technology for the treatment of waste and wastewater to recover energy and nutrients. It is a versatile method to process a wide range of waste streams. Globally, the actual biogas production from AD is only 35 million tonnes of oil equivalent (Mtoe), whereas the actual biogas potential is about 16 times higher at 570 Mtoe (World Energy Outlook, 2020). This is due to the underutilisation of biomass that is readily available and also that is conventionally not exploited. The World Resources Institute has recommended phasing out the dedicated use of land to grow energy feedstock to generate bioenergy and biofuels which undermines the efforts to combat climate change and to achieve a sustainable food future (Searchinger and Heimlich, 2015). Typically, the feedstocks for AD include crop residues, animal manure, municipal and industrial solid waste and wastewater. It is imperative that research on identifying and demonstrating feedstocks that are largely underutilised for AD is necessary for their commercial implementation. By doing so, can we enable a more sustainable and productive biogas sector, which does not compete with food production and fertile agricultural land?

Lipids in wastewater can be classified into four major groups, viz. triacylglycerols including long chain fatty acids (LCFAs), glycolipids, phospholipids, and cholesterol (Husain et al., 2014). Among the lipids, the most abundant are LCFAs and triacylglycerols (popularly referred to as fats and oils), and among the LCFAs, the most abundant are palmitic, oleic, and linoleic acids (Holohan et al., 2022). Fat, oil and grease (FOG) wastewater streams are generated by various industries, viz. dairy, slaughterhouses, edible oil production and fish canning factories whose characteristics vary highly and are dependent on the production process (Logan et al., 2021). The presence of lipids leads to bioreactor issues such as adsorption, sludge flotation, washout and microbial inhibition (Diamantis et al., 2021). Therefore, they are usually removed ahead as a pretreatment (such as screening, sedimentation, dissolved air floatation (DAF), flocculation and/or precipitation) ahead of biological treatment. Despite these challenges, lipids have gained interest for methanogenesis owing to their high energy content. Theoretically, the biogas yield for lipids is 1.4 L g^{-1}, when compared to 0.9 L g^{-1} for proteins and 0.8 L g^{-1} for carbohydrates, respectively (Alves et al., 2009).

In industries, such as food processing, dairy, petrochemical, and pulp and paper manufacturing, a dissolved air floatation (DAF) unit removes the FOG content in wastewater (Ross et al., 2003). Typically, the concentrated DAF slurry that is generated could hold up to

85% of the separated FOG. There has been no comprehensive review on the biorefinery options for DAF slurries. Therefore, this chapter attempts to focus on the avenues of AD of DAF slurries.

On the other hand, several waste streams are often laden with inorganic salts such as sulfate and selenate. In the last few decades, anaerobic remediation of these inorganic wastewaters has been studied as bioreduction in their excessive (or the highest possible) concentration. However, these wastewaters are perceived as not appropriate feedstocks for AD in full-scale plants. Sulfate- or selenate- reducing bacteria can be dominant (more than methanogenic archaea) when their respective concentrations are higher, which is detrimental to complete the AD process. This background has driven the AD research community to establish the optimal dosage of these inorganic concentrations that enhance process performance at lower concentrations, but might lead to inhibition at elevated concentrations. While few streams like sulfate-rich wastewater have been extensively investigated, others have not yet been studied. This chapter presents a state-of-the-art review of the research progress on AD of sulfate-rich and selenate-rich wastewaters.

2.2 Exploring dissolved air floatation slurry as a substrate for AD

2.2.1 Dissolved air floatation systems

DAF systems were introduced in the 1960s and quickly gained popularity since they are associated with superior treatment capacity, compact space requirements, temperature resistance and high clarifying performance (Cagnetta et al., 2019). In a typical DAF unit (Figure 2.1), the raw and untreated wastewater is initially mixed with chemicals for an optional pH adjustment. Thereafter, an aluminium or ferric coagulant (with an optional coagulant aid polymer) is added, followed by flocculation in a dedicated two- or three-stage flocculation zone (Crossley and Valada, 2006).

The wastewater is then subjected to microbubbles formed by supersaturating a proportion of the clarified stream (DAF recycle) with air in a pressurized vessel, then releasing the pressure and injecting the DAF recycle flow. The micro-bubbles in turn attach to the flocculated particles and rise to the surface of the tank. The resulting dense foam is periodically removed by skimming or hydraulic flooding. The clarified water is drawn from underneath the bubble zone by collection manifolds or by an opening at the end of the tank (Crossley and

Valada, 2006). DAF systems can generate microbubbles and/or nanobubbles in the bubble size distribution range of 20–80 µm and 50–800 nm, respectively (Azevedo et al., 2018). Recently, the effects of influent physiochemical characteristics on air dissolution, bubble size and rise velocity in DAF have been reviewed by Rajapakse et al. (2022). The surface loading of DAF systems usually ranges between 10–40 m/h.

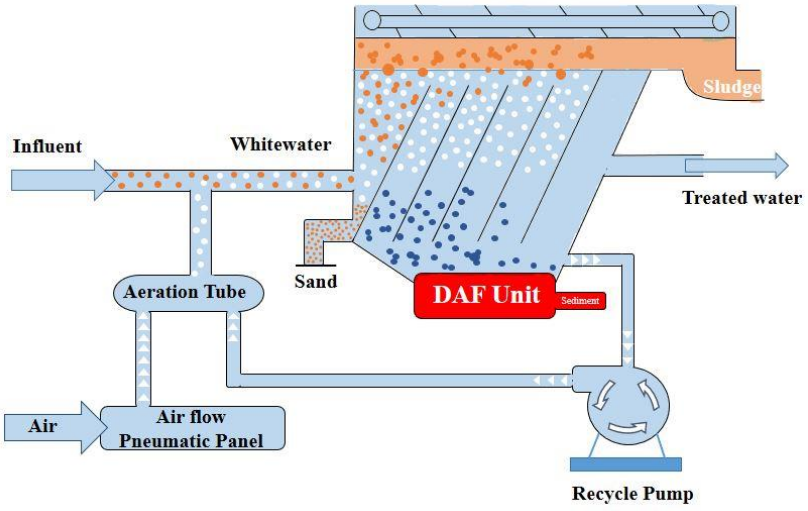

Figure 2.1 Typical dissolved air floatation unit for removal of FOG from dairy wastewater

Recent developments in DAF technology have reduced capital costs by optimizing flocculation, reducing hydraulic detention time (from 20 to 5 min) and increasing surface loading (from 10 to 40 m/h) (Crossley and Guiraud, 2016). There are still developments on novel methods for forming micro- and nano-bubbles with the proper characteristics for enhanced flotation of fats.

2.2.2 Dissolved air floatation sludge

After the hydrophobic interactions in a DAF unit, two wastewater fractions are produced. Traditionally, the dilute wastewater with lower FOG content is treated by biological methods. The concentrated wastewater is generally not managed by biological methods owing to the associated process challenges (Logan et al., 2021). Through DAF systems, up to 85% of the FOG content can be concentrated in the DAF sludge. The characteristics of DAF slurries reported in the literature are reviewed in Table 2.1.

Table 2.1 Characteristics of DAF slurry generated by different industrial processes

Source	**Coagulant**	**Concentration**	**Lipid content**	**pH**	**Reference**
Meat processing wastewater	n.a.	TSS = 150.33 g/m.	Lipid content = 12.98 (wt.%, dry sludge basis)	8.23	Okoro et al., 2017
Personnel care products factory wastewater	Ferric chloride	COD_{total} = 645.7 ±53 mg/L TSS = 61.3 ±57 mg/L	O&G content = 45.6 ±10 mg/L	8.41 ±0.15	El-Gohary et al., 2010
Personnel care products factory wastewater	Alum	COD_{total} = 512 ±154 mg/L TSS = 46 ±35 mg/L	O&G content = 36.3 ±4 mg/L	6.93 ±0.2	El-Gohary et al., 2010
Personnel care products factory wastewater	Ferrous sulfate	COD_{total} = 735 ±64 mg/L TSS = 65 ±58 mg/L	O&G content = 47.5 ±0.7 mg/L	8.9 ±0.2	El-Gohary et al., 2010
Slaughterhouse waste	Sodium hydroxide and Ferrous sulfate	TOC = 675,000 mg/kg TS TS = 22 %	Fat = 57.9 % of TS	n.a.	Pitk et al., 2012
Cheese processing waste	n.a.	TS = 7.8 0.3%	n.a.	n.a.	Browne et al., 2013
Slaughterhouse waste	n.a.	COD_{total} = 205 g/L $COD_{soluble}$ = 33.5 g/L TS = 14.56 ±0.61 %	FOG content = 90000 mg/L	4.16	Harris et al., 2017

FOG: Fats, Oil and Grease; O&G: Oil and Grease; n.a. – not available

Ding et al. (2015) reported the removal of 81% of influent TSS and 67 % of COD in DAF. Because of the ability to retain high solid concentrations in the sludge, a DAF system also leads to economic advantages since it suppresses the need for a sludge thickening step and replaces the combination of a settler and thickener (Cagnetta et al., 2019, Wang et al., 2005). The characteristics of sludge produced from the DAF process are highly dependent on the type of influent wastewater processed, specific coagulant used, bubble size distribution, gas to liquid mass transfer efficiency, hydrodynamics and the operating conditions (Rajapakse et al., 2022, El-Gohary et al., 2010).

2.2.2.1 AD of dissolved air floatation slurry

A lipid-rich DAF slurry follows the typical anaerobic biodegradation pathway as illustrated in Figure 2.2. LCFAs, the primary component of FOG, are degraded anaerobically via the β-oxidation pathway to acetate and H_2, which are subsequently converted to methane. The β-oxidation pathway (shown in the equation below) begins when the fatty acid is activated with coenzyme A and the resulting oxidation leads to the release of acetyl-CoA and the formation of a fatty acid chain, which is shortened by two carbons (Long et al., 2012). Acetyl-CoA is oxidized by the citric acid cycle pathway and the process of β-oxidation is repeated (Madigan et al., 2006).

$CH_3(CH_2)_nCOOH + 2H_2O \rightarrow CH_3(CH_2)_{n-2}COOH + CH_3COOH + 2H_2$ (Kim et al., 2004)

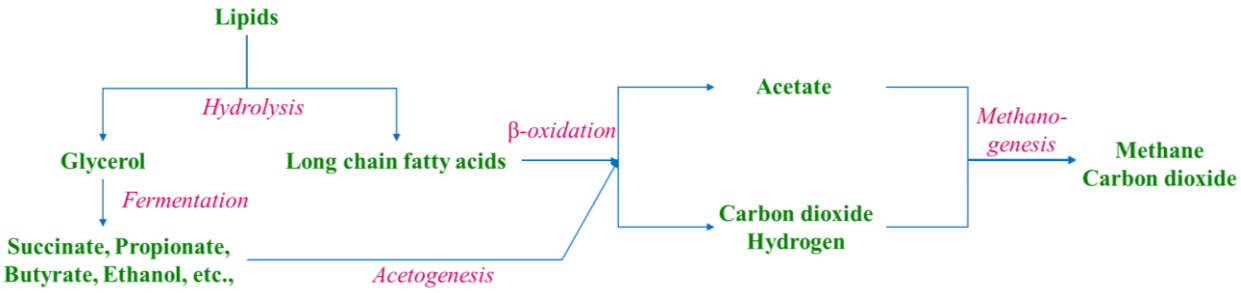

Figure 2.2 Pathway of anaerobic lipid biodegradation

Table 2.2 Methane production from DAF slurries from different wastewater types

DAF slurry	Inoculum	System	pH	Tempe-rature (°C)	Working volume (mL)	Inoculum to substrate ratio	Methane yield	Reference
Slaughterhouse waste	Primary and secondary sludge mixture treating domestic and industrial wastewater	OxiTop-C respirometric system	n.a.	37.5	200	0.5	650 mL/g VS	Pitk et al., 2012
Cheese processing waste	Cattle slurry, poultry litter and grease trap waste mixture	Automated BMP (AMPTS II)	~7	37	400	2	787 mL/g VS	Browne et al., 2013
Slaughterhouse waste	Anaerobic sludge treating slaughterhouse waste	Automated BMP (AMPTS II)	n.a.	37	400	3	759 mL/g VS	Harris et al., 2017
Dairy wastewater	Anaerobic granular sludge treating dairy wastewater	Automated BMP (AMPTS II)	6.0-8.0	37	50	0.9	743 mL/g VS	Logan et al., 2021
Dairy wastewater	Waste activated sludge treating domestic wastewater	Manual BMP	7.0-8.0	30	250	0.1	659 mL/g VS	Logan et al., 2022a

n.a. – not available

As such, the high FOG content in DAF slurries poses a challenge for biological treatment. The insolubility of FOG forms a separate phase-out of the liquid and is not easily biodegradable. LCFA components (especially palmitate) in DAF slurry accumulate or are absorbed onto the biomatrix (Neves et al., 2009). AD of a DAF slurry can be destabilised by the high LCFA concentrations which might have a detrimental effect by inhibiting methanogenic bacteria as a result of damage to their cellular membrane (Worwag et al., 2011) or inducing reduced mass transfer due to the formation of a layer of LCFAs on the bacteria or granules, thus hindering the substrate access to the cells and biogas release (Long et al., 2011, Martinez et al., 2016). Flotation due to LCFA entrapment can make the substrate inaccessible to the anaerobic biomass and disrupt the AD (Martinez et al., 2016). DAF slurry also undergoes slow acidification which means a longer retention time is required (Li et al., 2013).

Despite these challenges, few studies have demonstrated the AD of DAF slurries. The methane yields from DAF slurries derived from different waste streams in biomethane potential assays are presented in Table 2.2. However, there is no literature that has reported pilot- or full-scale methane production from the AD of DAF slurry.

Lipolytic bacteria in anaerobic digesters have been proposed to belong to the families Caldilineaceae (phylum Firmicutes), Bacteroidaceae (phylum Bacteroidetes) and to the genera Trichococcus (phylum Firmicutes), Devosia, and Psycrobacter (phylum Proteobacteria) (Westerholm and Schnürer, 2019). Bacteria identified that are capable of β-oxidizing LCFA in syntrophy with methanogens belong to the families Syntrophomonadaceae and Syntrophaceae. *Methanosaeta* and *Methanosarcina* are dominant methanogenic archaea in anaerobic digesters treating FOG waste (Salama et al., 2019).

In addition to the option of methane recovery from DAF slurry in optimized operational conditions, two popular approaches can be applied, viz. pretreatment before AD and anaerobic co-digestion, which are explained in the subsequent sections.

2.2.2.1.a Pre-treatment technologies

Pre-treatment refers to the treatment of the wastewater to enhance the availability of substrates to microbes and thereby improve the removal of organics and increase reaction kinetics and total biogas production (Harris and McCabe, 2015). Prior to digestion, pre-treatment such as thermal, chemical, thermochemical, mechanical and biological methods may be applied.

Though there is very little literature on DAF slurries, successful pretreatments reported with FOG waste could be easily adopted.

Thermal pre-treatment of FOG waste at elevated temperatures to solubilise larger biomolecules is also promising. Li et al. (2017) reported that thermal pretreatment enhanced the degradation efficiency of FOG-rich kitchen waste by upto 36%. Acid pretreatment of DAF slurry derived from dairy wastewater was conducted in this thesis, which improved methane production by 23% (Logan et al., 2021). Similarly, biodegradable soluble materials improved to over 66% with alkaline treatment (Linyi et al., 2020). Harris et al. (2017) recommended thermobaric pre-treatment as viable in an industrial context for AD of DAF slurry from slaughterhouse waste. Ozone treatment was found to enhance the biodegradability of DAF slurry derived from refinery wastewater (Haak et al., 2016). Microwave pretreatment that ruptures cell wall resulted in a maximum methane yield which was 155% higher than the control, i.e. thickened waste activated sludge and FOG waste (Alqaralleh et al., 2019).

Meng et al. (2017) reported up to 158% improvement in the biomethane production rate from crude lipid through hydrolysis by enzymatic pretreatment. Biosurfactants have been shown to pretreat cattle slaughterhouse wastes with high FOG concentrations (Harris et al., 2018). A pre-digestion (two-stage AD) has greatly improved process performance. The maximum methane yield from waste cooking oil and sewage sludge co-digestion in a two-stage continuous stirred tank reactor (CSTR) was 39% higher than that of a single stage CSTR system (Yan et al., 2021).

2.2.2.1.b Anaerobic co-digestion

In general, lab-scale studies show that it is more feasible for FOG wastes such as DAF slurry to be used as a (co-)substrate during anaerobic treatment. There have been several publications which have reported successful co-digestion of FOG waste (Salama et al., 2019). For instance, co-digesting sewage sludge with a grease trap waste resulted in about 93% higher specific methane yield than mono-digestion (Grosser and Neczaj, 2016). Similarly, biogas production increased by 350% when FOG was co-digested with waste activated sludge (Li et al., 2011). Significant improvement in productivity has been reported from co-digestion of FOG waste with food waste, municipal solid waste, animal manure and microalgae (Solé-Bundó et al., 2019, Salama et al., 2019, Long et al., 2012). With only very few studies that have investigated biomethane recovery from DAF slurry, it can be anticipated that DAF slurry might receive

attention (similar to other FOG wastes) as a co-substrate for AD in the future. There is huge scope to explore this possibility which could not only accomplish higher methane productivity via synergistic effects, but also overcome potential toxic effects on methanogenesis as discussed above (Logan et al., 2021). In addition, conductive material supplementation could improve lipid degradation to methane and promote syntrophic and electroactive microorganisms.

2.2.2.2 Biorefinery approaches for dissolved air floatation slurry

In addition to the aforementioned challenges (such as prolonged lag phase and LCFAs toxicity), requirements for mixing, pumping, and digestate handling increases operational costs (Fagbohungbe et al., 2015). This could be overcome with additional biorefinery options. The conversion of DAF slurries to biodiesel may be achieved either via modified transesterification processes or the two-step integrated hydrolysis and esterification process (Veljković et al., 2015). A DAF slurry can be used as an inexpensive carbon feedstock to produce polyhydroxyalkanoates or bioplastics (Sangkharak et al, 2021). Similarly, pyrolysis of DAF slurry can yield biooil (Trabelsi et al, 2020). Carboxylic acid production from DAF slurry remains yet to be explored. Though interest in the production of methane is gaining momentum, hydrogen generation through dark fermentation of DAF slurry is yet to be investigated extensively. Research developments on microbial fuel cells for the treatment of FOG wastes for bioelectricity production are recently advancing (Lawan et al., 2022). Enhanced productivity of microalgae cultivated in DAF slurries can also be achieved for biofuel production (Chen et al., 2015). DAF slurries can also be used as an electron donor for the bioremediation of inorganic wastewaters (Logan et al., 2022a).

2.3 Realising methane production from wastewaters with high inorganic content

Several industries such as dye, textile, pesticides and pharmaceutical and coal mining generate wastewater laden with high inorganic content (Hayat et al., 2015). These inorganic wastewaters can be treated via physical methods (such as distillation, adsorption, extraction and membrane filtration), where the pollutants are only transferred rather than converted or decomposed (Saravanan et al., 2021). On the other hand, chemical oxidative techniques (such as advanced oxidation processes and Fenton oxidation process) are associated with high removal and degradation ability, however, the cost of the chemical reagents used is prohibitive (Chen et al., 2021). Biological conversion to a non-toxic stable form has emerged as an effective and eco-

friendly method. The activated sludge process (ASP) is capable of degradation and mineralization of pollutants, nevertheless, it comes with the downside of aeration requirement (which could cost 75% of the total energy expenditure in treatment plants) along with the excess amount of sludge generated (Rosso et al., 2008). AD overcomes the drawbacks of the conventional ASP, with its ability to recover bioenergy from wastes, its low biomass (excess sludge) yield and strong tolerance to high organic loading rates (Kong et al., 2019). Though the removal of inorganics such as selenate and sulfate has been widely demonstrated in anaerobic bioreactors, the realisation of simultaneous methanogenesis is seldom focused on.

In the subsequent sections, the effect of sulfate and selenate on methanogenesis is reviewed. An external carbon source is often supplemented for bioreduction of these inorganics. The potential reactions and their free energies for methane production and reduction of sulfate and selenate is presented in Table 2.3. From a thermodynamic point of view, the reactions involving the reduction of these oxyanions are dominant over methanogenesis. As such, methanogenesis is adversely affected at higher concentrations of sulfate and selenate.

Table 2.3 Stoichiometry of the anaerobic degradation of acetate and molecular hydrogen for production of methane and reduction of selenate and sulfate
(Costa et al., 2020, Chung et al., 2006)

Reactions	**$\Delta G^{0'}$ (KJ/mol)**
Acetate:	
$CH_3COO^- + H_2O \rightarrow CH_4 + HCO_3^-$	-31
Selenate	
$3CH_3COO^- + 4SeO_4^{2-} + 11H^+ \rightarrow 6CO_2 + 4Se^0 + 10H_2O$	-930
Sulfate	
$CH_3COO^- + SO_4^{2-} \rightarrow 2HCO_3^- + HS^-$	-47.6
Hydrogen:	
$4H_2 + HCO_3^- + H^+ \rightarrow CH_4 + 3H_20$	-33
Selenate	
$3H_2 + SeO_4^{2-} + 2H^+ \rightarrow Se^0 + 4H_2O$	-71
Sulfate	
$4H_2 + SO_4^{2-} + H^+ \rightarrow HS^- + 4H_2O$	-38.1

2.3.1 Sulfate-rich wastewaters

Sulfate-rich wastewaters are generated from fermentation, tanneries, pulp and seafood processing industry (Robles et al., 2020). Due to their presence in several wastewaters, the effect of sulfate has been studied extensively. Under anaerobic conditions, dissimilatory sulfate-reducing bacteria use sulfate as a terminal electron acceptor for the degradation of organic compounds and hydrogen, which results in the generation of sulfide. A major problem in the biological treatment of sulfate-rich wastewaters is the production of hydrogen sulfide. Gaseous and dissolved sulfides are corrosive and pose biological toxicity constraints that may lead to AD process failure (Magowo et al., 2020).

Microbial activity inhibition due to sulfide is related to two mechanisms: substrate competition and toxicity. Much of the research on methane production focuses on the competition between sulfate-reducing bacteria and methanogenic archaea (Cetecioglu et al., 2019). Sulfate-reducing bacteria and methane-producing archaea coexist together and therefore methane production will not be inhibited in anaerobic reactors treating wastewaters with a COD/SO_4^{2-} ratio higher than 10 (Lens et al., 1998). Theoretically, a COD/SO_4^{2-} ratio of 0.67 is required for complete sulfate removal. Successful methane production has been reported in bioreactors treating wastewaters with low COD/SO_4^{2-} ratio and complex organic substances (Zan and Hao, 2020). However, the predominance of sulfate-reducing bacteria over methane-producing archaea is achieved after an extended operational period as shown in Figure 2.3. Sulfide toxicity is caused by the undissociated sulfide diffusing through the cell membrane to denature proteins, and precipitation of metal sulfides resulting in decreased bioavailability of micronutrients (Jung et al., 2022). Sulfate-reducing bacteria can act as a complete oxidizer (mineralize organic compounds to CO_2) or an incomplete oxidizer (partially oxidize organic compounds and generate acetate as a by-product, but are unable to use acetate as an electron donor) (Muyzer and Stams, 2008). Incomplete oxidizers account for the majority of sulfate-reducing bacteria (Hao et al. 2014).

The outcome of the competition between sulfate-reducing bacteria and methanogenic archaea is dependent on inoculum composition (type of seed sludge, bacterial composition, operational duration and bio-augmentation), influent composition (type of COD, COD/SO_4^{2-} ratio, concentration of acetate, sulfate, sulfide, Ca^{2+} and Mg^{2+}), and operational conditions (pH, mixed liquor, salinity and temperature) (Costa et al., 2020). Various studies have proposed

measures to reduce the sulfide concentration in the reactor, thus allowing the integration of methanogenesis and sulfate reduction. The simplest is the dilution of the influent with non-sulfate containing water or recycling of the effluent after removal of sulfide (by stripping, precipitation, and oxidation to elemental sulfur). The unionized sulfide concentration can be decreased by increasing pH and temperature, sulfide precipitation, electrolysis application and reactor liquid stripping. A two-stage AD that separates sulfide production and methanogenesis can also be a way forward (Lopes et al., 200).

The adverse effect of sulfate could be reversible. Lackner et al. (2020) reported that the sulfate addition affects the carbon flow shifting the end product from methane and carbon dioxide to acetate and carbon dioxide. However, methane production quickly resumed when sulfate was no longer present in the system. During AD of sulfate-rich wastewaters, the abundance of methanogens (*Methanoculleus, Methanosarcina* and *Methanosaeta*) was reduced, while sulfate-reducing bacteria (*Desulfovibrio, Desulfomicrobium, Desulfurella, Coprothermobacter, Desulfobacca, Desulfatirhabdium, Desulfotomaculum, Candidatus Desulforudis, Desulfobacterium* and *Desulfobulbus*) increased in the presence of sulfate (Kibangou et al., 2022; Lackner et al., 2020; Oliveira et al., 2021; Sarti et al., 2010).

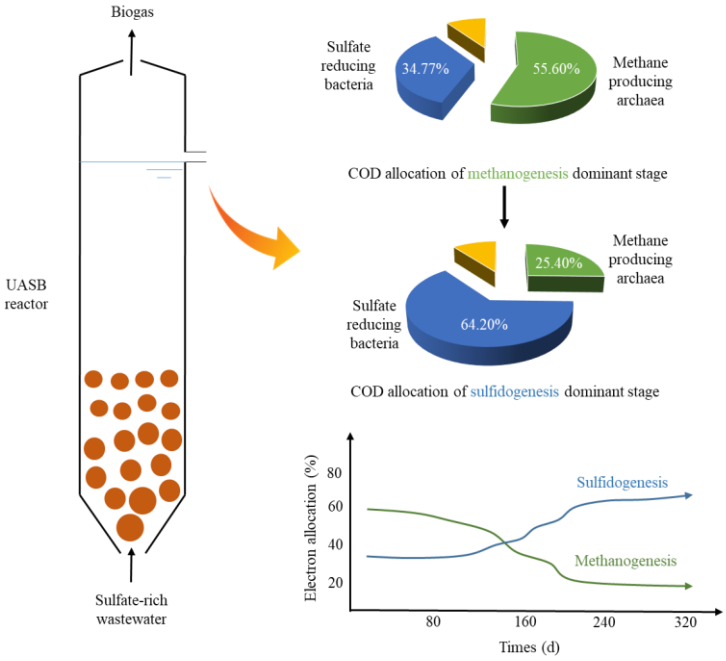

Figure 2.3 Gradual change between methanogenesis and sulfidogenesis during long-term anaerobic treatment of sulfate-rich wastewater. Adapted from Wu et al. (2018).

Sulfate is an oxyanion that has received immense attention in the past few decades, whose perception has been changing now to toxicant for useful bioprocess. Recently, Zan and Hao (2020) concluded that the presence of sulfate (400 mg/L) can stimulate sulfate-reducing bacteria acting as acetogens to convert propionate to acetate, and accelerate methanogenesis. Novel applications recently developed include recycling precious metals and rare earth elements from secondary sources (such as electronic waste) in a biogenic sulfide unit (Işıldar et al., 2019).

2.3.2 Selenate-rich wastewaters

Unlike sulfate, selenate rich wastewaters have not been investigated thoroughly as shown in Figure 2.4. There have been very few batch assays conducted to study the toxicity of selenate (Logan et al., 2022a). Through this thesis, it is clear that the COD/selenate ratio is not found to influence the process performance (chapter 7). However, the selenate concentration is found to govern the AD process performance. With the substrate concentration being ruled out, methanogenic inhibition is related to the toxicity mechanism.

As shown in Table 2.3, the detoxification of selenate by their reduction to elemental Se is favoured prior to the commencement of the AD process. Lenz et al. (2008a) reported that selenate treating granules showed elemental Se deposits only in their outer layer (compared to selenite treating granules contained elemental Se deposits over the whole cross section). The incomplete inhibition observed in the presence of selenate could thus be due to the protection of methane-producing archaea in the core of the granules. However, in terms of removal, selenate is less reactive and forms weakly bound complexes with organic matter and is therefore difficult to remove from the wastewater (Cálix et al., 2019). This is in contrast to selenite which has high reactivity to form strong and stable bonds with organic matter (Lussier et al., 2003) which allows for its quick removal. It is possible that the selenium deposits in the biomass could result in delay in lag phase and impair methane production (Martinez et al., 2016).

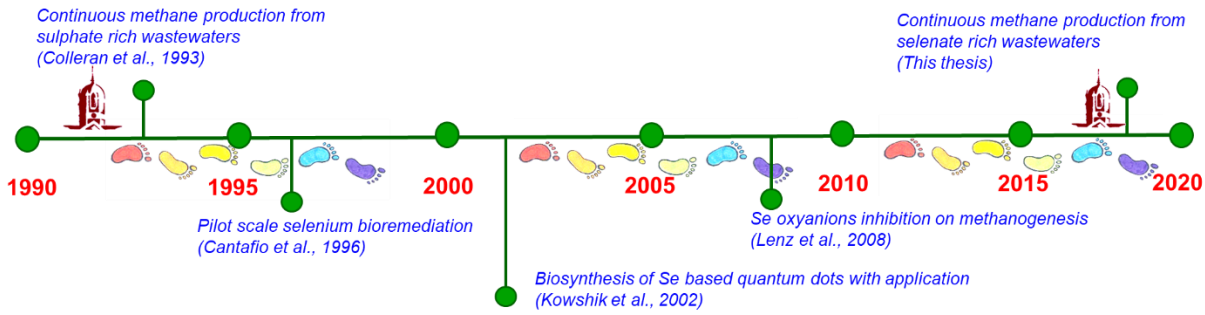

Figure 2.4 Historical and current research progress on the anaerobic treatment of selenate rich wastewaters

Selenate toxicity could also be due to synergistic toxicity from additional inhibitors formed during the conversion of Se oxyanion (e.g. hydrogen selenide, which could in turn form selenocysteine and selenomethionine), change in enzyme functionality, accumulation of carboxylic acids, and increased production of reactive oxygen species to which anaerobes are sensitive (Dong et al., 1994; Lenz et al., 2008a).

There is recent literature which focused on the microbial communities during AD of different substrates in the presence of selenium. Higher relative abundance (RA) of the bacteria *Chlorofelxi* and *Synergistes*, and archaea *Methanosaeta* and *Methanosarcina* were observed during anaerobic treatment of pig manure with 30 mg/L Se (Liang et al., 2020). Roy et al. (2022) reported a higher RA of bacteria *Turneriella*, *Rhodobacter*, *Planctomyces*, *Allochromatium*, *Nannocystis*, and *Rhodogerax*, and the archaea *Methanosarcina*, *Methanospirillum*, *Methanosaeta*, and *Methanocorpusculum* in AD of waste sewage sludge with supplementation of up to 50 mg/L sodium selenite. *Firmicutes*, *Chloroflexi*, *Bacteroidetes* and *Proteobacteria* were reported in the AD of rice straw with 100 mg/L Se (Cai et al., 2018). The activity of the methanogenic archaea *Methanosaeta* was inhibited at 500 µM SeO_4^{2-} as described in chapter 7 of this thesis. On the other hand, the presence and activity of selenium reducing bacteria (such as *Pseudomonas*, *Acinetobacter*, and *Dechloromonas*) were strengthened.

2.3.3 Biorefinery approaches for treatment of inorganic wastewater

Volatile fatty acid production from sulfate wastewaters has been demonstrated by Bertolino et al. (2012). In this thesis too, enhanced volatile fatty acid production was investigated from selenate wastewater (chapter 6). Since, selenate or sulfate can act as a chemical methanogenic

inhibitor at concentrations above the co-existence (with methanogenesis) threshold, further studies on volatile fatty acids production from these wastewaters are required. Bioelectrical energy generation with oxyanion reduction in microbial fuel cells has been reported (Rodrigues and Leão, 2020). The commercialisation of phytoremediation and phycoremediation is also promising for treatment and resource recovery from inorganic wastewaters (Mustafa and Hayder, 2021).

2.4 Conclusion

Lipid-rich dissolved air floatation slurries, sulfate- and selenate- rich wastewaters as substrates for methane production in anaerobic digestion were reviewed in this chapter. Lipid-rich wastewaters could serve as a carbon source or electron donor for anaerobic treatment of sulfate- and selenate-rich wastewaters. Novel pre-treatment methods could maximise and/or accelerate methane production from DAF slurry. Innovative strategies such as two-stage digesters and combinations of physio-chemical methods for prior removal could be beneficial for anaerobic treatment of inorganic wastewaters. The COD/sulfate ratio is reported to govern the AD process performance, however, the COD/selenate ratio does not play a similar critical role. Though the effect of the concentration of the inorganic compounds on methanogenesis are currently being understood, the evaluation on the effect of co-pollutants is necessary. Further research and development on anaerobic degradation of lipid-rich and selenium-rich wastewaters is required for commercial implementation.

2.5 References

Alqaralleh, R.M., Kennedy, K., Delatolla, R., 2019. Microwave vs. alkaline-microwave pretreatment for enhancing Thickened Waste Activated Sludge and fat, oil, and grease solubilization, degradation and biogas production. Journal of Environmental Management 233, 378-392. https://doi.org/10.1016/j.jenvman.2018.12.046

Alves, M.M., Pereira, M.A., Sousa, D.Z., Cavaleiro, A.J., Picavet, M., Smidt, H., Stams, A.J.M., 2009. Waste Lipids to Energy: How to Optimize Methane Production from Long-Chain Fatty Acids (LCFA). Microbial Biotechnology 2 (5), 538– 550. https://doi.org/10.1111/j.1751-7915.2009.00100.x

Azevedo, A., Oliveira, H.A., Rubio, J., 2018. Treatment and water reuse of lead-zinc sulphide ore mill wastewaters by high rate dissolved air flotation. Minerals Engineering 127, 114-121. https://doi.org/10.1016/j.mineng.2018.07.011

Bertolino, S.M., Rodrigues, I.C., Guerra-Sá, R., Aquino, S.F., Leão, V.A., 2012. Implications of volatile fatty acid profile on the metabolic pathway during continuous sulfate reduction. Journal of Environmental Management 103, 15-23. https://doi.org/10.1016/j.jenvman. 2012.02.022

Browne, J.D., Allen, E., Murphy, J.D., 2013. Evaluation of the biomethane potential from multiple waste streams for a proposed community scale anaerobic digester. Environ. Technol. 34, 2027-2038. https://doi.org/10.1080/09593330.2013.812669

Cagnetta, C., Saerens, B., Meerburg, F.A., Decru, S.O., Broeders, E., Menkveld, W., Vandekerckhove, T.G., De Vrieze, J., Vlaeminck, S.E., Verliefde, A.R., De Gusseme, B., 2019. High-rate activated sludge systems combined with dissolved air flotation enable effective organics removal and recovery. Bioresource Technology, 291, 121833. https://doi.org/10.1016/j.biortech.2019.121833

Cai, Y., Zheng, Z., Zhao, Y., Zhang, Y., Guo, S., Cui, Z., Wang, X., 2018. Effect of molybdenum, selenium and manganese supplementation on the performance of anaerobic digestion and the characteristics of bacterial community in acidogenic stage. Bioresource Technology 266, 166-175. https://doi.org/10.1016/j.biortech.2018.06.061

Cálix, E.M., Tan, L.C., Rene, E.R., Nancharaiah, Y.V., van Hullebusch, E.D., Lens, P.N.L., 2019. Simultaneous removal of sulfate and selenate from wastewater by process integration of an ion exchange column and upflow anaerobic sludge blanket bioreactor. Sep. Sci. Technol. 54(8), 1387-1399. https://doi.org/10.1080/01496395.2018.1533562

Cetecioglu, Z., Dolfing, J., Taylor, J., Purdy, K.J., Eyice, Ö., 2019. COD/sulfate ratio does not affect the methane yield and microbial diversity in anaerobic digesters. Water research 155, 444-454. https://doi.org/10.1016/j.watres.2019.02.038

Chen, Y-d., Duan, X., Zhou, X., Wang, R., Wang, S., Ren, N.Q., Ho, S-H., 2021. Advanced oxidation processes for water disinfection: Features, mechanisms and prospects. Chemical Engineering Journal 409, 128207. https://doi.org/10.1016/j.cej.2020.128207

Chen, G., Zhao, L., Qi, Y., 2015. Enhancing the productivity of microalgae cultivated in wastewater toward biofuel production: a critical review. Applied Energy 137, 282-291. https://doi.org/10.1016/j.apenergy.2014.10.032

Chung, J., Nerenberg, R., Rittman, B.E., 2006. Bioreduction of selenate using a hydrogen-based membrane biofilm reactor. Environ. Sci. Technol. 40, 1664-1671. https://doi.org/10.1021/es051251g

Costa, R.B., O'Flaherty, V., Lens, P.N.L., 2020. Biological treatment of organic sulfate-rich wastewaters. In book: Environmental Technologies to Treat Sulphur Pollution: Principles and Engineering. IWA Publishing, London, UK. http://dx.doi.org/10.2166/9781789060966_0167

Creamer, K.S., Chen, Y., Williams, C.M. and Cheng, J.J., 2010. Stable thermophilic anaerobic digestion of dissolved air flotation (DAF) sludge by co-digestion with swine manure. Bioresource Technology, 101, 3020-3024. https://doi.org/10.1016/j.biortech.2009.12.029

Crossley, I.A., Guiraud, P., 2016. In: Crossley, I.A., Guiraud, P. (Eds.), Proceedings of the 7th International IWA Conference on Flotation for Water and Wastewater Systems. IWA Publishing, Toulouse, France.

Crossley, I.A., Valade, M.T., 2006. A review of the technological developments of dissolved air flotation. Journal of Water Supply: Research and Technology – Aqua 55, 7- 8.

Diamantis, V., Eftaxias, A., Stamatelatou, K., Noutsopoulos, C., Vlachokostas, C., Aivasidis, A., 2021. Bioenergy in the era of circular economy: Anaerobic digestion technological solutions to produce biogas from lipid-rich wastes. Renewable Energy 168, 438-447. https://doi.org/10.1016/j.renene.2020.12.034

Ding, H.B., Doyle, M., Erdogan, A., Wikramanayake, R., Gallagher, P., 2015. Innovative use of dissolved air flotation with biosorption as primary treatment to approach energy neutrality in WWTPs. Water Practice and Technology, 10(1), 133-142. https://doi.org/10.2166/ wpt.2015.015

El-Gohary, F., Tawfik, A., Mahmoud, U., 2010. Comparative study between chemical coagulation/precipitation (C/P) versus coagulation/dissolved air flotation (C/DAF) for pre-treatment of personal care products (PCPs) wastewater. Desalination 252(1-3), 106-112. https://doi.org/10.1016/j.desal.2009.10.016

Fagbohungbe, M.O., Dodd, I.C., Herbert, B.M.J., Li, H., Ricketts, L., Semple K.T., 2015. High solid anaerobic digestion: Operational challenges and possibilities. Environmental Technology and Innovation 4, 268-284. https://doi.org/10.1016/j.eti.2015.09.003

Grosser, A., Neczaj, E., 2016. Enhancement of biogas production from sewage sludge by addition of grease trap sludge. Energy Conversation and Management 125, 301-308. https://doi.org/10.1016/j.enconman.2016.05.089

Haak, L., Roy, R., Pagilla, K., 2016. Toxicity and biogas production potential of refinery waste sludge for anaerobic digestion. Chemosphere, 144, 1170-1176. https://doi.org/10.1016/j.chemosphere.2015.09.099

Hao, T-W., Xiang, P-Y., Mackey, H.R., Chi, K., Lu, H., Chui, H-K., van Loosdrecht, M.C.M., Chen, G.H., 2014. A review of biological sulfate conversions in wastewater treatment. Water Research 65, 1–21. https://doi.org/10.1016/j.watres.2014.06.043

Harris, P.W., McCabe, B.K., 2015. Review of pre-treatments used in anaerobic digestion and their potential application in high-fat cattle slaughterhouse wastewater. Applied Energy 155, 560-575. https://doi.org/10.1016/j.apenergy.2015.06.026

Harris, P.W., Schmidt, T., McCabe, B.K., 2018. Bovine bile as a bio-surfactant pre-treatment option for anaerobic digestion of high-fat cattle slaughterhouse waste. Journal of Environmental Chemical Engineering 6(1), 444-450. https://doi.org/10.1016/j.jece.2017.12.034

Harris, P.W., Schmidt, T., McCabe, B.K., 2017. Evaluation of chemical, thermobaric and thermochemical pre-treatment on anaerobic digestion of high-fat cattle slaughterhouse waste. Bioresource Technology 244, 605–610. https://doi.org/10.1016/j.biortech.2017.07.179

Hayat, H., Mahmood, Q., Pervez, A., Bhatti, Z. A., Baig, S. A., 2015. Comparative decolorization of dyes in textile wastewater using biological and chemical treatment. Separation and Purification Technology 154, 149–153. https://doi.org/10.1016/j.seppur.2015.09.025

Husain, I.A., Ma, A.F.A., Jammi, M.S., Mirghani, M.E., Zainudin, Z.B., Hoda, A., 2014. Problems, control, and treatment of fat, oil, and grease (FOG): a review. Journal of oleo science ess13182.

Holohan, B.C., Duarte, M.S., Szabo-Corbacho, M.A., Cavaleiro, A.J., Salvador, A.F., Pereira, M.A., Ziels, R.M., Frijters, C.T., Pacheco-Ruiz, S., Carballa, M., Sousa, D.Z., 2022. Principles, advances, and perspectives of anaerobic digestion of lipids. Environmental Science and Technology. https://doi.org/10.1021/acs.est.1c08722

Işıldar, A., van Hullebusch, E.D., Lenz, M., Du Laing, G., Marra, A., Cesaro, A., Panda, S., Akcil, A., Kucuker, M.A., Kuchta, K., 2019. Biotechnological strategies for the recovery of valuable and critical raw materials from waste electrical and electronic equipment (WEEE) – A review. Journal of Hazardous Materials 362, 467–481. https://doi.org/10.1016/j.jhazmat. 2018.08.050

Jiang, Y., McAdam, E., Zhang, Y., Heaven, S., Banks, C., Longhurst, P., 2019. Ammonia inhibition and toxicity in anaerobic digestion: A critical review. Journal of Water Process Engineering 32, 100899. https://doi.org/10.1016/j.jwpe.2019.100899

Jung, H., Kim, D., Choi, H., Lee, C., 2022. A review of technologies for in-situ sulfide control in anaerobic digestion. Renewable and Sustainable Energy Reviews 157, 112068. https://doi.org/10.1016/j.rser.2021.112068

Kiuru, H.J., 2001. Development of dissolved air flotation technology from the first generation to the newest (third) one (DAF in turbulent flow conditions). Water Science and Technology 43, 1-7.

Kibangou, V.A., Lilly, M., Mpofu, A.B., de Jonge, N., Oyekola, O.O., Welz, P.J., 2022. Sulfate-reducing and methanogenic microbial community responses during anaerobic digestion of tannery effluent. Bioresource Technology 347, 126308. https://doi.org/10.1016/ j.biortech.2021.126308

Kim, S.H., Han, S.K., Shin, H.S., 2004. Kinetics of LCFA inhibition on acetoclastic methanogenesis, propionate degradation and β-oxidation. Journal of Environmental Science and Health, Part A, 39(4),1025-1037. https://doi.org/10.1081/ESE-120028411

Kong, Z., Li, L., Xue, Y., Yang, M., Li, Y.Y., 2019. Challenges and prospects for the anaerobic treatment of chemical-industrial organic wastewater: a review. Journal of Cleaner Production 231, 913-927. https://doi.org/10.1016/j.jclepro.2019.05.233

Lackner, N., Wagner, A.O., Illmer, P., 2020. Effect of sulfate addition on carbon flow and microbial community composition during thermophilic digestion of cellulose. Applied

Microbiology and Biotechnology 104, 4605–4615. https://doi.org/10.1007/s00253-020-10546-7

Lawan, J., Wichai, S., Chuaypen, C., Nuiyen, A., Phenrat, T., 2022. Constructed sediment microbial fuel cell for treatment of fat, oil, grease (FOG) trap effluent: Role of anode and cathode chamber amendment, electrode selection, and scalability. Chemosphere 286, 131619. https://doi.org/10.1016/j.chemosphere.2021.131619

Lens, P.N.L., Visser, A., Janssen, A.J.H., Hulshoff Pol, L.W., Lettinga, G., 1998. Biotechnological Treatment of Sulfate-Rich Wastewaters. Critical Reviews in Environmental Science and Technology 28, 41–88. https://doi.org/10.1080/10643389891254160

Lenz, M., Janzen, N., Lens, P.N.L., 2008a. Selenium oxyanion inhibition of hydrogenotrophic and acetoclastic methanogenesis. Chemosphere 73(3), 383-388. https://doi.org/10.1016/j.chemosphere.2008.05.059

Lenz, M., van Hullebusch, E.D., Hommes, G., Corvini, P.F.X., Lens, P.N.L., 2008b. Selenate removal in methanogenic and sulfate-reducing upflow anaerobic sludge bed reactors. Water Research 42(8-9), 2184-2194. https://doi.org/10.1016/j.watres.2007.11.031

Li, C., Champagne, P., Anderson, B., 2011. Evaluating and modelling biogas production from municipal fat, oil and grease and synthetic kitchen waste in anaerobic co-digestions. Bioresource Technology 102(20), 9471-9480. https://doi.org/10.1016/j.biortech.2011.07.103

Li, Y., Jin, Y., Li, J., Li, H., Yu, Z., Nie, Y., 2017. Effects of thermal pretreatment on degradation kinetics of organics during kitchen waste anaerobic digestion. Energy 118, 377-386. https://doi.org/10.1016/j.energy.2016.12.041

Liang, Y.G., Bao, J., Ding, J., Tang, J.Y., Li, W., Zhang, L.G., Zhang, Y.H., 2020. Process performance and microbial communities in response to selenite addition during anaerobic digestion of pig manure. International Journal of Environmental Science and Technology 17, 3947-3954. https://doi.org/10.1007/s13762-020-02744-7

Linyi, C., Yujie, Q., Buqing, C., Chenglong, W., Shaohong, Z., Renglu, C., Shaohua, Y., Lan, Y., Zhiju, L., 2020. Enhancing degradation and biogas production during anaerobic digestion of food waste using alkali pretreatment. Environmental Research 188, 109743. https://doi.org/10.1016/j.envres.2020.109743

Logan, M., Tan, L.C., Lens, P.N.L., 2022a. Anaerobic co-digestion of dissolved air floatation slurry and selenium rich wastewater for simultaneous methane production and selenium bioremediation. International Biodeterioration and Biodegradation 172, 105425. https://doi.org/10.1016/j.ibiod.2022.105425

Logan, M., Tan, L.C., Nzeteu, C.O., Lens, P.N.L., 2022b. Enhanced anaerobic digestion of dairy wastewater in a granular activated carbon amended sequential batch reactor. GCB Bioenergy 14(7), 840-857. https://doi.org/10.1111/gcbb.12947

Logan, M., Tan, L.C., Nzeteu, C.O., Lens, P.N.L., 2022c. Effect of selenate on treatment of glycerol containing wastewater in UASB reactors. Renewable Energy (Under Review).

Logan, M., Ravishankar, H., Tan, L.C., Lawrence, J., Fitzgerald, D., Lens, P.N.L., 2021. Anaerobic digestion of dissolved air floatation slurries: Effect of substrate concentration and pH. Environmental Technology and Innovation 21, 101352. https://doi.org/10.1016/j.eti. 2020.101352

Long, J.H., Aziz, T.N., Francis III, L., Ducoste, J.J., 2012. Anaerobic co-digestion of fat, oil, and grease (FOG): A review of gas production and process limitations. Process Safety and Environmental Protection 90(3), 231-245. https://doi.org/10.1016/j.psep.2011.10.001

Lopes, S.I.C., Capela, M.I., Lens, P.N.L., 2010. Sulfate reduction during the acidification of sucrose at pH 5 under thermophilic (55°C) conditions. II: Effect of sulfide and COD/SO_4^{2-} ratio. Bioresource Technology 101, 4278–4284. https://doi.org/10.1016/j.biortech.2009. 12.132

Ma, H., Guo, Y., Qin, Y., Li, Y.-Y., 2018. Nutrient recovery technologies integrated with energy recovery by waste biomass anaerobic digestion. Bioresource Technology 269, 520-531. https://doi.org/10.1016/j.biortech.2018.08.114

Madigan, M.T., Martinko, J.M., Parker, J., 2006. Brock biology of microorganisms 11, 136. Upper Saddle River, NJ: Pearson Prentice Hall.

Magowo, W.E., Sheridan, C., Rumbold, K., 2020. Global Co-occurrence of acid mine drainage and organic rich industrial and domestic effluent: biological sulfate reduction as a co-treatment-option. Journal of Water Process Engineering 38, 101650. https://doi.org/10.1016/j.jwpe.2020. 101650

Mahmoud, A., Hamza, R.A., Elbeshbishy, E., 2022. Enhancement of denitrification efficiency using municipal and industrial waste fermentation liquids as external carbon sources. Science of the Total Environment 816, 151578. https://doi.org/10.1016/j.scitotenv.2021.151578

Meng, Y., Luan, F., Yuan, H., Chen, X. and Li, X., 2017. Enhancing anaerobic digestion performance of crude lipid in food waste by enzymatic pretreatment. Bioresource Technology 224, 48-55. https://doi.org/10.1016/j.biortech.2016.10.052

Mustafa, H.M., Hayder, G., 2021. Recent studies on applications of aquatic weed plants in phytoremediation of wastewater: A review article. Ain Shams Engineering Journal 12(1), 355-365. https://doi.org/10.1016/j.asej.2020.05.009

Muyzer, G., Stams, A.J.M., 2008. The ecology and biotechnology of sulphate-reducing bacteria. Nature Reviews – Microbiology 6, 441–454. https://doi.org/10.1038/nrmicro1892

Nancharaiah, Y.V., Lens, P.N.L., 2015a. Ecology and biotechnology of selenium-respiring bacteria. Microbiology and Molecular Biology Reviews 79, 61-80. https://doi.org/10.1128/MMBR.00037-14

Nancharaiah, Y.V., Lens, P.N.L., 2015b. Selenium biomineralization for biotechnological applications. Trends in Biotechnology 33(6), 323-330. https://doi.org/10.1016/j.tibtech.2015.03.004

Neves, L., Pereira, M.A., Mota, M., Alves, M.M., 2009. Detection and quantification of long chain fatty acids in liquid and solid samples and its relevance to understand anaerobic digestion of lipids. Bioresource Technology 100, 91-96. https://doi.org/10.1016/j.biortech.2008.06.018

Okoro, O.V., Sun, Z., Birch, J., 2017. Meat processing dissolved air flotation sludge as a potential biodiesel feedstock in New Zealand: A predictive analysis of the biodiesel product properties. Journal of Cleaner Production 168, 1436-1447. https://doi.org/10.1016/j.jclepro.2017.09.128

Oliveira, C.A., Fuess, L.T., Soares, L.A., Damianovic, M.H.R.Z., 2021. Increasing salinity concentrations determine the long-term participation of methanogenesis and sulfidogenesis in the biodigestion of sulfate-rich wastewater. Journal of Environmental Management 296, 113254. https://doi.org/10.1016/j.jenvman.2021.113254

Pitk, P., Kaparaju, P., Vilu, R., 2012. Methane potential of sterilized solid slaughterhouse wastes. Bioresource Technology 116, 42-46. https://doi.org/10.1016/j.biortech.2012.04.038

Rajapakse, N., Zargar, M., Sen, T., Khiadani, M., 2022. Effects of influent physicochemical characteristics on air dissolution, bubble size and rise velocity in dissolved air flotation: A review. Separation and Purification Technology 289, 120772. https://doi.org/10.1016/j.seppur.2022.120772

Robles, A., Vinardell, S., Serralta, J., Bernet, N., Lens, P.N.L., Steyer, J-P., Astals, S., 2020. Anaerobic treatment of sulfate-rich wastewaters: process modeling and control. In: Piet N. L. Lens (Eds.), Environmental Technologies to Treat Sulphur Pollution: Principles and Engineering, IWA Publishing, 277-317.

Rodrigues, I.C.B., Leão, V.A., 2020. Producing electrical energy in microbial fuel cells based on sulphate reduction: a review. Environmental Science and Pollution Research 27(29), 36075-36084. https://doi.org/10.1007/s11356-020-09728-7

Ross, C.C., Valentine, G.E., Smith, B.M., Pierce, J.P., 2003. Recent advances and applications of dissolved air flotation for industrial pretreatment. In Industrial Water/Wastewater Program North Carolina AWWA/WEA Conference, Greensboro–North Carolina.

Rosso, D., Larson, L.E., Stenstrom, M.K., 2008. Aeration of large-scale municipal wastewater treatment plants: state of the art. Water Science and Technology 57(7), 973-978. https://doi.org/10.2166/wst.2008.218

Roy, C.K., Hoshiko, Y., Toya, S., Maeda, T., 2022. Effect of different concentrations of sodium selenite on anaerobic digestion of waste activated sludge. Environmental Technology and Innovation 27, 102403. https://doi.org/10.1016/j.eti.2022.102403

Salama, E.S., Saha, S., Kurade, M.B., Dev, S., Chang, S.W., Jeon, B.H., 2019. Recent trends in anaerobic co-digestion: fat, oil, and grease (FOG) for enhanced biomethanation. Progress in Energy and Combustion Science 70, 22-42. https://doi.org/10.1016/j.pecs.2018.08.002

Sangkharak K., Khaithongkaeo P., Chuaikhunupakarn T., Choonut A., Prasertsan P., 2021. The production of polyhydroxyalkanoate from waste cooking oil and its application in biofuel production. Biomass Conversion and Biorefinery 11, 1651-1664. 10.1007/s13399-020-00657-6

Saravanan, A., Kumar, P.S., Jeevanantham, S., Karishma, S., Tajsabreen, B., Yaashikaa, P.R., Reshma, B., 2021. Effective water/wastewater treatment methodologies for toxic pollutants removal: Processes and applications towards sustainable development. Chemosphere 280, 130595. https://doi.org/10.1016/j.chemosphere.2021.130595

Sarti, A., Pozzi, E., Chinalia, F.A., Ono, A., Foresti, E., 2010. Microbial processes and bacterial populations associated to anaerobic treatment of sulfate-rich wastewater. Process biochemistry 45(2), 164-170. https://doi.org/10.1016/j.procbio.2009.09.002

Searchinger, T., Heimlich, R., 2015. Avoiding Bioenergy Competition for Food Crops and Land. Working Paper, Installment 9 of Creating a Sustainable Food Future. Washington, DC: World Resources Institute. Available online at http://www.worldresourcesreport.org.

Solé-Bundó, M., Passos, F., Romero-Güiza, M.S., Ferrer, I., Astals, S., 2019. Co-digestion strategies to enhance microalgae anaerobic digestion: A review. Renewable and Sustainable Energy Reviews 112, 471-482. https://doi.org/10.1016/j.rser.2019.05.036

Sun, Y., Zhao, J., Chen, L., Liu, Y., Zuo, J., 2018. Methanogenic community structure in simultaneous methanogenesis and denitrification granular sludge. Front. Environ. Sci. Eng., 12 (2018), p. 10. https://doi.org/10.1007/s11783-018-1067-2

Trabelsi A.B.H., Zaafouri K., Baghdadi W., Naoui S., Ouerghi A., 2020. Second generation biofuels production from waste cooking oil via pyrolysis process. Renewable Energy 126, 888-896. 10.1016/j.renene.2018.04.002

Veljković, V.B., Banković-Ilić, I.B., Stamenković, O.S., 2015. Purification of crude biodiesel obtained by heterogeneously-catalyzed transesterification. Renewable and Sustainable Energy Reviews 49, 500-516. https://doi.org/10.1016/j.rser.2015.04.097

Wang, L.K., Hung, Y.-T., Shammas, N.K., 2005. Physicochemical Treatment Processes. Handbook of Environmental Engineering, vol. 3, Humana Press, New Jersey, USA. https://doi.org/10.1385/159259820x

Westerholm, M., Schnürer, A., 2019, Microbial Responses to Different Operating Practices for Biogas Production Systems. In J. R. Banu (Ed.), Anaerobic Digestion, IntechOpen, London. 10.5772/intechopen.82815.

Wu, J., Niu, Q., Li, L., Hu, Y., Mribet, C., Hojo, T., Li, Y.Y., 2018. A gradual change between methanogenesis and sulfidogenesis during a long-term UASB treatment of sulfate-rich chemical wastewater. Science of the Total Environment 636, 168-176. https://doi.org/10.1016/j.scitotenv.2018.04.172

Yan, W., Vadivelu, V., Maspolim, Y., Zhou, Y., 2021. In-situ alkaline enhanced two-stage anaerobic digestion system for waste cooking oil and sewage sludge co-digestion. Waste Management 120, 221-229. https://doi.org/10.1016/j.wasman.2020.11.047

Yenigün, O., Demirel, B., 2013. Ammonia inhibition in anaerobic digestion: A review. Process Biochemistry 48, 901–911. https://doi.org/10.1016/j.procbio.2013.04.012

World Energy Outlook, 2020. Outlook for biogas and biomethane: Prospects for organic growth.

Zan F., Hao, T., 2020. Sulfate in anaerobic co-digester accelerates methane production from food waste and waste activated sludge. Bioresource Technology 298, 122536. https://doi.org/10.1016/j.biortech.2019.122536

Chapter 3 Anaerobic digestion of dissolved air floatation slurries: effect of substrate concentration and pH

A modified version of this chapter has been published as:

Logan, M., Ravishankar, H., Tan, L.C., Lawrence, J., Fitzgerald, D., Lens, P.N.L., 2021. Anaerobic digestion of dissolved air floatation slurries: effect of substrate concentration and pH. Environmental Technology and Innovation 21, 101352. https://doi.org/10.1016/j.eti.2020.101352

Abstract

Dissolved air floatation (DAF) slurries are a promising substrate for anaerobic digestion owing to their high COD concentrations, mainly consisting of lipids. Batch anaerobic digestion of DAF slurry was conducted to investigate the methane production through dilution of the slurry (with mineral salt medium, MSM) and by adjusting the initial pH (to 6.0, 5.5, 5.0 and 4.5). The performance of two different inocula, namely waste activated sludge (WAS) treating domestic wastewater and anaerobic granular sludge (AGS) treating dairy wastewater, was compared. The DAF slurry had a pH of 7.03 (± 0.07), conductivity of 6.69 (± 0.54) mS/cm, and a COD and ammonium concentration of 85.96 (± 8.32) g/L and 168.49 (± 1.79) mg N/L, respectively. DAF slurry without dilution produced a maximum methane yield of 58.60 (± 1.97) mL/g COD after 30 days of incubation. Dilution with MSM up to three folds, improved the methane yield by about 67 – 105% and 67 – 177% with WAS and AGS as the inoculum, respectively. Higher methane productivity was achieved at an inoculum to substrate ratio of at least 1.5 for WAS and 2.0 for AGS, respectively. AGS was more effective with a 20% increase in methane production from 3-fold diluted DAF slurry when compared with WAS. Adjustment of the initial pH of the DAF slurry to 6.0 resulted in a methane yield of 316.78 (± 28.82) mL/g COD, which was 23% higher than the control without pH adjustment. This study demonstrated that the methane yield from DAF slurries can be enhanced through substrate dilution and initial pH adjustment.

3.1 Introduction

Fat, oil and grease (FOG) wastewaters are generated during food processing and industrial activities such as palm oil mill effluent and automobile workshop discharge (Husain et al., 2014). FOG consists of lipids and are composed of long chain saturated and unsaturated fatty acids, triacylglycerols and lipid-soluble hydrocarbons (Voet et al., 2012). FOG waste poses a huge challenge in the operation of wastewater treatment plants owing to their potential for mechanical disruption, reduced oxygen transfer, and odour issues. General practice for the treatment of FOG-rich wastewaters is to separate FOG in a skimming tank at the primary treatment stage to avoid issues further downstream in the anaerobic treatment process. For this, physical and chemical technologies such as dissolved air floatation, centrifugation and ultrafiltration are used to separate FOG from the wastewater (Coca et al., 2010). Unsustainable management of lipid-rich FOG overlooks their substantial calorific value thus represents a huge economic loss. It is estimated that there is an economic loss of recoverable biochemical

products from wasted FOG of approximately €100 million, often due to lack of cost-effective utilisation routes (Wallace et al., 2017). Further, regulations might necessitate stabilisation of FOG prior to disposal. Moreover, the European Union has targeted by 2030 to meet 32% of its energy consumption from renewable energy sources such as waste biomass with the Renewable Energy Directive 2 or RED II (directive 2018/2001/EC).

Anaerobic treatment offers simultaneous waste stabilisation along with the production of renewable energy and other value-added products (Wickham et al., 2016). The anaerobic digestion (AD) process begins with the rapid hydrolysis of lipids to glycerol and long chain fatty acids (LCFAs), with subsequent slow LCFA degradation via β-oxidation to acetate and hydrogen, which are further converted to methane. Theoretically, degradation of lipids produces more methane (990 mL/g) when compared with proteins (634 mL/g) or carbohydrates (415 mL/g) (Alves et al., 2009). However, anaerobic treatment of FOG is a challenge due to the presence of LCFA, which are toxic to methanogens (Malayil and Chanakya, 2020), induce flotation (Usman et al., 2020) and are only slowly degraded resulting in longer retention times (Li et al., 2013). Therefore, the FOG content of industrial wastewaters is separated with specialised technologies such as dissolved air floatation (DAF) prior to the AD.

DAF is used in several industries including food processing, petrochemical, as well as pulp and paper manufacturing (Ross et al., 2003). Flocculants and coagulants are added to the wastewater and fine air bubbles, generated by injecting pressurized air, attach to the particulate matter, which rises to the surface forming a slurry. DAF treatment removes insoluble particulate matter from wastewaters and the DAF slurry is hence characterized by high suspended solids and biological oxygen demand (BOD) concentrations, which is partly composed of FOG. DAF slurries from dairy industry can contain chemical oxygen demand (COD) concentrations and a fat content as high as 200 g/L and 100 g/kg, respectively (Lutze and Engelhart, 2020; Silvestre et al., 2011).

When the COD concentration is too high and exceeds the tolerance of methanogens, it causes an imbalance between the hydrolysis/acidogenesis and methanogenesis steps, and thus methane production is hampered (Güngör-Demirci and Demirer, 2004). Feng et al. (2019) indicated reduction in cost during digester operation with optimal COD level. An appropriate substrate concentration favours enhanced metabolic activity, improved biogas production, lower accumulation of intermediate compounds, limits overloading and reduces the influence of toxic compounds (Long et al., 2011). The effects of the substrate concentration during

anaerobic digestion has been studied with only a few substrates such as food waste (Zhang et al., 2017), organic fraction of municipal solid waste (Fernández et al., 2008), piggery waste (Sánchez et al., 2001), cellulose, soymilk and sugar (Wang et al., 2015). Since, only few microorganisms are capable of anaerobic degradation of FOG waste, identifying a suitable inoculum is imperative for the AD of FOG waste (Rajput and Sheikh, 2019). Initial pH adjustment by acid addition might facilitate hydrolysis, and thus enhance the biogas yield. To the best of our knowledge, improving methane yield by dilution and acid addition in DAF slurry using different inocula has not yet been studied. Therefore, the objective of this study is to evaluate the effect of substrate concentration and initial pH using two inocula (i.e., anaerobic granular sludge and waste activated sludge), during mesophilic batch anaerobic digestion of a DAF slurry.

3.2 Materials and Methods

3.2.1 Source of biomass

The anaerobic granular sludge (AGS) was collected from a 200 m^3 up-flow anaerobic sludge bed (UASB) reactor treating dairy wastewater at 20 °C with a hydraulic retention time (HRT) of 9-12 h (Kilconnel, Ireland). The total solid (TS) and volatile solid (VS) content of AGS were 37.8 g/kg and 32.0 g/kg of wet weight, respectively. The waste activated sludge (WAS) was obtained from the secondary clarifier fed WAS chamber with varying HRT of 12-24 h under ambient temperature at the Tuam Municipal Wastewater Treatment Plant (Tuam, Ireland). The WAS had a TS and VS content of 45.0 g/kg and 31.2 g/kg, respectively. The inocula were stored at 4 °C until use.

3.2.2 Substrate and media

The DAF slurry was collected from an AD plant treating dairy wastewater (Kilconnel, Ireland). Table 3.1 shows the characteristics of the DAF slurry used as the substrate in this study. Mineral salt medium (MSM) used for substrate dilution was prepared following Pham et al. (2012): 1 g/L KH_2PO_4, 1 g/L Na_2HPO_4, 1 g/L $NaHCO_3$, 0.3 g/L $MgCl_2$, 0.3 g/L NH_4Cl. The pH of the MSM was 7.07 (± 0.04). The substrate and MSM were also stored at 4 °C until use. The DAF slurry without dilution or pH adjustment was used as the control.

Table 3.1 Characterisation of the DAF slurry substrate

Parameter	Unit	Concentration
Conductivity	mS/cm	6.69 ± 0.54
pH	-	7.03 ± 0.07
Total Solids	g/kg	30.96 ± 0.05
Volatile Solids	g/kg	23.51 ± 0.13
Ammonium	mg N/L	168.49 ± 1.79
Sulphate	mg/L	11.49 ± 0.48
COD_{tot}	mg/L	85957.60 ± 831.98

3.2.3 Biomethane potential tests

Biomethane potential (BMP) tests were performed in batch assays using either manual or an automatic BMP Nautilus system (Anaero Techology, UK). BMP tests for substrate concentration were done with manual monitoring of biogas using 120 mL serum bottles at 30 ºC and 150 rpm. The substrate was diluted with MSM at the following ratios: 1:0 (only DAF), 1:1 (30 ml MSM:30 ml DAF), 1:2 (20 ml DAF:40 ml MSM), and 1:3 (15 ml DAF: 45 ml MSM). This corresponded to an inoculum to substrate ratio (w/w, VS basis) of 0.6, 1.1, 1.7 and 2.2, respectively. The working volume of the manual BMP bottles was 62.5 mL, with 2.5 mL (1.3 g VS/L) of WAS or AGS as the inoculum. Digestate and biogas samples were extracted using valves from the top cap of the bottles. At the start of the experiment, nitrogen was purged to ensure strict anaerobic conditions. The experiment was conducted for a 30 day period, while a 2 ml sample was extracted every second or third day for volatile fatty acid (VFA) analysis. Prior to taking gas and liquid samples from each bottle, the pressure was recorded using a pressure transducer (Keller Druckmesstechnik Mano Leo1 81000.2, Range 0 – 4 bar abs). The biogas samples were collected and the bottles were then restored to atmospheric pressure by releasing excess pressure.

The effect of the initial pH on the BMP was studied using an automated BMP Nautilus system. The equipment had robust stainless-steel mixers and wide mouth HDPE bottles for sample handling. The total volume was 1 litre, with a working volume of 750 mL. The equipment allowed access to the HDPE bottles via an air-tight port during the tests for pH monitoring, nutrient supplementation, or sampling. The reactors were flushed with nitrogen at

the start of the test. Each HDPE bottle was equipped with paddles for gentle mixing at approximately 75 rpm and an Arduino gas flow meter. The temperature of the water bath was 37 °C. AGS inoculum was provided at 2 g VS/L in automated BMP tests, following the results from the manual BMP assays. The inoculum to substrate ratio (w/w, VS basis) was 0.9. Undiluted DAF slurry was used as the substrate in the study of the effect of the initial pH. Acid solution (1 M HCl) was used to adjust the initial pH to 4.5, 5.0, 5.5 and 6.0 only once at the start of the experiment. The variation in pH during the batch experiment was monitored at regular intervals.

3.2.4 Analytical techniques

The conductivity was measured using a conductivity probe (Fisherbrand Accumet Basic AB30 Conductivity Meter), whereas the pH was measured by a Cole-Parmer pH meter (pH/ORP 300) which was connected to a Hamilton SlimTrode electrode. Total solids (TS, in g/kg) and Volatile Solids (VS, in g/kg) were determined by oven drying at 105 °C for 24 h and furnace drying at 550 °C for 2 h, respectively (APHA, 2017). Total (COD_{tot}, in mg/L) and soluble (COD_{sol}, in mg/L) COD were measured using the closed reflux, colorimetric method (APHA, 2017). Ammonium (in mg N/L) and sulphate (in mg/L) were determined using Gallery Plus Automated Chemistry Analyser (Thermo Scientific).

VFA concentrations were measured using a gas chromatograph (GC) equipped with a flame ionization detector and a capillary column BP21 (30 m x 0.25 m x 0.25 µm) (Agilent Technologies 7890B). The detector temperature was set at 250 °C. The methane concentration in the biogas samples was determined using a gas chromatograph (GC) equipped with a thermal conductivity detector (Agilent Technologies 7890B) and a Porapak Q column (2.74 m x 2 mm). The oven temperature was kept constant at 60 °C. The temperature of the injection port and the detector were maintained constant at 250 °C. Helium was used as the carrier gas for both methane and VFA analyses. The FOG concentration could not be determined due to analytical limitations.

3.2.5 Theoretical BMP based on COD

The theoretical BMP can be calculated using Eq. (3.1) as described by Nielfa et al. (2015):

$$BMP_{thCOD} = \frac{n_{CH_4} RT}{p\, VS_{added}} \qquad \text{Eq. (3.1)}$$

where BMP_{thCOD} is the theoretical methane production, R is the gas constant (R = 0.082 atm L/mol K), T is the temperature (K), p is the atmospheric pressure (1 atm), VS added (g) are the volatile solids of the substrate and n_{CH_4} is the amount of methane (mol) determined from Eq. (3.2):

$$n_{CH_4} = \frac{COD}{64} \quad \text{Eq. (3.2)}$$

where COD is the chemical oxygen demand (g)

3.2.6 Statistical analysis

BMP tests were conducted in either duplicates or triplicates. All results are reported as average values. Analysis of variance (ANOVA) was performed on the methane production data by using SPSS 16 software (IBM Corp., Ireland) at 5% level of significance.

3.3 Results

3.3.1 Effect of substrate concentration on anaerobic digestion of DAF slurry

Figure 3.1 presents the cumulative methane yield obtained from the DAF slurry at different substrate concentrations using the two different inocula. The control without dilution gave the lowest cumulative methane yield of 58.60 (± 1.97) mL/g COD with WAS after 30 days of incubation. The substrate concentration of 1:1 (DAF:MSM) achieved a higher cumulative methane yield of 98.28 (± 0.23) mL/g COD with WAS. A slightly higher cumulative methane yield of 119.92 (± 2.90) mL/g COD and 119.82 (± 11.08) mL/g COD was achieved at 2-fold and 3-fold dilutions (corresponding to an inoculum to substrate ratio of, respectively, 1.66 and 2.21), respectively, which were not significantly different ($p > 0.05$). The methane yields from the other test conditions of 1:0 (only DAF) and 1:1 (DAF:MSM) were significantly different ($p < 0.05$) from the other WAS incubations.

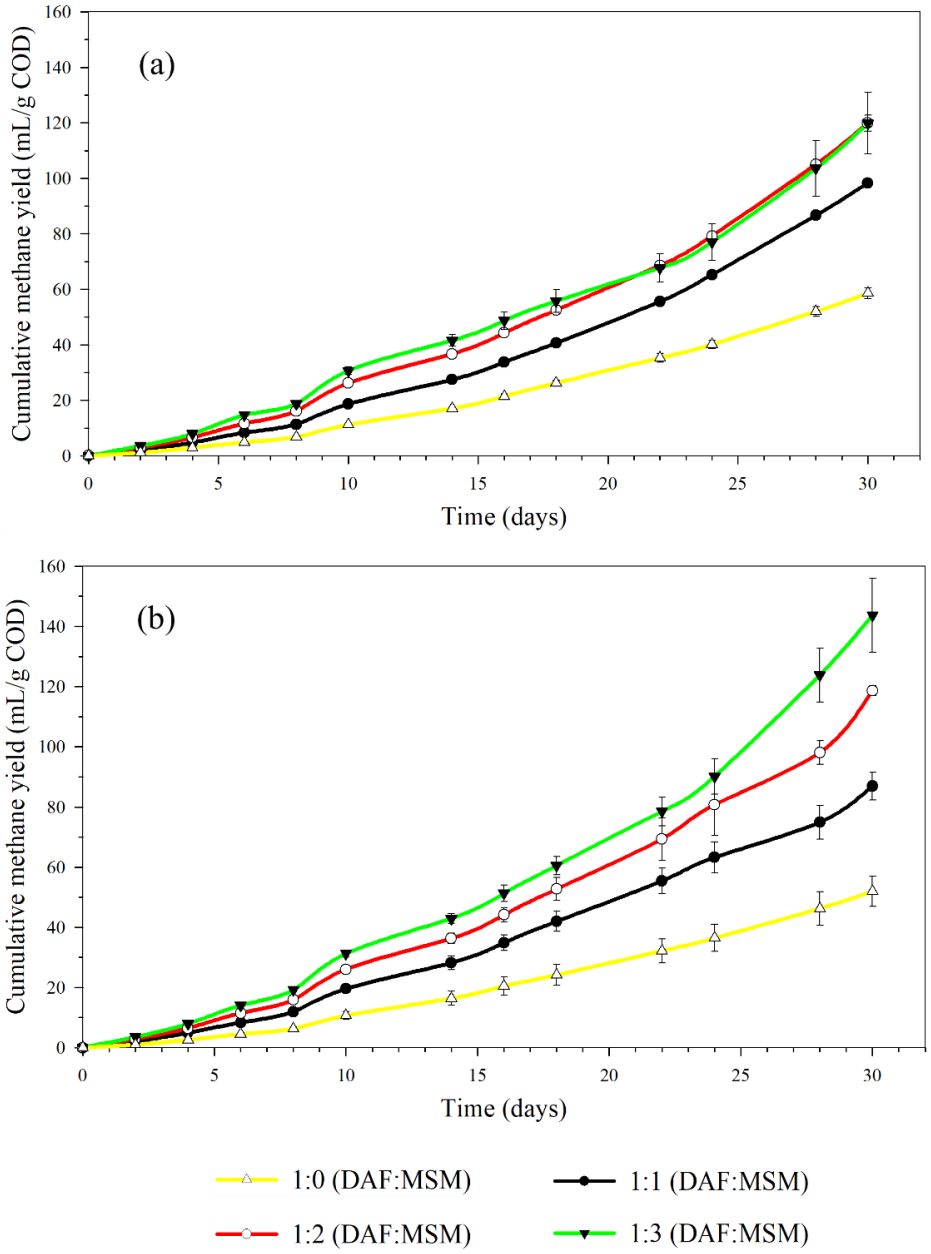

Figure 3.1 Methane production from dissolved air floatation slurry at different substrate concentrations with (a) waste activated sludge and (b) anaerobic granular sludge as inoculum.

At the end of the incubation, AGS showed the highest cumulative methane yield of 143.69 (± 12.28) mL/g COD when the DAF slurry was diluted by three times (inoculum to substrate ratio of 2.27) (Figure 3.1). The lowest cumulative methane yield (51.94 (± 5.06) mL/g COD) was observed for the control with AGS. Unlike with WAS, significant differences were observed in the methane yields at the different substrate dilutions when AGS was used as the inoculum. About 30.9% of the initial COD was converted to methane at 2-fold dilution using WAS as the inoculum, when compared with 15.1% for the control sample at the end of the incubation. About 37.0% of the initial COD was converted to methane at the 3-fold dilution, when compared with only 13.4% for the control with AGS as the inoculum.

Figure 3.2 shows the fluctuation of the net soluble COD concentrations during the experiment, corresponding to the sum of its production and consumption. Acetate and propionate were the main VFA produced with about 70% of the VFA composed of acetate. The peak acetic acid concentrations amounted to 2200, 1415, 1125 and 1085 mg COD/L (day 6) and the peak propionic acid concentrations were 935 mg COD/L (day 30), 570 mg COD/L (day 18), 450 mg COD/L (day 18) and 360 mg COD/L (day 30) at 1:0 (only DAF), 1:1 (DAF:MSM), 1:2 (DAF:MSM) and 1:3 (DAF:MSM), respectively, with AGS as the inoculum (Figure 3.2). With WAS as the inoculum, substrate dilution resulted in peak acetic acid concentrations of 2900 mg COD/L (day 6), 1600 mg COD/L (day 6), 930 mg COD/L (day 6) and 720 mg COD/L (day 10) and peak propionic acid concentrations of 800 mg COD/L (day 18), 490 mg COD/L (day 18), 375 mg COD/L (day 18) and 330 mg COD/L (day 18), respectively, for the 1:0, 1:1, 1:2 and 1:3 incubations. Noteworthy, the COD_{sol} and total VFA balance implies that up to about 70% of COD_{sol} was unaccounted for incubation period from days 20 – 30 (Figure 3.2). This indicates that other organic compounds such as glycerol and long chain carboxylic acids (Johannesson et al., 2020; Creamer et al., 2010), which were not analysed in this study, might have been formed during the DAF slurry incubation. Therefore, the monitoring of different intermediates, such as glycerol and (long chain) fatty acids during anaerobic treatment of DAF slurry should be considered in future studies.

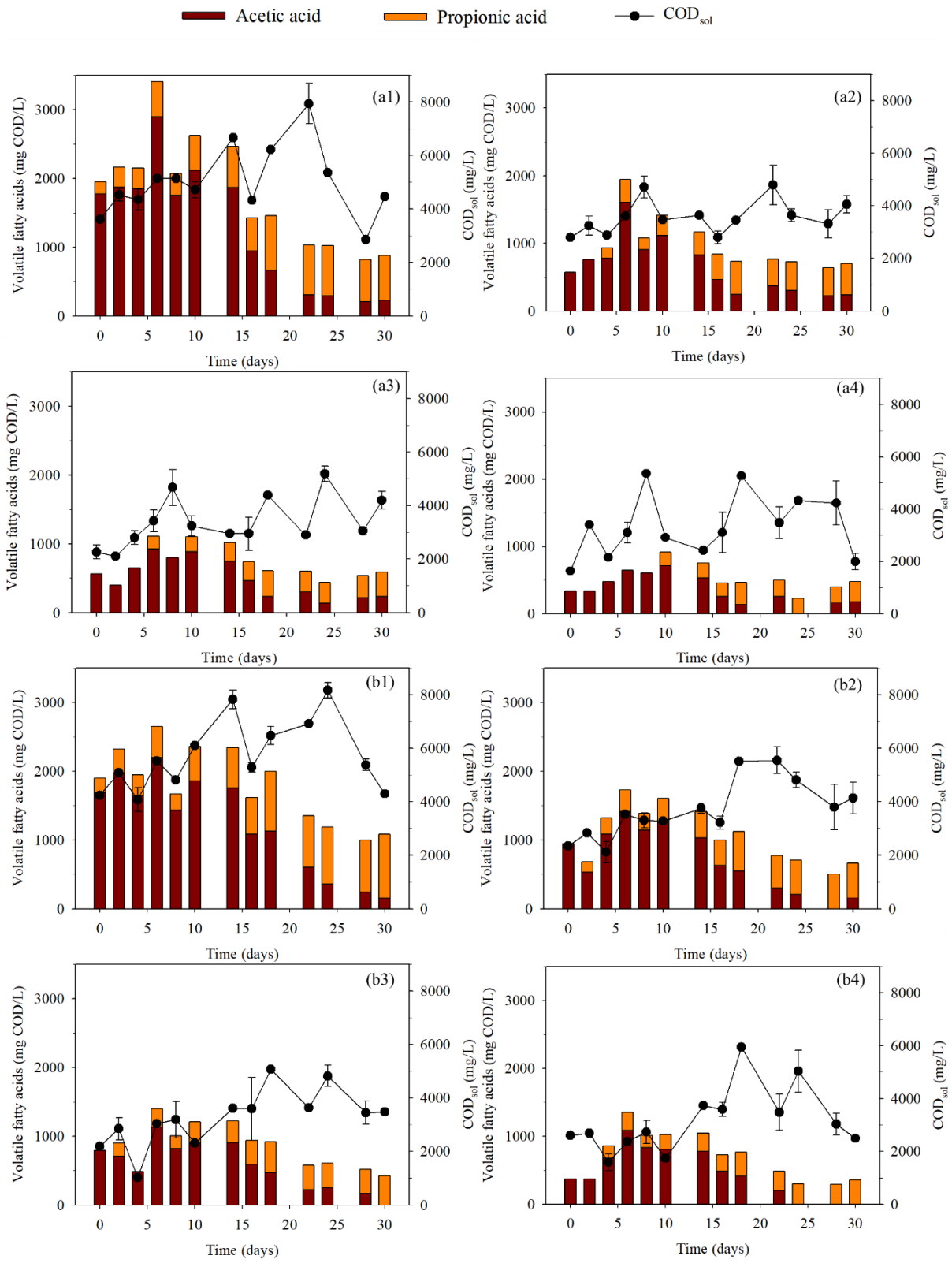

Figure 3.2 COD_{sol}, acetic and propionic acid profile for (a) waste activated sludge and (b) anaerobic granular sludge at different DAF to MSM ratio: (1) 1:0; (2) 1:1; (3) 1:2; and (4) 1:3.

3.3.2 Effect of initial pH on methane production from DAF slurry

AGS was selected as the inoculum for the study on the effect of initial pH, since it produced about 20% increased methane yield (at the 3-fold dilution) when compared with WAS. Figure 3.3 shows the effect of the initial pH on the methane production from the undiluted DAF slurry. Adjustment of the initial pH of the DAF slurry to 6.0 resulted in an enhancement of the methane yield by 23%, with the highest cumulative methane yield of 316.78 (± 28.82) mL/g COD. Following this, the initial pH of 5.5 and 7.0 (control) resulted in cumulative methane yields of 294.12 (± 25.69) mL/g COD and 258.22 (± 38.97) mL/g COD, respectively, at the end of the 35 days incubation. The methane yield attained saturation by the end of 35 days, possibly due to a different batch of AGS inoculum and the automated method used where the gas produced was released continuously without any pressure build-up (unlike the manual BMP test where the gas was released only at regular intervals). Conversely, there was complete inhibition of the methane production when the initial pH was adjusted to 5.0 and 4.5. Notably, there was a significant difference in methane yield ($p < 0.05$) at the different initial pH values (Figure 3.3).

For the incubation with initial pH of 5.5 and 6.0, the pH of the medium increased above 6.8 after 5 days (Figure 3.3), suggesting that the initial VFAs present were immediately consumed. After commencement of the exponential phase, the intermediates from the DAF slurry degradation were quickly utilised, and the methane production hit a plateau by the end of day 24 (Figure 3.3). On the contrary, an initial pH value below 5.5 resulted in inhibition of methanogenesis. VFA profiling revealed that acetic, propionic and butyric acid were the main VFAs produced in these incubations (Figure 3.4). The highest acetic acid concentration of 1785 mg COD/L (day 12) and 1630 mg COD/L (day 12), propionic acid concentration of 1400 mg COD/L (day 35) and 235 mg COD/L (day 12) and butyric acid concentration of 570 mg COD/L (day 12) and 440 mg COD/L (day 24) was observed at initial pH 7.0 and 6.0, respectively. Figure 3.4 suggests that hydrolysis, acidogenesis, acetogenesis and methanogenesis occurred at the initial DAF slurry pH of 5.5, 6.0 and 7.0. At an initial pH of 4.5 and 5.0, hydrolysis still occurred, however, the subsequent acidogenesis, acetogenesis and methanogenesis steps were inhibited.

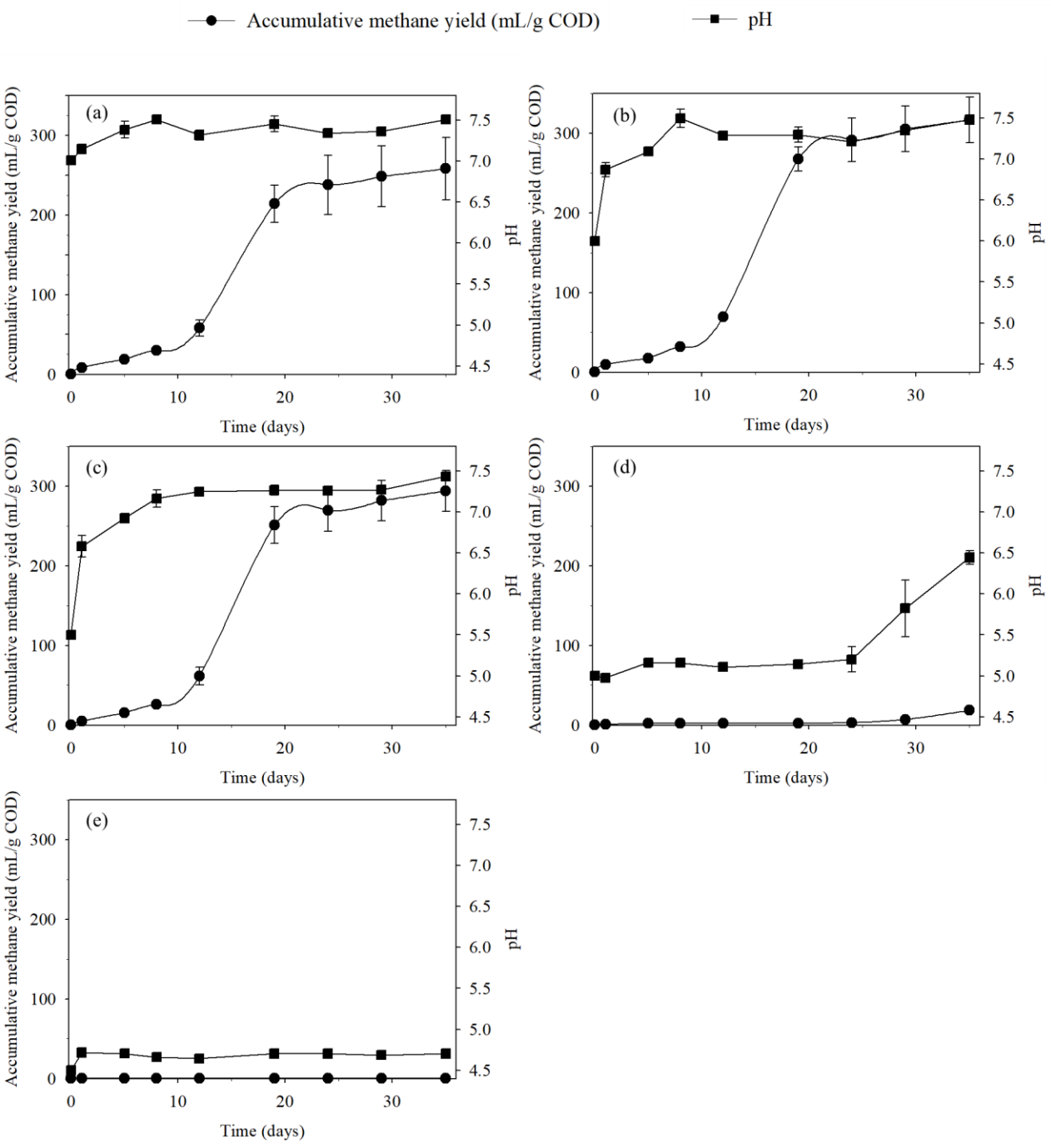

Figure 3.3 Methane production and pH variation during automated BMP test with initial pH of (a) 7.0; (b) 6.0; (c) 5.5; (d) 5.0; and (e) 4.5.

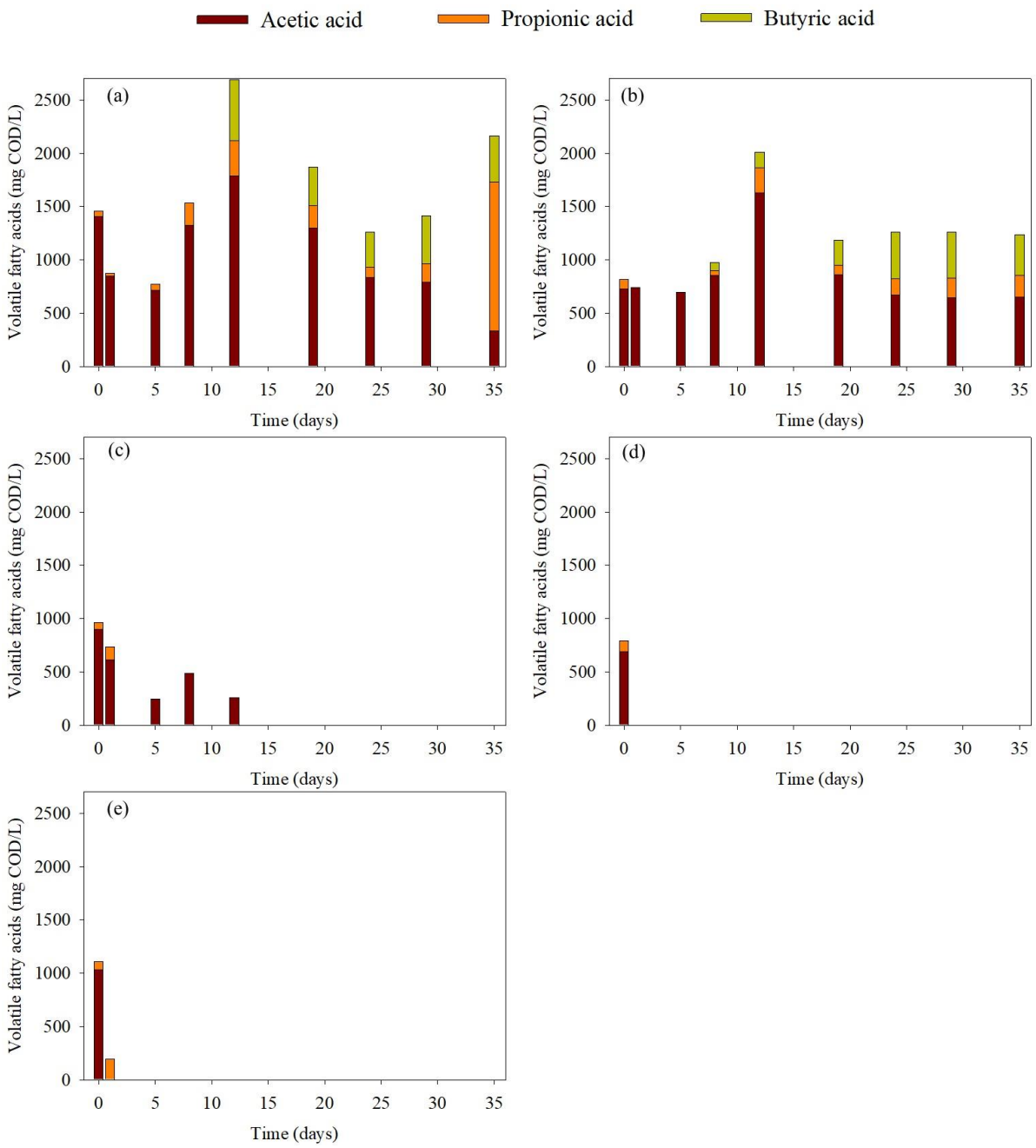

Figure 3.4 Volatile fatty acid profile at initial pH of (a) 7.0; (b) 6.0; (c) 5.5; (d) 5.0 and (e) 4.5

3.4 Discussion

3.4.1 Role of substrate concentration on methanogenesis of DAF slurry

This study shows that substrate dilution (using MSM) from 85 g/l COD_{tot} to 22.5 g/l COD_{tot} improved the methane production from DAF, an uncommon feedstock for AD with a high COD

concentration. AD of a DAF slurry can be destabilised by the high LCFA concentrations released. LCFA might have a detrimental effect by inhibiting methanogenic bacteria as a result of damage to their cellular membrane (Worwag et al., 2011) or inducing reduced mass transfer due to the formation of a layer of LCFAs on the bacteria or granule, thus hindering the substrate access to the cells and biogas release (Long et al., 2011; Martinez et al., 2016). Furthermore, flotation due to LCFA entrapment can make the substrate inaccessible to the anaerobic biomass and disrupt the AD (Martinez et al., 2016).

LCFA inhibition of methanogenesis has been investigated by Alves et al. (2001) and Salminen et al. (2000). Cirne et al. (2007) observed alleviation of the LCFA toxicity when the lipid concentration was decreased from 47% to 18% (w/w, COD basis). Sánchez et al. (2001) reported that the increase in the initial pig slurry concentration caused reduction of the COD removal rate and increase in the total volatile fatty acids to total alkalinity (TVFA/TA) ratio. An increase in TVFA/TA ratio is an indicator for process instability in AD processes (Chuenchart et al., 2020). This suggests that the DAF slurry after dilution using mineral medium might result in process stability with lower TVFA/TA ratio. Wang et al. (2015) also showed a positive effect on the degradation rates of cellulose, soymilk and sugar after dilution by a nutrient solution.

Altamira et al. (2008) reported that the methane potential of different industrial wastewaters could be improved with an increase of the inoculum-to-substrate ratio. A lower inoculum-to-substrate ratio could lead to overloading caused by the accumulation of carboxylic acids, resulting in process inhibition. Therefore, lower accumulation of carboxylic acids could be a possible reason for higher methane production at lower substrate concentration.

When the inoculum to substrate ratio was decreased from 2.27 to 0.57, the methane productivity from the DAF slurry also decreased. This study recommends an inoculum to substrate ratio of at least 1.5 for WAS and 2.0 for AGS, respectively. Similarly, Raposo et al. (2009) showed inhibition by the sunflower oil cake concentration when the inoculum (granular sludge) to substrate ratio was decreased from 3.0 to 0.5. Moreover, TVFA/TA ratios were lower than the failure limit values (0.3-0.4), indicating a high stability of the AD process in the inoculum to substrate ratio ranging from 0.8 to 3.0 (Raposo et al., 2009). Sri Bala Kameswari et al. (2012) also reported a significant drop in specific methane production at an inoculum (waste activated sludge) to substrate (tannery solid wastes) ratio below 1.0.

3.4.2 Effect of inoculum

The syntrophic association between acetogenic and methanogenic archaea in AGS could be a possible reason for the higher methane yield from DAF slurry, when compared with WAS. There is, however, ambiguity on that microorganisms can degrade both saturated and unsaturated fatty acids in methanogenic environments (Sousa et al., 2007). Improper selection of the inoculum is therefore a main bottleneck and can lead to process failures during FOG waste digestion (Long et al., 2011). Only a few bacterial species have been identified so far that are capable of anaerobic degradation of fatty acids with more than 4 and up to 18 carbon atoms (Sousa et al., 2007). Bioaugmentation with these species could be used to increase the methane production rate and reduce the lag phase (Worwag et al., 2011; Creamer et al., 2010). Alternatively, direct interspecies electron transfer between fermenting bacteria and methanogens could be promoted by electrochemically active substances stored in the EPS (Xiao et al., 2017) or conductive materials such as granular activated carbon (Tan et al., 2020).

This study shows that AGS sourced from a UASB reactor treating dairy wastewater is an efficient inoculum for treatment of DAF slurry. de Vrieze et al. (2015) recommend the application of granular sludge as an inoculum for industrial substrates because of its higher methanogenic abundance and activity, and protection from bulk solutions, compared with suspended sludges. Posmanik et al. (2020) found that granular sludge inocula yielded an overall higher biomethane potential and had faster kinetics than suspended biomass, when daily manure and waste activated sludge were used as the substrates.

Comparison of granular to suspended sludges for methane production have contrasting conclusions, and their suitability appears to be case-specific (Singh et al., 2019). The specific methanogenic activity and biogas production rate from municipal and industrial wastewaters are positively proportional to the granular size (Bhunia and Ghangrekar, 2007; Wu et al., 2016). Notably, large granules with layered internal structures are composed of acetoclastic methanogens, whereas small granules have a uniform internal structure with mainly hydrogenotrophic methanogens (Owusu-Agyeman et al., 2019). Therefore, both acetoclastic and hydrogenotrophic methanogenesis could be present in the AGS with heterogeneous size distribution. With better settling characteristics that prevent biomass washout than suspended sludge (Tassew et al., 2019), AGS is thus a better inoculum for practical applications treating DAF slurry.

3.4.3 Use of pH adjustment for improved methanogenesis of DAF slurry

This study shows that adjustment of the initial pH of a DAF slurry results in enhanced methane production (Figure 3.3). This could be attributed to improved hydrolysis at pH 6.0 that led to breakdown of the DAF slurry to substrates for acidogenic and methanogenic bacteria. The test conditions with initial pH of 4.5 and 5.0 might be dominated by hydrolysis of the fat content in the DAF slurry to long chain carboxylic acids, whose energy value could still be exploited by further downstream digestate processing. An initial lag phase duration of 8-10 days was reported during AD of lipid-rich waste by Cirne et al. (2006). Effect of the adjustment of the initial pH, along with their associated cost, should be studied under a continuous mode of operation to evaluate commercial implementation.

Devlin et al. (2011) reported that acid pre-treatment (pH 1 to 6) leads to solubilisation of EPS, carbohydrates and proteins resulting in enhanced biogas production. The solubilisation of the DAF slurry upon pH adjustment also improves the mass transfer during DAF slurry degradation. Maspolim et al. (2015) stated that the pH adjustment to 5.0 and 11.0 led to an increased solubilisation of the organics, which in turn converted a fraction of the recalcitrant material to a more degradable form. Therefore, adjustment of the initial pH with acids contributes to an increase in the hydrolysis rate, a rate-limiting step for DAF slurry digestion. The acid pre-treatment of DAF slurry thus releases LCFA for β-degradation and glycerol for acidogenesis, which eventually results in a higher methane production rate with a relatively shorter lag phase. Similarly, Wilson et al. (2009) reported subsequent LCFA inhibition resulting from thermal pre-treatment, which in turn extended the lag period. Wang et al. (2015) also observed that dilution had no strong influence on the lag time when using cellulose, soymilk and sugar as the substrates.

A pH below 5.0 led to a poor acidification efficiency of the lipid-rich DAF slurry. This indicates the detrimental impact of the abiotic effects by acid dosage and resulting acidic condition to the biotic contribution to hydrolysis. Higher solubilisation resulting from the acid treatment does not result into higher VFA production (Zhang et al., 2009). Maspolim et al. (2015) reported that total enzymatic activities reduced by more than 50% at pH 5.0 and below. Further, solubilisation by adjustment to low pH resulted in higher molecular weight organics with lower biodegradability and thus unfavourable for subsequent biological processes. Strong acid addition might also result in the production of inhibitory by-products and loss of fermentable sugar due to the increased

degradation of complex substrates (Ariunbaatar et al., 2014). Additionally, the stressed condition of low pH might also lead to the reduced acidogenic activities (Kevbrin et al., 2005). The inhibition of methanogenesis from DAF slurry is thus a result of impaired acidogenesis in the acidic environment (pH < 5.0).

3.4.4 Practical implications for AD of FOG waste

BMP tests are as a screening tool to optimize biogas yield from the substrate being investigated (Angelidaki et al., 2009). However, their limitation is differences in the BMP results among different studies due to substrate properties, BMP equipment, operational conditions, inocula and nutrient media used as well as analyses and reporting (Jensen et al., 2011). This study serves as a screening test for the identification of suitable inoculum, substrate dilution, inoculum to substrate ratio and initial pH for DAF slurry as the substrate. Before designing and constructing a full-scale operational digester, the results from the BMP assay with the DAF slurry should be further evaluated in continuously loaded bench-scale digesters.

Following the substrate concentration and pH adjustment, various other operational parameters could also be studied to enhance the AD of FOG waste. Thermophilic degradation of FOG could possibly improve process performance. Martinez et al. (2016) reported the formation of fatty aggregates in thermophilic regimes to protect biomass to the toxic effect of high LCFA concentrations thereby avoiding process failure. There have been few studies on AD of FOG waste in the thermophilic regime to establish a clear comparison with mesophilic digestion. Moreover, FOG accumulation onto the biomass induces sludge floatation and biomass washout. The sludge loss in the bed increased the FOG loading to the biomass and induced failure (Jeganathan et al., 2006). At higher DAF loads, ammonia and LCFA accumulation could become restrictive to biogas production (Creamer et al., 2010). Therefore, there is a huge scope to further evaluate the operational conditions such as organic loading rate or hydraulic retention time during AD of DAF slurries.

The BMP of a DAF slurry cannot only be improved by optimising the operational conditions, but also through anaerobic co-digestion or pre-treatment. A higher nitrogen content in the lipid-rich FOG waste can be exploited for optimising the carbon to nitrogen ratio for anaerobic co-digestion. An enhanced methane yield and stability can thus be achieved through synergistic

microbial activity, buffer and nutrient availability during anaerobic co-digestion (Chuenchart et al., 2020). Recent studies have explored the potential of anaerobic co-digestion for the treatment of different FOG wastes (Kurade et al., 2019, Sunada et al., 2018, Amha et al., 2017; Wickham et al., 2016). For instance, Marchetti et al., (2019) achieved a methane yield of 811 mL/g, with a 15.5 % increase in overall methane production and a lag phase shortened by 58.3 % in a laboratory batch mesophilic reactor with waste cooking oil and pig slurry as the substrates. Also other pre-treatment options including mechanical, thermal, chemical and biological pre-treatments, could be exploited individually or in combination for improved lipids biodegradation (Salama et al., 2019; Habashi et al., 2016). Low cost, less energy and chemicals consuming pre-treatment technologies should be identified based on the desired end-use application.

The AD of DAF slurries paves the way to a 'FOG waste bio-refinery', enabling the production of alternative products, e.g. bioplastic, biodiesel and biooil production. Polyhydroxyalkanoates (PHAs) or bioplastics can be produced by bacterial fermentation using FOG waste as a feedstock. Utilizing waste cooking oil as an inexpensive carbon feedstock for PHA production at lab scale was demonstrated by Sangkharak et al. (2020). Biodiesel can be produced from FOG waste through a catalyzed-transesterification process (Abomohra et al, 2020). Biooil was produced and characterized by pyrolysis of waste cooking oil in a fixed bed reactor by Trabelsi et al. (2020). These alternate technologies do not replace, but complement AD towards a sustainable and circular economy (Abomohra et al., 2020).

3.5 Conclusion

The effect of substrate concentration and initial pH on AD of a DAF slurry was evaluated. The methane production doubled after 2-fold dilution with WAS and tripled after 3-fold dilution with AGS. This could be attributed to lower LCFA toxicity, higher inoculum to substrate ratio, lower VFA accumulation, and better nutrient availability from the mineral medium at lower substrate concentrations. The methane yield increased by 23% when the initial pH of the DAF slurry was adjusted to 6.0, possibly due to improved hydrolysis. However, when the initial pH was set to 5.0 and 4.5, there was complete inhibition of methane production. Anaerobic granular sludge is a more suitable inoculum for methane production from lipid-rich DAF slurry when compared with waste activated sludge.

3.6 References

Abomohra, A.E., Elsayed, M., Esakkimuthu, S., El-Sheekh, M., Hanelt, D., 2020. Potential of fat, oil and grease (FOG) for biodiesel production: a critical review on the recent progress and future perspectives. Progress in Energy and Combustion Science 81. https://doi.org/10.1016/j.pecs.2020.100868

Altamira, L.M., Baun, A., Angelidaki, I., Schmidt, J.E., 2008. Influence of wastewater characteristics on methane potential in food-processing industry wastewaters. Water Research 42(8-9), 2195-203. https://doi.org/10.1016/j.watres.2007.11.033

Alves, M.M., Pereira, M.A., Sousa, D.Z., Cavaleiro, A.J., Picavet, M., Smidt, H., Stams, A.J.M., 2009. Waste Lipids to energy: how to optimize methane production from long-chain fatty acids (LCFA). Microbial Biotechnology 5, 538-550. https://doi.org/10.1111/j.1751-7915.2009.00100.x

Alves, M.M., Vieira, J.A.M., Pereira, R.M.A., Pereira, M.A., Novais, J.M., Mota, M., 2001. Effects of lipids and oleic acid on biomass development in anaerobic fixed reactors. Part II: oleic acid toxicity and biodegradability. Water Research 35, 264-270. https://doi.org/10.1016/S0043-1354(00)00242-6

Amha, Y.M., Sinha, P., Lagman, J., Gregori, M., Smith, A.L., 2017. Elucidating microbial community adaptation to anaerobic co-digestion of fats, oils, and grease and food waste. Water Research 123, 277-289. https://doi.org/10.1016/j.watres.2017.06.065

Angelidaki, I., Alves, M., Bolzonella, D., Borzacconi, L., Campos, J.L., Guwy, A.J., Kalyuzhnyi, S., Jenicek, P., van Lier, J.B., 2009. Defining the biomethane potential (BMP) of solid organic wastes and energy crops: a proposed protocol for batch assays. Water Science and Technology: Journal of the International Association on Water Pollution Research 59, 927-934. https://doi.org/10.2166/wst.2009.040.

APHA, Standard methods for the examination of water and wastewater (23rd edition). American Public Health Association, Washington, D.C., USA (2017). ISBN: 9780875532875.

Ariunbaatar, J., Panico, A., Esposito, G., Pirozzi, F., Lens, P.N.L., 2014. Pretreatment methods to enhance anaerobic digestion of organic solid waste. Applied Energy 123, 143-156. https://doi.org/10.1016/j.apenergy.2014.02.035

Atlaş, L., 2009. Inhibitory effect of heavy metals on methane-producing anaerobic granular sludge. Journal of Hazardous Materials 162 (2-3), 1551-1556. https://doi.org/10.1016/j.jhazmat.2008.06.048

Bhunia, P., Ghangrekar, M.M., 2007. Required minimum granule size in UASB reactor and characteristics variation with size. Bioresource Technology 98, 994-999. https://doi.org/10.1016/j.biortech.2006.04.019

Chuenchart, W., Logan, M., Leelayouthayotin, C., Visvanathan, C., 2020. Enhancement of food waste thermophilic anaerobic digestion through synergistic effect with chicken manure. Biomass and Bioenergy 136. https://doi.org/10.1016/j.biombioe.2020.105541

Cirne, D.G., Paloumet, X., Bjornsson, L., Alves, M.M., Mattiasson, B., 2006. Anaerobic digestion of lipid –rich waste – Effects of lipid concentration. Renewable Energy. 32(6), 965-975. https://doi.org/10.1016/j.renene.2006.04.003

Coca, J., Gutierrez, G., Benito, J.M., 2010. Treatment of oily wastewater. In: Coca-Prados, J., Gutierrez-Cervello, G. (eds) Water Purification and Management. NATO Science for Peace and Security Series C: Environmental Security. Springer, Dordrecht. https://doi.org/10.1007/978-90-481-9775-0_1

Creamer, K.S., Chen, Y., Williams, C.M., Cheng, J.J., 2010. Stable thermophilic anaerobic digestion of dissolved air flotation (DAF) sludge by co-digestion with swine manure, Bioresource Technology 10 (9), 3020-3024. https://doi.org/10.1016/j.biortech.2009.12.029

Devlin, D.C., Esteves, S.R.R., Dinsdale, R.M., Guwy, A.J., 2011. The effect of acid pretreatment on the anaerobic digestion and dewatering of waste activated sludge. Bioresource Technology 102(5), 4076-4082. http://dx.doi.org/10.1016/j.biortech.2010.12.043

de Vrieze, J., Raport, L., Willems, B., Verbrugge, S., Volcke, E., Meers, E., Angenent, L.T., Boon, N., 2015. Inoculum selection influences the biochemical methane potential of agro-industrial substrates. Microbial Biotechnology 8(5), 776-86. https://doi.org/10.1111/1751-7915.12268

Feng, S., Hong, X., Wang, T., Huang, X., Tong, Y., Yang, H., 2019. Reutilization of high COD leachate via recirculation strategy for methane production in anaerobic digestion of municipal solid

waste: Performance and dynamic of methanogen community. Bioresource Technology 288, 121509. https://doi.org/10.1016/j.biortech.2019.121509

Fernández, J., Pérez, M., Romero, L.I., 2008. Effect of substrate concentration on dry mesophilic anaerobic digestion of organic fraction of municipal solid waste (OFMSW). Bioresource Technology 99(14), 6075-6080. https://doi.org/10.1016/j.biortech.2007.12.048

Güngör-Demirci, G., Demirer, G.N., 2004. Effect of initial COD concentration, nutrient addition, temperature and microbial acclimation on anaerobic treatability of broiler and cattle manure. Bioresource Technology 93, 109-117. https://doi.org/10.1016/j.biortech.2003.10.019

Habashi, N., Mehrdadi, N., Mennerich, A., Alighardashi, A., Torabian, A., 2016. Hydrodynamic cavitation as a novel approach for pretreatment of oily wastewater for anaerobic co-digestion with waste activated sludge. Ultrasonics Sonochemistry 31, 362-370. http://dx.doi.org/10.1016/j.ultsonch.2016.01.022

Husain, I.A.F., Alkhatib, M.F., Jammi, M.S., Mirghani, M.E.S., Zainudin, Z.B., Hoda, A., 2014. Problems, Control, and Treatment of Fat, Oil, and Grease (FOG): A Review. Journal of Oleo Science 63 (8), 747-752. https://doi.org/10.5650/jos.ess13182

Jeganathan, J., Nakhla, G., Bassi, A., 2006. Long-term performance of high-rate anaerobic reactors for the treatment of oily wastewater. Environmental Science and Technology 40 (20), 6466-6472. https://doi.org/10.1021/es061071m

Jensen, P.D., Ge, H., Batstone, D.J., 2011. Assessing the role of biochemical methane potential tests in determining anaerobic degradability rate and extent. Water Science and Technology 64, 880. https://doi.org/10.2166/wst.2011.662

Johannesson, G.H., Crolla, A., Lauzon, J.D., Gilroyed, B.H., 2020. Estimation of biogas co-production potential from liquid dairy manure, dissolved air flotation waste (DAF) and dry poultry manure using biochemical methane potential (BMP) assay. Biocatalysis and Agricultural Biotechnology 25, 101605. https://doi.org/10.1016/j.bcab.2020.101605

Kevbrin, V.V., Romanek, C.S., Wiegel, J., 2005. Alkalithermophiles: A Double Challenge From Extreme Environments. In: Seckbach J. (eds) Origins. Cellular Origin, Life in Extreme Habitats and Astrobiology, vol 6. Springer, Dordrecht. https://doi.org/10.1007/1-4020-2522-X_24

Kurade, M. B., Saha, S., Salama, E., Patil, S.M., Govindwar, S.P., Jeon, B., 2019. Acetoclastic methanogenesis led by *Methanosarcina* in anaerobic co-digestion of fats, oil and grease for enhanced production of methane. Bioresource Technology 272, 351-359.

Li, C., Champagne, P., Anderson, B.C., 2013. Biogas production of mesophilic and thermophilic anaerobic co-digestion with fat, oil, and grease in semi-continuous flow digesters: effects of temperature, hydraulic retention time, and organic loading rate. Environmental Technology 34, 2125-2133. https://doi.org/10.1080/09593330.2013.824010

Long, J.H., Aziz, T.N., de los Reyes III, F.L., Ducoste, J.J., 2011, Anaerobic co-digestion of fat oil, and grease (FOG): A review of gas production and process limitations. Process Safety and Environmental Protection 90 (3), 231-245. https://doi.org/10.1016/j.psep.2011.10.001

Lutze, R., Engelhart, M., 2020. Comparison of CSTR and AnMBR for anaerobic digestion of WAS and lipid-rich flotation sludge from the dairy industry. Water Resources and Industry 23, 100122. https://doi.org/10.1016/j.wri.2019.100122

Malayil, S., Chanakya, H. N., 2020. Biogas production from fat, oil and grease and effect of pre-treatment. In: Ghosh, S., Sen, R., Chanakya, H., Pariatamby, A., (eds). Bioresource Utilization and Bioprocess. Springer, Singapore. https://doi.org/10.1007/978-981-15-1607-8_7

Marchetti, R., Vasmara, C., Fiume, F., 2019. Pig slurry improves the anaerobic digestion of waste cooking oil. Applied Microbiology and Biotechnology 103(19), 8267-8279. https://doi.org/10.1007/s00253-019-10087-8

Martinez, E.J., Gil, M.V., Fernandez, C., Rosas, J.G., Gomez, X., 2016. Anaerobic codigestion of sludge: addition of butcher's fat waste as a cosubstrate for increasing biogas production. PLoS One. 11(4). https://dx.doi.org/10.1371%2Fjournal.pone.0153139

Maspolim, Y., Zhou, Y., Guo, C., Xiao, K., Ng, W.J., 2015. The effect of pH on solublization of organic matter and microbial community structures in sludge fermentation. Bioresource Technology 190, 289-298. https://doi.org/10.1016/j.biortech.2015.04.087

Nielfa, A., Cano, R., Fdz-Polanco, M., 2015. Theoretical methane production generated by the co-digestion of organic fraction municipal solid waste and biological sludge. Biotechnology Reports 5, 14-21. https://doi.org/10.1016/j.btre.2014.10.005

Owusu-Agyeman, I., Eyice, O., Cetecioglu, Z., Plaza, E., 2019. The study of structure of anaerobic granules and methane producing pathways of pilot-scale UASB reactors treating municipal wastewater under sub-mesophilic conditions. Bioresource Technology 290. https://doi.org/10.1016/j.biortech.2019.121733

Pham, T.N., Nam, W.J., Jeon, Y.J., Yoon, H.H., 2012. Volatile fatty acids production from marine macroalgae by anaerobic fermentation. Bioresource Technology 124, 500-503. https://doi.org/10.1016/j.biortech.2012.08.081

Posmanik, R., Kim, A.H., Labatut, R.A., Usack, J.G., Angenent, L. T., 2020. Granular sludge is a preferable inoculum for the biochemical methane potential assay for two complex substrates. Bioresource Technology 309. https://doi.org/10.1016/j.biortech.2020.123359

Rajput, A.A., Sheikh, Z., 2019. Effect of inoculum type and organic loading on biogas production of sunflower meal and wheat straw. Sustainable Environment Research 29(4). https://doi.org/10.1186/s42834-019-0003-x

Raposo, F., Borja, R., Martín, M.A., Martín, A., de la Rubia, M.A., Rincón, B., 2009. Influence of inoculum-substrate ration on the anaerobic digestion of sunflower oil cake in batch mode: process stability and kinetic evaluation. Chemical Engineering Journal 149(1-3), 70-77. https://doi.org/10.1016/j.cej.2008.10.001

Ross, C.C., Valentine, G.E., Smith, B.M., Pierce, J.P., 2003. Recent advances and applications of dissolved air flotation for industrial pretreatment. In Industrial Water/Wastewater Program North Carolina AWWA/WEA Conference, Greensboro, North Carolina.

Salama, E., Saha, S., Kurade, M.B., Dev, S., Chang, S.W., Jeon, B., 2019. Recent trends in anaerobic co-digestion: fat, oil, and grease (FOG) for enhanced biomethanation. Progress in Energy and Combustion Science 70, 22-42. https://doi.org/10.1016/j.pecs.2018.08.002

Salminen, E., Rintala, J., Lokshina, L. Ya., Vavilin, V.A., 2000. Anaerobic batch degradation of solid poultry slaughterhouse waste. Water Science and Technology 41, 33-41. https://doi.org/10.2166/wst.2000.0053

Sánchez, E., Borja, R., Weiland, P., Travieso, L., Martin, A., 2001. Effect of substrate concentration and temperature on the anaerobic digestion of piggery waste in a tropical climate. Process Biochemistry 37 (5), 483-489. https://doi.org/10.1016/s0032-9592(01)00240-0

Sangkharak, K., Khaithongkaeo, P., Chuaikhunupakarn, T., Choonut, A., Prasertsan, P., 2020. The production of polyhydroxyalkanoate from waste cooking oil and its application in biofuel production. Biomass Conversion and Biorefinery https://doi.org/10.1007/s13399-020-00657-6

Silvestre, G., Rodríguez-Abalde, A., Fernández, B., Flotats, X., Bonmatí, A., 2011. Biomass adaptation over anaerobic co-digestion of sewage sludge and trapped grease waste. Bioresource Technology 102, 6830-6836. https://doi.org/10.1016/j.biortech.2011.04.019

Singh, S., Rinta-Kanto, J.M., Kettunen, R., Lens, P., Collins, G., Kokko, M., Rintala, J., 2019. Acetotrophic activity facilitates methanogenesis from LCFA at low temperatures: screening from mesophilic inocula. Archaea. https://doi.org/10.1155/2019/1751783

Sousa, D.Z., Pereira, M.A., Stams, A.J.M., Alves, M.M., Smidt, H., 2007. Microbial communities involved in anaerobic degradation of unsaturated or saturated long-chain fatty acids. Applied and Environmental Microbiology 73(4): 1054-1064. https://dx.doi.org/10.1128%2FAEM.01723-06

Sri Bala Kameswari, K., Kalyanaraman, C., Porselvam, S., Thanasekaran, K., 2012. Optimization of inoculum to substrate ratio for bio-energy generation in co-digestion of tannery sold wastes. Clean Technologies and Environmental Policy 14, 241-250. https://dx.doi.org/10.1007/s10098-011-0391-z

Sunada, N.S., Orrico, A., Orrico, M., de Lucas J Jr., Lopes, W., Schwingel, A., 2018. Anaerobic co-digestion of animal manure at different waste cooking oil concentrations. Ciência Rural 48. https://doi.org/10.1590/0103-8478cr20170517

Tan, L.C., Lin, R., Murphy, J.D., Lens, P.N.L. 2020. Granular activated carbon supplementation enhances anaerobic digestion of lipid-rich wastewaters. Renewable Energy 171, 958-970. http://dx.doi.org/10.1016/j.renene.2021.02.087

Tassew, F.A., Bergland, W.H., Dinamarca, C., Bakke, R., 2019. Settling velocity and size distribution measurement of anaerobic granular sludge using microscopic image analysis. Journal of Microbiological Methods. 159, 81-90. https://doi.org/10.1016/j.mimet.2019.02.013

Trabelsi, A.B.H., Zaafouri, K., Baghdadi, W., Naoui, S., Ouerghi, A., 2020. Second generation biofuels production from waste cooking oil via pyrolysis process. Renewable Energy 126, 888-896. https://doi.org/10.1016/j.renene.2018.04.002

Usman, M., Zha, L., Abomohra, A.E., Li, X., Zhang, C., Salama, E., 2020. Evaluation of animal- and plant-based lipidic waste in anaerobic digestion: kinetics of long-chain fatty acids degradation. Critical Reviews in Biotechnology https://doi.org/10.1080/07388551.2020.1756215

Voet, D., Voet, J., Pratt, C. 2012. In: Fundamentals of Biochemistry: Life at Molecular Level (4th edition). Wiley, United States.

Wallace, T., Gibbons, D., O'Dwyer, M., Curran, T.P., 2017. International evolution of fat, oil and grease (FOG) waste management – A review. Journal of Environmental Management 187, 424-435. https://doi.org/10.1016/j.jenvman.2016.11.003

Wang, B., Strömberg, S., Li, C., Nges, I.A., Nistor, M., Deng, L., Liu, J., 2015. Effects of substrate concentration on methane potential and degradation kinetics in batch anaerobic digestion. Bioresource Technology 194, 240-246. https://doi.org/10.1016/j.biortech.2015.07.034

Wickham, R., Galway, B., Bustamante, H., Nghiem, L.D., 2016. Biomethane potential evaluation of co-digestion of sewage sludge and organic wastes. International Biodeterioration and Biodegradation 113, 3-8. https://doi.org/10.1016/j.ibiod.2016.03.018

Wilson, C.A., Novak, J.T., Murthy, S.N., 2009. Thermal hydrolysis of the lipid and protein fractions of wastewater sludge: impactions for digester performance and operational considerations, Water Environment Federation.

Worwag, M., Neczaj, E., Grosser, A., Krzeminska, D., 2011. Methane production from fat-rich materials. Civil and Environmental Engineering Reports 6, 147-162.

Wu, J., Afridi, Z.U.R., Cao, Z.P., Zhang, Z.L., Poncin, S., Li, H.Z., Zuo, J.E., Wang, K.J., 2016. Size effect of anaerobic granular sludge on biogas production: a micro scale study. Bioresource Technology 2020, 165-171. https://doi.org/10.1016/j.biortech.2015.12.006

Xiao, Y., Zhang, E., Zhang, J., Dai, Y., Yang, Z., Christensen, H.E.M., Ulstrup, J., Zhao, F., 2017. Extracellular polymeric substances are transient media for microbial extracellular electron transfer. Journal of Applied Science and Engineering 3(7). https://doi.org/10.1126/sciadv.1700623

Zhang, P., Chen, Y., Zhou, Q., 2009. Waste activated sludge hydrolysis and short-chain fatty acids accumulation under mesophilic and thermophilic conditions: effect of pH. Water Research 43(15), 3735-3742. https://doi.org/10.1016/j.watres.2009.05.036

Zhang, W., Lang, Q., Fang, M., Li, X., Bah, H., Dong, H., Dong, R., 2017. Combined effect of crude fat content and initial substrate concentration on batch anaerobic digestion characteristics of food waste. Bioresource Technology 232, 304-312. https://doi.org/10.1016/j.biortech.2017.02.039

Zwietering, M., Jongenburger, I., Rombouts, F., Van't Riet, K., 1990. Modeling of the bacterial growth curve. Applied and Environmental Microbiology 56 (6), 1875-1881.

Chapter 4 Enhanced anaerobic digestion of dairy wastewater in a granular activated carbon amended sequential batch reactor

A modified version of this chapter has been published as:

Logan, M., Tan, L.C., Nzeteu, C.O., Lens, P.N.L., 2022. Enhanced anaerobic digestion of dairy wastewater in a granular activated carbon amended sequential batch reactor. GCB Bioenergy 14(7), 840-857. https://doi.org/10.1111/gcbb.12947

Abstract

This study investigated the potential of granular activated carbon (GAC) supplementation to enhance anaerobic degradation of dairy wastewater. Two sequential batch reactors (SBR; 0.8 L working volume), one control and another amended with granular activated carbon, were operated at 37 ^{o}C and 1.5-1.6 m/h upflow velocity for a total of 120 days (four cycles of 30 days each). The methane production at the end of each cycle run increased by about 68, 503, 110, and 125% in the GAC-amended SBR when compared to the Control SBR. Lipid degradation was faster in the presence of GAC. Conversely, the organic compounds, especially lipids, accumulated in the absence of the conductive material. In addition, a reduction in lag phase duration by 46-100% was observed at all four cycles in the GAC-amended SBR. RNA-based bacterial analysis revealed enrichment of *Synergistes* (0.8% to 29.2%) and *Geobacter* (0.4% to 11.3%) in the GAC-amended SBR. *Methanolinea* (85.8%) was the dominant archaea in the biofilm grown on GAC, followed by *Methanosaeta* (11.3%), at RNA level. Overall, this study revealed that GAC supplementation in anaerobic digesters treating dairy wastewater can promote stable and efficient methane production, accelerate lipid degradation and might promote the activity of electroactive microorganisms.

4.1 Introduction

Ireland has targeted for a 51% reduction in greenhouse gas (GHG) emissions by 2030 against the 2018 levels with a further aim of a net zero GHG emission by 2050 (Climate Action and Low Carbon Development Act, 2021). One of the ways to achieve this is through the recovery of biogas, where this sector alone has the potential to reduce the worldwide GHG emission by 10-13% (World Biogas Association, 2019). Biomethane, i.e. upgraded biogas, can save up to 202% of GHG emissions, compared to EU fossil fuels (European Commission, 2017). Therefore, biomethane deployment will contribute to future renewable energy production and help in achieving the targets set out for carbon emission reduction (Scarlat et al., 2018). The anaerobic digestion (AD) technology can help to meet the demand for biomethane, concomitantly managing the issue of waste and wastewater treatment. Ireland has a biogas potential of about a million tonne, but less than 2% of this is currently utilized (SEAI, 2016). Using waste substrates that are readily available in abundance for AD could help to leverage this biogas potential.

An untapped substrate material for AD is dairy wastewater that has high concentrations of fat, oil and grease (FOG) (Salama et al., 2019). The global dairy industry is expected to grow by 35% by the year 2030 (ICFN, 2018) with Ireland's diary industry ranking as the most profitable in Europe in 2020 (Shalloo et al., 2020). In 2019 alone, 19.5 million tons of liquid milk and 6.4 million tons of cheese were produced, and over 46 billion tons of fresh dairy products were consumed in the European Union (EU) (Shahbandeh, 2020). Due to the growth in production and demand of dairy products, waste/wastewater generated from this process is also increasing. For instance, about 1-2 m^3 of wastewater is generated per m^3 of manufactured milk (Paulo et al., 2020). While various characteristics of dairy wastewater (high COD and BOD, proteins, lipids and fat content) makes it favourable for AD (Bella and Rao, 2021), it is also difficult to process due to substrate accumulation and mass transfer limitations caused by the intermediate long chain fatty acids (LCFAs). This leads to process failure particularly if no proper strategies are implemented during AD operation. Currently, various practices and strategies are employed to deal with dairy wastewater loaded with high LCFA, such as utilizing dissolved air flotation for fat removal prior to AD (Logan et al., 2021); low or intermittent organic loading (Ziels et al., 2017); treatment after a start-up period with step feeding, i.e. sequencing continuous feeding and batch feeding (Cavaleiro et al., 2009); pre-treatments such as microwave (Zielińska et al., 2013), ozone or ultrasound (Chen et al., 2021); and/or modified reactor configurations (McAteer et al., 2020). However, these methods are associated with either high operational cost or difficulties with deployment in the existing AD systems.

One of the ways to improve the process is by targeting the acidogenic stage of AD, where LCFAs are slowly degraded into shorter chain volatile fatty acids. This can be done through the application of carbon-based or metal-based conductive materials (CMs) such as iron nanoparticles, stainless steel or carbon nanotubes, which have shown evidence of accelerated reaction rates and improved hydrolysis-acidification and methanogenesis (Liu et al., 2021). In addition, CMs can help to overcome the deterioration of AD from acidification or elevated H_2 partial pressures (Gao et al., 2019, Zhao et al., 2017). Besides, syntrophic activity in microbial communities can be increased in CM amended bioreactors (Zhao et al., 2020).

Current research on CM is mainly performed in batch reactors or experiments feeding with model and simple substrates, whereas investigations on long term pilot-scale reactor operation with real wastewater are still deficient (Wu et al., 2020). Furthermore, very few studies have

utilized granular activated carbon (GAC) as the CM, targeting treatment of complex wastewaters such as lipid rich wastewaters (Shrestha et al., 2014; Dang et al., 2017). Our previous work showed that biomethane potential assays with GAC supplementation improved lipid (oleate) degradation by 50% and decreased the lag phase time by 1000% (Tan et al., 2021). Notably, Ziels et al. (2017) reported higher microbial bioconversion kinetics and functional stability at pulse feeding rather than continuous feeding of lipid-rich wastewaters. A discontinuous operation of LCFA accumulation during continuous feeding and subsequent batch degradation of the biomass-associated substrate achieved an efficient methane production rate (Cavaleiro et al., 2009). Consequently, the evaluation of the long-term process performance and stability of GAC supplementation to bioreactors treating high strength, unprocessed and fat-rich dairy wastewater is necessary. In addition, the linkage between microbial activity and physiological changes in the presence of CMs has not yet been evaluated. Hence, this study investigated the enhancement of anaerobic degradation of dairy wastewater with GAC supplementation in a sequential batch reactor (SBR). The effect of GAC addition on the microbial community composition was studied as well.

4.2 Materials and methods

4.2.1 Inoculum, substrate and GAC

The GAC (granular activated carbon, Alfa Aesar™ Carbon, Norit ROW) was purchased from Fisher Scientific (Dublin, Ireland). The GAC was rod shaped with an average diameter and length of 0.8 mm and 3 mm, respectively. Prior to use, GAC was soaked in demiwater overnight to remove any particulate carbon attached to the GAC and subsequently air dried. GAC was provided at 2 g/L as optimized previously (Tan et al. 2021).

Anaerobic granular sludge collected from a full-scale AD plant (Kilconnell, Galway, Ireland) treating dairy wastewater at ambient temperature (3–19 ^{o}C) was used as the inoculum. The sludge was crushed to provide better contact between substrate, GAC and microorganisms. A sludge concentration of 5 g VS/L with a total solid content of 62.5 g TS/kg wet sludge and a volatile to total solid percentage of 89% was used. Dairy wastewater was also collected from the same location as the inoculum (Kilconnell, Galway, Ireland). When not in use, inoculum and dairy wastewater were kept at 4°C. Table 4.1 shows the characteristics of the dairy wastewater fed to the SBR.

Table 4.1 Characteristics of the dairy wastewater fed to the sequential batch reactors

Composition	Unit	Amount
Total COD	mg COD/L	5040 (±366)
Soluble COD	mg COD/L	134 (±22)
Carbohydrate[1]	mg COD/L	28 (±2)
Protein[2]	mg COD/L	37 (±4)
Lipids[3]	mg COD/L	4800 (±310)
Ammonium	mg N/L	41 (±10)
pH		7.17 (±0)
Conductivity	mS/cm	3.47 (±0)
TS	g/kg	4 (±0)
VS	g/kg	2 (±0)
VS/TS	%	40 (±0)

[1] 1.07 g COD/g glucose

[2] 1.47 g COD/g BSA

[3] 1.26 g COD/g light mineral oil [$C_{16}H_{10}N_2Na_2O_7S_2$]

4.2.2 Sequential bed reactor (SBR) set-up and operation

The effect of GAC on the anaerobic digestion reactor treating dairy wastewater was investigated using two 1.0 L double-jacketed glass upflow anaerobic sludge bed reactors – Control and GAC-amended SBR – operated in sequential batch mode at a 30 d operation cycle. Figure 4.1 shows the schematic diagram of the reactor set-up**.**

The reactors had a total working volume of 0.8 L and an inner diameter of 76.2 mm. The upflow velocity was kept at 1.5-1.6 m/h using a peristaltic pump (Masterflex L/S, Cole-Parmer, USA). Temperature was maintained at 37 °C using a recirculating water bath (Grant Tc120, UK). Biogas lines were connected to the V-count gas counter and on-line monitoring CH_4 sensors (BlueSens, Germany) for measurement of biogas volume and CH_4 composition, respectively.

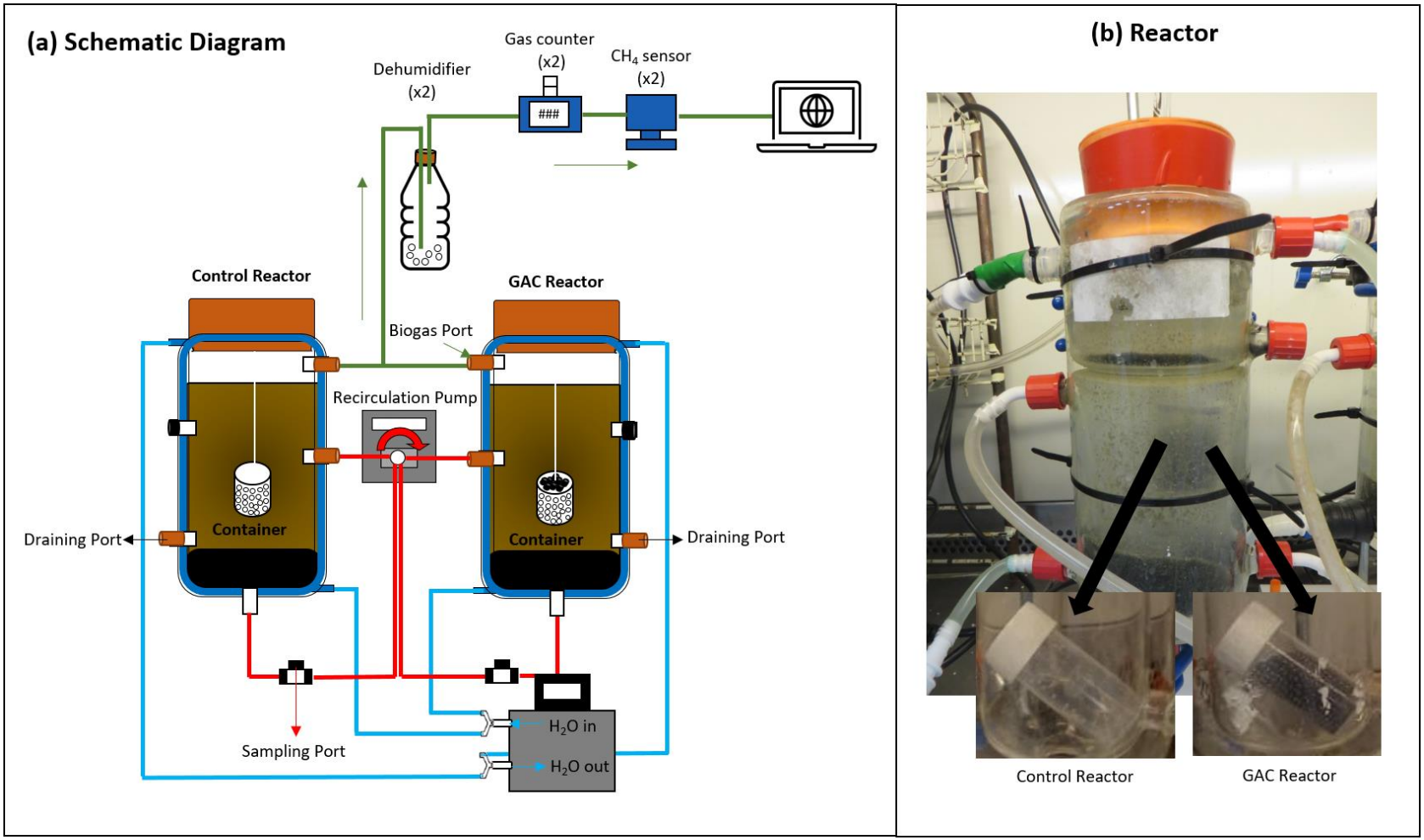

Figure 4.1 Schematic diagram (a) and image (b) of the UASB reactors (1 L total and 0.8 L working volume) treating dairy wastewater operated in sequential batch cycle mode for a total of 120 days (four cycles of 30 days each) at 37 °C and an upflow velocity at 1.5 – 1.6 m/h. The GAC-amended reactor was provided with a polypropylene container with 1 mm diameter holes to contain the GAC material (2 g/L). The control reactor was also provided with a similar polypropylene container without GAC.

A 20 ml polypropylene container was used to contain the GAC material within the GAC-amended SBR. Holes, approximately 1 mm in diameter, were made on the container using an 18-gauge needle. This was provided to allow the GAC to have contact with both the wastewater and sludge, while preventing its wash-out. A similar empty polypropylene container was placed in the Control SBR to ensure that the only difference between the two reactors was the presence of GAC. The container was suspended in the middle of the reactors using a nylon wire attached to the cap and tied to the neopropene rubber stopper used to seal the reactor airtight.

The reactors were operated for a total of 4 cycles, for a duration of 30 d each. Liquid samples were taken from the recirculation line connected to a glass 3-way connector with the sampling port sealed by a septum and aluminum cap. Samples were taken at definite sampling interval points on days 0, 1, 3, 6, 8, 10, 14, 17, 21, 25 and 30 of each cycle run. At the end of the cycle, the recirculation pump was stopped to allow for sludge settling. Approximately 80% of the reactor volume (draining port located near the bottom of the reactor) was drained and new dairy wastewater influent was fed to fill the 0.8 L reactor volume. To ensure anaerobic conditions, a nitrogen gas bag was attached to the headspace line to pump in nitrogen or withdraw headspace gas whenever liquid samples were withdrawn or added. Liquid samples were analyzed for their COD, protein, carbohydrates, NH_4^+, VFA and total lipid concentration. At the end of the operation run (120 d), sludge samples were taken for total solids (TS), volatile solids (VS), extracellular polymeric substances (EPS) and specific methanogenic activity (SMA) analysis.

4.2.3 Analytical method

TS, VS and total COD were measured according to standard procedures (APHA, 2017). Ammonium and soluble proteins were measured using an Nutrient analyser (Gallery Plus, Thermo Scientific, Waltham, USA). Carbohydrates were measured following the colorimetric protocol described by DuBois et al. (1956) and quantified using an UV-Spectrophotometer (UV-1900, Shimadzu, Tokyo, Japan).

Liquid samples for VFA analysis (C_2 to C_7) were prepared by adding a known amount and concentration of internal standard (ethyl butyric acid in 10% phosphoric acid) and filtering with a 1740.20 µm filter syringe (Chromafil Xtra Syringe Filters, PET-20/25). After analysis, VFA concentrations were reported as total VFA COD equivalent. For LCFA analysis (C_{10} to C_{18}), samples were prepared by lyophilizing at -56 °C and 0.050 mbar for 1 week using a freeze dryer

L-200 basic with Edwards nXDS6iC dry scroll vacuum pump (Buchi, Mason Technology, Dublin, Ireland). After lyophilization, LCFA was extracted and esterified using methanol and hexane following the procedure mentioned by Guihéneuf et al. (2015) with modification. The detailed process for the LCFA extraction is described in Tan et al. (2021).

Total lipid quantification was carried out using Wilks Infracal 2 HATR/ATR-SP (Hach, Loveland, USA). Prior to total lipid quantification, 4 ml of the liquid sample were taken and lypolised. After lypolisation, recovered powder was dissolved in hexane and quantified. The amount of lipids was reported in its COD equivalent following the conversion factor 1.26 g COD/g light mineral oil [$C_{16}H_{10}N_2Na_2O_7S_2$]. Light mineral oil (provided by the manufacturer) was used as the standard for the calibration of a Wilks Infracal 2 HATR/ATR-SP (Hach, Loveland, USA).

A specific methanogenic activity (SMA) assay was performed using the sludge sampled from the Control and GAC-amended SBRs at the end of the fourth cycle (day 120) with acetate (30 mM) as the substrate following the procedure described by Colleran et al. (1992). The total volume of the bottles was 120 ml with a working volume of 20 ml. The anaerobic buffer was prepared with 0.4 mg/L resazurin and 3.05 g/L sodium bicarbonate. The amount of sludge added in each bottle was 2 g VS/L. L-cysteine hydrochloride (3.2 mM) was used as the reducing agent.

Loosely bound EPS was extracted from a 15 ml sample of the inoculum and both reactor sludges at the end of operation (120 d) through centrifugation at a speed of 10000 *g* and 4 °C for 20 minutes (Mal et al. 2017). Extracted EPS was quantified for TOC content and normalized at 10 mg/L. Fluorescence emission excitation matrix (FEEM) spectra were recorded on a Shimadzu RF-6000 (Kyoto, Japan), set to scan samples from 200 nm to 550 nm (excitation and emission wavelengths) at 6000 nm min^{-1} with an excitation and emission bandwidth of 3.0 nm.

TEM images of the suspensions from both reactors and SEM images of GAC were recorded at the end of 120 d operation. The protocol followed for TEM and SEM preparation, fixation and imaging were described in detail by, respectively, Florentino et al. (2020) and Tan and Lens (2021).

4.2.4 Microbial community analyses

Approximately 15 ml of sludge samples were taken at the end of each cycle run for microbial community analysis (DNA and rRNA) for further rRNA sequencing for taxonomic characterization of microbial communities. In addition to suspended sludge samples, the biofilm grown in the GAC at the end of the operational run was also harvested and analysed for its microbial community. After sampling, the samples were immediately centrifuged at 8000 × g for 15 min. The resulting pellet was re-suspended in a 2 mL RNA tube for 5 hours and centrifuged at 10,000 g for 10 min. The supernatant was discarded and the pellet was flash-frozen using liquid nitrogen before storing at -80 ^{o}C. The pellets were used for RNA and DNA extractions based on the method described by Thorn et al. (2019). RNA purification was carried out using the TURBO DNA-free™ Kit (Ambion, Dublin, Ireland) in accordance with the manufacturer's instructions. Complementary deoxyribonucleic acid (cDNA) was generated from DNA-free RNA samples using the superscript reverse transcriptase III kit (Invitrogen, Dublin, Ireland) with random hexamer primers following the manufacturer's instructions.

Both DNA and cDNA were purified using sodium acetate precipitation (Thermo fisher scientific, Dublin, Ireland). The purified DNA and cDNA were normalised to a final concentration of 20 ng μl^{-1} and sent to an external laboratory (RTL Genomics, Texas, US) for *16S rRNA* amplicon sequencing using the MiSeq Illumina platform. In brief, after denoising and chimera checking, the sequences were clustered into OTUs using the UPARSE algorithm (Edgar, 2013). The centroid sequence from each cluster was then run against either the USEARCH global alignment algorithm or the Ribosomal Database Project (RDP) Classifier against a database of high-quality sequences derived from the National Center for Biotechnology Information (NCBI) database. The output was then analyzed using python program that assigns taxonomic information to each sequence. The minimum number of reads was on average of 10,000 reads per sample. The primers used to sequence the V3 – V4 region of the bacteria *16S rRNA* genes at both DNA and cDNA level were 357wF (CCTACGGGNGGCWGCAG) and 806R (GGACTACHVGGGTWTCTAAT) (Lemons et al., 2017). Similarly, the V4 – V5 region of the archaeal *16S rRNA* genes was sequenced by the universal primary set for archaea: 517F (GCYTAAAGSRNCCGTAGC) and 909R (TTTCAGYCTTGCGRCCGTAC) at both DNA and cDNA level (Florentino et al., 2019). RTL Genomics' data analysis and methodology can be

accessed in the following link: http://www.rtlgenomics.com/docs/Data_Analysis_Methodology.pdf. The detailed protocol can also be found in previous literature (Pérez-Rangel el et al., 2021, Tianero et al., 2015, Loganathachetti et al, 2015).

4.2.5 Calculations and statistical analyses

Methane production data were fitted to the modified Gompertz model as described by Logan et al. (2021). Analysis of variance (ANOVA) and the kinetic fitting using the modified Gompertz model were performed using SPSS 16 software. Non-metric multi-dimensional scaling (NMDS) analyses applying the Bray-Curtis similarity index was performed by means of the R package "vegan". The analysis carried out plots the rank order of similarity of DNA- and RNA-based bacterial and archaeal community profiles at the end of different cycles of the Control and GAC-amended SBRs (Ziganshin et al., 2013). NMDS ordination positions each sample as a function of its distance from all other data points (greater distances represent larger dissimilarities) (Joyce et al., 2018).

4.3 Results

4.3.1 Process performance of GAC-amended SBR

The methane production profile per 30 d cycle run for both the Control and GAC-amended SBRs is presented in Figure 4.2. The methane production at the end of the first 30 d cycle run was about 68 % higher for the GAC-amended SBR when compared to the Control SBR. The highest methane yield was realised at the second cycle run in the GAC-amended SBR, which was about 503 % higher than the Control SBR. The GAC-amended SBR also showed a 110 and 125 % increment in methane yield at the third and fourth 30 d cycle, when compared to the Control. The methane and carbon dioxide concentrations in the biogas ranged between 70-80 % and 10-20 %, respectively, throughout the experimental period.

The organic compound profile for each 30 d cycle for both the Control and GAC-amended SBR are presented in Figure 4.3. The COD fraction converted to methane was more than 75 % at all cycles in the GAC-amended SBR. The lipid degradation was more profound in the GAC-amended SBR than in the Control SBR. More than 50 % of the COD, mostly in the form of lipids which might deteriorate the AD performance, accumulated in the Control SBR. Only very low LCFA concentrations could be detected using the analytical methods used (data not shown).

Accurate sampling and measurement of the LCFA concentration remains difficult as LCFAs are likely to accumulate in the solid phase, particularly palmitate, which is the limiting step product in LCFA degradation, and is adsorbed onto the biomass matrix (Neves et al., 2009). Samples taken from the effluent thus only represent a fraction of the LCFA concentration. The challenge lies in the extraction of the LCFAs from the solid phase, which is not practical in a semi-continuous reactor setting.

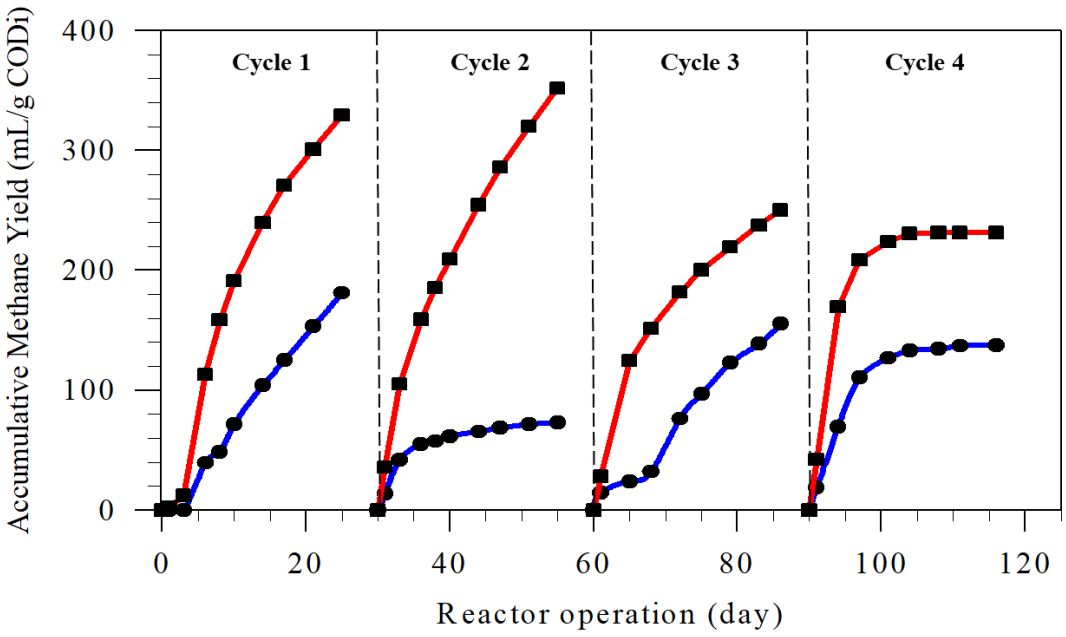

Figure 4.2 Methane production at all four cycles in the Control and GAC-amended SBR. The profile of the Control SBR is represented by the blue line with circle, whereas GAC-amended SBR is represented by the red line with square.

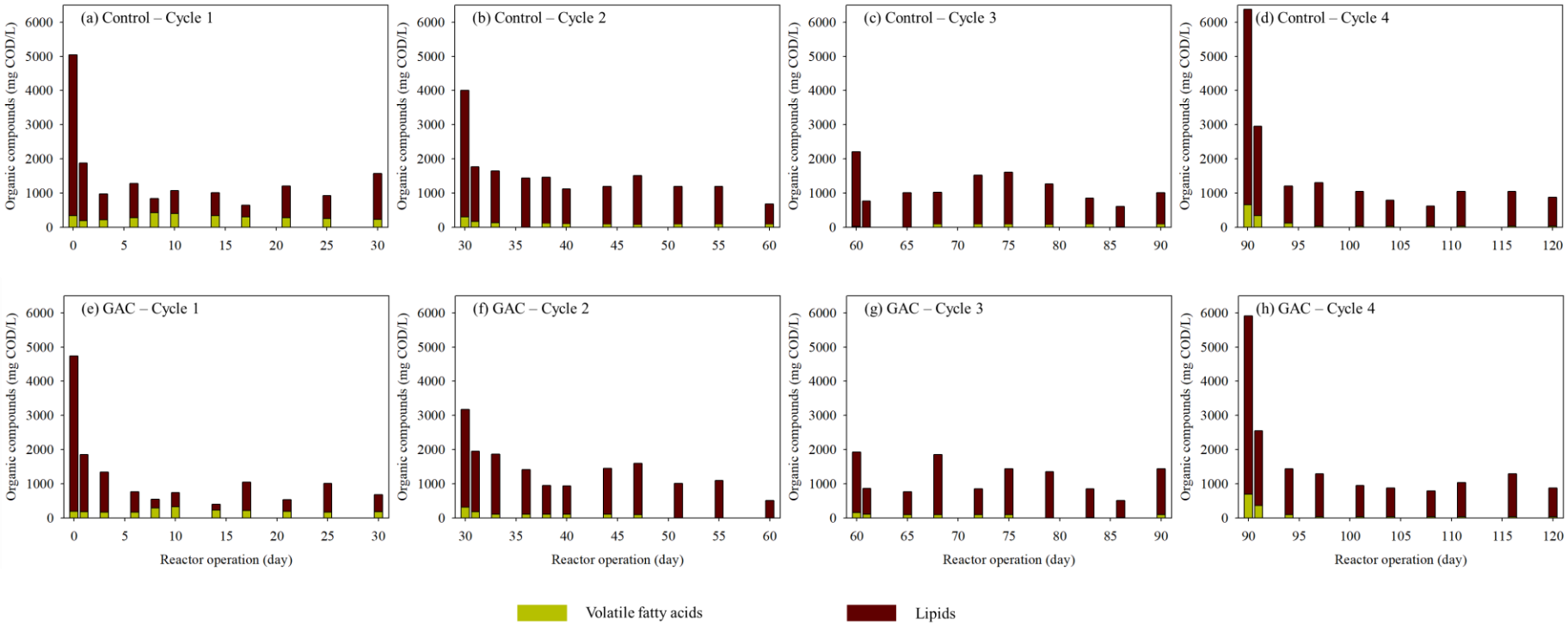

Figure 4.3 Organic compound profiling for each 30 d cycle run for the Control (a-d) and GAC-amended (e-h) reactor.

Table 4.2 Specific methanogenic activity (SMA) of sludge taken at the end of the reactor run and calculated kinetic parameters from the modified Gompertz method from each cycle of reactor operation.

		SMA	CH_4 $yield_{max}$	λ	T_{max}	R^2
		ml CH_4/gVS-d	mL/$gCOD_i$	d	d	
Control SBR	Cycle 1	123.2 (±6.3)	247	3.3	12.6	0.9891
	Cycle 2		62	0.3	3.0	0.9839
	Cycle 3		185	3.0	9.9	0.9813
	Cycle 4		154	0.5	3.8	0.9824
GAC-amended SBR	Cycle 1	167.9 (±10.4)	339	1.8	7.6	0.9813
	Cycle 2		348	0.0	7.6	0.9895
	Cycle 3		247	0.0	5.0	0.9841
	Cycle 4		247	0.2	2.7	0.9936

Kinetic parameters are CH_4 $yield_{max}$ – maximum methane yield; λ – lag-phase duration and T_{max} – peak time of methane yield.

The pH of the mixed liquor at the start of each cycle was around 7.35 (± 0.15), which decreased to 7.1 (± 0.24) at the end of each cycle for both reactors. The carbohydrate and protein concentrations in the effluent of each cycle were less than 100 mg/L COD in both SBRs, with ammonium reaching a maximum concentration of 120 mg/L N. The TS content of the Control SBR was 15.7 (±1.3) g TS/g wet sludge with 73 (±2) % VS/TS, whereas a reduced TS content of 11.5 (±1.2) g TS/g wet sludge and 74 (±2) % VS/TS was observed in the GAC-amended SBR at the end of the experimental run.

The kinetic parameters (R^2 > 0.98) for each cycle of reactor operation estimated by the modified Gompertz model is presented in Table 4.2. The lag phase duration reduced by 46-100% in the GAC-amended SBR, when compared with the Control. The sludge taken at the end of the operation of the GAC-amended SBR had a SMA of 167.9 (± 10.4) ml CH_4/g VS-d, which was 36 % higher than that of the Control SBR.

4.3.2 Sludge characterisation from Control and GAC supplemented SBR

FEEM characterisation revealed that the EPS extracted from the sludge at the end of the Control SBR operation contained high amounts of TOC that consisted of aromatic proteins, fulvic acid and humic substances with low indication of soluble microbial product-like compounds (Figure 4.4b). Opposite to this, the EPS extracted from the sludge of the GAC-amended SBR showed a low TOC concentration with mainly aromatic proteins present along with a small percentage of fulvic acid and humic substances (Figure 4.4c).

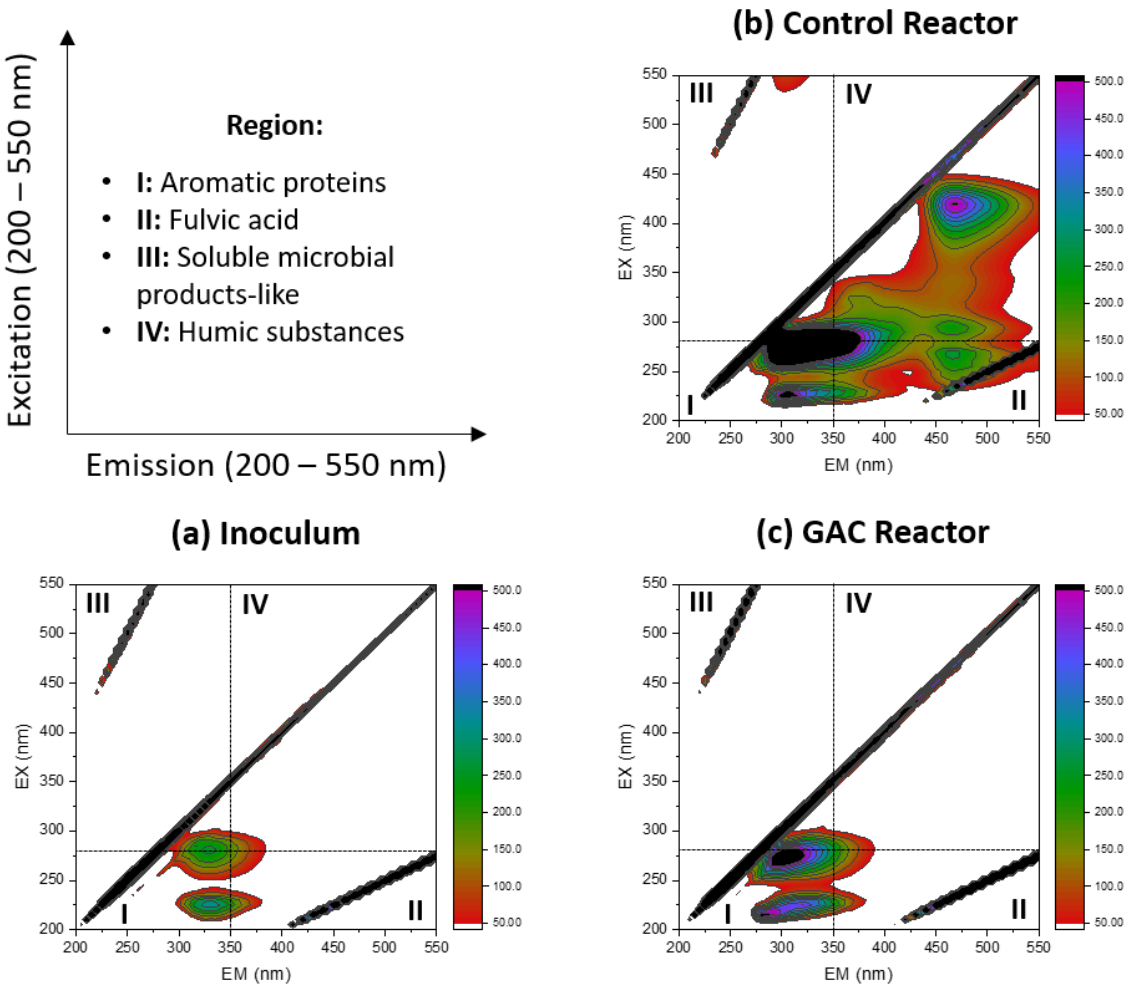

Figure 4.4 FEEM characterisation analyses of extracellular polymeric substances (EPS) extracted from the initial inoculum (a), sludge from the Control SBR after 120 d or end of cycle 4 (b) and sludge from the GAC-amended SBR (c) after 120 d (end of cycle 4). Prior to FEEM analyses, the TOC content was normalized to 10 mg/L.

Figure 4.5 presents the SEM images of GAC taken from the GAC-amended SBR, along with the TEM images of the suspensions from the Control and GAC-amended SBR at the end of the reactor operation. SEM images show evidence of biofilm growth on the GAC surface (Figure 4.5b) with pili-like structures observed on the attached microorganisms (Figure 4.5c). TEM images taken from the GAC-supplemented SBR similarly showed long connecting structures (Figure 4.5f) between microorganisms that were not evident in the images from the Control SBR (Figure 4.5e).

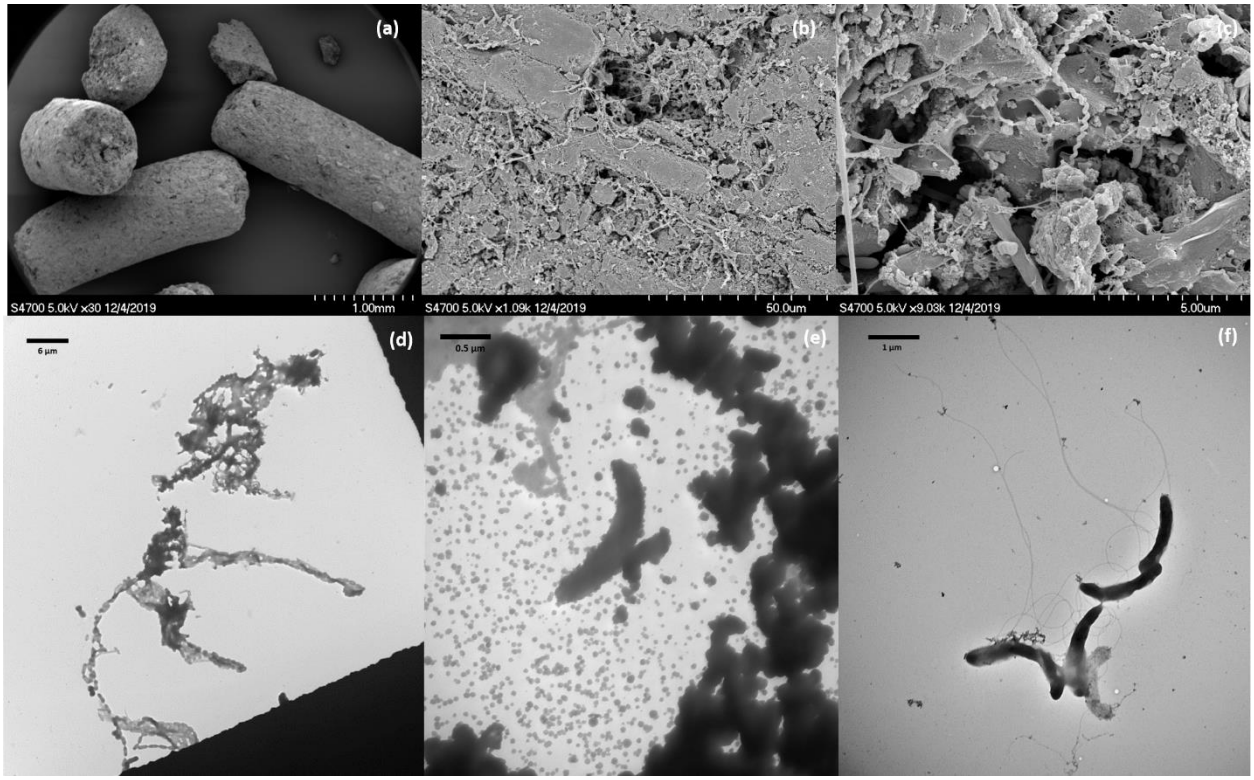

Figure 4.5 Electron microscopic images. SEM images at different magnification of GAC taken from the GAC-amended SBR at the end of 120 days of operation (a-c), as well as TEM images of particles present in dairy wastewater (d), suspension of the Control SBR mixed liquor (e) and suspension from the GAC-amended SBR mixed liquor (f). Both suspensions were taken at the end of the reactor run (day 120).

4.3.3 Microbial community dynamics

The microbial community structure of sludge growing in the Control and the GAC amended SBR were investigated by means of *16S rRNA* profiling from DNA and cDNA samples (Figure 4.6 and Figure 4.7). The bacterial and archaeal communities present initially in the dairy wastewater and

the inoculum that was previously adapted to dairy wastewater are also presented in Figures 4.6 and 4.7.

The DNA-based bacterial communities of the GAC-biofilm revealed that the main genera were *Mesotoga* (31.1%), *Synergistes* (19.4%), *Chlorobium* (11.1%), *Geobacter* (8.9%), *Chlorobaculum* (7.7%), *Desulfuromonas* (1.0%) and *Trichococcus* (0.5%). *Geobacter* showed a progressively increasing relative abundance growing from 1.1% up to 6.3% at DNA level by the end of the operation. The relative abundance of *Synergistes* also increased from 8.0% to 21.7% at DNA level by the end of the four cycles. Figure 4.6 shows *Geobacter* and *Synergistes* were enriched in the suspension of the GAC-amended SBR, relative to the Control SBR, accompanied with a slight enrichment of *Trichococcus, Clostridium, Deslfuromonas* and *Caldithrix*.

RNA-based bacterial analysis revealed similar enrichment of *Synergistes* (0.8% to 29.2%) and *Geobacter* (0.4% to 11.3%) in the GAC-amended SBR, compared to the Control SBR (Figure 4.6). A slight increase in *Arcobacter, Trichococcus, Clostridium, Brachymonas, Cytophaga, Desulfuromonas, Sulfuricurvum, Acinetobacter, Pseudomonas, Azonexus* and *Caldithrix* was observed at cDNA level due to GAC supplementation, relative to the Control. At cDNA level, the biofilm developed on the GAC constituted of *Synergistes* (19%), *Geobacter* (17.5%), *Desulfuromonas* (9.9%), *Chlorobaculum* (8.5%), *Chlorobium* (5.7%), *Mesotoga* (2.7%) and *Azonexus* (0.5%). An NMDS plot stress value below 0.1 indicates that the two-dimensional representation is ideal for data interpretation (Rees et al., 2004). The NMDS clustering of bacterial communities presence in the Control and GAC-amended SBR visibly separated at cDNA level (R^2: 0.997; Stress: 0.053) (Figure 4.8). In contrast, there was no distinct NMDS clustering at DNA level (R^2: 0.994; Stress: 0.076).

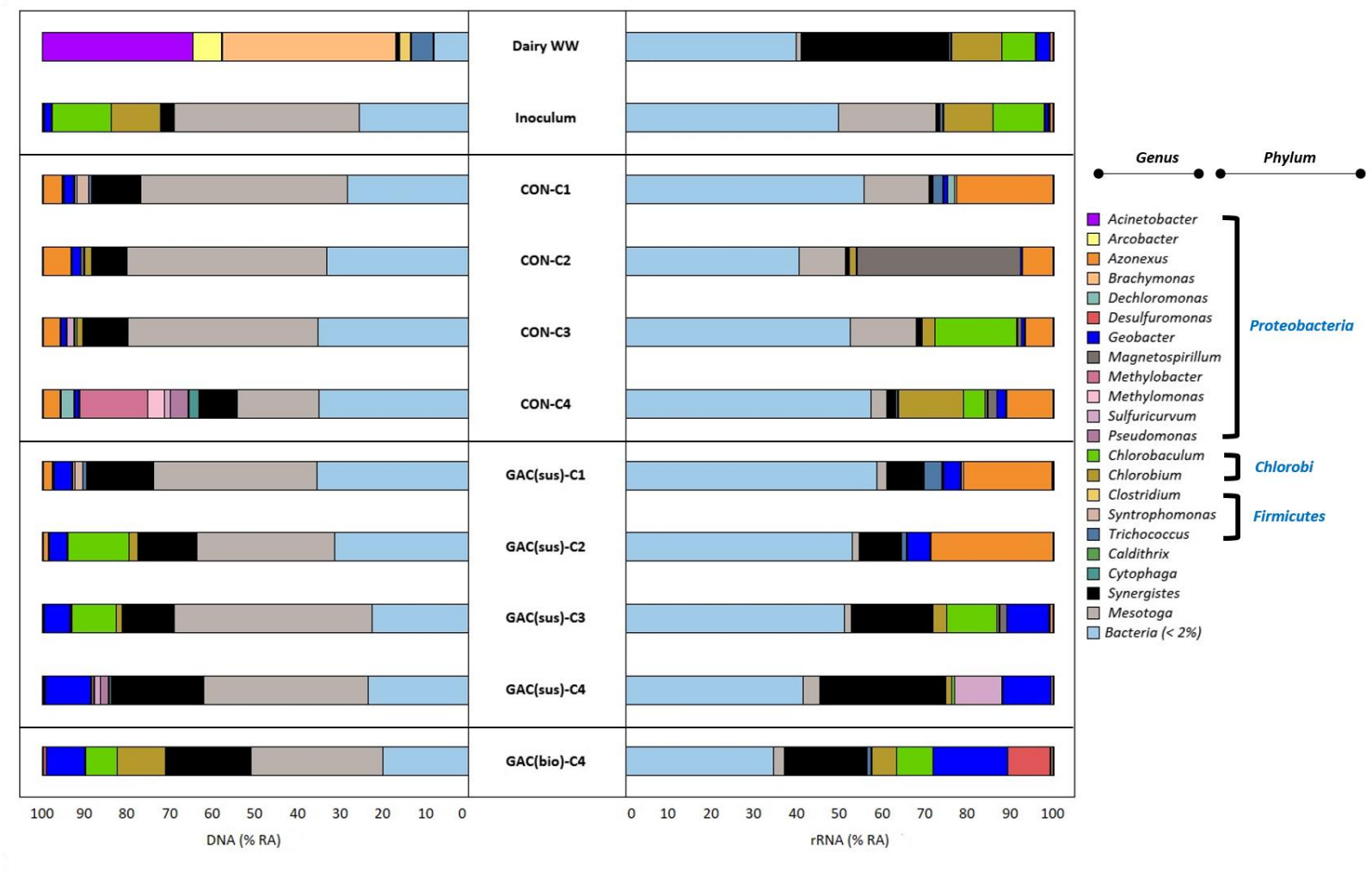

Figure 4.6 Relative abundance of bacteria at genus level in samples collected from dairy wastewater, inoculum, Control and GAC-amended SBR (at the end of each cycle run), and biofilm grown in the GAC at the end of the experiment. Genus level with relative abundance lower than 2% were included in unclassified groups.

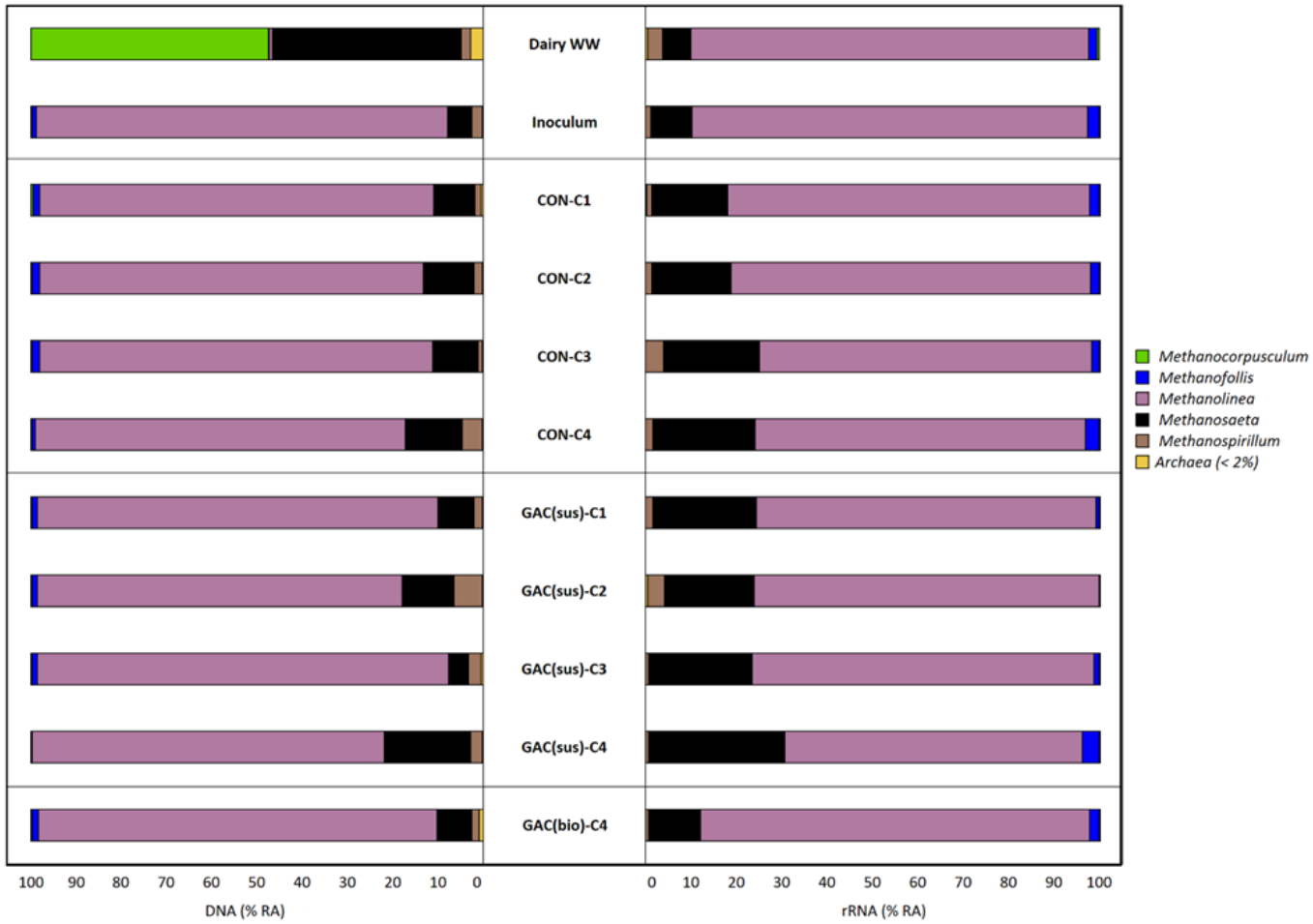

Figure 4.7 Relative abundance of archaea at genus level in samples collected from dairy wastewater, inoculum, Control and GAC-amended SBR (at the end of each cycle run), and biofilm grown in the GAC at the end of the operation. Genus level with relative abundance lower than 2% were included in unclassified groups.

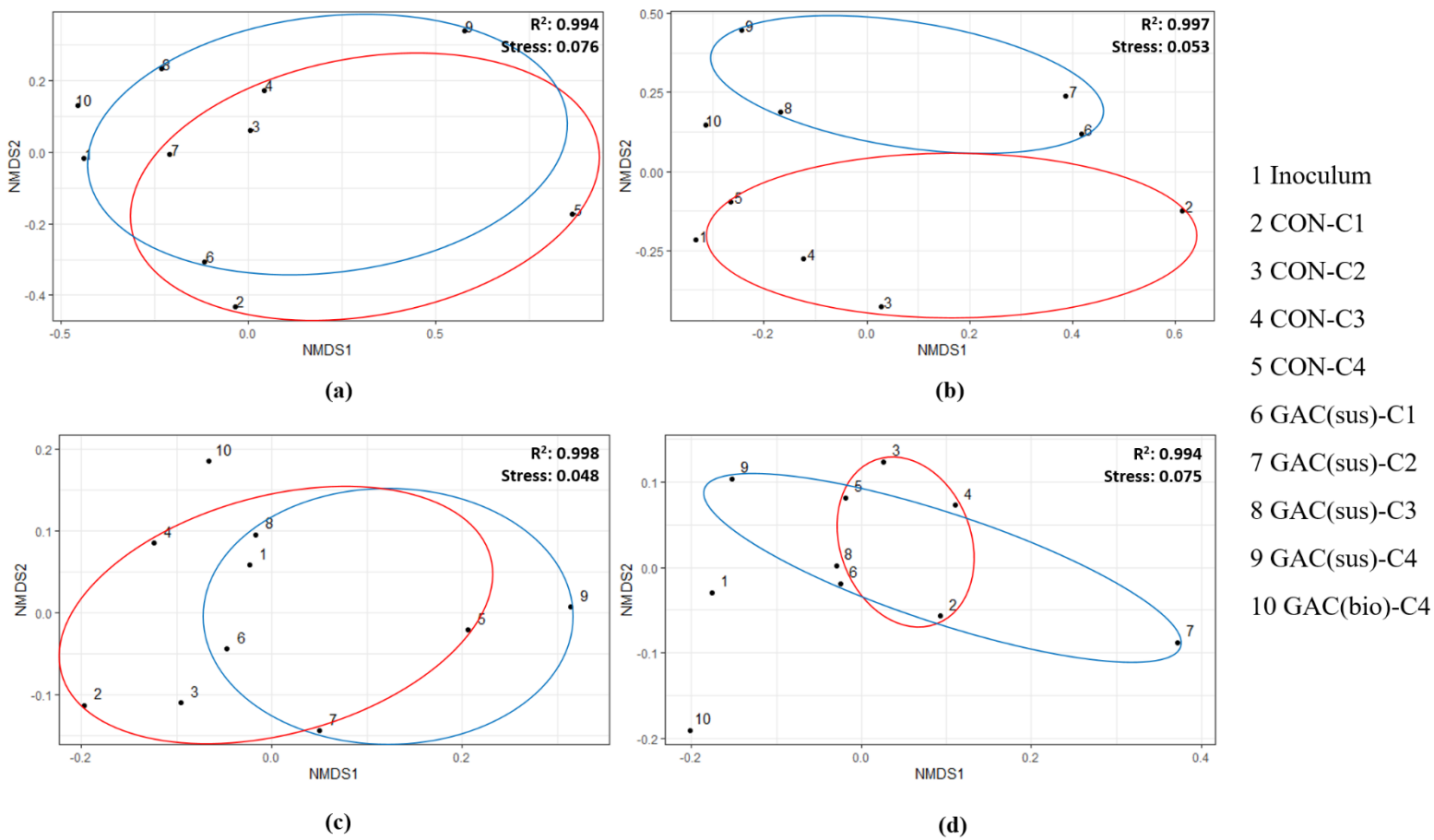

Figure 4.8 Nonmetric multidimensional scaling (NMDS) ordination with (a) DNA-based bacterial communities, (b) RNA-based bacterial communities, (c) DNA-based archaeal communities and (d) RNA-based archaeal communities. The Bray-Curtis index was performed to generate NMDS to visualize microbiome similarities. The red and blue cluster denote the Control and GAC(sus) microbiome, respectively. A stress value < 0.05 is considered an excellent fit; 0.05-0.1 indicates a good fit; > 0.2 indicates a poor fit.

As depicted in Figure 4.7, DNA-based archaeal community analysis shows *Methanolinea* (88.1%), *Methanosaeta* (7.7%), *Methanospirillum* (1.7%) and *Methanofollis* (1.6%) had a remarkable prevalence in the GAC-biofilm. The relative abundance of *Methanospirillum* increased from 0.9% to 6.3% and *Methanolinea* increased from 86.7% to 91.0% at DNA level in the suspension of the GAC-amended SBR. The relative abundance of *Methanosaeta* and *Methanospirillum* increased from 16.66% to 22.71% and 1.20% to 1.62% at cDNA level in the GAC-amended SBR after the first feeding cycle, which was not significantly enriched at the subsequent cycles. *Methanolinea* (85.8%) was the dominant archaea in the biofilm grown on GAC, followed by *Methanosaeta* (11.3%), *Methanofollis* (2.2%) and *Methanospirillum* (0.6%) at cDNA level. The NMDS plot revealed that there was no distinct clustering of the archaeal communities at both DNA (R^2: 0.998; Stress: 0.048) and RNA (R^2: 0.994; Stress: 0.075) level related to the GAC supplementation. The bacterial and archaeal communities developed in the GAC biofilm were clearly distinct at both DNA and cDNA levels compared to the Control-SBR suspensions (Figure 4.8 a-d).

4.4 Discussion

4.4.1 Improvement of AD of dairy wastewater by GAC supplementation

This study demonstrates GAC supplementation in anaerobic digesters could promote syntrophic metabolism to improve methane recovery from a complex industrial wastewater, i.e. dairy wastewater (Figure 4.2). This study confirms significant improvement in the COD conversion to methane and specific methanogenic activity can be achieved through the addition of GAC during the AD of dairy wastewater (Table 4.2).

Lipids are rapidly hydrolysed to glycerol and LCFAs, and the LCFAs are subsequently converted to acetate and hydrogen through the β-oxidation pathway, cleaving 2-carbon atoms at a time concomitantly with the release of acetyl-CoA, and finally to methane (Tan and Lens, 2021). Though the LCFA components could not be clearly quantified, it is highly likely that they had either accumulated or were absorbed onto the solid phase, i.e. biomass (Neves et al., 2009). These LCFAs might have a detrimental effect by either damaging the cellular membrane of methanogenic bacteria, reducing microbial-substrate interaction via encapsulation, or inducing flotation via entrapment (Logan et al., 2021). Slow acidification also leads to a prolonged degradation time and extended lag phase duration (Wu et al., 2017). AD of dairy wastewater in the absence of GAC witnessed lipid accumulation in the sequential batch reactor (Figure 4.3). However, the supplementation of GAC as CM in AD of dairy wastewater

facilitated lipid degradation, with increased lipid degradation and VFA conversion (Figure 4.3). Therefore, this study shows that GAC amendment could improve both the fermentation and methanogenesis steps.

The lag phase reduction by 100% upon GAC addition (Table 4.2) indicates it induced faster methane production from dairy wastewater. Dębowski et al. (2020) evaluated AD of dairy wastewater in a multi-section horizontal flow reactor equipped with microwave and ultrasonic generators (OLR: 1-4 g COD/L.d; 85% organic removal and 0.23 L/g COD methane yield). This resulted in a decreased productivity at higher OLR. Bela and Rao (2021) showed AD of dairy wastewater can be enhanced by pretreatment or co-digestion with substrates such as animal manure, agro waste, municipal waste and sewage sludge. A pilot scale magneto-active hybrid anaerobic biofilm reactor (OLR: 6-8 g COD/L.d; 80% COD removal; 0.26 – 0.32 L/g COD biogas yield) was demonstrated by Dębowski et al. (2018). Rajesh Banu et al. (2007) evaluated two-stage hybrid UASB reactors (OLR: 10.7-21.4 g COD/L.d; 98% COD removal; 3.2 m^3/m^3 of reactor volume/d biogas yield) for anaerobic treatment of dairy wastewater. Unlike the high cost associated with the aforementioned strategies, faster (reduced lag phase) and improved methane production was relatively easily realised in this study with the addition of GAC. The improvement in the methane yield in the GAC-amended SBR was more evident in Cycle 1 and Cycle 2, than in Cycle 3 and Cycle 4 (Figure 4.2). Therefore, it might be possible that the presence of GAC is crucial only during the start-up period of anaerobic digesters. This could be ascertained through a long term operation of the control and GAC-amended bioreactors. Notably, other strategies such as step feeding during start-up could promote sludge acclimation and is conducive to the development of anaerobic microbial communities for efficient LCFA mineralization (Cavaleiro et al., 2009).

Based on the comparison between degradation (Figure 4.3) and microbial community (Figures 4.6 and 4.7) profiles, GAC supplementation could be effective in enriching electroactive microorganisms, overcoming the bottleneck of lipid breakdown. The inhibition alleviation observed in the GAC amended SBR can be linked to the porosity, conductivity and adsorption properties of GAC. GAC provides a large specific surface area to enhance the growth and proliferation of methanogens (Johnravindar et al., 2020). The electrical conductivity of GAC is reported to be about 3000 S/cm, which is 100% greater than other organic CMs such as biochar (Baek et al., 2018). As such, GAC has a huge potential to serve as an electron conduit, allowing for electron transfer from bacteria to methanogenic archaea. It is noteworthy that high strength wastewaters, such as dairy, improve methanogenesis due to GAC addition, also overcoming the inhibition due to GAC adsorption of low-strength

wastewater (Florentino et al., 2019). Calabrò et al. (2021) also reported that the inhibitory compounds (e.g., LCFAs, VFAs and alcohols) are adsorbed onto the GAC. The enhanced GAC-induced methane recovery from dairy wastewater might also be due to improvement in sludge conductivity (Liu et al., 2021) or increased biomass concentration (Guo et al., 2020).

Electroactive bacteria oxidize organics, and then the released electrons are directly transferred through pili to methanogens, which reduce CO_2 to CH_4 (Rotaru et al., 2014). The SEM imaging of GAC-biofilm showed various cell types, suggesting multiple microorganisms are involved in the CM-induced methanogenesis (Figure 4.5). The microorganisms with rich pili-like structures (Figures 4.5b and c) might facilitate biofilm formation and direct interspecies electron transfer (DIET) (Guo et al., 2020). However, both the quantification and the conductivity of these pili-like structures needs to be ascertained in future research. Pili deficient strains could not convert ethanol to methane unless in the presence of biochar as CM (Chen et al., 2014), by utilizing 86% of the electrons released from ethanol oxidation for methane production. Further investigations are required to confirm, first, the percentage of the improved DIET process due to GAC supplementation and second, whether the e-pili concentration increased and assisted in the exogenous electron transfer via GAC acting as the conduit.

The humic substances and redox proteins present in the EPS matrix are widely reported to be electrochemically active and enhance AD (Xiao et al., 2017). FEEM characterisation revealed that the EPS composition was not altered in the sludge from the GAC-amended SBR compared with the Control SBR (Figure 4.4). Therefore, the improved mechanism with the addition of conductive material was not via enriched EPS compounds. This contrasts Yan et al (2018), who found that the presence of CMs greatly enriched certain EPS compounds such as proteins and humic substances that can act as electron shuttles. Notably, higher EPS concentrations in the control sludge without the presence of GAC also suggests the microbes were retained in stress conditions induced from lipid accumulation. Conversely, GAC amendment could have alleviated this stress condition with improved electron transfer and reduced LCFA toxicity, thereby showing less EPS compounds (Figure 4.4).

4.4.2 Effect of GAC addition on microbial community composition

Improved lipid degradation to methane is accompanied by the enrichment of fermentative bacteria (such as *Synergistes* and *Geobacter*) and methanogenic archaea (such as *Methanolinea* and *Methanosaeta*) that could possibly establish syntrophic relationships in the presence of

GAC (Figures 4.6 and 4.7). Kang et al. (2019) also reported that GAC significantly enriched *Geobacter* species. Bioaugmentation of syntrophic microorganisms such as *Geobacter* and *Synergistes* identified in this study could be evaluated in future studies on enhanced AD process performance (Zhang et al., 2018).

Interestingly, the biofilm developed on the GAC had a remarkable presence of electrotrophic methanogenic archaea, especially *Methanolinea* and *Methanosaeta* (Figure 4.7). Both *Methanolinea and Methanosaeta* are reported as syntrophic partners of *Geobacter* (Lee et al., 2016, Mei et al., 2018, Yang et al., 2019, Jiang et al., 2020). Looking closely at the organisms enriched in the reactor, *Geobacter* and *Methanosaeta* were identified to perform DIET using pili to shuttle electrons (Venkiteshwaran et al., 2016). The cells of these syntrophic partners attach to the carbon-based materials for interspecies electron exchange since the CMs could save cell energy to produce extracellular electrical connections (Zhao et al., 2015). Pyrosequencing of *16S rRNA* genes from the biomass attached to GAC by Lee et al. (2016) also demonstrated the enrichment of the exoelectrogen *Geobacter* and hydrogenotrophic methanogen *Methanolinea. Geobacter* species form electrically conductive aggregates composed of c-type cytochromes and conductive type IV pili (Aulenta et al., 2020).

Zhang et al. (2020) states that GAC stimulated the e-pili gene expression in the AD reactor, leading to a higher pili production, thereby increasing the electron transfer efficiency and thus syntrophic methanogenesis. Further investigation is required to show evidence of e-pili genes in the GAC-amended SBR through metagenomics and transcriptomic quantification (Holmes et al., 2017). The evaluation of the conductivity of the e-pili observed due to GAC supplementation by two-probe or four-probe conductivity methods is also required (Lovley, 2017).

Nakasaki et al. (2019) stated that *Synergistes* bacteria enhance the lipid degradation through active acetate degradation. Similarly, *Geobacter* was reported to degrade LCFAs for methane production with iron as electron acceptor (Cavaleiro et al., 2020). In addition to *Geobacter* and *Synergistes*, the presence and activity of LCFAs degrading bacteria such as *Acinetobacter, Arcobacter, Azonexus, Syntrophomonas, Pseudomonas* and *Clostridium* were observed due to GAC presence (Wongfaed et al., 2020, Zhu et al., 2015, Westerholm and Schnürer, 2019, Baserba et al., 2012, Ning et al., 2018). Likewise, *Methanospirillum* has been proposed as important hydrogen-utilizing partner for LCFA-degrading bacteria, while *Methanosaeta* is reported to be tolerant to LCFAs (Amha et al., 2017, Treu et al., 2016). The microbial community evolution in this study further suggests that GAC supplementation could have

resulted in effective utilization of the LCFAs, thus overcoming the bottleneck of degradation of lipids in dairy wastewater.

Zhang and Lu (2016) reported on conductive ferrosoferric oxide (Fe_3O_4) nanoparticles accelerating syntrophic methane production from butyrate oxidation in lake sediments. Guo et al. (2020) found a syntrophic partnership between propionate-oxidizing bacteria and methanogenic archaea in the presence of CM. Zhang et al. (2020) reported that GAC amendment improved conversion of propionate to methane by 100% at a high H_2 partial pressure (0.17 atm). Zhao et al. (2017) reported that carbon-based CM enhanced the resistance of semi-continuous digesters treating butanol to acidic impacts and maintained stable methanogenesis. *Synergistes* bacteria especially utilize acetate through syntrophic acetate oxidation coupled with hydrogenotrophic methanogens (Ito et al., 2011). This clearly explains the reason for effective VFA conversion in the anaerobic digestion systems amended with conductive materials (Kumar et al., 2021).

Several studies report that CM supplementation has introduced only small changes in the microbial community composition without changing the dominant microorganisms (Guo et al., 2020, Zhang et al., 2020). Van Steendam et al. (2019) asserted that the RNA-based community analysis is essential to understand the effects of GAC on DIET performing microorganisms. Further, Guo et al. (2020) stated that DNA-based communities are not significantly different between the reactors with and without GAC supplementation. DNA microbial community analysis in our earlier batch study also revealed similar relative abundance in GAC supplemented and control assays with the dominant bacterial families *Clostridiacea, Synergistaceae* and the archaea family *Methanomicrobiaceae* (Tan and Lens, 2021). In this study too, no distinct NMDS clustering was visualized after GAC amendment in bacterial communities at DNA level and archaeal communities at DNA and cDNA levels (Figure 4.8). In contrast, the NMDS clustering of bacterial communities was dissimilar at cDNA level with and without the presence of GAC. Further studies focused on metatranscriptomic and metaproteomic profiles of DIET-mediated AD mixed cultures are suggested to further establish if the GAC amendment induces changes in the functional phylogenetic members.

4.4.3 Practical aspects of GAC amendment for efficient dairy wastewater AD

This study suggests that GAC amendment significantly improved AD of dairy wastewater which could be attributed to several possible reasons as discussed above including the enhancement of DIET process which needs to be confirmed using microbial (fluorescence in

situ hybridization, meta-omic methods for detecting genes, transcripts and proteins), electrochemical (cyclic voltammetry measurement) and/or metabolic (carbon isotope analysis and inhibitor tests) characterisation (van Steendam et al., 2019). At present, costly and unsustainable strategies are adopted for anaerobic treatment of dairy wastewaters, including pre-treatments or operation with low OLRs, to overcome process inhibition from LCFAs accumulation and the resulting mass transfer limitation. Dairy wastewaters are generated in large volumes and due to the presence of lipids, a DAF process is employed prior to the AD reactor as a standard operating procedure. This is done to remove lipids and prevent complications during digestion as well as allow high loading rates to process the large volume of wastewater produced. Zhang et al. (2020) stated that the organic loading rates of industrial wastewater could be increased by GAC amendment. This study confirms a higher organic loading rate of dairy wastewater to AD reactors can be realised with GAC supplementation. Consequently, this study affirms Lee et al. (2016), who suggest CMs addition is an effective approach to increase methane production rates, ultimately reducing the volume of anaerobic digesters.

Conductive materials amended digesters sustain treatment of complex wastewaters and harsh operational conditions (Mostafa et al., 2020). The potential of GAC to act as an electron conduit could be explored to improve mass and electron transfer between substrate-microbes and bacteria-archaea, respectively. Existing AD reactors could easily employ CMs such as GAC. However, reactor design and modification is necessary in order to prevent CM washout, along with an optimized recirculation flow for better contact between substrate and CMs. Furthermore, GAC regeneration and recycling are not required since biofilms develop on the GAC surfaces, which can help to bio-regenerate the GAC (Zhang et al., 2020). Therefore, a sequential batch reactor with a submerged GAC encased porous container, as envisaged in this study (Figure 4.1), could be adopted. Lü et al. (2019) reported that powdered CMs (biochar) doubled the microbial enrichment and increased the methane production from oil by 30%. Thus, formulation of a modified carrier infused with activated carbon could also be considered for the anaerobic treatment of complex wastewaters.

4.5 Conclusion

Traditionally, dairy wastewaters abundant in fats and oils have difficulties in achieving high methane recovery due to accumulation and slow degradation of intermediate LCFAs which results in an extended lag phase duration. This study demonstrates that GAC augmentation in a sequential batch reactor resulted in substantial improvement in performance, whereby a

decrease in lag phase duration (46-100%) and increase in methane production (68-503%) were observed when compared to the control reactor. Faster reduction and removal of the lipid content were evident both visibly and quantitatively in the GAC supplemented reactor, overcoming LCFA inhibition likely due to improved contact between substrate and microorganism. Further metabolic investigation is required to confirm the mechanistic pathway for the improved performance efficiency of the GAC augmented reactor, in particular confirming the occurrence of direct electron interspecies transfer via electrically conductive pili. Active bacterial genera such as *Synergistes* and *Geobacter*, as well as the methanogens *Methanolinea* and *Methanosaeta* were observed in the presence of GAC. Overall, GAC supplementation via retrofitting of AD reactors treating dairy wastewater shows a huge potential in improving reactor performance and methane recovery leading to a stable and efficient operation.

4.6 References

Amha, Y,M., Sinha, P., Lagman, J., Gregori, M., Smith, A.L., 2017. Elucidating microbial community adaptation to anaerobic co-digestion of fats, oils, and grease and food waste. Water Research 123, 277-289. https://doi.org/10.1016/j.watres.2017.06.065

APHA, 2017. APHA Standard Methods for the Examination of Water and Wastewater (23rd edition), 9780875532875, American Public Health Association, Washington, D.C., USA.

Aulenta, F., Tucci, M., Viggi, C.C., Dolfing, J., Head, I.M., Rotaru, A-E., 2020. An underappreciated DIET for anaerobic petroleum hydrocarbon-degrading microbial communities. Microbial Biotechnology 14, 2-7. https://doi.org/10.1111/1751-7915.13654

Baserba, M.G., Angelidaki, I., Karakashev, D., 2012. Effect of continuous oleate addition on microbial communities involved in anaerobic digestion process. Bioresource Technology 106, 74-84. https://doi.org/10.1016/j.biortech.2011.12.020

Bella, K., Rao, P.V., 2021. Anaerobic digestion of dairy wastewater: effect of different parameters and co-digestion options – a review. Biomass Conversion and Biorefinery. https://doi.org/10.1007/s13399-020-01247-2

Baek, G., Kim, J., Kim, J., Lee, C., 2018. Role and potential of direct interspecies electron transfer in anaerobic digestion. Energies 11, 107. https://doi.org/10.3390/en11010107

Calabrò, P.S., Fazzino, F., Limonti, C., Siciliano A., 2021. Enhancement of anaerobic digestion of waste-activated sludge by conductive materials under high volatile fatty acids-to-alkalinity ratios. Water 13, 391. https://doi.org/10.3390/w13040391

Cavaleiro, A.J., Salvador, A.F., Alves, J.I., Alves, M., 2009. Continuous high rate anaerobic treatment of oleic acid based wastewater is possible after a step feeding start-up. Environmental Science and Technology 43, 2931 – 2936. https://doi.org/10.1021/es8031264

Chen, S., Rotaru, A.E., Shrestha, P.M., Malvankar, N.S., Liu, F., Fan, W., Nevin, K.P., Lovley, D.R., 2014. Promoting interspecies electron transfer with biochar. Scientific Reports 4, 5019. https://doi.org/10.1038/srep05019

Chen, X., Tang, R., Wang, Y., Yuan, S., Wang, W., Ali, I.M., Hu, Z., 2021. Effect of ultrasonic and ozone pretreatment on the fate of enteric indicator bacteria and antibiotic resistance genes, and anaerobic digestion of dairy wastewater. Bioresource Technology 320, 124356. https://doi.org/10.1016/j.biortech.2020.124356

Climate Action and Low Carbon Development (Amendment) Act, 2021. Ireland. https://data.oireachtas.ie/ie/oireachtas/act/2021/32/eng/enacted/a3221.pdf

Colleran, E., Concannon, F., Golden, T., Geoghegan, F., Crumlish, B., Killilea, E., Henry, M., Coates, J., 1992. Use of methanogenic activity tests to characterize anaerobic sludges, screen for anaerobic biodegradability and determine toxicity threshold against individual anaerobic trophic groups and species. Water Science and Technology 25, 31-40.

Dang, Y., Sun, D., Woodard, T.L., Wang, L., Nevin, K.P., Holmes, D.E., 2017. Stimulation of the anaerobic digestion of the dry organic fraction of municipal solid waste (OFMSW) with carbon-based conductive materials. Bioresource Technology 238, 30-38. https://doi.org/10.1016/j.biortech.2017.04.021

Dębowski, M., Zieliński, M., Kisielewska, M., Kazimierowicz, J., 2020. Evaluation of anaerobic digestion of dairy wastewater in an innovative multi-section horizontal flow reactor. Energies 13, 2392. https://doi.org/10.3390/en13092392

Dębowski, M., Zieliński, M., Kisielewska, M., Kazimierowicz, J., Makowska, M., Grądkowski, M., Tor-Świątek, A., 2018. Simulated dairy wastewater treatment in a pilot plant scale magneto-active hybrid anaerobic biofilm reactor (MA-HABR). Brazilian Journal of Chemical Engineering 35, 553-562. https://doi.org/10.1590/0104-6632.20180352s20170036

DuBois, M., Gilles, K.A., Hamilton, J.K., Rebers, P.A., Smith, F., 1956. Colorimetric method for determination of sugars and related substances. Analytical Chemistry 28, 3, 350-356. https://doi.org/10.1021/ac60111a017

Edgar, R.C., 2013. UPARSE: highly accurate OTU sequences from microbial amplicon reads, Nature Methods 10, 996-998. https://doi.org/10.1038/nmeth.2604

European Commission, 2017. Solid and gaseous bioenergy pathways: input values and GHG emission. Joint Research Center Science for Policy Report. https://doi.org/10.2790/27486

Florentino, A.P., Costa, R.B., Hu, Y., O'Flaherty, V., Lens, P.N.L., 2020. Long chain fatty acid degradation coupled to biological sulfidogenesis: A prospect for enhanced metal recovery. Frontiers in Bioengineering and Biotechnology 8, 550253. https://doi.org/10.3389/fbioe.2020.550253

Florentino, A.O., Sharaf, A., Zhang, L., Liu, Y., 2019. Overcoming ammonia inhibition in anaerobic blackwater treatment with granular activated carbon: the role of electroactive microorganisms. Environmental Science: Water Resource and Technology 5, 383-396. https://doi.org/10.1039/C8EW00599K

Florentino, A.P., Xu, R., Zhang, L., Liu, Y., 2018. Anaerobic digestion of blackwater assisted by granular activated carbon: From digestion inhibition to methanogenesis enhancement. Chemosphere 233, 462-471. https://doi.org/10.1016/j.chemosphere.2019.05.255

Guihéneuf., F., Schmid, M., Stengel, D.B., 2015. Lipids and fatty acids in algae: Extraction, fractionation into lipid classes, and analysis by gas chromatography coupled with flame ionization detector (GC-FID). Methods in Molecular Biology, Springer Science, New York, USA, 173–190.

Guo, B., Zhang, Y., Zhang, L., Zhou, Y., Liu, Y., 2020. RNA-based spatial community analysis revealed intra-reactor variation and expanded collection of direct interspecies electron transfer microorganisms in anaerobic digestion. Bioresource Technology 298, 122534. https://doi.org/10.1016/j.biortech.2019.122534

Holmes, D., Shrestha, P.M., Walker, D.J.F., Dang, Y., Nevin, K.P., Woodard, T.L., Lovley, D.R., 2017. Metatranscriptomic evidence for direct interspecies electron transfer between *Geobacter* and *Methanothrix* species in methanogenic rice paddy soils. Applied and Environmental Microbiology 83, 9. https://doi.org/10.1128/AEM.00223-17

ICFN, 2018. International Farm Comparison Network Dairy Research Network Dairy Report.

Ito, T., Yoshiguchi, K., Ariesyady, H.D., Okabe, S., 2011. Identification of a novel acetate-utilizing bacterium belonging to *Syngergistes* group 4 in anaerobic digester sludge. The ISME journal 5, 1844-1856. https://doi.org/10.1038/ismej.2011.59

Jiang, Q., Chen, Y., Yu, S., Zhu, R., Zhong, C., Zou. H., Gu, L., He, Q., 2020. Effects of citrus peel biochar on anaerobic co-digestion of food waste and sewage sludge and its direct interspecies electron transfer pathway study. Chemical Engineering Journal 398, 125643. https://doi.org/10.1016/j.cej.2020.125643

Johnravindar, D., Liang, B., Fu, R., Luo, G., Meruvu, H., Yang, S, Yuan, B., Fei, Q., 2020. Supplementing granular activated carbon for enhanced methane production in anaerobic co-digestion of post-consumer substrates. Biomass and Bioenergy 136, 105543. https://doi.org/10.1016/j.biombioe.2020.105543

Joyce, A., Ijaz, U.Z., Nzeteu, C., Vaughan, A., Shirran, S.L., Botting, C.H., Quince, C., O'Flaherty, V., Abram, F., 2018. Linking microbial community structure and function during the acidified anaerobic digestion of grass. Frontiers in Microbiology 9, 540. https://doi.org/10.3389/fmicb.2018.00540

Kang, H., Lee, S., Lim, T., Park, H., 2019. Effect of inoculum concentration on methanogenesis by direct interspecies electron transfer: Performance and microbial community composition. Bioresource Technology 291, 121881. https://doi.org/10.1016/j.biortech.2019.121881

Kumar, V., Nabaterega, R., Khoei, S., Eskicioglu, C., 2021. Insight into interactions between syntrophic bacteria and archaea in anaerobic digestion amended with conductive materials. Renewable and Sustainable Energy Reviews 144, 110965. https://doi.org/10.1016/ j.rser.2021.110965

Lee, J.Y., Lee, S.H., Park, H.D., 2016. Enrichment of specific electro-active microorganisms and enhancement of methane production by adding granular activated carbon in anaerobic reactors. Bioresource Technology 205, 205-212. https://doi.org/10.1016/j.biortech. 2016.01.054

Lemons, A.R., Hogan, M.B., Gault, R.A., Holland, K., Sobek, E., Olsen-Wilson, K.A., Park, Y., Park, J., Gu, J.K., Kashon. M.L., Green, B.J., 2017. Microbial rRNA sequencing analysis of evaporative cooler indoor environments located in the Great Basin Desert region of the

United States. Environmental Science: Processes and Impacts 19, 101-110. https://doi.org/10.1039/C6EM00413J

Liu, Y., Li, X., Wu, S., Tan, Z., Yang, C., 2021. Enhancing anaerobic digestion process with addition of conductive materials. Chemosphere 278, 130449. https://doi.org/10.1016/j.chemosphere.2021.130449

Logan, M., Ravishankar, H., Tan, L.C., Lawrence, J., Fitzgerald, D., Lens, P.N.L., 2021. Anaerobic digestion of dissolved air floatation slurries: effect of substrate concentration and pH. Environmental Technology and Innovation 21, 101352. https://doi.org/10.1016/j.eti.2020.101352

Loganathachetti, D.S., Sadaiappan, B., Poosakkannu, A., Muthuraman, S., 2016. Pyrosequencing-Based Seasonal Observation of Prokaryotic Diversity in Pneumatophore-Associated Soil of *Avicennia marina*. Current Microbiology 72, 68–74. https://doi.org/10.1007/s00284-015-0920-9

Lovley, D.R., 2017. Electrically conductive pili: Biological function and potential applications in electronics. Current Opinion in Electrochemistry 4, 190-198. http://dx.doi.org/10.1016/j.coelec.2017.08.015

Lü, F., Liu, Y., Shao, L., He, P., 2019. Powdered biochar doubled microbial growth in anaerobic digestion of oil. Applied Energy 247, 605-614. https://doi.org/10.1016/j.apenergy.2019.04.052

Mal, J., Yarlagadda, V.N., Maheshwari, N., van Hullebusch, E.D., Lens, P.N.L., 2017. Continuous removal and recovery of tellurium in an upflow anaerobic granular sludge bed reactor. Journal of Hazardous Materials 327, 79-88. http://doi.org/10.1016/j.jhazmat.2016.12.052

Martins, G., Salvador, A.F., Pereira, L., Alves, M.M., 2018. Methane production and conductive materials: a critical review. Environmental Science and Technology 52, 10241-10253. https://doi.org/10.1021/acs.est.8b01913

McAteer, P.G., Trego, A.C., Thorn, C., Mahony, T., Abram, F., O'Flaherty, V., 2020. Reactor configuration influences microbial community structure during high-rate, low-temperature anaerobic treatment of diary wastewater. Bioresource Technology 307, 123221. https://doi.org/10.1016/j.biortech.2020.123221

Mei, R., Nobu, M.K., Narihiro, T., Yu, J., Sathyagal, A., Willman, E., Liu, W., 2018. Novel *Geobacter* species and diverse methanogens contribute to enhanced methane production in media-added methanogenic reactors. Water Research 147, 403-412. https://doi.org/10.1016/j.watres.2018.10.026

Mostafa, A., Im, S., Song, Y., Ahn, Y., Kim, D., 2020. Enhanced anaerobic digestion by stimulating DIET reaction. MDPI Processes 8, 424. https://doi.org/10.3390/pr8040424

SEAI, 2017. Economic Assessment of Biogas and Biomethane in Ireland. Sustainable Energy Authority Ireland.

Nakasaki, K., Koyama, M., Maekawa, T., Fujita, J., 2019. Changes in the microbial community during the acclimation process of anaerobic digestion for treatment of synthetic lipid-rich wastewater. Journal of Biotechnology 306, 32-37. https://doi.org/10.1016/j.jbiotec.2019.09.003

Neves, L., Pereira, M.A., Mota, M., Alves, M.M., 2009. Detection and quantification of long chain fatty acids in liquid and solid samples and its relevance to understand anaerobic digestion of lipids. Bioresource Technology 100, 91-96. https://doi.org/10.1016/j.biortech.2008.06.018

Ning, Z., Zhang, H., Li, W., Zhang, R., Liu, G., Chen, C., 2018. Anaerobic digestion of lipid-rich swine slaughterhouse waste: Methane production performance, long-chain fatty acids profile and predominant microorganisms. Bioresource Technology 269, 426-433. https://doi.org/10.1016/j.biortech.2018.08.001

O'Connor, S., Ehimen, E., Pillai, S.C., Power, N., Lyons, G.A., Bartlett, J., 2021. An investigation of the potential adoption of anaerobic digestion for energy production in Irish farms. Environments 8, 8. https://doi.org/10.3390/environments8020008

Park, J.-H., Kang, H.-J., Park, K,-H., Park, H.-D., 2018. Direct interspecies electron transfer via conductive materials: a perspective for anaerobic digestion applications. Bioresource Technology 254, 300-311. https://doi.org/10.1016/j.biortech.2018.01.095

Paulo, L. M., Castilla-Archilla, J., Ramiro-Garcia, J., Es-camez-Picón, J.A., Hughes, D., Mahony, T., Murray, M., Wilmes, P., O'Flaherty, V., 2020. Microbial community redundancy and resilience underpins high-rate anaerobic treatment of dairy-processing wastewater at ambient temperatures. Frontiers in Bioengineering and Biotechnology 8, 192. https://doi.org/10.3389/fbioe.2020.00192

Pérez-Rangel, M., Barboza-Corona, J.E., Navarro-Díaz, M., Escalante, A.E., Valdez-Vazquez, I., 2021. The duo Clostridium and Lactobacillus linked to hydrogen production from a lignocellulosic substrate. Water Science and Technology 83, 3033-3040. https://doi.org/10.2166/wst.2021.186

Rajesh Banu, J., Kaliappan, S., Yeom, I., 2007. Two-stage anaerobic treatment of dairy wastewater using HUASB with PUF and PVC Carrier. Biotechnology and Bioprocess Engineering 12, 257-264. https://di.org/10.1007/BF02931101

Rees, G.N., Baldwin, D.S., Watson, G.O., Perryman, S., Nielsen, D.L., 2004. Ordination and significance testing of microbial community composition derived from terminal restriction fragment length polymorphisms: application of multivariate statistics. Antonie Van Leeuwenhoek 86, 339-347. https://doi.org/10.1007/s10482-004-0498-x

Rotaru, A., Shrestha, P., Liu, F., Shrestha, M., Shrestha, D., Embree, M., Zengler, K., Wardman, C., Nevin, K., Lovley, D., 2014. A new model for electron flow during anaerobic digestion: Direct interspecies electron transfer to *Methanosaeta* for the reduction of carbon dioxide to methane. Energy and Environmental Science 7, 408-415. https://doi.org/10.1039/C3EE42189A

Salama, E., Saha, S., Kurade, M.B., Dev, S., Chang, S.W., Jeon, B., 2019. Recent trends in anaerobic co-digestion: Fat, oil, and grease (FOG) for enhanced biomethanation. Progress in Energy and Combustion Science 70, 22-42. https://doi.org/10.1016/j.pecs.2018.08.002

Scarlat, N., Dallemand, J., Fahl, F., 2018. Biogas: Developments and perspectives in Europe. Renewable Energy 129, 457-472. https://doi.org/10.1016/j.renene.2018.03.006

Shahbandeh, M., 2020. Dairy industry in Europe – Statistics and facts. Accessed May 5, 2021. https://www.statista.com/topics/3955/dairy-industry-in-europe/#dossierSummary

Shalloo, L., Connor, D. O., Cele, L., Thorne, F., 2020. An analysis of the Irish dairy sector post quota. Teagasc and Cork Institute of Technology. Accessed https://www.teagasc.ie/media/website/publications/2020/An-Analysis-of-the-Irish-Dairy-Sector-Post-Quota.pdf on 15 April 2021

Shrestha, P.M., Malvankar, N.S., Werner, J.J., Franks, A.E., Elena-Rotaru, A., Shrestha, M., Liu, F., Nevin, K.P., Angenent, L.T., Lovley, D.R., 2014. Correlation between microbial community and granule conductivity in anaerobic bioreactors for brewery wastewater

treatment. Bioresource Technology 174, 306-310. https://doi.org/10.1016/j.biortech.2014.10.004

Sousa, D.Z., Salvador, A.F., Ramos, J., Guedes, A.P., Barbosa, S., Stams, A.J.M., 2013. Activity and viability of methanogens in anaerobic digestion of unsaturated and saturated long-chain fatty acids. Applied and Environmental Microbiology 79, 4239-4245. https://doi.org/10.1128/aem.00035-13

Tan, L.C., Lens, P.N.L., 2021. Addition of granular activated carbon during anaerobic oleate degradation overcomes inhibition and promotes methanogenic activity. Environmental Science: Water Research and Technology 7, 762-774. https://doi.org/10.1039/d0ew01093f

Tan, L.C., Lin, R., Murphy, J.D., Lens, P.N.L., 2021. Granular activated carbon supplementation enhances anaerobic digestion of lipid-rich wastewaters. Renewable Energy 171, 958-970. https://doi.org/10.1016/j.renene.2021.02.087

Thorn, C.E., Bergesch, C., Joyce, A., Sambrano, G., McDonnell, K., Brennan, F., Heyer, R., Benndorf, D., Abram, F., 2018. A robust, cost-effective method for DNA, RNA and protein co-extraction from soil, other complex microbiomes and pure cultures. Molecular Ecology Resources 19, 439-455. https://doi.org/10.1111/1755-0998.12979

Tianero, M.D.B., Kwan, J.C., Wyche, T.P., Presson, A.P., Koch, M., Barrows, L.R., Bugni, T.S., Schmidt, E.W., 2015. Species specificity of symbiosis and secondary metabolism in ascidians. The ISME Journal 9, 615-628. https://doi.org/10.1038/ismej.2014.152

Treu, L., Campanaro, S., Kougias, P.G., Zhu, X., Angelidaki, I., 2016. Untangling the effect of fatty acid addition at species level revealed different transcriptional responses of the biogas microbial community members. Environmental Science and Technology 50, 6079-6090. https://doi.org/10.1021/acs.est.6b00296

Van Steendam, C., Smets, I., Skerlos, S., Raskin, L., 2019. Improving anaerobic digestion via direct interspecies electron transfer requires development of suitable characterization methods. Current Opinion in Biotechnology 57, 183-190. https://doi.org/10.1016/j.copbio.2019.03.018

Venkiteshwaran, K., Bocher, B., Maki, J., Zitomer, D., 2016. Relating anaerobic digestion microbial community and process function. Microbiology Insights https://doi.org/10.4137%2FMBI.S33593

Westerholm, M., & Schnürer, A. 2019. Microbial Responses to Different Operating Practices for Biogas Production Systems. In (Ed.), Anaerobic Digestion. IntechOpen. https://doi.org/10.5772/intechopen.82815

Wongfaed, N., Kongjan, P., Prasertsan, P., O-Thong, S., 2020. Effect of oil and derivative in palm oil mill effluent on the process imbalance of biogas production. Journal of Cleaner Production 247, 119110. https://doi.org/10.1016/j.jclepro.2019.119110

World Biogas Association, 2019. Global Potential of Biogas. https://www.worldbiogasassociation.org/wp-content/uploads/2019/09/WBA-globalreport-56ppa4_digital-Sept-2019.pdf

Wu, L.J., Kobayashi, T., Li, Y.Y., Xu, K.Q., Lv, Y., 2017. Determination and abatement of methanogenic inhibition from oleic and palmitic acids. International Biodeterioration and Biodegradation 123, 10-16. https://doi.org/10.1016/j.ibiod.2017.05.021

Wu, Y., Wang, S., Liang, D., Li, N., 2020. Conductive materials in anaerobic digestion: From mechanism to application. Bioresource Technology 298, 122403. https://doi.org/10.1016/j.biortech.2019.122403

Xiao, Y., Zhao, F., 2017. Electrochemical roles of extracellular polymeric substances in biofilms. Current Opinion in Electrochemistry 4, 206-211. https://doi.org/10.1016/j.coelec.2017.09.016

Yan, W., Sun, F., Liu, J., Zhou, Y., 2018. Enhanced anaerobic phenol degradation by conductive materials via EPS and microbial community alteration. Chemical Engineering Journal 352, 1-9. https://doi.org/10.1016/j.cej.2018.06.187

Yang, P., Tan, G.A., Aslam, M., Kim, J., Lee, P.H., 2019. Metatranscriptomic evidence for classical and RuBisCO-mediated CO_2 reduction to methane facilitated by direct interspecies electron transfer in a methanogenic system. Scientific Reports 9, 4116. https://doi.org/10.1038/s41598-019-40830-0

Yun, S., Xing, T., Han, F., Shi, J., Wang, Z., Fan, Q., Xu, H., 2021. Enhanced direct interspecies electron transfer with transition metal oxide accelerants in anaerobic digestion. Bioresource Technology 320, 124294. https://doi.org/10.1016/j.biortech.2020.124294

Zhang, S., Chang, J., Liu, W., Pan, Y., Cui, K., Chen, X., Liang, P., Zhang, X., Wu, Q., Qiu, Y., Huang, X., 2018. A novel bioaugmentation strategy to accelerate methanogenesis via

adding *Geobacter sulfurreducens* PCA in anaerobic digestion system. Science of The Total Environment 642, 322-326. https://doi.org/10.1016/j.scitotenv.2018.06.043

Zhang, Y., Guo, B., Zhang, L., Liu, Y., 2020. Key syntrophic partnerships identified in a granular activated carbon amended UASB treating municipal sewage under low temperature conditions. Bioresource Technology 312, 123556. https://doi.org/10.1016/j.biortech.2020.123556

Zhang, J., Lu, Y., 2016. Conductive Fe_3O_4 nanoparticles accelerate syntrophic methane production from butyrate oxidation in two different lake sediments. Frontiers in Microbiology: Aquatic Microbiology 7, 1316. https://doi.org/10.3389/fmicb.2016.01316

Zhang, Y., Zhang, L., Guo, B., Zhou, Y., Gao, M., Sharaf, A., Liu, Y., 2020. Granular activated carbon stimulated microbial physiological changes for enhanced anaerobic digestion of municipal sewage. Chemical Engineering Journal 400, 125838. https://doi.org/10.1016/j.cej.2020.125838

Zhao, Z., Li, Y., Zhang, Y., Lovley, D.R., 2020. Sparking anaerobic digestion: Promoting direct interspecies electron transfer to enhance methane production. iScience 23, 101794. https://doi.org/10.1016/j.isci.2020.101794

Zhao, Z., Zhang, Y., Li, Y., Dang, Y., Zhu, T., Quan, X., 2017. Potentially shifting from interspecies hydrogen transfer to direct interspecies electron transfer for syntrophic metabolism to resist acidic impact with conductive carbon cloth. Chemical Engineering Journal 313, 10-18. http://dx.doi.org/10.1016/j.cej.2016.11.149

Zhao, Z., Zhang, Y., Woodard, T.L., Nevin, K.P., Lovley, D.R., 2015. Enhancing syntrophic metabolism in up-flow anaerobic sludge blanket reactors with conductive carbon materials. Bioresource Technology 11, 140-145. https://doi.org/10.1016/j.biortech.2015.05.007

Zhu, X., De Francisci, D., Treu, L., Kougias, P., Campanaro, S., Angelidaki, I., 2015. Metagenomic analysis on thermophilic biogas reactors fed with high load of Long Chain Fatty Acids (LCFA). Abstract from 14th World Congress on Anaerobic Digestion, Viña del Mar, Chile.

Zielińska, M., Cydzik-kwiatkowska, A., Zieliński, M., Dębowski, M., 2013. Impact of temperature, microwave radiation and organic loading rate on methanogenic community and

biogas production during fermentation of dairy wastewater. Bioresource Technology 129, 308-214. https://doi.org/10.1016/j.biortech.2012.11.093

Ziels, R.M., Beck, D.A.C., Stensel, H.D., 2017. Long-chain fatty acid feeding frequency in anaerobic codigestion impacts syntrophic community structure and biokinetics. Water Research 117, 218-229. https://doi.org/10.1016/j.watres.2017.03.060

Ziganshin, A.M., Liebetrau, J., Pröter, J., Kleinsteuber, S., 2013. Microbial community structure and dynamics during anaerobic digestion of various agricultural waste materials. Applied Microbiology and Biotechnology 97, 5161-5174. https://doi.org/10.1007/s00253-013-4867-0

Chapter 5 Effect of selenium oxyanions on anaerobic digestion of dissolved air floatation slurry for simultaneous methane production and selenium bioremediation

A modified version of this chapter has been published as:

Logan, M., Tan, L.C., Lens, P.N.L., 2022. Anaerobic co-digestion of dissolved air floatation slurry and selenium rich wastewater for simultaneous methane production and selenium bioremediation. International Biodeterioration and Biodegradation 172, 105425. https://doi.org/10.1016/j.ibiod.2022.105425

Abstract

Dissolved air floatation (DAF) slurry, a lipid-rich waste, is largely disregarded as a substrate for anaerobic digestion. On the other hand, selenium (Se) contaminated wastewaters are perceived as unsuitable feedstocks because of their toxicity. This study aimed to evaluate the effect of Se oxyanions on anaerobic digestion of a DAF slurry using anaerobic granular sludge and waste activated sludge as the inocula. Anaerobic batch assays of DAF slurry supplemented with 0.05, 0.10, 0.25 and 0.50 mM selenate (SeO_4^{2-}) and selenite (SeO_3^{2-}), along with a control (without Se) were performed at 30 ºC. Methanogenesis of the DAF slurry using anaerobic granular sludge was realised up to 0.50 mM SeO_4^{2-}, whereas SeO_3^{2-} was already toxic from 0.05 mM onwards. DAF slurry supplemented with 0.05 and 0.10 mM Se oxyanions (both selenate and selenite) achieved a similar cumulative methane yield of about 180 mL/g COD as that of digestion of Se free DAF slurry after 65 days of incubation using waste activated sludge. Simultaneously, more than 90% removal of Se was accomplished. The lag phase duration was, however, extended by 50 and 90 % in the presence of 0.05 and 0.10 mM Se, respectively. The half maximal inhibitory concentration (IC_{50}) for methane production using waste activated sludge was 0.08 mM for SeO_4^{2-} and 0.07 mM for SeO_3^{2-}. The IC_{50} amounted to 2.10 mM for SeO_4^{2-} and 0.08 mM for SeO_3^{2-} with anaerobic granular sludge. SeO_4^{2-} and SeO_3^{2-} were reduced to elemental Se nanoparticles, as shown by transmission electron microscopy. This study indicates the feasibility of methane production from a DAF slurry, codigested with wastewaters containing up to 0.10 mM SeO_4^{2-} or SeO_3^{2-}.

5.1 Introduction

The anaerobic digestion (AD) technology benefits industries to produce methane, generates revenue streams (as volatile fatty acids), and decreases the environmental impact of their emissions. Lipid-rich slurries are generated in dissolved air floatation (DAF) systems when particulate matter present in fat, oil and grease (FOG) rich wastewaters rises to the surface upon injecting pressurized air (Tan et al., 2020). The DAF slurry has a high biomethane potential and calorific value, although frequently not considered as feedstock for AD (Awe et al., 2018). This represents a huge energy loss as a DAF slurry can serve as an excellent carbon source for methane production with improved energy yield through co-digestion with other organic substrates (Logan et al., 2021). Apart from a source of energy via methane production, a DAF slurry and its degradation intermediates can also provide as range of electron donors for redox reactions. The DAF slurry undergoes hydrolysis producing long chain fatty acids (LCFAs),

with subsequent β–oxidation of these LCFA to acetate and hydrogen, which are finally converted to methane (Alves et al., 2009). These intermediates from the DAF slurry might potentially serve as an electron donor for reduction of oxyanion pollutants present in the AD process, e.g. sulfate (Florentino et al., 2020) or selenate/selenite (this study).

Large amounts of selenium (Se) are released by agricultural and industrial activities including mining, coal-fired power generation, and photoelectric production (Table 5.1). Selenium is present as selenate (SeO_4^{2-}) and selenite (SeO_3^{2-}), which both have acute and chronic toxicity (Kagami et al., 2013, Zhang et al., 2019). Especially industries such as oil refineries generate effluents with high lipid and Se concentrations (Hansen et al., 2019). The cost and energy limitation of physico-chemical methods to achieve the stringent Se regulatory discharge limit of 5 µg Se/L can be overcome through microbial Se remediation (Tan et al., 2016). Anaerobic treatment of Se contaminated waste streams offers the possibility to convert soluble selenium oxyanions (SeO_4^{2-} and SeO_3^{2-}) to insoluble, less toxic elemental selenium (Se^0), and simultaneously conserve energy as methane from the organic matter present (Lenz et al., 2008a). Notably, some Se-containing wastewaters are inorganic and need to be externally supplemented with an electron donor for anaerobic treatment (Sinharoy and Lens, 2020). Further, the elemental Se produced can be recovered as nanoparticles that have high revenue potential in several industries, ranging from metallurgy, glass to chemical manufacturing (Nancharaiah and Lens, 2015b).

Microbial processes thriving on various redox processes can co-exist together (Sela-Alder et al., 2017). For instance, long-term and continuous methane production and sulfate reduction have been extensively studied in the past three decades (Sun et al., 2016). Se oxyanions, which share reduction pathways similar to sulfur oxyanions, can influence fermentation and methanogenesis either directly via inhibition of the microbial groups involved (Lenz et al., 2008b) or indirectly by altering the electron flow in the food web as Se respirers use the substrates as electron donor for Se reduction (Wu et al., 2018). The inhibition of SeO_4^{2-} and SeO_3^{2-} on methanogenic systems is crucial for the operation of anaerobic digesters, since a decrease in methanogenic activity will reduce the potential of the bioreactor to degrade the organic matter and recover energy via methane. The co-existence of methanogenic and Se reducing micro-organisms while sharing a common substrate is yet to be clearly understood.

Table 5.1 Characteristics of selenium laden industrial wastewaters

Waste stream	Province, Country	Se content (µg/L)	pH	Concentration	Reference
Aquaculture wastewater	Foshan City, China	115	8.1	COD = 2.25 mg/L TDS = 34,870 mg/L	Han et al., 2020
Oil refinery wastewater	Valparaiso, Chile	300	7.13	TS = 12.6 mg/L Oil and grease = 6.41 mg/L	Hansen et al., 2019
Coal ash wastewater	Kentucky, USA	10	n.a.	n.a.	Lemly, 2018
Flue gas desulphurized wastewater	Ontario, Canada	4440	n.a.	Soluble COD = 241± 86 mg/L	Andalib et al., 2016
Agricultural drainage water	California, USA	9000	n.a.	n.a.	Schmidt et al., 2013
Selenium refinery plant	Hyogo, Japan	74000	1.0	COD = 74000 mg/L	Soda et al., 2011

n.a. – not available

The stoichiometry and their free energies for the anaerobic degradation of acetate and molecular hydrogen for methane production and selenium reduction is presented below (Costa et al., 2020; Lundquist et al., 1994; Chung et al., 2006):

Acetate:

$CH_3COO^- + H_2O \rightarrow CH_4 + HCO_3^-$ ($\Delta G^{0'}$ = -31 KJ/mol) Eq. (5.1)

$3CH_3COO^- + 4SeO_4^{2-} + 11H^+ \rightarrow 6CO_2 + 4Se^0 + 10H_2O$ ($\Delta G^{0'}$ = -930 kJ/mol) Eq. (5.2)

$2CH_3COO^- + 4HSeO_3^- + 6H^+ \rightarrow 4CO_2 + 4Se^0 + 8H_2O$ ($\Delta G^{0'}$ = -884 kJ/mol Eq. (5.3)

Hydrogen:

$4H_2 + HCO_3^- + H^+ \rightarrow CH_4 + 3H_20$ ($\Delta G^{0'}$ = -33 KJ/mol) Eq. (5.4)

$SeO_4^{2-} + 3H_2 + 2H^+ \rightarrow Se^0 + 4H_2O$ ($\Delta G^{0'}$ = -71 kJ/mol) Eq. (5.5)

$HSeO_3^- + 2H_2 + H^+ \rightarrow Se^0 + 3H_2O$ ($\Delta G^{0'}$ = -65 kJ/mol) Eq. (5.6)

Trace Se concentrations of 0.32 – 0.63 µM enhanced the anaerobic digestion of food waste by 30 – 35 % (Ariunbaatar et al., 2016). The inhibitory effects of Se towards hydrogenotrophic and acetoclastic methanogenesis was evaluated in toxicity assays by Lenz et al. (2008a). However, to the best of our knowledge, there have been no studies to establish simultaneous Se reduction and methane production during biomethane potential tests of Se-laden lipid rich wastewaters. The inhibitory concentrations of Se oxyanions need to be clearly established for AD processes to prevent their overdosing (Cai et al., 2018).

This study aims to evaluate the effect of Se oxyanions on anaerobic digestion of DAF slurry. Towards this, the inhibition of methanogenesis of DAF slurry at different SeO_4^{2-} and SeO_3^{2-} concentrations was investigated. Degradation tests were conducted as biomethane potential (BMP) assays to track the simultaneous production of methane and Se oxyanion removal. Finally, to ascertain the Se toxicity was due to inhibition of fat or LCFA biodegradation, the specific methanogenic activity with simpler substrates (acetate and H_2/CO_2) at equimolar Se concentrations was investigated as well.

5.2 Materials and Methods

5.2.1 Source of biomass

The anaerobic granular sludge (AGS) was obtained from a 200 m^3 up-flow anaerobic sludge bed (UASB) reactor treating dairy wastewater at 20 °C with a hydraulic retention time (HRT) of 9-12 h (Kilconnel, Ireland). The total solid (TS) and volatile solid (VS) content of AGS was 37.8 g/kg and 32.0 g/kg of wet weight, respectively. The waste activated sludge (WAS) was collected from the secondary clarifier fed WAS chamber at the Tuam Municipal Wastewater Treatment Plant (Tuam, Ireland). The chamber was operated with varying HRT of 12-24 h at ambient temperature. The WAS had a TS and VS content of 45.0 g/kg and 31.2 g/kg, respectively.

5.2.2 Source of substrates

DAF slurry collected from an AD plant treating dairy wastewater was used as the substrate. The total COD of the DAF slurry amounted to 85958 (± 832) mg/L. The total solids (TS) and volatile solids (VS) content was 31.0 (± 0.1) and 23.5 (± 0.1) g/kg, respectively. The characteristics of the DAF slurry are detailed by Logan et al. (2021). Sodium selenate and sodium selenite salts were purchased from Alfa Aesar (Fisher Scientific, UK) and dissolved in distilled water to obtain 100 mM stock solutions of SeO_4^{2-} and SeO_3^{2-}. Subsequently, the synthetic selenate or selenite wastewater containing 0.1, 0.2, 0.5 and 1 mM was prepared from the stock solution. Se free DAF slurry was used as the control. The substrates and inocula were stored at 4 ^oC until use.

5.2.3 Inhibition and degradation assays

Batch inhibition assays were performed to study the effect of the SeO_4^{2-} or SeO_3^{2-} concentration in 60 ml working volume vials at 30 ^oC and 120 rpm. 50% of the working volume of the vials was synthetic selenate or selenite wastewater (0.1, 0.2, 0.5 and 1 mM), i.e. 30 ml synthetic selenate/selenite wastewater and 30 ml DAF slurry. This resulted in the DAF slurry supplemented with selenate concentrations of 0.05 mM SeO_4^{2-} (7.15 mg/L SeO_4^{2-}), 0.10 mM SeO_4^{2-} (14.30 mg/L SeO_4^{2-}), 0.25 mM SeO_4^{2-} (35.74 mg/L SeO_4^{2-}), 0.50 mM SeO_4^{2-} (71.49 mg/L SeO_4^{2-}), or selenite concentrations of 0.05 mM SeO_3^{2-} (6.35 mg/L SeO_3^{2-}), 0.10 mM SeO_3^{2-} (12.70 mg/L SeO_3^{2-}), 0.25 mM SeO_3^{2-} (31.74 mg/L SeO_3^{2-}), and 0.50 mM SeO_3^{2-} (63.49 mg/L SeO_3^{2-}). Se oxyanion supplementation resulted in a COD/selenate ratio of 5596, 2798,

1119 and 560, and COD/selenite ratio of 6300, 3150, 1260 and 630, respectively. The batch assays were conducted with and without 1.5 ml (0.8 g VS/L) inoculum (AGS or WAS). A total of six sets of experiments were conducted as depicted in Table 5.2.

The non-inhibitory SeO_4^{2-} and SeO_3^{2-} concentrations of 0.05 and 0.10 mM determined from the inhibition tests were employed for the degradation test. The batch study was conducted in 250 ml working volume vials (125 ml DAF slurry and 125 ml synthetic selenate/selenite wastewater) at 30 ^oC and 120 rpm. 6.3 ml (0.8 g VS/L) of waste activated sludge was added as the inoculum in each bottle during the degradation test. Five sets of experiments were conducted as presented in Table 5.2.

During the start of the inhibition and degradation experiments, the batch bottles were purged with nitrogen gas to ensure anaerobic conditions. Pressure reading was measured using a pressure transducer (Keller Druckmesstechnik Mano Leo1 81000.2, Range 0 – 4 bar abs, Jestetten, Germany) before the gas sample was collected for methane content analysis. The gas samples were collected using a 10 ml syringe and were analysed for their methane content on the same day. 2 ml of liquid samples were extracted at regular intervals to measure pH as well as COD and Se concentrations in the degradation test. After each sampling in the inhibition and degradation tests, the bottles were vented to release the excess built up pressure.

Table 5.2 Experimental sets conducted in this study with DAF slurry as the substrate

Experimental sets	Inoculum	Conditions
Inhibition test		
I	No Inoculum	Control, 0.05, 0.10, 0.25 and 0.50 mM SeO_4^{2-}
II	No Inoculum	Control, 0.05, 0.10, 0.25 and 0.50 mM SeO_3^{2-}
III	AGS	Control, 0.05, 0.10, 0.25 and 0.50 mM SeO_4^{2-}
IV	AGS	Control, 0.05, 0.10, 0.25 and 0.50 mM SeO_3^{2-}
V	WAS	Control, 0.05, 0.10, 0.25 and 0.50 mM SeO_4^{2-}
VI	WAS	Control, 0.05, 0.10, 0.25 and 0.50 mM SeO_3^{2-}
Degradation test		
VII	WAS	Control
VIII	WAS	0.05 mM SeO_4^{2-}

IX	WAS	0.10 mM SeO_4^{2-}
X	WAS	0.05 mM SeO_3^{2-}
XI	WAS	0.10 mM SeO_3^{2-}

a) 0.05, 0.10, 0.25 and 0.50 mM SeO_4^{2-} corresponds to COD/selenate ratio of 5596, 2798, 1119 and 560, respectively.

b) 0.05, 0.10, 0.25 and 0.50 mM SeO_3^{2-}corresponds to COD/selenite ratio of 6300, 3150, 1260 and 630, respectively.

5.2.4 Specific methanogenic activity (SMA) assays

A specific methanogenic activity (SMA) assay was performed following the procedure described by Colleran et al. (1992) using acetate and H_2/CO_2 (80:20) as the soluble and gaseous direct methanogenic substrates, respectively. SMA using WAS as inoculum was tested in the presence and absence of Se oxyanions at SeO_4^{2-} and SeO_3^{2-} concentrations of 0.05, 0.10, 0.25 and 0.50 mM, respectively. The volume of the bottles used was 120 ml for SMA assays with acetate, while a bottle of larger volume (160 ml) was used for the gaseous (H_2/CO_2) substrate assays. The working volume for both conditions was 20 ml. L-cysteine hydrochloride was used as reducing agent and resazurin as indicator.

5.2.5 Analytical techniques

The pH was measured by a pH meter (Cole-Parmer 300 pH/ORP, Cambridgeshire, UK) which was connected to a Hamilton SlimTrode electrode. Chemical oxygen demand (COD), total solids (TS) and volatile solids (VS) of the DAF slurry and inocula used were determined using standard methods (APHA, 2017).

Liquid samples collected during degradation tests were analyzed for Se oxyanion concentrations. The collected liquid samples were centrifuged at 37,000 g for 15 min and filtered with 0.22 µm (Filtropur S, Sarstedt, Germany) to remove suspended cells and Se^0 particles before. The supernatant was used for the analysis of Se oxyanions as described by Jain et al. (2015). SeO_4^{2-} and SeO_3^{2-} were determined using an ion chromatograph equipped with an electrical conductivity detector (Dionex™ Aquion™, Thermo Scientific, Waltham, USA) (Florentino et al., 2020). Samples for Se^0 and total Se analyses were prepared following the protocol described by Mal et al. (2016) and quantified using an inductively coupled plasma

– optical emission spectroscopy 5110 synchronous vertical dual view (ICP-OES 5110, Agilent Technologies, Santa Clara, USA). The operational conditions of ICP-OES were RF power: 1300 W, argon plasma flow rate: 8 $L.min^{-1}$, auxiliary argon flow rate: 0.3 $L.min^{-1}$, nebulizer argon flow rate: 0.80 $L.min^{-1}$. Se was read on axial mode at 196.02 nm.

Biogas volume was calculated using the ideal gas law accounting for the headspace volume of the bottle during each sampling interval. Methane concentration in biogas was determined using a gas chromatograph equipped with a thermal conductivity detector (GC, 7890B, Agilent Technologies, Santa Clara, USA) and a Porapak Q (2.74 m x 2 mm) column (Logan et al., 2021).

The Se nanostructures present in the WAS were extracted, fixed and observed on a Hitachi H7000 transmission electron microscope (TEM, Hitachi, Tokyo, Japan) at the Centre for Microscopy and Imaging (NUI Galway, Ireland).

5.2.6 Kinetic calculations

The kinetic model fitting was performed by using the modified Gompertz model for the inhibition test and logistic function model for the degradation test as described by Rajput et al. (2018) using SPSS 16 software (IBM Corp., Dublin, Ireland). The model with better fit for the data was selected and presented in Table 5.4.

5.2.7 Statistical analysis

All the test conditions were conducted in triplicates and results are reported as average values. Analysis of variance (ANOVA) was performed by using SPSS 16 software (IBM Corp., Dublin, Ireland) at 5% level of significance. IC_{50} values were calculated as mentioned by Cai et al. (2018).

5.3 Results

5.3.1 Inhibition of methanogenesis of DAF slurry by selenium oxyanions

The impact of Se oxyanions on the methane production from the DAF slurry using anaerobic granular sludge (AGS) is shown in Figure 5.1 with calculated IC_{50} values presented in Table 5.3. The batch assays with AGS showed that the maximum methane production yield was similar to the control at the end of the incubation with the exception of the highest SeO_4^{2-}

concentration tested. However, the methane production rate decreased by about 10% at SeO_4^{2-} concentrations of 0.05 and 0.10 mM (Table 5.4). The rate of methane production was further impaired by about 30% and 50% at SeO_4^{2-} concentrations of 0.25 and 0.50 mM, respectively. Similarly, though the lag phase did not significantly reduce at lower SeO_4^{2-} concentrations, the lag phase duration increased by about 1 day and 4 days at SeO_4^{2-} concentrations of 0.25 and 0.50 mM, respectively. On the other hand, toxicity due to SeO_3^{2-} on methanogenesis was observed. The maximum methane yield from the DAF slurry decreased by about 80, 90, 93 and 97 % at SeO_3^{2-} concentrations of 0.05, 0.10, 0.25 and 0.50 mM, respectively. The IC_{50} amounted to 2.10 mM for SeO_4^{2-}, conversely it was lower at 0.08 mM for SeO_3^{2-} with AGS inoculum.

During the inhibition batch assays with WAS, there was no reduction in methane yield and rate in the presence of 0.05 and 0.10 mM SeO_4^{2-}; however, the lag phase extended by about 4 and 7 days, respectively (Table 5.4). At 0.25 mM SeO_4^{2-}, the maximum methane yield and rate were impaired by about 88 and 92%, respectively. There was complete inhibition of methanogenesis from the DAF slurry at 0.50 mM SeO_4^{2-} with WAS. The lag phase duration extended by about 6 and 9 days in the presence of 0.05 and 0.10 mM, respectively. Complete inhibition of methanogenesis was observed at SeO_4^{2-} and SeO_3^{2-} concentrations of, respectively, 0.25 mM (Figure 5.1e) and 0.50 mM (Figure 5.1f). More than 90% Se reduction was observed at these higher concentrations. The IC_{50} amounted to 0.08 mM for SeO_4^{2-} and 0.07 mM for SeO_3^{2-} when using WAS as the inoculum (Table 5.3).

Table 5.3 Half maximal inhibitory concentrations (IC_{50}) of selenium oxyanions on methane production using DAF slurry as the substrate

Inoculum	**Se species**	**IC_{50} (mM)**	**R^2**
No Inoculum	SeO_4^{2-}	0.01 (± 0.00)	0.79
	SeO_3^{2-}	0.01 (± 0.00)	0.80
AGS	SeO_4^{2-}	2.10 (± 0.03)	0.64
	SeO_3^{2-}	0.08 (± 0.00)	0.41
WAS	SeO_4^{2-}	0.08 (± 0.01)	0.96
	SeO_3^{2-}	0.07 (± 0.01)	0.96

Table 5.4 Calculated kinetic parameters for the inhibition test conditions. $M_{measured}$ – Measured methane yield (mL/g COD), M_o – Maximum methane yield (mL/g COD), R_m – Maximum methane production rate (mL/g COD-d), λ – Lag phase (d), T_m – Peak time (d).

Conditions	**M_o (mL/g COD)**	**R_m (mL/ g COD-d)**	**λ (d)**	**T_m (d)**	**R^2**
Anaerobic granular sludge					
Control	232.11	17.18	6.83	11.80	0.990
0.05 mM SeO_4^{2-}	231.91	15.83	6.41	11.79	0.993
0.1 mM SeO_4^{2-}	239.05	15.32	6.59	12.33	0.994
0.25 mM SeO_4^{2-}	252.22	12.37	7.57	15.07	0.995
0.5 mM SeO_4^{2-}	275.14	7.76	10.88	23.93	0.994
0.05 mM SeO_3^{2-}	48.30	2.63	-0.80	5.97	0.977
0.1 mM SeO_3^{2-}	21.82	1.78	-0.23	4.29	0.977
0.25 mM SeO_3^{2-}	15.17	0.77	-1.15	6.12	0.981
0.5 mM SeO_3^{2-}	6.69	0.55	0.84	5.35	0.978
Waste activated sludge					
Control	300.36	6.09	12.85	30.98	0.998
0.05 mM SeO_4^{2-}	332.22	6.41	16.55	35.62	0.998
0.1 mM SeO_4^{2-}	362.75	6.42	19.98	40.76	0.998
0.25 mM SeO_4^{2-}	37.19	0.47	7.67	36.97	0.977

0.5 mM SeO_4^{2-}	n.p.	n.p.	n.p.	n.p.	n.p.
0.05 mM SeO_3^{2-}	332.88	5.78	18.75	39.89	0.997
0.1 mM SeO_3^{2-}	231.54	5.65	21.87	36.93	0.997
0.25 mM SeO_3^{2-}	n.p.	n.p.	n.p.	n.p.	n.p.
0.5 mM SeO_3^{2-}	n.p.	n.p.	n.p.	n.p.	n.p.
No inoculum					
Control	757.82	5.75	41.51	90.02	0.996
0.05 mM SeO_4^{2-}	140839.64	433.06	182.87	302.51	0.994
0.1 mM SeO_4^{2-}	1.29	1.038	6.64	7.09	1
0.25 mM SeO_4^{2-}	n.p.	n.p.	n.p.	n.p.	n.p.
0.5 mM SeO_4^{2-}	n.p.	n.p.	n.p.	n.p.	n.p.
0.05 mM SeO_3^{2-}	42608.76	178.70	134.75	222.47	0.997
0.1 mM SeO_3^{2-}	3.58	0.41	36.21	39.37	1
0.25 mM SeO_3^{2-}	n.p.	n.p.	n.p.	n.p.	n.p.
0.5 mM SeO_3^{2-}	n.p.	n.p.	n.p.	n.p.	n.p.

n.p. – cannot be predicted from the available data at the process failure conditions

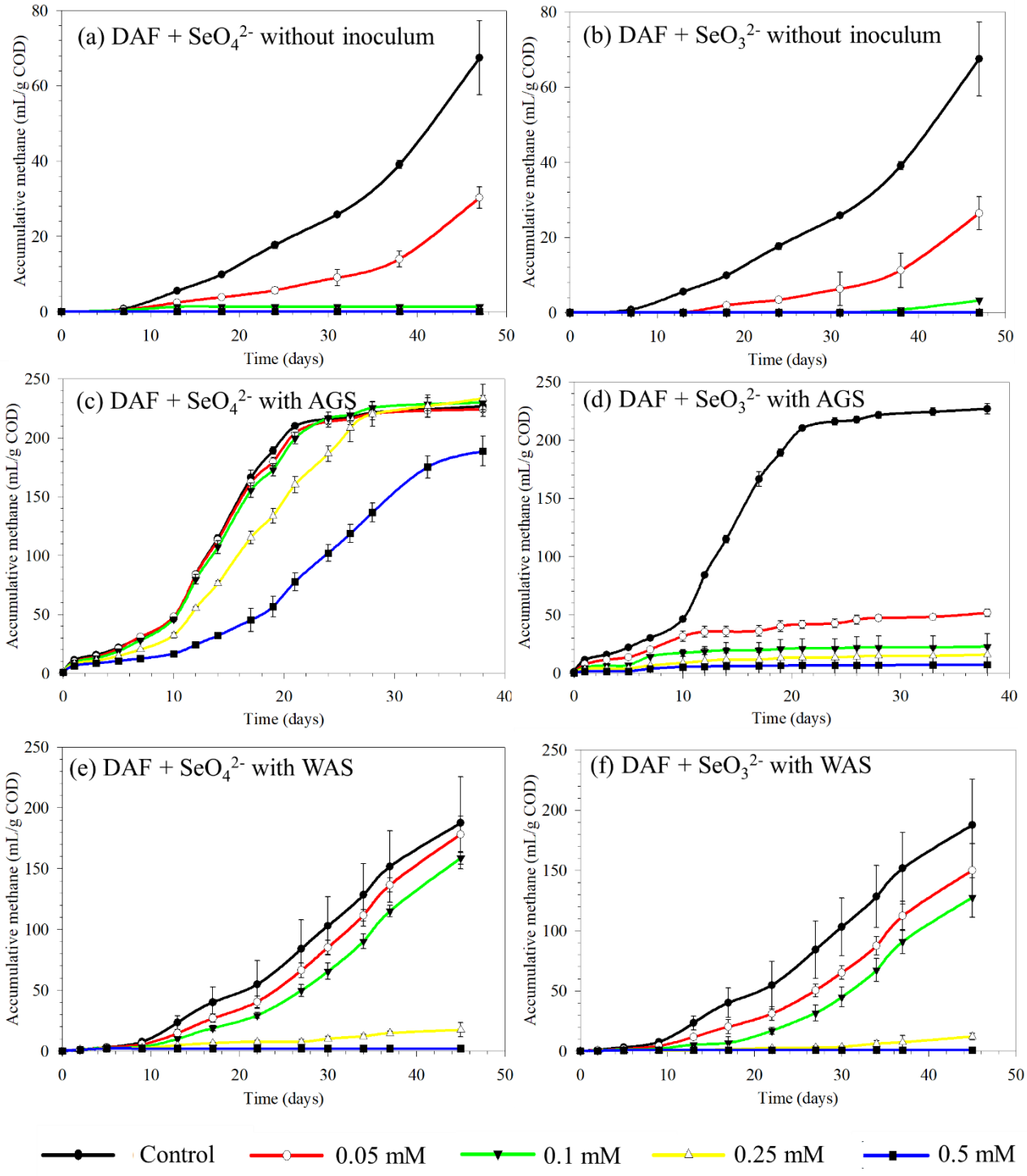

Figure 5.1 Inhibition due to selenium oxyanions with and without anaerobic granular sludge and waste activated sludge

For the batch assays without any inoculum, the inhibition of methanogenesis occurred early with single exposure at a concentration of 0.10 mM SeO_4^{2-} and SeO_3^{2-}. Though methanogenesis of the DAF slurry was still realised at 0.05 mM SeO_4^{2-} and SeO_3^{2-}, it is unfeasible with a delayed lag phase estimated at more than 100 days (Table 5.4). The inhibition assays established that the efficient inoculum for methanogenesis from Se oxyanions supplemented DAF slurry was as follows: DAF slurry with waste activated sludge > anaerobic granular sludge > no inoculum. Therefore, the subsequent degradation tests with DAF slurry were carried out with the WAS at the non-inhibitory SeO_4^{2-} and SeO_3^{2-} concentrations of 0.05 and 0.10 mM.

5.3.2 Simultaneous methanogenesis and Se oxyanion reduction during degradation of selenium supplemented DAF slurry

Figure 5.2 depicts the methane production during AD of DAF slurry with and without supplementation of Se oxyanions. Table 5.5 gives the corresponding estimated kinetic parameters from the logistic function model. The AD of the DAF slurry with SeO_4^{2-} and SeO_3^{2-} contaminated wastewater (0.05 and 0.10 mM) achieved a cumulative methane yield of about 180 mL/g COD after 65 days of incubation. This was statistically not different ($p < 0.05$) from the (Se free) Control. The maximum methane production and rate estimated at both SeO_4^{2-} and SeO_3^{2-} concentrations (0.05 and 0.10 mM) did not show huge difference with that of the control. However, the lag phase extension was more than 6 and 11 days in the presence of 0.05 and 0.10 mM SeO_4^{2-}. Similarly, the lag phase extended by about 7 and 12 days upon the addition of 0.05 and 0.10 mM SeO_3^{2-}. The peak time correspondingly increased by more than 6 and 11 days at 0.05 and 0.10 mM SeO_4^{2-}, and 6 and 13 days at 0.05 and 0.10 mM SeO_3^{2-}. The initial pH of 7.3 increased after the lag phase and was maintained above 7.5 till the end of the incubation (Figure 5.3). Figure 5.4 presents the COD profile during the degradation test, which shows that more than 80% initial COD removal was accomplished. At the end of 65 days of incubation, about 50 % of the initial COD was converted to methane.

Figure 5.2 presents Se removal during the degradation test. Only about 10% of Se removal was observed after 2 days of incubation, which increased to about 95 % of Se removal at the end of day 4 of incubation, for both 0.05 and 0.10 mM SeO_4^{2-}. About 95 % of Se removal was accomplished after a day of incubation at 0.05 and 0.10 mM SeO_3^{2-}. Se profiling of the subsequent days also confirmed the removal of Se. The deposition of biogenic elemental Se within the pellets was confirmed through quantification after acidification (Figure 5.5) and with

TEM imaging (Figure 5.7). Figure 5.5 shows that more than 90% soluble Se was completely reduced to insoluble Se^0 in the solid fraction of the digestate. TEM imaging clearly shows the formation of extracellular Se nanospheres in the WAS flocs (Figure 5.7).

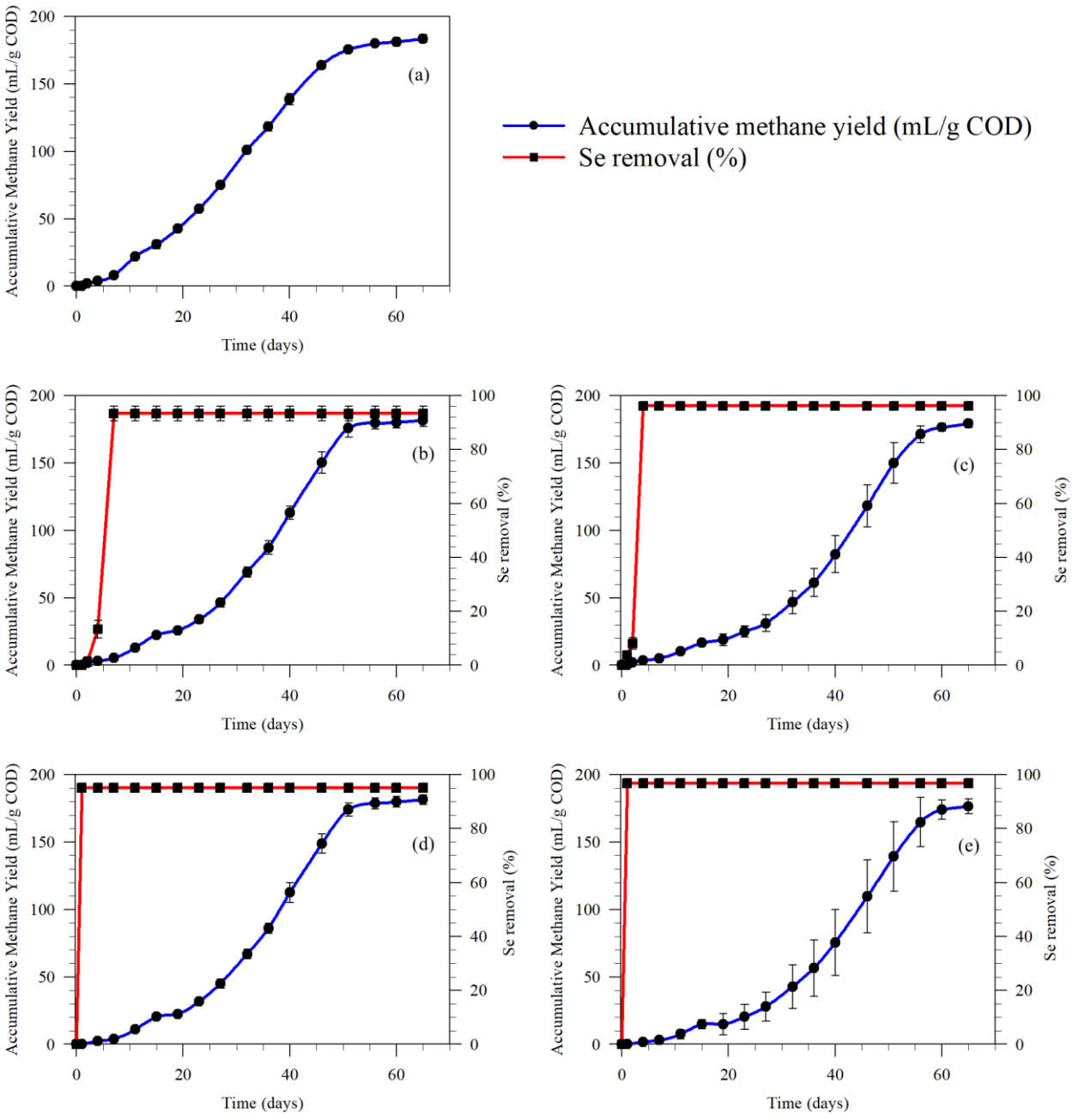

Figure 5.2 Methane production and selenium removal at (a) Control; (b) 0.05 mM SeO_4^{2-}; (c) 0.10 mM SeO_4^{2-}; (d) 0.05 mM SeO_3^{2-} and (e) 0.10 mM SeO_3^{2-}

Table 5.5 Calculated kinetic parameters for the anaerobic digestion of dissolved air floatation (DAF) slurry with and without Se supplementation

Conditions	**$M_{measured}$ (mL/ g COD)**	**M_o (mL/ g COD)**	**Difference (%)**	**R_m (mL/ g COD-d)**	**λ (d)**	**T_m (d)**	**Se removal (%)**	**R^2**
Control	183.49	188.96	2.98	5.39	13.13	26.03	-	0.998
0.05 mM SeO_4^{2-}	181.62	194.96	7.35	5.76	19.69	32.15	93.33	0.995
0.10 mM SeO_4^{2-}	179.16	202.76	13.17	5.51	24.26	37.80	96.19	0.996
0.05 mM SeO_3^{2-}	181.32	193.15	6.53	5.92	20.47	32.47	95.10	0.997
0.10 mM SeO_3^{2-}	176.43	201.00	13.93	5.51	25.71	39.13	96.80	0.997

$M_{measured}$ – Measured methane yield (mL/g COD), M_o – Maximum methane yield (mL/g COD), R_m – Maximum methane production rate (mL/g COD-d), λ – Lag phase (d), T_m – Peak time (d).

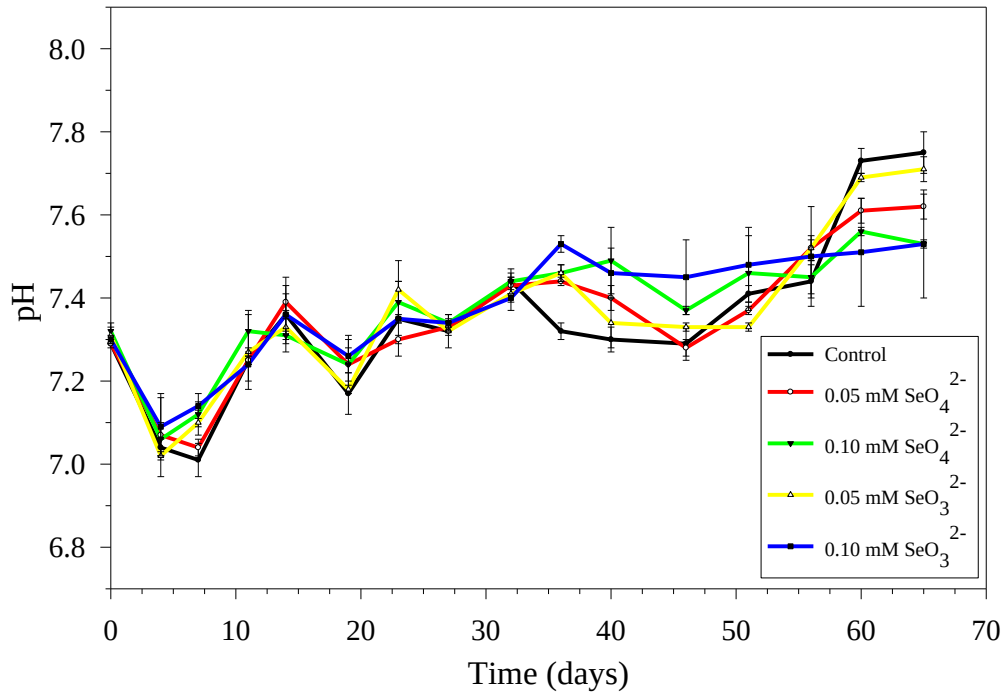

Figure 5.3 pH variation during degradation of selenium supplemented dissolved air floatation slurry

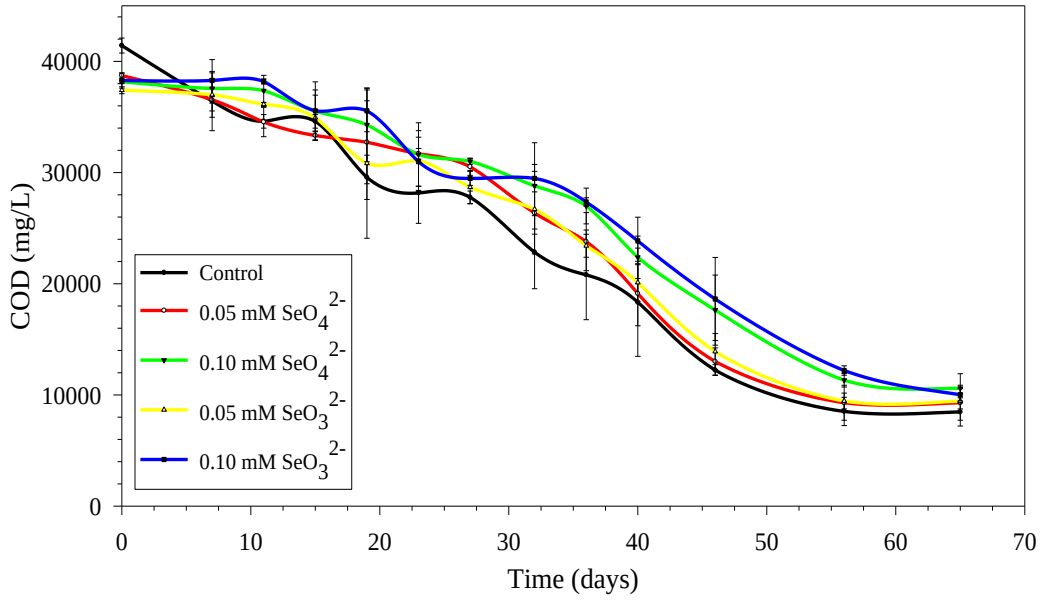

Figure 5.4 COD reduction during degradation of selenium supplemented dissolved air floatation slurry

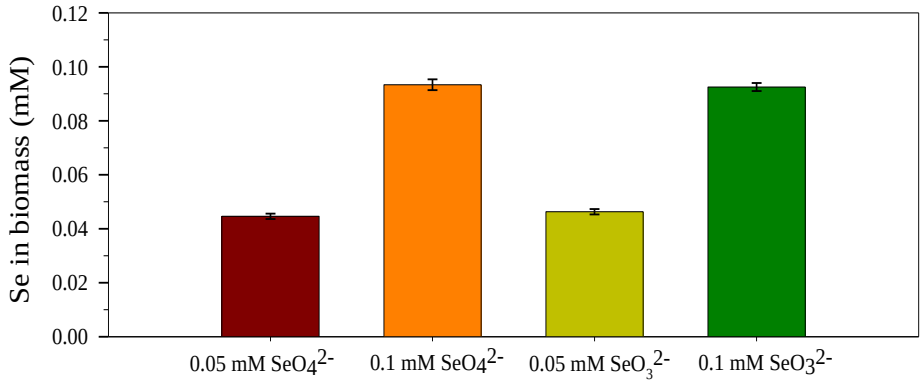

Figure 5.5 Selenium concentration in biomass at the end of the degradation of selenium supplemented dissolved air floatation slurry

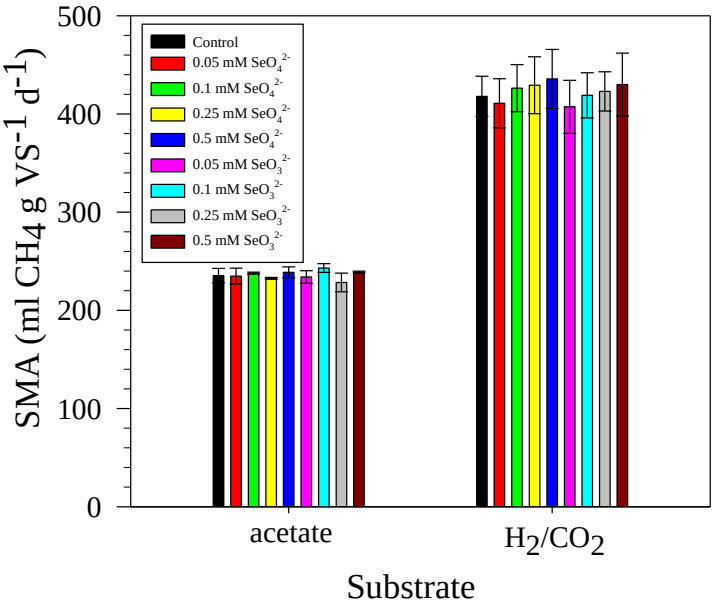

Figure 5.6 Specific methanogenic activity (SMA) test (30 ºC, 120 rpm, 48 hours) using simple substrates (acetate and H_2/CO_2) with waste activated sludge and with and without the presence of selenate and selenate concentrations (0.05, 0.1, 0.25 and 0.5 mM)

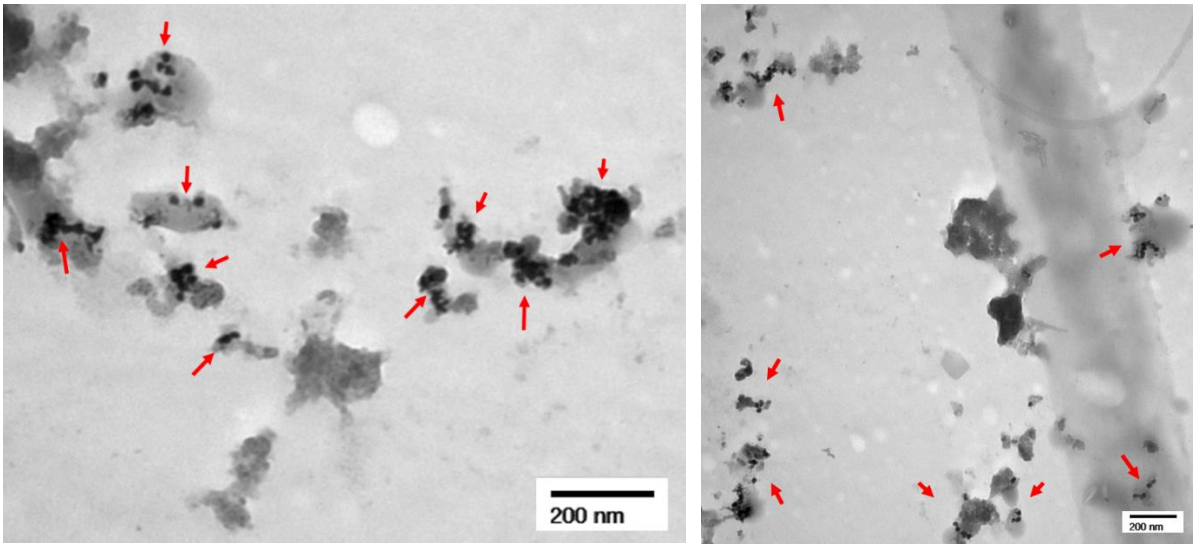

Figure 5.7 TEM images showing the presence of selenium nanoparticles inside the waste activated sludge flocs (red arrow marked showed presence of selenium)

5.3.3 Specific methanogenic activity of acetate and H_2/CO_2 in the presence of Se oxyanions

Unlike DAF slurry, using simple direct methanogenic substrates showed no Se oxyanion toxicity even at the higher concentrations tested up to 0.50 mM (Figure 5.6). No significant differences ($p > 0.05$) were observed in the SMA for all conditions reaching an activity of 235 ml CH_4 g VS^{-1} d^{-1} with acetate as the substrate. Likewise, a higher SMA of about 420 ml CH_4 g VS^{-1} d^{-1} was recorded with H_2/CO_2 as the substrate, which was not significantly different ($p > 0.05$) for all Se concentrations tested.

5.4 Discussion

5.4.1 Concomitant methane production and selenium bioremediation during anaerobic digestion of DAF slurry in selenium oxyanion presence

This study showed the feasibility of simultaneous methane generation and Se removal during AD of DAF slurry mixed with selenate or selenite rich wastewater. Most of the Se contaminated wastewaters have a low COD content and therefore the cost for the electron donor is a main concern for an economical process. Therefore, along with the methane recovery, the operational costs could be partially retrieved by mixing Se-rich (and COD poor) wastewaters with other substrates. In this study, the intermediate compounds from the DAF slurry were used as the electron donors for Se reduction (Figure 5.8).

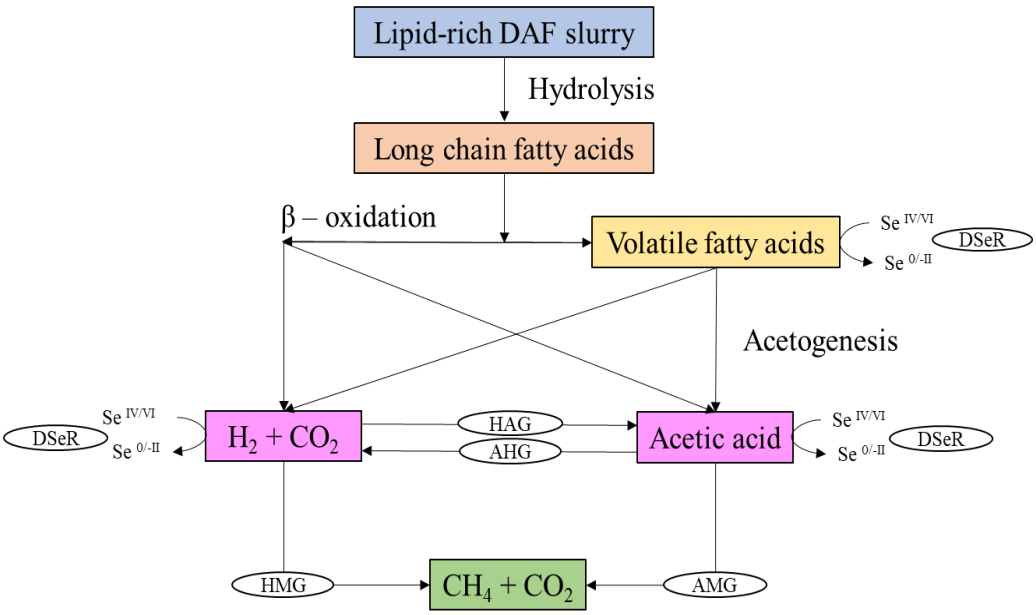

Figure 5.8 Possible pathway for anaerobic digestion of dissolved air floatation slurry supplemented with selenium oxyanions (DSeR = dissimilatory selenium reducers; AHG = acetoclastic hydrogenogens; HAG = hydrogenotrophic acetogens; AMG = acetoclastic methanogens; HMG = hydrogenotrophic methanogens)

Few studies have demonstrated complex organic wastes are suitable as electron donors for Se reduction, such as rice straw (Siddique et al., 2005) and molasses (Zhang et al., 2008). Though microbial reduction of both SeO_4^{2-} and SeO_3^{2-} under anaerobic conditions have been documented, to the best of our knowledge, there have been no studies on the reduction of these oxyanions in BMP assays using DAF slurry as the substrate.

In addition to the anaerobic microbial processes (e.g. dissimilatory reduction) and detoxification mechanisms, Se interactions and other processes (e.g. adsorption and precipitation) might also contribute to the removal of Se from the Se-containing wastewater (Mal et al., 2017). Additionally, the cost from chemical (acid/alkaline) addition can be avoided when Se-laden wastewaters mixed with organic substrates results in a desirable near neutral pH. The optimal pH for the biological reduction of SeO_4^{2-} and SeO_3^{2-} is near neutral (~7.0) for most anaerobic bacteria (Sinharoy and Lens, 2020), which is also the optimal range for methanogenic activity. Lowering the pH to 5.0 reduces the Se removal efficiency by 20-30% (Tan et al., 2018), and acidic environments (pH < 6.5) can also be detrimental to methanogens (Logan et al., 2019). This indicates that both selenium reduction and methanogenesis can occur simultaneously in a single-stage reactor.

The Pourbaix diagram for selenium indicating the thermodynamically preferred oxidation states of selenium within bioreactor operational conditions has been presented by Alhasan et al. (2019). Alterations in pH and redox conditions may cause a shift in equilibrium distributions of individual Se species. In a methanogenic bioreactor operated at near neutral pH, the selenium species of SeO_4^{2-}, $HSeO_3^-$, Se^0 and HSe^- are predominately expected, depending on the redox potential. Interaction of these intermediates (especially the unstable HSe^- species) can occur with minerals or other acid metabolites present. Se speciation and redox potential measurements were not included in this study and can be further considered in future works to elucidate the metabolite formation and interactions.

Mixed microbial communities of granular and activated sludge, instead of pure cultures are more suitable inocula for anaerobic digesters (Piacenza et al., 2017). Several bacterial species including *Pseudomonas* (Otsuka et al., 2020), *Clostridium* (Bao et al., 2013), *Rhodopseudomonas* (Li et al., 2014), *Rhodobacter* (Borghese et al., 2014), *Bacillus* (Bao et al., 2016), *Chrysiogenetes* and *Deferribacteres* (Narasingarao and Häggblom, 2007) produce elemental Se nanoparticles from Se oxyanions using different substrates in anaerobic environments. Very few microorganisms, such as *Syntrophomonas* sp., and *Thermosyntropha* sp., are capable of utilizing mono- and/or polyunsaturated LCFA during anaerobic treatment of wastewaters (Alves et al., 2009). The microbial community dynamics between MPA and SeRB should be investigated in future research. This will throw light on the inhibition of archaeal activity by SeRB.

This study indicates the ability of the SeO_4^{2-} and SeO_3^{2-} reducers to alter the electron flow from methanogens. This suggests that probably selenium-reducing bacteria have a higher substrate affinity than the MPA, and consume hydrogen below a minimum threshold for hydrogen metabolism by methanogens. This has also been observed between sulfate-reducing bacteria (SRB) and MPA in sulfate-rich environments (Kristjansson and Schönheit, 1983). In methanogenic dominant Se concentrations, the electron flow was shared between both MPA and selenium reducing bacteria (SeRB) (Wu et al., 2018). Whereas at higher inhibitory Se concentrations, the electron flow shifted towards SeRB for selenate/selenite reduction depriving MPA.

5.4.2 Toxicity of selenium oxyanions to methane production from DAF slurry

Despite methane production still being realised with AGS at higher SeO_4^{2-} concentrations (≤ 0.25 mM), the AD process suffered inhibition by SeO_3^{2-} toxicity (Figure 5.1). This study shows that SeO_3^{2-} is irreversibly inhibitory upon a single exposure with granular sludge (Figure 5.1). Using WAS, methane production was realised from Se-rich wastewaters up to 0.10 mM SeO_4^{2-} and SeO_3^{2-}. Unlike AGS, waste activated sludge did not exhibit SeO_3^{2-} toxicity and was able to achieve a similar methane yield as that of Se free substrate.

Only a few studies have reported about Se inhibition of methanogenesis. Lenz et al. (2008a) reported that the IC_{50} of both Se oxyanions was below 6.1 x 10^{-5} M in hydrogenotrophic assays, whereas acetoclastic methanogens were less inhibited: IC_{50} = 8.3 x 10^{-5} M and 5.5 x 10^{-4} M for SeO_3^{2-} and SeO_4^{2-}, respectively. Liang et al. (2020) found high selenium concentrations (30-120 mg/L) decreased the methane yield from pig manure by 23-100% and the methane production rate by 1.3-100% (IC_{50} = 77.3 mg/L). More recently, Roy et al. (2022) reported that AD of waste sewage sludge, which realized methane production at 50 mg/L sodium selenite, was completely inhibited at 100 mg/L sodium selenite. The toxic effects on AD of rice straw (IC_{50} = 79.9 mg/L) was observed when the supplemented Se concentration exceeded 100 mg/L (Cai et al., 2018). With DAF slurry, the IC_{50} value was 11.4 mg/L for SeO_4^{2-} and 8.9 mg/L for SeO_3^{2-}, as shown in Table 5.6.

Hydrogenotrophic activity showed a higher SMA compared to acetoclastic activity in the presence of Se oxyanions (Figure 5.6). Rinzema et al. (1992) showed that the obligate hydrogen producing acetogenic bacteria and hydrogenotrophic methanogens recover first from the toxic effect of LCFA, followed by acetotrophic methanogens. Similarly, Molaey et al. (2018) reported that hydrogenotrophic methanogens were the dominant pathway in AD of chicken manure with high ammonia concentrations by supplementing Se. The specific methanogenic activity was unaffected by Se with both simpler substrates (Figure 5.6), indicating Se oxyanions create inhibition in the initial steps of the LCFAs degradation in the lipid-rich DAF slurry. This suggests that less complex feedstocks (unlike DAF slurry) could be used as the carbon source for anaerobic treatment of Se-laden wastewaters with less concerns for inhibition.

This study indicates the detoxification of Se oxyanions by their reduction to elemental Se occurred prior to the commencement of the AD process (Figure 5.2). Lenz et al. (2008a) reported that SeO_3^{2-} treating granules contained elemental Se deposits over the whole cross

section, whereas SeO_4^{2-} treating granules showed elemental Se deposits only in the outer layer. The incomplete inhibition observed in the presence of SeO_4^{2-} compared to SeO_3^{2-} could thus be due to the protection of methane producing archaea (MPA) in the core of the granules. Future research is required on the role of the penetration and deposition of different Se species in granules on the inhibition of the microbial communities. The high reactivity of SeO_3^{2-} to form strong and stable bonds with organic matter (Lussier et al., 2003) allows for its easy and fast removal from waste streams (Figure 5.2), while SeO_4^{2-} is less reactive and forms weakly bound complexes and is therefore harder to remove from the wastewater (Cálix et al., 2019). Further, there is a longer lag phase before insoluble LCFAs (such as palmitate) are converted to shorter chains (Alves et al. 2009).

SeO_4^{2-} and SeO_3^{2-} toxicity at higher concentrations using WAS could also be due to synergistic toxicity from additional inhibitors formed during the conversion of Se oxyanion (e.g. hydrogen selenide, which could in turn form selenocysteine and selenomethionine), change in enzyme functionality, accumulation of carboxylic acids, and increased production of reactive oxygen species to which anaerobes are sensitive (Dong et al., 1994; Lenz et al., 2s008a). Similar toxicity due to sulfur oxyanions in AD is well established (Mahesh et al., 2018).

Table 5.6 IC_{50} values for different electron donor and Se speciation

Electron donor	**Inoculum**	**pH**	**Temperature (ºC)**	**Se speciation**	**IC_{50} (mg/L)**	**Reference**
Acetate	Anaerobic granular treating paper mill wastewater	~ 7	30	SeO_4^{2-} and SeO_3^{2-}	8.7	Lenz et al., 2008
Hydrogen	Anaerobic granular treating paper mill wastewater	~ 7	30	SeO_4^{2-}	78.6	Lenz et al., 2008
Hydrogen	Anaerobic granular treating paper mill wastewater	~ 7	30	SeO_3^{2-}	10.5	Lenz et al., 2008
Rice straw	Biogas plant treating cow manure	n.a.	35	SeO_3^{2-}	79.9	Cai et al., 2018
Pig manure	Anaerobic culture	6.8-7.8	35	SeO_3^{2-}	77.3	Liang et al., 2020
DAF slurry (from dairy wastewater)	Waste activated sludge treating domestic wastewater	7.0-8.0	30	SeO_4^{2-}	11.4	This study
DAF slurry (from dairy wastewater)	Waste activated sludge treating domestic wastewater	7.0-8.0	30	SeO_3^{2-}	8.9	This study

n.a. – not available

5.4.3 Prospects for anaerobic digestion of selenium laden wastewater

This study demonstrated an integrated approach of simultaneous methane (Figure 5.1) and Se nanoparticles recovery (Figure 5.7). This finds application and relevance in oil refinery industries that generate effluents with high lipid as well as Se concentrations. For instance, an Se content of 0.30 mg/L and an oil and grease concentration of 6.41 mg/L in petroleum refinery wastewaters was reported by Hansen et al. (2019). Refineries typically use the DAF technique to remove free and emulsified oil from refinery wastewater, thus producing DAF slurry (Haak et al., 2016). However, wastewater from oil refineries will become contaminated with other compounds such as nitrogen, sulfur, and an array of toxic organic compounds such as phenols and volatile aromatics (El-Naas et al., 2014). These toxic contaminants need to be removed from these oil refinery effluents as well before being used as feed in AD plants. Future studies are therefore required to investigate the effects from co-contaminants on AD. This study serves as a benchmark providing an alternative approach to dealing with oil refinery waste and establishing whether DAF slurry can be digested and how Se concentrations can impact the process.

Few studies have shown that volatile fatty acids, intermediates from the AD of DAF slurry, can serve as an electron donor for Se reduction (Nanchariah and Lens, 2015a). Therefore, DAF slurry can also serve as electron donor for Se reduction (Figure 5.2). AD bioreactors with a high Se removal efficiency may serve as an alternate option to cost-, energy- and chemical-intensive physico-chemical Se removal techniques such as precipitation and electrocoagulation. The biogenic Se nanoparticles synthesised are mostly located in the extracellular spaces and retained in the biomass (Jain et al., 2017).

With realisation of methane yield but with an extended lag phase duration, continuous methane production from Se rich wastewaters through a longer initial hydraulic retention time or acclimatization phase during the start-up of the bioreactor should be investigated in future research. Additionally, the optimization of the operational parameters viz., pH, temperature, loading rate, retention time, and solid content that determine the methane production rate from Se rich wastewater is required in future research (Meegoda et al., 2018). Evaluation of long term and repeated exposure of Se oxyanions on methanogenesis needs to be evaluated as well.

To the best of our knowledge, there are no established pilot and full scale anaerobic digesters treating DAF slurry or Se-rich wastewater, owing to their process challenges as

discussed in this chapter and their high operational and maintenance costs. There is a huge scope for a detailed techno-economic assessment of AD of these two substrates, which has so far not been conducted. The operational cost of AD of DAF slurry and Se-rich wastewater is estimated to be higher due to their prolonged lag phase and requirements of mixing, pumping and digestate handling (Fagbohungbe et al., 2015). Further, the collection of Se-rich wastewater for AD, and transportation of selenium enriched digestate for land application on Se-deficit soils will add up to the overall costs.

5.5 Conclusion

This study demonstrates an integrated approach of methane production and selenium bioremediation during anaerobic treatment of Se oxyanion containing wastewaters. AD of a DAF slurry at 0.10 mM SeO_4^{2-} and SeO_3^{2-} realised a similar cumulative methane yield of about 180 mL/g COD as that of Se free Control after 65 days of incubation, however with an up to double fold increase in the lag phase duration. The IC_{50} value for methane production was 0.08 and 0.07 mM, respectively, for SeO_4^{2-} and SeO_3^{2-} with WAS as the inoculum. AGS allowed methane recovery from the DAF slurry in the presence of selenate (IC_{50} = 2.10 mM), but suffered inhibition by selenite (IC_{50} = 0.08 mM). More than 90 % of the Se concentration was removed by day 4 of incubation. TEM images suggest the formation of extracellular Se nanospheres inside the flocs of the WAS.

5.6 References

Alhasan, R., Nasim, M.J., Jacob, C., Gaucher, C., 2019. Selenoneine: a unique reactive selenium species from the blood of tuna with implications for human diseases. Current Pharmacology Reports 5, 163 – 173. https://doi.org/10.1007/s40495-019-00175-8

Alves, M.M., Pereira, M.A., Sousa, D.Z., Cavaleiro, A.J., Picavet, M., Smidt, H., Stams, A.J.M., 2009. Waste lipids to energy: how to optimize methane production from long-chain fatty acids (LCFA). Microbial Biotechnology 5, 538-550. https://doi.org/10.1111/j.1751-7915.2009.00100.x

Alves, M.M., Vieira, J.A.M., Pereira, R.M.A., Pereira, M.A., Novais, J.M., Mota, M., 2001. Effects of lipids and oleic acid on biomass development in anaerobic fixed reactors. Part II: oleic acid toxicity and biodegradability. Water Research 35, 264-270. https://doi.org/10.1016/S0043-1354(00)00242-6

Andalib, M., Arabi, S., Dold, P., Bye, C., 2016. Mathematical modelling of biological selenium removal from flue gas desulfurization (FGD) wastewater treatment. Proceedings of the Water Environment Federation 11, 228-248.

Angelonidi, E., Smith, S.R., 2015. A comparison of wet and dry anaerobic digestion processes for the treatment of municipal solid waste and food waste. Water and Environment Journal 29, 549-557. https://doi.org/10.1111/wej.12130

APHA, 2017. APHA Standard Methods for the Examination of Water and Wastewater (23rd edition), American Public Health Association, Washington, D.C., USA. ISBN: 9780875532875.

Ariunbaatar, J., Esposito, G., Yeh, D.H., Lens, P.N.L., 2016. Enhanced anaerobic digestion of food waste by supplementing trace elements: role of Selenium (VI) and Iron (II). Frontiers in Environmental Science and Engineering 4(8). https://doi.org/10.3389/fenvs.2016.00008

Astratinei, V., van Hullebusch, E., Lens, P.N.L., 2006. Bioconversion of selenate in methanogenic anaerobic granular sludge. Journal of Environmental Quality 35, 1873-1883. https://doi.org/10.2134/jeq2005.0443

Awe, O.W., Zhao, Y., Nzihou, D., Pham Minh, D., Lyczko, N., 2018. Anaerobic co-digestion of food waste and FOG with sewage sludge – realising its potential in Ireland. International Journal of Environmental Studies 75, 496-504. https://doi.org/10.1080/00207233.2017.1380335

Bao, P., Huang, H., Hu, Z.Y., Häggblom, M.M., Zhu, Y.G., 2013. Impact of temperature, CO_2 fixation and nitrate reduction on selenium reduction, by a paddy soil Clostridium strain. Journal of Applied Microbiology 114, 703-12. https://doi.org/10.1111/jam.12084

Borghese, R., Baccolini, C., Francia, F., Sabatino, P., Turner, R.J., Zannoni, D., 2014. Reduction of chalcogen oxyanions and generation of nanoprecipitates by the photosynthetic bacterium *Rhodobacter capsulatus.* Journal of Hazardous Materials 269, 24-30. https://doi.org/10.1016/j.jhazmat.2013.12.028

Browne, J.D., Allen, E., Murphy, J.D., 2013. Evaluation of the biomethane potential from multiple waste streams for a proposed community scale anaerobic digester. Environmental Technology 34, 2027-2038. https://doi.org/10.1080/09593330.2013.812669

Buchs, B., Evangelou, M.W.H., Winkel, L.H.E., Lenz, M., 2013. Colloidal properties of nanoparticular biogenic selenium govern environmental fate and bioremediation effectiveness. Environmental Science and Technology 47, 2401-2407. https://doi.org/10.1021/es304940s

Cai, Y., Zheng, Z., Zhao, Y., Zhang, Y., Guo, S., Cui, Z., Wang, X., 2018. Effects of molybdenum, selenium and manganese supplementation on the performance of anaerobic digestion and the characteristics of bacterial community in acidogenic stage. Bioresource Technology 266, 166-175. https://doi.org/10.1016/j.biortech.2018.06.061

Cálix, E.M., Tan, L.C., Rene, E.R., Nancharaiah, Y.V., van Hullebusch, E.D., Lens, P.N.L., 2019. Simultaneous removal of sulfate and selenate from wastewater by process integration of an ion exchange column and upflow anaerobic sludge blanket bioreactor. Seperation Science and Technology 54(8), 1387-1399. https://doi.org/10.1080/01496395.2018.1533562

Caporaso, J.G., Lauber, C.L., Walters, W.A., Berg-Lyons, D., Lozupone, C.A., Turnbaugh, P.J., Fierer, N., Knight, R., 2011. Global patterns of 16S rRNA diversity at a depth of millions of sequences per sample. Proceedings of the National Academy of Sciences of the United States of America 108(1), 4516-4522. https://doi.org/10.1073/pnas.1000080107

Chuenchart, W., Logan, M., Leelayouthayotin, C., Visvanathan, C., 2020. Enhancement of food waste thermophilic anaerobic digestion through synergistic effect with chicken manure. Biomass and Bioenergy 136, 105541. https://doi.org/10.1016/j.biombioe.2020.105541

Chung, J., Nerenberg, R., Rittman, B.E., 2006. Bioreduction of selenate using a hydrogen-based membrane biofilm reactor. Environmental Science and Technology 40, 1664-1671. https://doi.org/10.1021/es051251g

Colleran, E., Concannon, F., Golden, T., Geoghegan, F., Crumlish, B., Killilea, E., Henry, M., Coates, J., 1992. Use of methanogenic activity tests to characterize anaerobic sludges, screen for anaerobic biodegradability and determine toxicity threshold against individual anaerobic trophic groups and species. Water Science and Technology 25, 31-40.

Colleran, E., Finnegan, S., Lens, P., 1995. Anaerobic treatment of sulphate-containing waste streams. Antonie van Leeuwenhoek 67, 29-46. https://doi.org/10.1007/BF00872194

Colleran, S., Pender, S., 2002. Mesophilic and thermophilic anaerobic digestion of sulphate-containing wastewaters. Water Science and Technology 45, 231-235. https://doi.org/10.2166/wst.2002.0339

Costa, R.B., O'Flaherty, V., Lens, P.N.L., 2020. Biological treatment of organic sulfate-rich wastewaters. In book: Environmental Technologies to Treat Sulphur Pollution: Principles and Engineering. IWA Publishing, London, UK. http://dx.doi.org/10.2166/9781789060966_0167

Dong, X., Plugge, C.M., Stams, A.J.M., 1994. Anaerobic degradation of propionate by a mesophilic acetogenic bacterium in coculture and triculture with different methanogens. Applied and Environmental Microbiology 60, 2834-2838.

Fagbohungbe, M.O., Dodd, I.C., Herbert, B.M.J., Li, H., Ricketts, L., Semple K.T., 2015. High solid anaerobic digestion: Operational challenges and possibilities. Environmental Technology and Innovation 4, 268-284. https://doi.org/10.1016/j.eti.2015.09.003

Fellowes, J.W., Pattrick, R.A.D., Lloyd, J.R., Charnock, J.M., Coker, V.S., Mosselmans, W., Weng, T.C., Pearce, C.I., 2013. Ex situ formation of metal selenide quantum dots using bacterially derived selenide precursors. Journal of Nanotechnology 24, 145603-145612. https://doi.org/10.1088/0957-4484/24/14/145603

Florentino, A.P., Costa, R.B., Hu, Y., O'Flaherty, V., Lens, P.N.L., 2020. Long chain fatty acid degradation coupled to biological sulfidogenesis: A prospect for enhanced metal recovery. Frontiers in Bioengineering and Biotechnology 8, 550253. https://doi.org/10.3389/ fbioe.2020.550253

Griffiths, R.I., Whiteley, A.S., O'Donnell, A.G., Bailey, M.J., 2000. Rapid method for coextraction of DNA and RNA from natural environments for analysis of ribosomal DNA- and rRNA- based microbial community composition. Applied and Environmental Microbiology 66(12), 5488-5491. https://dx.doi.org/10.1128/AEM.66.12.5488-5491.2000

Haak, L., Roy, R., Pagilla, K., 2016. Toxicity and biogas production potential of refinery waste sludge for anaerobic digestion. Chemosphere 144, 1170-1176. https://doi.org/10.1016/j.chemosphere.2015.09.099

Han, W., Mao, Y., Wei, Y., Shang, P., Zhou, X., 2020. Bioremediation of aquaculture wastewater with algal-bacterial biofilm combined with the production of selenium rich biofertilizer. Water 12, 7. https://doi.org/10.3390/w12072071

Hansen, H.K., Pena, S.F., Gutiérrez, C., Lazo, A., Lazo, P., Ottosen, L.M., 2019. Selenium removal from petroleum refinery wastewater using an electrocoagulation technique. Journal of Hazardous Materials 364, 78-81. https://doi.org/10.1016/j.jhazmat.2018.09.090

Harris, P.W.; Schmidt, T.; McCabe, B.K. 2017. Evaluation of chemical, thermobaric and thermochemical pre-treatment on anaerobic digestion of high-fat cattle slaughterhouse waste. Bioresource Technology 244, 605–610. https://doi.org/10.1016/j.biortech.2017.07.179

Haug, A., Graham, R.D., Christophersen, O.A., Lyons, G.H., 2007. How to use the world's scarce selenium resources efficiently to increase the selenium concentration in food. Microbial Ecology in Health and Disease 19, 209-228. https://doi.org/10.1080/08910600701698986

Illumina, 2013. 16S Metagenomic Sequencing Library Preparation. http://support.illumina.com/content/dam/illumina-support/documents/documentation/chemistry_documentation/16s/16s-metagenomic-library-prep-guide-15044223-b.pdf.

Jain, R., Seder-Colomina, M., Jordan, N., Dessi, P., Cosmidis, J., van Hullebusch, E.D., Weiss, S., Farges, F., Lens, P.N.L., 2015. Entrapped elemental selenium nanoparticles affect physiochemical properties of selenium fed activated sludge. Journal of Hazardous Materials 295, 193-200. https://doi.org/10.1016/j.jhazmat.2015.03.043

Jain, R., van Hullebusch, E.D., Lenz, M., Farges, F., 2017. Understanding selenium biogeochemistry in engineered ecosystems: transformation and analytical methods. Bioremediation of selenium contaminated wastewater. Springer. https://doi.org/10.1007/978-3-319-57831-6_2

Kagami, T., Narita, T., Kuroda, M., Notaguchi, E., Yamashita, M., Sei, K., Soda, S., Ike, M., 2013. Effective selenium volatilization under aerobic conditions and recovery from the aqueous phase by *Pseudomonas stutzeri* NT-I. Water Research 47(3), 1361-1368. https://doi.org/10.1016/j.watres.2012.12.001

Koster, I.W., Rinzema, A., de Vegt, A.L., Lettinga, G., 1986. Sulfide inhibition of the methanogenic activity of granular sludge at various pH-levels. Water Research 20, 1561-1567. https://doi.org/10.1016/0043-1354(86)90121-1

Kozich, J.J., Westcott, S.L., Baxter, N.T., Highlander, S.K., Schloss, P.D., 2013. Development of a dual-index sequencing strategy and curation pipeline for analyzing amplicon sequence data on the miseq illumine sequencing platform. Applied and Environmental Microbiology 79, 5110-5120. https://doi.org/10.1128/AEM.01043-13

Kristjansson, J.K., Schönheit, P., 1983. Why do sulfate-reducing bacteria outcompete methanogenic bacteria for substrates. Oecologia, 60(2), 264-266.

Lemly, A.D., 2018. Selenium poisoning of fish by coal ash wastewater in Herrington Lake, Kentucky. Ecotoxicology and Environmental Safety 150, 49-53. https://doi.org/10.1016/j.ecoenv.2017.12.013

Lenz, M., Janzen, N., Lens, P.N.L., 2008a. Selenium oxyanion inhibition of hydrogenotrophic and acetoclastic methanogenesis. Chemosphere 73(3), 383-388. https://doi.org/10.1016/j.chemosphere.2008.05.059

Lenz, M., van Hullebusch, E.D., Hommes, G., Corvini, P.F.X., Lens, P.N.L., 2008b. Selenate removal in methanogenic and sulfate-reducing upflow anaerobic sludge bed reactors. Water Research 42(8-9), 2184-2194. https://doi.org/10.1016/j.watres.2007.11.031

Li, C., Champagne, P., Anderson, B.C, 2013. Biogas production of mesophilic and thermophilic anaerobic co-digestion with fat, oil, and grease in semi-continuous flow digesters: effects of temperature, hydraulic retention time, and organic loading rate. Environmental Technology 34, 2125-2133. https://doi.org/10.1080/09593330.2013.824010

Li, B., Liu, N., Li, Y., Jing, W., Fan, J., Li, D., et al. 2014. Reduction of selenite to red elemental selenium by *Rhodopseudomonas palustris* strain. N. PLoS One. 9:e95955. https://doi.org/10.1371/journal.pone.0095955

Liang, Y.G., Bao, J., Ding, J., Tang, J.Y., Li, W., Zhang, L.G., Zhang, Y.H., 2020. Process performance and microbial communities in response to selenite addition during anaerobic digestion of pig manure. International Journal of Environmental Science and Technology 17, 3947-3954. https://doi.org/10.1007/s13762-020-02744-7

Logan, M., Tan, L.C., Nzeteu, C.O., Lens, P.N.L., 2022. Enhanced anaerobic digestion of dairy wastewater in a granular activated carbon amended sequential batch reactor. GCB-Bioenergy 14(7), 840-857. https://doi.org/10.1111/gcbb.12947

Logan, M., Ravishankar, H., Tan, L.C., Lawrence, J., Fitzgerald, D., Lens, P.N.L., 2021. Anaerobic digestion of dissolved air floatation slurries: Effect of substrate concentration and pH. Environmental Technology and Innovation https://doi.org/10.1016/j.eti.2020.101352

Logan, M., Safi, M., Lens, P., Visvanathan, C., 2019. Investigating the performance of internet of things based anaerobic digestion of food waste. Process Safety and Environmental Protection 127, 277-287. https://doi.org/10.1016/j.psep.2019.05.025

Lundquist, T.J., Baily Green, F., Blake Tresan, R., Newman, R.D., Oswald, W.J., Gerhardt, M.B., 1994. The algal-bacterial selenium removal system: mechanisms and field study. In: Selenium in the Environment. Pergamon Press, New York, USA.

Lussier, C., Veiga, V., Baldwin, S., 2003. The geochemistry of selenium associated with coal waste in the Elk River Valley, Canada. Journal of Environmental Geology 44, 905-913. https://doi.org/10.1007/S00254-003-0833-Y

Madden, P., Al-Raei, A.M., Enright, A.M., Chinalia, F.A., de Beer, D., O'Flaherty, V., Collins, G., 2014. Effect of sulfate on low-temperature anaerobic digestion. Frontiers in Microbiology 5, 376. https://doi.org/10.3389/fmicb.2014.00376

Mahesh, M., Arivizhivendhan, K.V., Nivetha, K., Swarnalatha, S., Sekaran, G, 2018. Anaerobic digestion of sulphate-rich post-tanning wastewater at different COD/sulphate and F/M ratios. 3 Biotechnology 8(2), 130. https://dx.doi.org/10.1007%2Fs13205-018-1154-x

Mal, J., Nancharaiah, Y.V., van Hullebusch, E.D., Lens, P.N.L., 2016. Effect of heavy metal co contaminants on selenite bioreduction by anaerobic granular sludge. Bioresource Technology 206, 1-8. https://doi.org/10.1016/j.biortech.2016.01.064

Mal, J., Nancharaiah, Y.V., Bera, S., Maheshwari, N., van Hullebusch, E.D., Lens, P.N.L., 2017. Biosynthesis of CdSe nanoparticles by anaerobic granular sludge. Environmental Science: Nanotechnology, 4, 824-833. https://doi.org/10.1039/C6EN00623J

Martinez, E.J., Gil, M.V., Fernandez, C., Rosas, J.G., Gomez, X., 2016. Anaerobic co-digestion of sludge: addition of butcher's fat waste as a cosubstrate for increasing biogas production. PLoS One 11(4). https://doi.org/10.1371/journal.pone.0153139

Meegoda, J.N., Li, B., Patel, K., Wang, L.B., 2018. A review of the processes, parameters and optimization of anaerobic digestion. International Journal of Environmental Research and Public Health 15, 2224. https://doi.org/10.3390/ijerph15102224

Molaey, R., Bayrakdar, A., Calli, B., 2018. Long-term influence of trace element deficiency on anaerobic mono-digestion of chicken manure. Journal of Environmental Management 223, 743-748. https://doi.org/10.1016/j.jenvman.2018.06.090

Molaey, R., Bayrakhar, A., Sürmeli, R.Ö., Bariş, Ç., 2018. Anaerobic digestion of chicken manure: mitigating process inhibition at high ammonia concentrations by selenium

supplementation. Biomass and Bioenergy 108, 439-446. https://doi.org/10.1016/j.biombioe.2017.10.050

Nancharaiah, Y.V., Lens, P.N.L., 2015a. Ecology and biotechnology of selenium-respiring bacteria. Microbiology and Molecular Biology Reviews 79, 61-80. https://doi.org/10.1128/MMBR.00037-14

Nancharaiah, Y.V., Lens, P.N.L., 2015b. Selenium biomineralization for biotechnological applications. Trends in Biotechnology 33(6), 323-330. https://doi.org/10.1016/j.tibtech.2015.03.004

Narasingarao, P., Häggblom, M.M., 2007. Identification of anaerobic selenate-respiring bacteria from aquatic sediments. Applied and Environmental Microbiology 73, 3519-27. https://doi.org/10.1128/AEM.02737-06

O'Flaherty, V., Lens, P., Leahy, B., Colleran, E., 1998. Long-term competition between sulphate-reducing and methane-producing bacteria during full-scale anaerobic treatment of citric acid production wastewater. Water Research 32, 815-825. https://doi.org/10.1016/S0043-1354(97)00270-4

Otsuka, O., Yamashita, M., 2020. Selenium recovery from wastewater using the selenate-reducing bacterium *Pseudomonas stutzeri* NT-I. Hydrometallurgy 197, 105470. https://doi.org/10.1016/j.hydromet.2020.105470

Parada, A.E., Needham, D.M., Fuhrman, J.A., 2016. Every base matters: Assessing small subunit rRNA primers for marine microbiomes with mock communities, time series and global field samples. Environmental Microbiology 18, 1403-1414. https://doi.org/10.1111/1462-2920.13023

Piacenze, E., Presentato, A., Zonaro, E., Lampis, S., Vallini, G., Turner, R.J., 2017. Microbial-based bioremediation of selenium and tellurium compounds. Biosorption. IntechOpen. 117-147. http://dx.doi.org/10.5772/intechopen.72096

Pitk, P., Kaparaju, P., Vilu, R., 2012. Methane potential of sterilized solid slaughterhouse wastes. Bioresource Technology 116, 42-46. https://doi.org/10.1016/j.biortech.2012.04.038

Rajput, A.A., Zeshan, Visvanathan, C., 2018. Effect of thermal pretreatment on chemical composition, physical structure and biogas production kinetics of wheat straw. Journal of Environmental Management 221, 45-52. https://doi.org/10.1016/j.jenvman.2018.05.011

Rinzema, A., Boone, M., van Knippenberg, K., Lettinga, G., 1994. Bactericidal effect of long chain fatty acids in anaerobic digestion. Water Environment Research 66, 40-49.

Roy, C.K., Hoshiko, Y., Toya, S., Maeda, T., 2022. Effect of different concentrations of sodium selenite on anaerobic digestion of waste activated sludge. Environmental Technology and Innovation 27, 102403. https://doi.org/10.1016/j.eti.2022.102403

Sarker, S., Lamb, J.J., Hjelme, D.R., Lien, K.M., 2019. A review of the role of critical parameters in the design and operation of biogas production plants. Applied Sciences 9, 1915. https://doi.org/10.3390/app9091915

Schloss, P.D., Westcott, S.L., Ryabin, T., Hall, J.R., Hartmann, M., Hollister, E.B., Lesniewski, R.A., Oakley, B.B., Parks, D.H., Robinson, C.J., Sahl, J.W., Stres, B., Thallinger, G.G., Van Horn, D.J., Weber, C.F., 2009. Introducing mother: Open-source, platform-independent, community-supported software for describing and comparing microbial communities. Applied and Environmental Microbiology 75, 7537-7541. https://doi.org/10.1128/AEM.01541-09

Schmidt, R., Tantoyotai, P., Fakra, S.C., Marcus, M.A., Yang, S.I., Pickering, I.J., Banuelos, G.S., Hristova, K.R., Freeman, J.L., 2013. Selenium biotransformations in an engineered aquatic ecosystem for bioremediation of agricultural wastewater via brine shrimp production. Environmental Science and Technology 47, 5057-5065. https://dx.doi.org/10.1021/es305001n

Schnürer, A.; Jarvis, Å. 2009. Microbiological Handbook for Biogas Plants-Swedish Waste Management. Swedish Gas Centre Report; Avfall Sverige, Svenskt Gastekniskt Center AB: Malmo, Sweden.

Segata, N., Izard, J., Waldron, L., Gevers, D., Miropolsky, L., Garrett, W.S., Huttenhower, C., 2011. Metagenomic biomarker discovery and explanation. Genome Biology 12. https://doi.org/10.1186/gb-2011-12-6-r60

Sela-Adler, M., Ronen, Z., Herut, B., Antler, G., Vigderovich, H., Eckert, W., Sivan, O., 2017. Co-existence of methanogenesis and sulfate reduction with common substrates in sulfate-rich estuarine sediments. Frontiers in Microbiology 8, 766.

https://dx.doi.org/10.3389%2F
fmicb.2017.00766

Siddique, T., Okeke, B.C., Zhang, Y., Arshad, M., Han, S.K., Frankenberger, W.T., 2005. Bacterial diversity in selenium reduction of agricultural drainage water amended with rice straw. Journal of Environmental Quality 34(1), 217-226.

Sinharoy, A., Lens, P.N.L., 2020. Biological removal of selenate and selenite from wastewater: options for selenium recovery as nanomaterials. Current Pollution Reports 6, 230-249. https://doi.org/10.1007/s40726-020-00146-4

Soda, S., Kashiwa, M., Kagami, T., Kuroda, M., Yamashita, M., Ike, M., 2011. Laboratory-scale bioreactors for selenium removal from selenium refinery wastewater using anaerobic sludge. Desalination 279(1-3), 433-438. https://doi.org/10.1016/j.desal.2011.06.031

Staicu, L.C., van Hullebusch, E.D., Lens, P.N.L., 2015. Production, recovery and reuse of biogenic elemental selenium. Environmental Chemistry Letters 13, 89-96. https://doi.org/10.1007/s10311-015-0492-8

Sun, J., Dai, X., Wang, Q., Pan, Y., Ni, B., 2016. Modelling methane production and sulfate reduction in anaerobic granular sludge reactor with ethanol as electron donor. Scientific Reports 6, 35312. https://doi.org/10.1038/srep35312

Tan, L.C., Lens, P.N.L., 2021. Addition of granular activated carbon during anaerobic oleate degradation overcomes inhibition and promotes methanogenic activity. Environ. Sci.: Water Research and Technology 7, 762-774. https://doi.org/10.1039/D0EW01093F

Tan, L.C., Lin, R., Murphy, J.D., Lens, P.N.L. 2020. Granular activated carbon supplementation enhances anaerobic digestion of lipid-rich wastewaters. Renewable Energy 171, 958-970. https://doi.org/10.1016/j.renene.2021.02.087

Tan, L.C., Nancharaiah, Y.V., Lu, S., van Hullebusch, E.D., Gerlach, R., Lens, P.N.L., 2018. Biological treatment of selenium-laden wastewater containing nitrate and sulfate in an upflow anaerobic sludge bed reactor at pH 5.0. Chemosphere 211, 684-693. https://doi.org/10.1016/j.chemosphere.2018.07.079

Tan, L.C., Nancharaiah, Y.V., van Hullebusch, E.D., Lens, P.N.L., 2016. Selenium: Environmental significance, pollution, and biological treatment technologies. Biotechnology Advances 34(5), 886-907. https://doi.org/10.1016/j.biotechadv.2016.05.005

Tarze, A., Dauplais, M., Grigoras, I., Lazard, M., Ha-Duong, N., Barbier, F., Blanquet, S., Plateau, P., 2007. Extracellular production of hydrogen selenide accounts for thiol-assisted toxicity of selenite against *Saccharomyces cerevisiae.* Journal of Biological Chemistry 282, 8759-8767. https://doi.org/10.1074/jbc.M610078200

Wall, D.M., Allen, E., Straccialini, B., O'Kiely, P., Murphy, J.D., 2014. The effect of trace element addition to mono-digestion of grass silage at high organic loading rates. Bioresource Technology 172, 349-355. https://doi.org/10.1016/j.biortech.2014.09.066

Wu, L.J., Kobayashi, T., Li, Y.Y., Xu, K.Q., Lv, Y., 2017. Determination and abatement of methanogenic inhibition from oleic and palmitic acids. International Biodeterioration and Biodegradation 123, 10-16. https://doi.org/10.1016/j.ibiod.2017.05.021

Wu, J., Niu, Q., Li, L., Hu, Y., Mribet, C., Hojo, T., Li, Y., 2018. A gradual change between methanogenesis and sulfidogenesis during a long-term UASB treatment of sulfate-rich chemical wastewater. Science of The Total Environment 636, 168-176. https://doi.org/10.1016/j.scitotenv.2018.04.172

Wu, L., 2004. Review of 15 years of research on ecotoxicology and remediation of land contaminated by agricultural drainage sediment rich in selenium. Ecotoxicology and Environmental Safety 57(3), 257-269. https://doi.org/10.1016/S0147-6513(03)00064-2

Zhang, Y., Kuroda, M., Arai, S., Kato, F., Inoue, D., Ike, M., 2019. Biological treatment of selenate-containing saline wastewater by activated sludge under oxygen-limiting conditions. Water Research 154, 327-335. https://doi.org/10.1016/j.watres.2019.01.059

Zhang, Y., Okeke, B.C., Frankenberger Jr., W.T., 2008. Bacterial reduction of selenate to elemental selenium utilizing molasses as a carbon source. Bioresource Technology 99, 1267-1273. https://doi.org/10.1016/j.biortech.2007.02.048

Zwietering, M., Jongenburger, I., Rombouts, F., Van't Riet, K., 1990. Modeling of the bacterial growth curve. Applied and Environmental Microbiology 56 (6), 1875-1881.

Chapter 6 Influence of pH, heat treatment of inoculum and selenium oxyanions on concomitant volatile fatty acids production and selenium bioremediation using food waste

Abstract

This study hypothesised to improve the VFA yield of food waste via three strategies viz., pH adjustment (5 and 10), chemical inhibitor addition (selenate, SeO_4^{2-} and selenite, SeO_3^{2-}; until 500 µM), and heat treatment of the inoculum (at 85 ^oC for 1 hour). The highest VFA yield of about 0.516 g COD/g VS was achieved at pH 10, which was 45% higher than the maximum VFA production (~ 0.355 g COD/g VS) at pH 5. Heat treatment (HT) of the inoculum resulted in VFA accumulation after day 10 in alkaline conditions, possibly due to its suppression of the methane conversion. Acetic and propionic acid contributed for about 80% of the VFA produced at the methanogenic condition of pH 10 with non-heat treated (NHT) inoculum. Conversely, the VFA composition diversified at pH 5 (HT and NHT) without isocaproate and pH 10 (HT) without caproate. The study suggests Se oxyanions could act as chemical inhibitor to improve the VFA yield in methanogenic conditions (pH 10 and NHT). Albeit VFA yields were not significantly different due to neither heat treatment of the inoculum nor Se oxyanion supplementation at acidic conditions. In the presence of SeO_4^{2-}, pH 10 with non-heat treated inoculum resulted in > 95% Se removal on day 1. Heat treatment (HT) was found to be detrimental for selenate reduction, with less than 15 % Se removal even after 20 days of incubation. On the other hand, ~ 95% Se removal was observed on day 1 with all the tested conditions in the presence of SeO_3^{2-}. Simultaneously biosynthesised Se nanoparticles were confirmed by TEM, SEM and SEM-EDX.

6.1 Introduction

Bio-based circular economy regards organic waste as a potential resource that can be utilized to recover valuable fuels, nutrients and chemicals. Resource recovery from waste streams helps to achieve the ambitious target of net-zero carbon emissions by 2050 as well as the United Nations Sustainable Development Goals (Lemaire and Limbourg, 2019). With one-third of food produced ending up as waste, food waste alone generates about 8 – 10% of the global greenhouse gas emissions (UNEP, 2021). Notably, Europe dominated the food waste management market and accounted for 32.4% share of the global revenue in 2019, owing to reasons such as excessive shopping, improper food management, overproduction and negligence for food wasted (Market Data Forecast, 2021).

Methane, which is the final end product of anaerobic digestion (AD), has low commercial value of less than € 0.1 per m^3 (Veluswamy et al., 2021). Further, challenges from

fugitive methane emissions and affordable solar and wind energy in the recent times raises concerns over the long term sustainability of the AD technology for renewable energy production. On the other hand, volatile fatty acids (VFAs) are the intermediate products of anaerobic treatment and have high value and marketability. The market demand for VFAs in 2020 was 18500 kilotons, and is projected to increase at an annual growth rate of 3% per year (Veluswamy et al., 2021). VFAs recovery helps carbon-intensive industries (such as agri-food, dairy, pharmaceutical, manufacturing and energy sector) to decarbonise their production, decrease the environmental impact, and generate revenue. Depending upon their molecular structure, VFAs have a 4 to 25 times higher market value than that of biogas (Owusu-Agyeman et al., 2020). A wide range of waste, including food waste, can be stabilized by VFA extraction from them (Atasoy et al., 2018). These VFAs derived from anaerobic fermentation can be transformed into electricity by microbial fuel cells (Yang et al., 2019). Alternatively, VFAs can also serve as an excellent carbon source for the production of polyhydroxyalkanoates or bioplastics (Atasoy and Cetecioglu, 2020). The use of VFA-rich fermentation liquids is a sustainable carbon source for biological removal of nutrients such as phosphorous and nitrogen (Liang et al., 2021). Research on production of single-cell protein to meet global food demand using VFAs are also gaining interest (Wainaina et al., 2020).

Optimizing the operational parameters such as pH can result in higher VFA yields. Though acidic pH was adopted conventionally for acidogenesis, few studies have successfully demonstrated that alkaline pH can vastly increase VFA productivity (Khatami et al., 2021). Similarly, pre-treating inoculum by temperature shocks could limit the growth of homoacetogenic bacteria and methanogenic archaea (Dessì et al., 2018). However, there have been very few studies showing improved VFA production due to heat treatment of the inoculum. Therefore, this study investigates enhancing VFA accumulation from food waste with heat treated inoculum. Meanwhile, chemicals such as 2-bromoethane sulfonic acid (BES) act as an inhibitor to suppress methanogenesis, resulting in improved VFA yield by preventing their consumption (Lukitawesa et al., 2020). However, the high cost of BES (~ € 900/kg) necessitates identifying cheap chemical inhibitors, especially from waste streams.

On the other hand, selenium (Se) wastewaters are of huge environmental concern owing to their acute and chronic toxicity (Tan et al., 2016). Anaerobic treatment of Se-laden wastewater offers the possibility to recover VFAs as well as to convert soluble Se oxyanions to insoluble and less toxic elemental Se. Similarly, the Se nanoparticles synthesised find

application in several industries ranging from health care, metallurgy, glass to chemicals manufacturing (Nancharaiah and Lens, 2015). Our previous long-term continuous study established that 500 µM Se oxyanion concentration caused methanogenic inhibition from VFA accumulation during AD of glycerol containing wastewater (Logan et al., 2022b). However, the influence of Se on the amount and composition of VFA produced is not clearly understood. To the best of our knowledge, no studies have focused on concomitant VFA production and Se reduction using food waste as the carbon source. Microbial studies establishing the coexistence of communities of fermentative as well as selenium reducing bacteria are also scarce.

Therefore, this study hypothesises to enhance VFA production via three different strategies, viz. pH adjustment (acidic and alkaline), chemical methanogenic inhibitor and heat treatment of the inoculum. The study will indicate the feasibility for the continuous and simultaneous VFA and Se nanoparticle production for commercial applications. The results from this paves the way for the circular economy and, energy and resource recovery in industries such as agri-food, mining, coal-fired power generation and oil refineries that generate food waste or Se-rich wastewaters. Demonstration of biogenic Se nanoparticle synthesis and VFA production will also cater to the needs of a wide range of industries.

6.2 Materials and Methods

6.2.1 Substrate and inoculum

Food waste collected from a pilot plant established at a wastewater treatment facility of KTH (Hammerby Sjöstadverket, Stockholm, Sweden) was used as the substrate. The digested sludge was collected from a full-scale anaerobic digester at the same wastewater treatment plant and was used as the inoculum. The characteristics of the food waste and digested sludge are presented in **Table 6.1.** Sodium selenate and sodium selenite salts were dissolved in distilled water to obtain stock solutions of selenate (SeO_4^{2-}) and selenite (SeO_3^{2-}).

Table 6.1 Characteristics of substrate and inoculum used in this study

Parameter	Food waste	Inoculum
TS (%)	9.37	2.61
VS (%)	8.10	1.66
pH	4.51	7.59
Total COD (mg/L)	204700	51900

Soluble COD (mg/L)	193933	49400

6.2.2 Experimental setup

Using food waste as the substrate, the effect of pH, heat treatment on the inoculum, and speciation and concentration of selenium oxyanions on VFA production, selenium removal and microbial communities was investigated. The batch assays were conducted in 150 mL serum bottles (with 100 mL working volume) at 35 ^{o}C (mesophilic regime) and 120 rpm. A substrate to inoculum ratio of 2 g COD/g VS was adopted to maximize VFA production (Khatami et al., 2021). The pH of the reactors was adjusted to 5.0 or 10.0 by using 1 M HCl or 1 M NaOH. SeO_4^{2-} concentrations supplemented were as follows: 0 (Control), 100 µM (14.30 mg/L), 300 µM (42.89 mg/L) and 500 µM (71.49 mg/L). Likewise, SeO_3^{2-} concentrations were 0 (Control), 100 µM (12.70 mg/L), 300 µM (38.09 mg/L) and 500 µM (63.49 mg/L). Each reactor was purged with nitrogen to ensure strict anaerobic conditions at the start of the experiment. Each test condition was conducted in triplicates for statistical analysis.

Table 6.2 Experimental sets conducted in this study

Experimental set	pH	Inoculum	Condition
I	5	NHT	Control 100, 300 and 500 µM SeO_4^{2-} 100, 300 and 500 µM SeO_3^{2-}
II	10	NHT	Control 100, 300 and 500 µM SeO_4^{2-} 100, 300 and 500 µM SeO_3^{2-}
III	5	HT	Control 500 µM SeO_4^{2-} 500 µM SeO_3^{2-}
IV	5	NHT	Control; 500 µM SeO_4^{2-} 500 µM SeO_3^{2-}
V	10	HT	Control 500 µM SeO_4^{2-} 500 µM SeO_3^{2-}
VI	10	NHT	Control 500 µM SeO_4^{2-} 500 µM SeO_3^{2-}

HT – heat treated inoculum; NHT – non-heat treated inoculum

Following this, the second phase of the experiment was conducted using the heat treated inoculum. The digested sludge was heated at 85 ^{o}C for 1 hour in a muffle furnace and then used in batch reactors. Each test condition was conducted in duplicates for statistical analysis. A 20-day retention period was adopted and the sacrificial bottles were set up to be taken down on day 1, 5, 10, 15 and 20. The experimental sets conducted in this study are shown in **Table 6.2**.

6.2.3 Analytical methods

The pH was measured by a pH-meter (Mettler Toledo FiveEasyTM pH bench meter, FE20). Total solids (TS, in %) and Volatile Solids (VS, in %) were determined by oven drying at 105 °C for 24 h and furnace drying at 550 °C for 2 h, respectively (APHA, 2017). Aliquots of the fermentation broth of each reactor were taken and centrifuged at 11000 rpm for 3 min. The supernatant was filtered with 0.45 and 0.2 μm polypropylene filters in order to determine the soluble chemical oxygen demand (sCOD) and VFA composition, respectively. The sCOD was measured using COD cuvette tests (LCK 514 Hach Lange, Düsseldorf, Germany) (Khatami et al., 2021). The composition of the VFAs was determined using a high performance liquid chromatograph (HPLC) (1260 Infinity II, Agilent, Santa Clara, USA) equipped with a Hi-Plex H (300 x 7.7 mm) column, heated at 60 ^{o}C and a refractive index detector (RID) set at 55 ^{o}C. A H_2SO_4 solution (5 mM) was used as the mobile phase at a flow rate of 0.7 mL/min and with a sample injection volume of 50 μL. The VFA concentrations measured are expressed as the COD equivalent. The COD conversion factor for acetic acid, propionic acid, butyric acid, valeric acid, isovaleric acid, caproic and isocaproic acid is 1.067, 1.512, 1.816, 2.037, 2.037, 2.207 and 2.207, respectively (Atasoy et al., 2020).

The liquid samples collected from the batch assays were analyzed for Se oxyanion concentration. The collected liquid samples were centrifuged at 11,000 rpm for 15 min and filtered with 0.2 um polypropylene filters to remove suspended cells and elemental selenium (Se^0) particles. Total Se was quantified using an inductively coupled plasma – optical emission spectroscopy 5110 synchronous vertical dual view (ICP-OES 5110, Agilent Technologies, Santa Clara, USA) (Logan et al., 2022a). Transmission electron microscopic (TEM) and scanning electron microscopic (SEM) imaging of selenium nanoparticles were studied. The protocols followed for preparation, fixing and imaging in TEM and SEM were described in detail by Florentino et al. (2020) and Tan and Lens (2021), respectively.

6.2.4 Calculations and statistical methods

The VFA production efficiency was calculated as the ratio of total VFA concentration to sCOD concentration (Jankowska et al., 2017). Analysis of variance (ANOVA) was performed on the averaged VFA production data by using SPSS 16 software (IBM Corp., Ireland) at 5% level of significance.

6.3 Results

6.3.1 Effect of acidic and alkaline pH

The initial VFA concentration introduced into the batch bottles from food waste is presented in **Table 6.3**. The profile of VFA production at different pH, and speciation and concentration of selenium with and without heat treatment is presented in **Figure 6.1**. The VFA production over time was in a decreasing trend at pH 10 (**Figure 6.1a**). The maximum VFA production at pH 10 was 9315 (± 652) mg COD/L on day 5. On the contrary, the VFA production profile was in an increasing trend, with the maximum VFA production of 6416 (± 591) mg COD/L on day 20 at pH 5. A higher VFA yield (by about 45.2%) was obtained in alkaline conditions in a shorter retention time, when compared with the acidic environment (**Figures 6.1 a and c**). At initial pH 10, the pH dropped to near neutral after 5 days, and thereafter was in the range between 7 and 8 until the end of the incubation. However, the pH was below 5.6 throughout the experiment for the 'initial pH 5' incubation (**Figure 6.3**). The composition of VFA at different test conditions is presented in **Figure 6.4**. About 80% of the VFAs produced in alkaline conditions was dominated by acetate and propionate. On the contrary, a diverse composition of all VFAs except isocaproate was present at acidic conditions (**Figure 6.2**).

Table 6.3 Initial average volatile fatty acid concentration (in mg COD/L) introduced into batch reactors from food waste

Acetate	Propionate	Isobutyrate	Butyrate	Isovalerate	Valerate	Total VFA
1365	206	749	128	187	34	2669

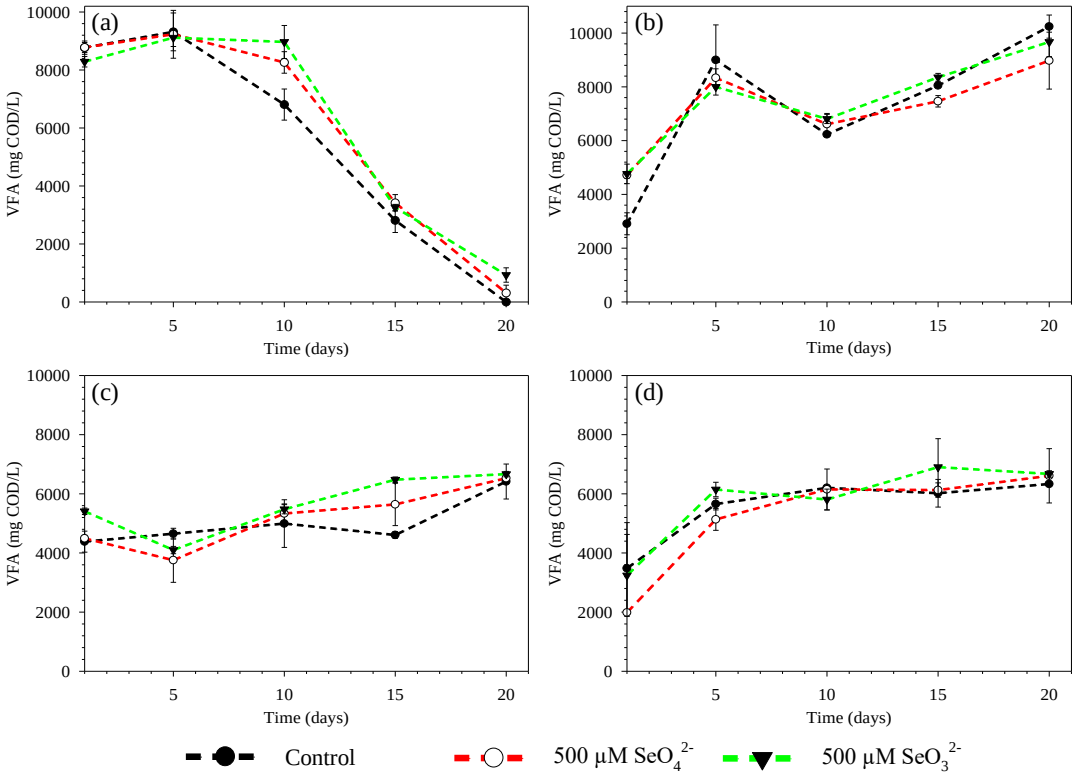

Figure 6.1 VFA profile at (a) pH 10, NHT; (b) pH 10, HT; (c) pH 5, NHT; and (d) pH 5, HT

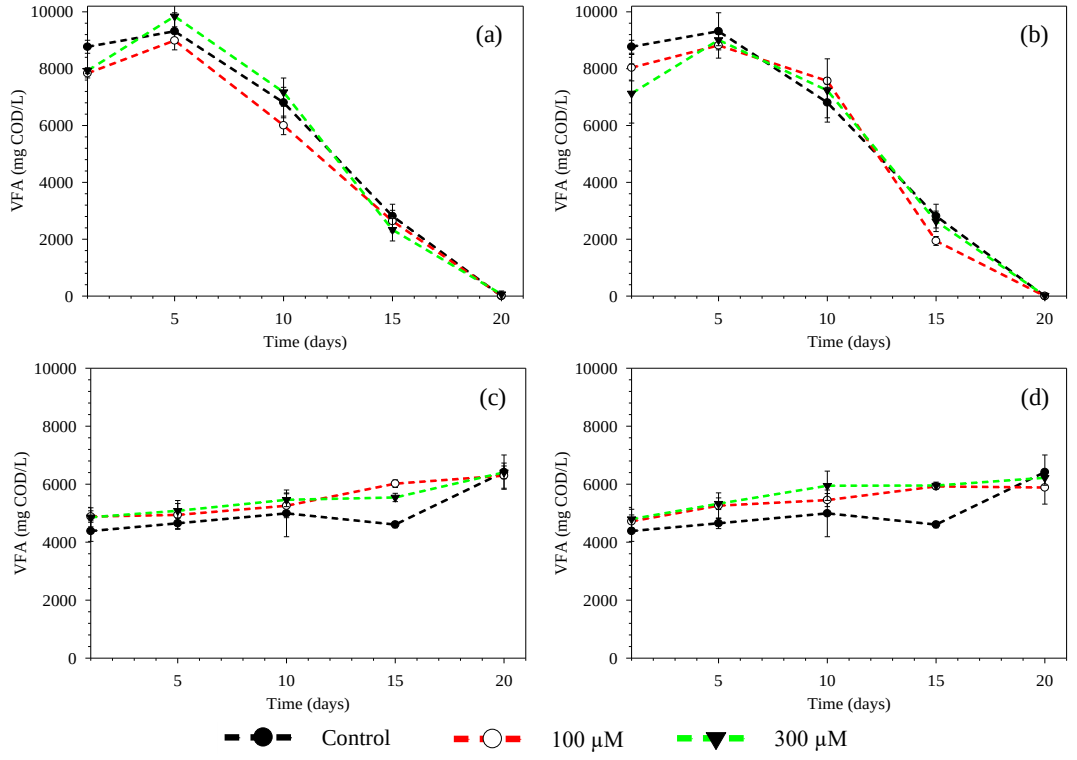

Figure 6.2 VFA profile at (a) pH 10, NHT, SeO_4^{2-}; (b) pH 10, HT, SeO_3^{2-}; (c) pH 5, NHT, SeO_4^{2-}; and (d) pH 10, HT, SeO_4^{2-}

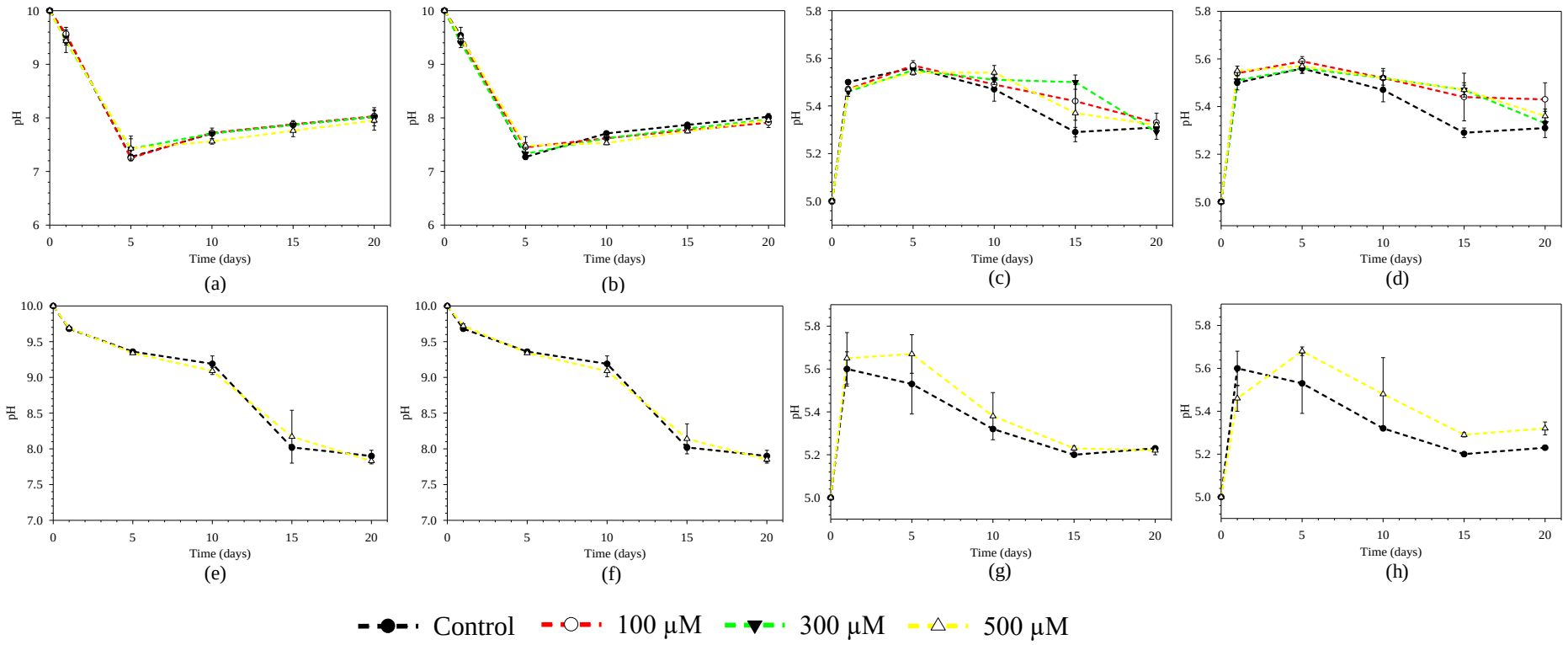

Figure 6.3 pH variation with non-heat treated inoculum at (a) pH 10, SeO_4^{2-}; (b) pH 10, SeO_3^{2-}; (c) pH 5, SeO_4^{2-}; and (d) pH 5, SeO_3^{2-}; and heat treated inoculum at (e) pH 10, SeO_4^{2-}; (f) pH 10, SeO_3^{2-}; (g) pH 5, SeO_4^{2-}; and (h) pH 5, SeO_3^{2-}

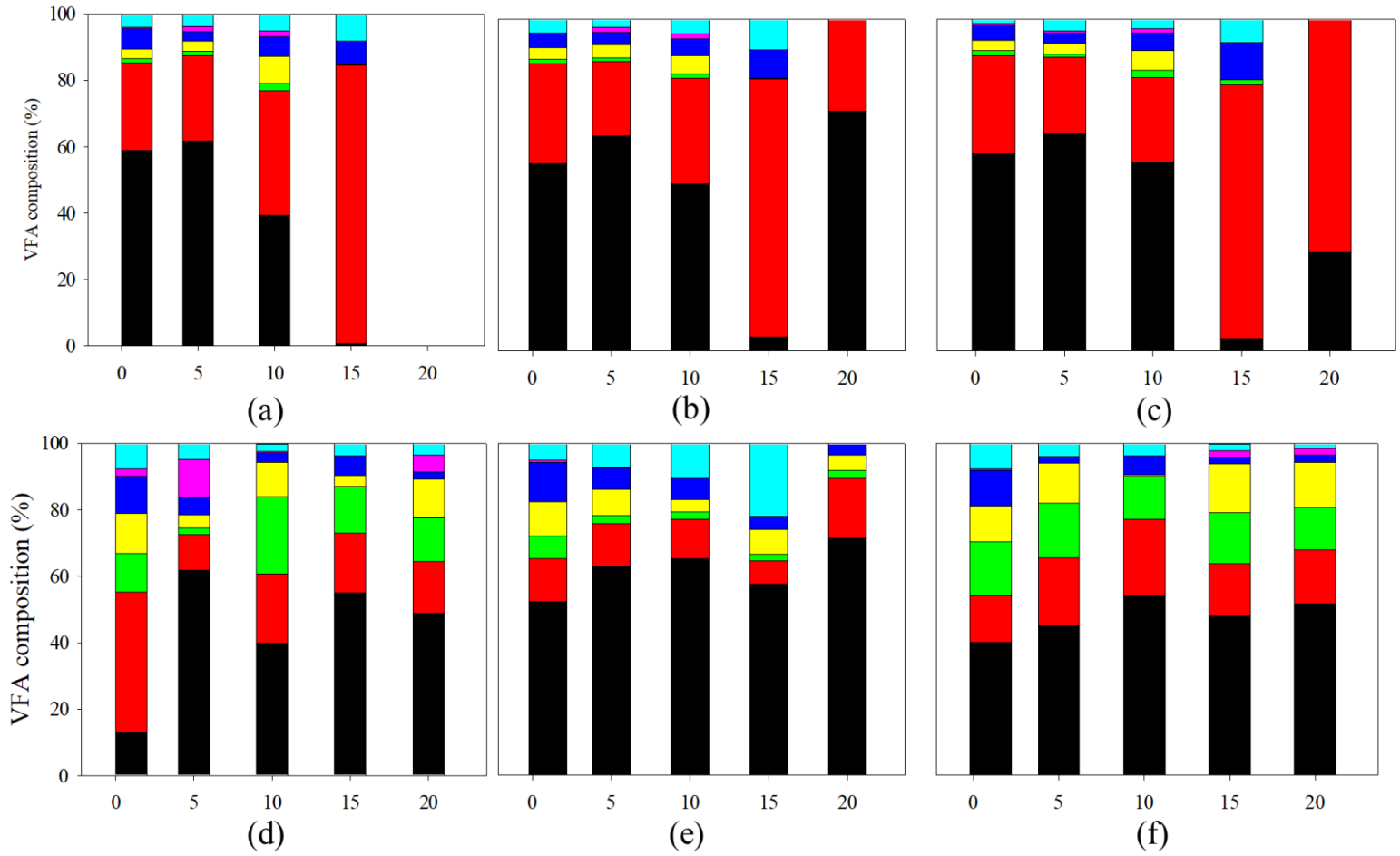
VFA composition (%)
100
80
60
40
20
0
0
5
10
15
20
(a)
(b)
(c)
(d)
(e)
(f)

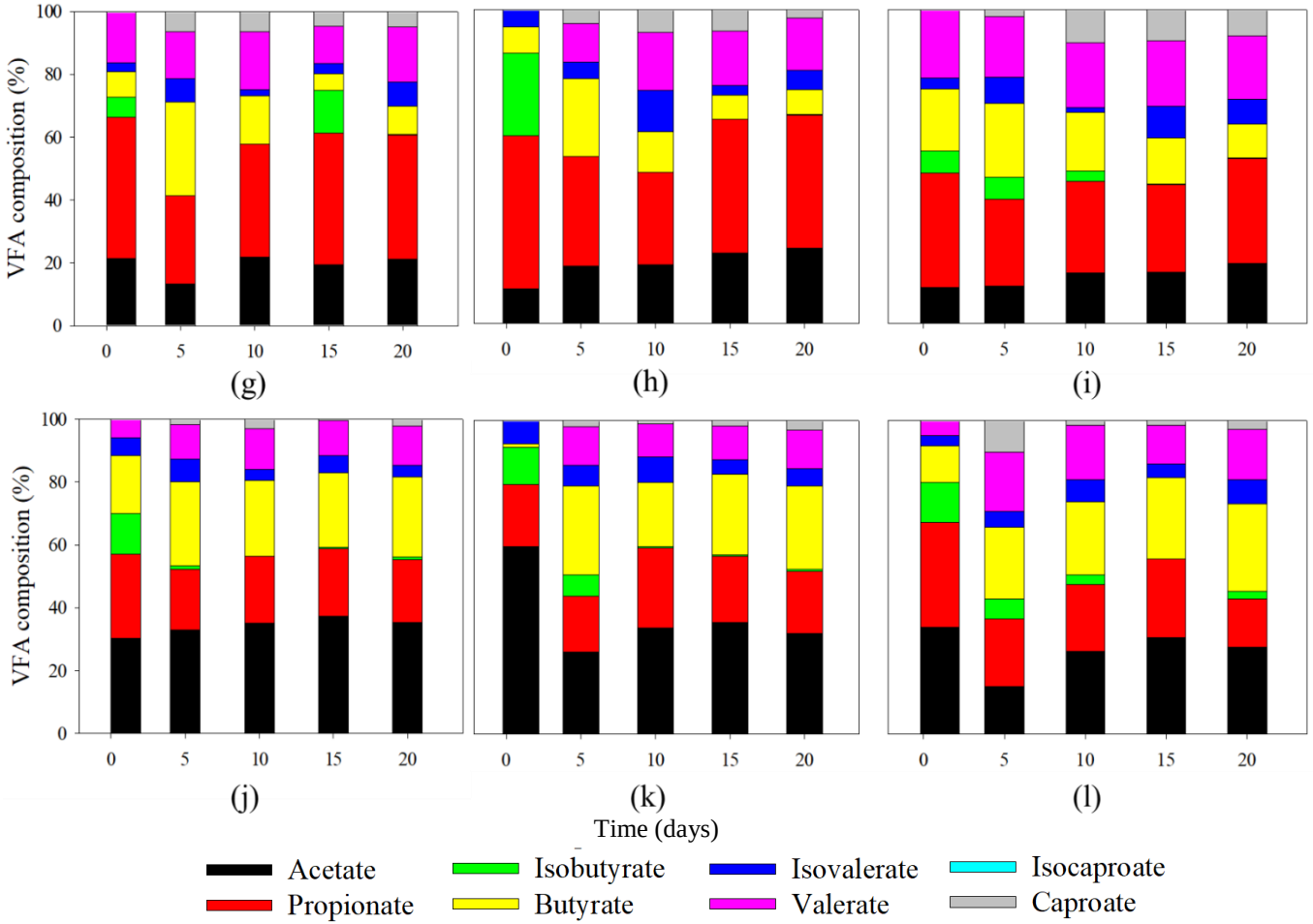

Figure 6.4 VFA composition at (a) pH 10, NHT, Control; (b) pH 10, NHT, 500 µM SeO_4^{2-}; (c) pH 10, NHT, 500 µM SeO_3^{2-}; (d) pH 10, HT, Control; (e) pH 10, HT, 500 µM SeO_4^{2-}; (f) pH 10, HT, 500 µM SeO_3^{2-}; (g) pH 5, NHT, Control; (h) pH 5, NHT, 500 µM SeO_4^{2-}; (i) pH 5, NHT, 500 µM SeO_3^{2-}; (j) pH 5, HT, Control; (k) pH 5, HT, 500 µM SeO_4^{2-}; and (l) pH 5, HT, 500 µM SeO_3^{2-}.

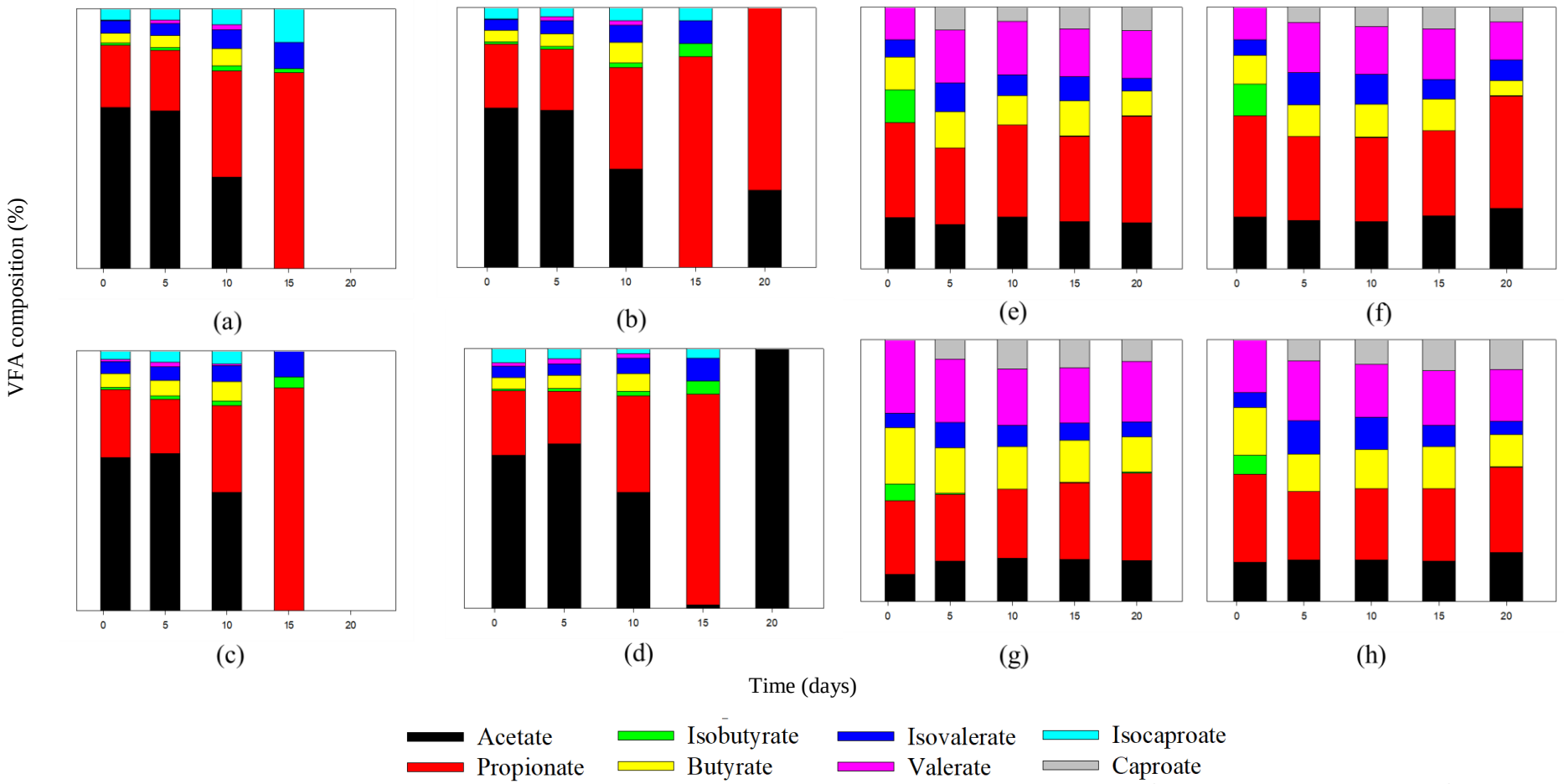

Figure 6.5 Volatile fatty acids composition with non-heat treated inoculum at (a) pH 10, 100 µM SeO_4^{2-}; (b) pH 10, 300 µM SeO_4^{2-}; (c) pH 10, 100 µM SeO_3^{2-}; (d) pH 10, 300 µM SeO_4^{2-}; (e) pH 5, 100 µM SeO_4^{2-} ; (f) pH 5, 300 µM SeO_4^{2-}; (g) pH 5, 100 µM SeO_3^{2-}; and (h) pH 5, 300 µM SeO_4^{2-}.

6.3.2 Effect of inoculum heat treatment

Heat treated inoculum resulted in VFA accumulation in an increasing trend to 10241 (±430) mg COD/L by day 20 at pH 10. On the contrary, without heat treatment, complete VFAs utilization resulted in the absence of VFAs on day 20 at pH 10 (**Figure 6.1a**). When compared to Se oxyanions (refer **Section 6.3.3**), VFAs accumulation was much more evident with heat treatment. Though heat treatment showed clear improvement in VFA yield in alkaline pH, there was no significant effect in acidic pH (**Figure 6.1b-d**). VFAs composition diversified due to heat treatment at alkaline conditions except caproic acid (**Figure 6.4a-f**). Heat treatment significantly changed the pH profile in alkaline conditions (**Figure 6.3**). pH gradually decreased to ~8 only after day 15.

6.3.3 Effect of selenium oxyanions and their concomitant reduction

Interestingly, selenium oxyanions overcame complete VFA conversion, which is remarkable on days 10, 15 and 20. In the presence of Se oxyanions, higher VFA yields were obtained on and after day 10 at pH 10. Selenate resulted in the highest VFA yield (8261 ± 371 mg COD/L) followed by selenite (8967 ± 569 mg COD/L) on day 10, which was about 21 % and 32 %, respectively. The presence of Se oxyanions did not significantly increase the VFA yields at acidic condition. **Figures 6.2 and 6.5** shows the VFA concentration and composition for 100 and 300 µM SeO_4^{2-} and SeO_3^{2-} at acidic and alkaline pH without heat treatment.

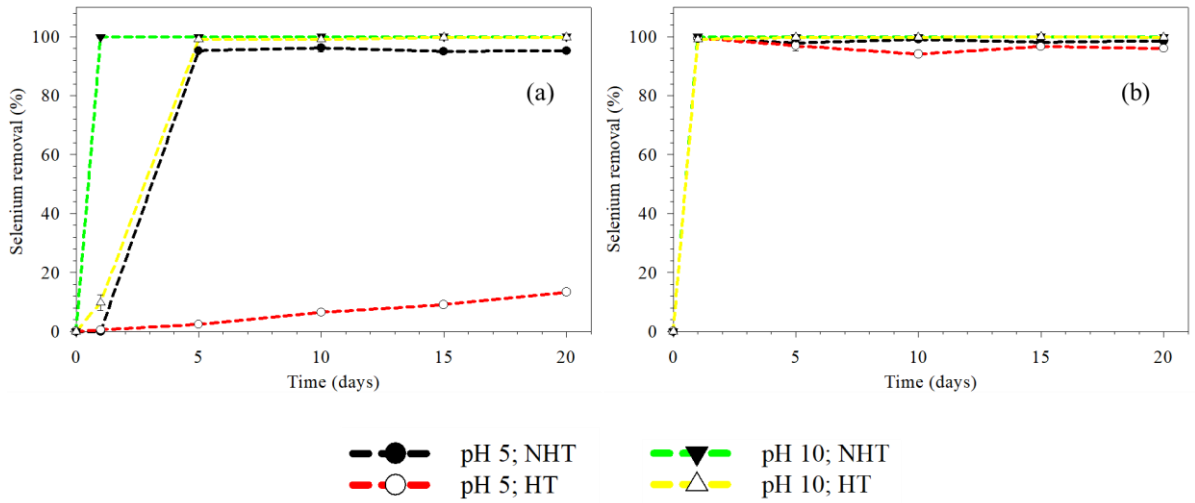

Figure 6.6 Selenium removal accomplished from (a) 500 µM SeO_4^{2-} and (b) 500 µM SeO_3^{2-} at pH 5 and 10 with non-heat treated (NHT) and heat treated (HT) inoculum

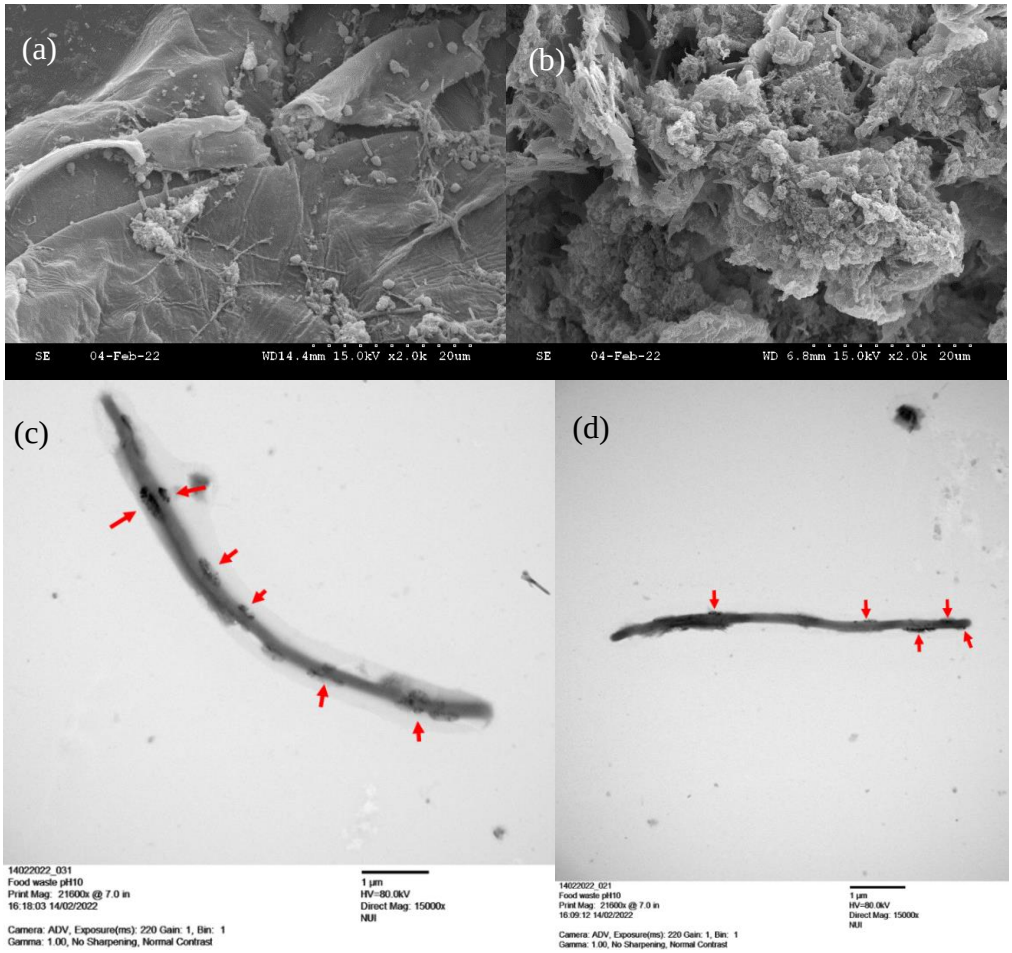

Figure 6.7 Electron microscopic images: SEM images (a,b); and TEM images (c,d) of the sludge taken at the end of the experiment (day 20) at pH 10 (NHT) to observe elemental selenium nanospheres deposited in the digested sludge flocs.

Se removal at acidic and alkaline pH with and without heat treatment is presented in **Figure 6.6.** More than 98% Se removal was observed at the end of day 1, in the presence of SeO_3^{2-}, at all tested conditions. On the other hand, above 95% Se removal was achieved on day 1 in the presence of SeO_4^{2-} at alkaline-NHT, however, heat treatment delayed Se removal (95%) on day 5 at pH 10. At acidic pH (NHT), about 95% SeO_4^{2-} removal efficiency was achieved on day 5. Interestingly, Se removal was less than 20% at acidic-NHT. Se removal at 100 and 300 µM SeO_4^{2-} and SeO_3^{2-} at pH 5 and 10 without heat treatment is presented in **Figure 6.8**. The reduction of Se oxyanions to elemental Se nanoparticles using food waste as the electron donor is supported by electron microscopic images. **Figure 6.7** shows the SEM and TEM images of elemental Se nanoparticles deposited in the digested sludge flocs. SEM-EDX confirms that the nanoparticles observed in electron microscopic images are indeed selenium nanoparticles, as shown in **Figure 6.9**.

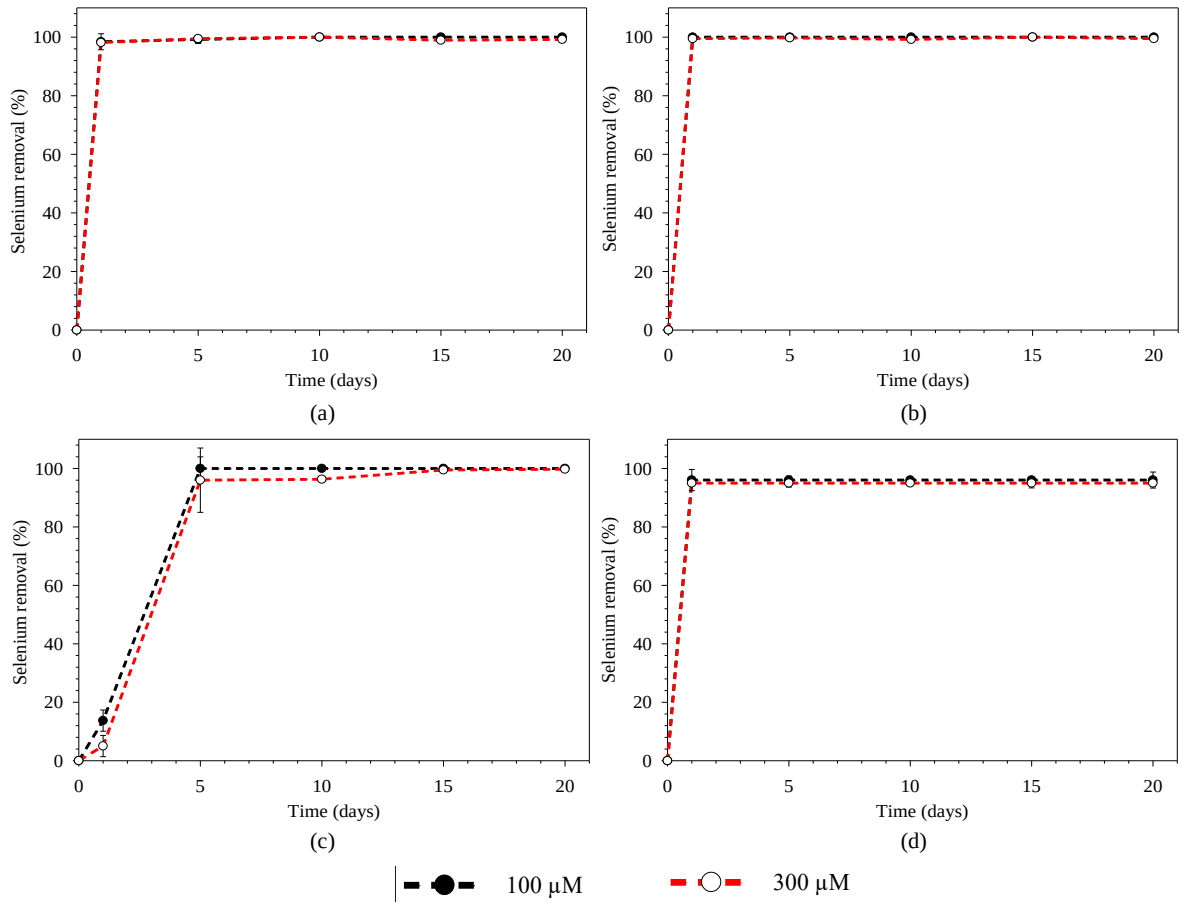

Figure 6.8 Selenium removal with non-heat treated inoculum at (a) pH 10, SeO_4^{2-}; (b) pH 10, SeO_3^{2-}; (c) pH 5, SeO_4^{2-}; and (d) pH 5, SeO_3^{2-}

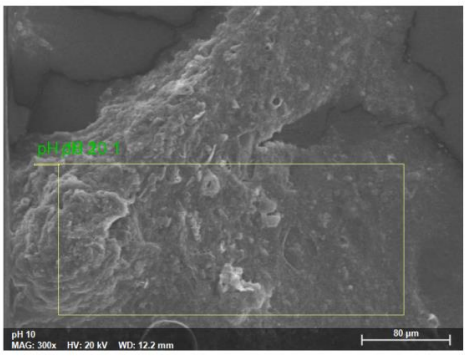

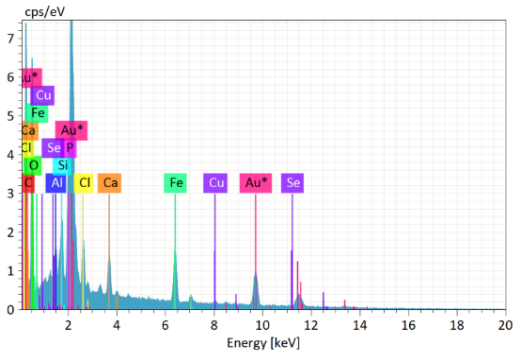

pH 10 1

Element	Mass Norm. [%]
Carbon	35.07
Oxygen	42.97
Aluminium	1.25
Silicon	1.82
Phosphorus	4.58
Chlorine	1.64
Calcium	2.85
Iron	8.96
Copper	0.71
Gold	0.00
Selenium	0.15
	100.00

Figure 6.9 SEM-EDX confirming biosynthesised selenium nanoparticles deposited in the digested sludge flocs.

6.4 Discussion

6.4.1 Novel strategies for enhancing volatile fatty acids production efficiency

6.4.1.1 Improved VFA yield at alkaline pH

This study shows that the initial alkaline conditions resulted in higher VFA production than under acidic conditions (**Figures 6.1a and c**). Alkaline pH promotes the hydrolysis of macromolecular substances and extracellular polymeric substances (EPS) of sludge flocs (Liang et al., 2021). This is because the alkaline pH induces the cleavage of covalent bonds of organic matter to increase the rupture of the cell membrane (Carrere et al., 2016). Under alkaline conditions, the charged functional groups in the EPS of sludge also get ionized and the accessibility of the soluble compounds is facilitated (Maddela et al., 2018). Further, OH^- ions breakdown peptide bonds for enhanced protein degradation (Dahiya et al., 2015). Recently, Lin and Li (2021) reported that alkaline pH (8 – 10) was more effective in VFA production by up to 46% than acidic pH (2 – 6) due to enzymatic activities.

The VFA composition (**Figure 6.4**) suggests that homoacetogenic microorganisms and propionic acid-producing microorganisms that consume hydrogen are favoured at alkaline pH (Figure 6.4). In addition, the phosphoroclastic pathway anticipated under alkaline pH is also likely the reason for the higher acetate production (Dahiya et al., 2015). Similar observations of acetate and propionate domination at alkaline conditions was reported by Chaganti et al. (2013). Jankowska et al. (2017) also concluded that a higher diversity of volatile and medium chain fatty acids are obtained at acidic conditions, compared to alkaline conditions.

6.4.1.2 VFA accumulation due to heat treated inoculum

VFA accumulation due to heat treatment was more evident in alkaline conditions than in acidic condition (**Figure 6.1**). This could be attributed to the prior inhibition of methanogenesis in acidic environment, and therefore heat treatment to eliminate methanogenic archaea might have a negligible effect. Moreover, the acidogenic bacteria can form spores when subjected to high temperatures, whereas methanogens lack that functionality, and therefore a heat shock at around 80–100 ^{o}C for 15–120 min can be employed to deactivate the methanogens (Mondylaksita et al., 2021). Sarkar et al. (2016) reported that a heat shock resulted in VFA accumulation, since it simultaneously selects acidogens and removes methanogens (Sarkar et al., 2016). Mondylaksita et al. (2021) also reported that heat treatment led to more VFA

accumulation than the chemical inhibitor (BES). The VFA production efficiency could be significantly improved through the simple method of using heat treated inoculum (**Figure 6.1b**), despite VFA production using inoculum without heat treatment is also well possible (Khatami et al., 2021). Therefore, further studies to clearly establish the effect of heat treatment of the inoculum on the VFA yield are necessary for implementation of bio-based VFAs recovery from food waste.

6.4.1.3 Simultaneous VFA production during selenium bioremediation

This study shows that food waste, one of the most abundant wastes, can be used for selenium remediation. Though literature is scarce on biological selenium oxyanion reduction using food waste as the carbon source, biological sulfate reduction using food industry waste has been reported. This study reveals that alkaline pH was more favourable for Se removal, than acidic pH (**Figure 6.6**). Tan et al. (2018) also reported a higher SeO_4^{2-} removal efficiency in alkaline conditions, however, lowering the pH to 5 was detrimental to the UASB reactor performance as the SeO_4^{2-} removal efficiency dropped by 20-30%. Additionally, a low polysaccharide (PS) to protein ratio in the soluble extracellular polymeric substance matrix of the biomass was observed at low pH, which can affect the biomass properties. pH values above 5 are pre-requisite for consumption of the carbon source for efficient sulfate reduction. For instance, Martins et al. (2009) supplemented calcite tailing that acts as a neutralizing and buffer material to increase pH from 4 to 6 for dissimilatory sulfate reduction.

The removal of selenite was accomplished earlier than that of selenate (**Figure 6.6**). This could be due to the high reactivity of SeO_3^{2-} to form strong stable bonds with organic matter in the food waste, leading to its easy and fast removal, while SeO_4^{2-} is less reactive and forms weakly bound complexes and is therefore harder to remove (Lussier et al., 2003, Cálix et al., 2019). Our previous study also showed the Se removal with SeO_3^{2-} was faster during the first day of incubation when compared to SeO_4^{2-} at the fourth day of incubation (Logan et al., 2022a). It should be noted that the effect of Se oxyanions was clearly evident only on and after day 10. This could be because the onset of the exponential phase of methanogenesis is typically with a lag phase of about 10 days for food waste (Hobbs et al., 2018). Mondylaksita et al. (2021) also observed that VFAs production started to accelerate only after the tenth day of the fermentation of the glucan-rich fraction of palm oil empty fruit bunch.

This study clearly indicates that heat treatment of the inoculum is detrimental for Se removal, in the presence of selenate, especially at acidic pH. Further research on the mechanism behind this phenomenon is required. Finally, the elemental Se nanoparticles synthesised in this study were in the shape of nanospheres (**Figure 6.7**) which are typical for mesophilic systems, compared to nanorods synthesised in thermophilic systems (Sinharoy and Lens, 2020).

Our earlier study in a UASB reactor treating selenate-rich wastewater showed that repeated exposure of Se oxyanions at higher concentrations led to reactor acidification and impaired methane production (Logan et al., 2022b). The lag-phase extension due to Se supplementation could have also resulted in the accumulation of volatile fatty acids (Kim and Kim, 2020). The toxicity of selenium on methanogenic archaea but less on fermentative bacteria could be leveraged, however further research is still required to recover fermentative products such as carboxylic acids and alcohols.

A commonly used methanogenic inhibitor such as 2-bromoethanesulfonate (BES) is a coenzyme M analog that acts as competitive inhibitor in methyl transfer reactions (Webster et al., 2016). β-cyclodextrin was also demonstrated as a chemical methanogenic inhibitor to improve hydrogen and VFA production by Kidanu et al. (2017). However, the market cost of β-cyclodextrin is high (~ € 1250/kg in 2022). Such high cost of external chemical addition might reduce the competitiveness of bio-based VFAs over petro-chemical based VFAs and therefore it is imperative to identify other cheap inhibitory compounds available in abundance. Industrial wastewaters laden with selenium at higher concentrations could be a good alternative for the existing chemical inhibitors such as BES and β-cyclodextrin.

6.4.2 Future perspectives for volatile fatty acid production and selenium bioremediation

As illustrated in **Figure 6.10**, there are two different approaches in the research area on bio-based VFAs, viz. 1) fermentation development and 2) primary product separation and recovery. A paradigm shift is needed on isolated approaches towards the development of the end product through integrated process design (Ramos-Suarez et al., 2021). Conventionally, the primary production is optimized through operational conditions such as inoculum, substrate, pH, temperature, and retention time. More diverse VFA presence in low concentrations discourages businesses to adopt them due to the concerns in terms of their recovery. However, biotechnological advances in the last decade are focussed to address this challenge. Novel strategies, such as bioaugmentation for targeted tailor-made VFA production (Atasoy and

Cetecioglu, 2021). Recently, the chain elongation process which occurs via the reversed β-oxidation pathway and the fatty acid biosynthesis pathway to produce less hydrophilic medium chain carboxylic acids ($C_6 – C_{12}$) through secondary fermentation of short-chain organic acids have gained interest as well (Nzeteu et al., 2022). VFAs can be developed for end-use applications such as alcohol, bioplastics, biodiesel, biological nutrient recovery and electricity generation (Khatami et al., 2021). Presently, the recovery methods include gas stripping with absorption, adsorption, solvent extraction, electrodialysis, reverse osmosis, nanofiltration and membrane contractor, however the prospects are unfolding for in-line recovery (Atasoy et al., 2018). Since research on anaerobic fermentation has high degrees of non-uniformity (from feedstocks to inoculum microbiome), technologies such as metagenomics and metatranscriptomic analysis would provide insights for generalized conclusions. Considering that these applications have huge commercial implications, several industries in a varied range of spectra will leverage from the research and developments on bio-based VFAs. This study indicates the feasibility of anaerobic treatment of acidic Se-laden wastewater such as mining wastewater in a single stage bioreactor for VFAs and Se nanoparticle production, without any additional cost of pretreatment for neutralization.

This study also implies that biological resource recovery could be concomitantly achieved during the anaerobic fermentation process for VFA production. This batch work necessitates that a long-term continuous bioreactor performance for simultaneous VFA and elemental Se nanoparticle production should be demonstrated. Additionally, the techno-economic and life cycle assessment will be beneficial for commercial implementation. Se levels in industrial wastewaters are higher (> 100 µM) and are reported to inhibit methanogenesis. Nanchariah and Lens (2015) stated that VFAs produced from AD of food waste could serve as an electron donor for Se reduction. Hence, remediation of Se wastewater could be achieved in a single stage bioreactor producing volatile fatty acids. Nonetheless, whenever Se regulatory discharge limits could not be met, additional post treatment methods should be employed. Coupling synthesis of selenium quantum dots together with VFA production could also be considered in future studies.

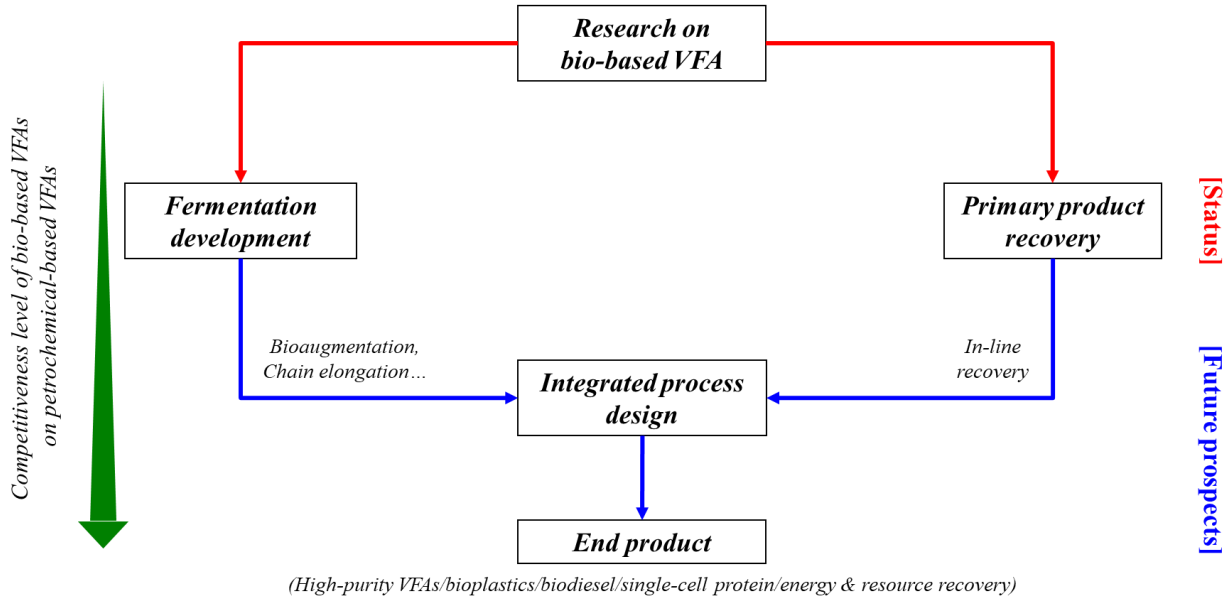

Figure 6.10 Current status and future prospects of bio-based VFA research

6.5 Conclusion

Exploring strategies for production of VFA from waste streams is the key to make it competitive over petrochemical-based VFAs. The effect of pH, heat treatment on the inoculum, and selenium speciation and concentration on concomitant VFA production, Se removal, and microbial community structure were investigated. A higher VFA yield was achieved in alkaline pH, when compared with acidic pH. Selenium acted as a chemical inhibitor to accumulate VFAs after day 10 in alkaline pH without heat treatment. Heat treatment resulted in VFAs accumulation in alkaline pH, but was detrimental to selenate removal. There was no significant difference observed neither in VFA concentration and composition nor in Se removal, by lowering the pH to 5 with or without heat treatment. Acetate and propionate were the dominant VFAs produced in alkaline condition without heat treatment, however a diverse VFA composition was observed in all other conditions tested.

6.6 References

Atasoy, M., Cetecioglu, Z., 2021. Bioaugmentation as a strategy for tailor-made volatile fatty acid production. Journal of Environmental Management 295, 113093. https://doi.org/10.1016/j.jenvman.2021.113093

Atasoy, M., Eyice, O., Cetecioglu, Z., 2020. A comprehensive study of volatile fatty acids production from batch reactor to anaerobic sequencing batch reactor by using cheese

processing wastewater. Bioresource Technology 311, 123529. https://doi.org/10.1016/j.biortech.2020.123529

Atasoy, M., Owusu-Agyeman, I., Plaza, E., Cetecioglu, Z., 2018. Bio-based volatile fatty acid production and recovery from waste streams: Current status and future challenges. Bioresource Technology 268 773-786. https://doi.org/10.1016/j.biortech.2018.07.042

APHA, 2017. Standard Methods for the Examination of Water and Wastewater (twenty-third ed.), 9780875532875, American Public Health Association. Washington, D.C., USA.

Cálix, E.M., Tan, L.C., Rene, E.R., Nancharaiah, Y.V., van Hullebusch, E.D., Lens, P.N.L., 2019. Simultaneous removal of sulfate and selenate from wastewater by process integration of an ion exchange column and upflow anaerobic sludge blanket bioreactor. Separation Science and Technology 54, 1387-1399. https://doi.org/10.1080/01496395.2018.1533562

Carrere, H., Antonopoulou, G., Affes, R., Passos, F., Battimelli, A., Lyberatos, G., Ferrer, I., 2016. Review of feedstock pretreatment strategies for improved anaerobic digestion: from lab-scale research to full-scale application. Bioresource Technology 199, 386-397. https://doi.org/10.1016/j.biortech.2015.09.007

Chaganti, S.R., Pendyala, B., Lalman, J.A., Veeravalli, S.S., Heath, D.D., 2013. Influence of linoleic acid, pH and HRT on anaerobic microbial populations and metabolic shifts in ASBRs during dark hydrogen fermentation of lignocellulosic sugars. International Journal Hydrogen Energy 38, 2212–2220. https://doi.org/10.1016/j.ijhydene.2012.11.137

Cetecioglu, Z., Ince, B., Gros, M., Rodriguez-Mozaz, S., Barceló, D., Ince, O., Orhon, D., 2015. Biodegradation and reversible inhibitory impact of sulfamethoxazole on the utilization of volatile fatty acids during anaerobic treatment of pharmaceutical industry wastewater. Science of The Total Environment 536, 667-674. https://doi.org/10.1016/j.scitotenv.2015.07.139

Dessì, P., Porca, E., Frunzo, L., Lakaniemi, A., Collins, G., Esposito, G., Lens, P.N.L., 2018. Inoculum pretreatment differentially affects the active microbial community performing mesophilic and thermophilic dark fermentation of xylose. International Journal of Hydrogen Energy 43, 9233-9245. https://doi.org/10.1016/j.ijhydene.2018.03.117

Florentino, A.P., Costa, R.B., Hu, Y., O'Flaherty, V., Lens, P.N.L., Long chain fatty acid degradation coupled to biological sulfidogenesis: A prospect for enhanced metal recovery. Frontiers in Bioengineering and Biotechnology 8, 550253.

Hobbs, S.R., Landis, A.E., Rittmann, B.E., Young, M.N., Parameswaran, P., 2018. Enhancing anaerobic digestion of food waste through biochemical methane potential assays at different substrate: inoculum ratios. Waste Management 71, 612-617. https://doi.org/10.1016/j.wasman.2017.06.029

Jankowska, E., Chwialkowska, J., Stodolny, M., Oleskowicz-Popiel, P., 2017. Volatile fatty acids production during mixed culture fermentation – The impact of substrate complexity and Ph. Chemical Engineering Journal 326, 901-910. https://doi.org/10.1016/j.cej.2017.06.021

Khatami, K., Atasoy, M., Ludtke, M., Baresel, C., Euice, O., Cetecioglu, Z., 2021. Bioconversion of food waste to volatile fatty acids: Impact of microbial community, pH and retention time. Chemosphere 275, 129981. https://doi.org/10.1016/j.chemosphere.2021.129981

Kim, M.J., Kim, S.H., 2020. Conditions of lag-phase reduction during anaerobic digestion of protein for high-efficiency biogas production. Biomass and Bioenergy 143, 105813. https://doi.org/10.1016/j.biombioe.2020.105813

Liang, T., Elmaadawy, K., Liu, B., Hu, J., Hou, H., Yang, J., 2021. Anaerobic fermentation of waste activated sludge for volatile fatty acid production: Recent updates of pretreatment methods and the potential effect of humic and nutrients substances. Process Safety and Environmental Protection 145, 321-339. https://doi.org/10.1016/j.psep.2020.08.010

Li, H., Zou, S., Li, C., Jin, Y., 2013. Alkaline post-treatment for improved sludge anaerobic digestion. Bioresource Technology 140, 187-191. https://doi.org/10.1016/j.biortech.2013.04.093

Lemaire, A., Limbourg, S., 2019. How can food loss and waste management achieve sustainable development goals? Journal of Cleaner Production 234, 1221-1234. https://doi.org/10.1016/j.jclepro.2019.06.226

Lin, L., Li, X., 2021. Effect of pH adjustment on the hydrolysis of Al-enhanced primary sedimentation sludge for volatile fatty acid production. Chemical Engineering Journal 346, 50-56. https://doi.org/10.1016/j.cej.2018.04.005

Logan, M., Ravishankar, H, Tan, L.C., Lawrence, J., Fitzgerald, D., Lens, P.N.L., 2021. Anaerobic digestion of dissolved air floatation slurries: effect of substrate concentration and pH. Environmental Technology and Innovation 21, 101352. https://doi.org/10.1016/j.eti.2020.101352

Logan, M., Tan, L.C., Lens, P.N.L., 2022a. Anaerobic co-digestion of dissolved air floatation slurry and selenium rich wastewater for simultaneous methane production and selenium bioremediation. International Biodeterioration and Biodegradation 172, 105425. https://doi.org/10.1016/j.ibiod.2022.105425

Logan, M., Tan, L.C., Nzeteu, C.O., Lens, P.N.L., 2022b. Long-term continuous methane production and selenium remediation in UASB treatment of selenate and glycerol containing wastewater. Renewable Energy (Under Review).

Lukitawesa, Patinvoh, R.J., Millati, R., Sárvári-Horváth, I., Taherzadeh, M.J., 2019. Factors influencing volatile fatty acids production from food wastes via anaerobic digestion. https://doi.org/10.1080/21655979.2019.1703544

Lussier, C., Veiga, V., Baldwin, S., 2003. The geochemistry of selenium associated with coal waste in the Elk River Valley, Canada. Environmental Geology 44, 905-913. https://doi.org/10.1007/S00254-003-0833-Y

Maddela, N.R., Zhou, Z., Yu, Z., Zhao, S., Meng, F., 2018. Functional determinants of extracellular polymeric substances in membrane biofouling: experimental evidence from pure-cultured sludge bacteria. Applied and Environmental Microbiology 84. https://doi.org/10.1128/AEM.00756-18

Market Data Forecast, 2021. Global Industry Analyses Size, Growth, Share, Trends Forecast Report 2021 – 2026. https://www.marketdataforecast.com/market-reports/food-waste-management-market

Magrini, F.E., de Almeida, G.M., Soares, D.M., Fuentes, L., Ecthebehere, C., Beal, L.L., da Silveira, M.M., Paesi, S., 2020. Effect of different heat treatments of inoculum on the production of hydrogen and volatile fatty acids by dark fermentation of sugarcane vinasse. Biomass Conversion and Biorefinery 11, 2443-2456. https://doi.org/10.1007/s13399-020-00687-0

Mondylaksita, K., Ferreira, J.A., Budhijanto, W., Niklasson, C., Taherzadeh, M.J., Millati, R., 2021. Enhanced Volatile Fatty Acid Production from Oil Palm Empty Fruit Bunch through Acidogenic Fermentation—A Novel Resource Recovery Strategy for Oil Palm Empty Fruit Bunch. Fermentation 7, 263. https://doi.org/10.3390/fermentation7040263

Nancharaiah, Y.V., Lens, P.N.L., 2015. Selenium biomineralization for biotechnological applications. Trends in Biotechnology 33(6), 323-330. https://doi.org/10.1016/j.tibtech.2015.03.004

Nzeteu, C.O., Coelho, F., Trego, A.C., Abram, F., Ramiro-Garcia, J., Paulo, L., O'Flaherty, V., 2022. Development of an enhanced chain elongation process for caproic acid production from waste-derived lactic acid and butyric acid. Journal of Cleaner Production 338, 130655. https://doi.org/10.1016/j.jclepro.2022.130655

Ramos-Suarez, M., Zhang, Y., Outram, V., 2021. Current perspectives on acidogenic fermentation to produce volatile fatty acids from waste. Reviews in Environmental Science and Bio/Technology 20, 439-478. https://doi.org/10.1007/s11157-021-09566-0

Sarkar, O., Kumar, A.N., Dahiya, S., Krishna, K.V., Yeruva, D.K., Mohan, S.V., 2016. Regulation of acidogenic metabolism towards enhanced short chain fatty acid biosynthesis from waste: metagenomic profiling. RSC Advances, 6, 18641–18653. https://doi.org/10.1039/c5ra24254a

Tan, L.C., Nancharaiah, Y.V., van Hullebusch, E.D., Lens, P.N.L., 2016. Selenium: Environmental significance, pollution, and biological treatment technologies. Biotechnol. Adv. 34(5), 886-907. https://doi.org/10.1016/j.biotechadv.2016.05.005

Tan, L.C., Espinosa-Ortiz, E.J., Nancharaiah, Y.V., van Hullebusch, E., Gerlach, R., Lens, P.N.L., 2018. Biological treatment of selenium-laden wastewater containing nitrate and sulfate in an upflow anaerobic sludge bed reactor at pH 5.0. Chemosphere 211, 684–93. https://doi.org/10.1016/j.chemosphere.2018.07.079.

Tan, L.C., Lens, P.N.L., 2021. Addition of granular activated carbon during anaerobic oleate degradation overcomes inhibition and promotes methanogenic activity. Environmental Science: Water Research and Technology 4.

UNEP, 2021. Food Waste Index Report 2021. United Nations Environment Programme. Nairobi. https://www.unep.org/resources/report/unep-food-waste-index-report-2021

Veluswamy, G.K., Shah, K., Ball, A.S., Guwy, A.J., Dinsdale, R.M., 2021. A techno-economic case for volatile fatty acid production for increased sustainability in the wastewater treatment industry. Environmental Science: Water Research and Technology 7, 927-941. https://doi.org/10.1039/D0EW00853B

Wainaina, S., Kisworini, A.D., Fanani, M., Wikandari, R., Millati, R., Niklasson, C., Taherzadeh, M.J., Utilization of food waste-derived volatile fatty acids for production of edible *Rhizopus obligosporus* fungal biomass. Bioresource Technology 310, 123444. https://doi.org/10.1016/j.biortech.2020.123444

Webster, T.M., Smith, A.L., Reddy, R.R., Pinto, A.J., Hayes, K.F., Raskin, L., 2016. Anaerobic microbial community response to methanogenic inhibitors 2-bromoethanesulfonate and propynoic acid. MicrobiologyOpen 5, 537–550. https://doi.org/10.1002/mbo3.349

Chapter 7 Effect of selenate on treatment of glycerol containing wastewater in UASB reactors

Abstract

The effect of selenate on the removal of glycerol in up-flow anaerobic sludge blanket (UASB) reactors was investigated. Two UASB reactors, $R_{Control}$ and $R_{Selenium,}$ were operated at a hydraulic retention time of 48 hours and an upflow velocity of 2 m/h at 37 ^{o}C. A GAL (glucose, acetate and lactate) and glycerol mixture were used as the only feedstock throughout the experiment for $R_{Control}$. After acclimation to GAL and glycerol in the start-up period, $R_{Selenium}$ was additionally exposed to selenate (SeO_4^{2-}) concentrations from 1.43 to 71.49 mg/L (10 to 500 µM) in a stepwise manner. An average daily methane yield of about 150 mL/g COD, which was comparable with $R_{Control}$, and 90% Se removal were achieved until 400 µM SeO_4^{2-}. Simultaneously, SeO_4^{2-} was reduced to elemental Se or metal selenide, supported by X-ray diffraction, as well as scanning and transmission electron microscopy. However, when the influent SeO_4^{2-} concentration was increased to 500 µM, the methane production rapidly deteriorated which was accompanied by a pH drop from 7.5 to less than 6.5, volatile fatty acid accumulation from 0.1 g/L to more than 2 g/L and COD removal efficiency drop from 98% to less than 20%. Electron flow calculations showed electron flow has shifted from methane producing archaea (MPA) to selenium reducing bacteria (SeRB) at 500 µM SeO_4^{2-}. The Se toxicity was evident from the reduction in the activity of *Methanosaeta*. Se facilitated sludge granulation evident from the increase in solids content and settling velocity of Se enriched granules (on day 130). This study showed that the SeO_4^{2-} concentration, but not the COD/SeO_4^{2-} ratio, governs the AD of selenate rich wastewaters.

7.1 Introduction

Anaerobic digestion (AD) plants utilize a range of feedstocks for digestion and production of methane that could be captured and utilized for various beneficial purposes such as power and biofuel production. A paradigm shift needs to be demonstrated on the approach of AD plants from ‘biogas-based optimization’ to ‘integrated biogas-digestate based optimization’, where along with biogas production, recovery of resources such as volatile fatty acids (VFAs), nitrogen, phosphorous, potassium and selenium should also be focussed on (Logan et al., 2019). Currently, industrial lipid-rich wastewaters, which are generated in huge amounts, are often underutilized for AD. On the other hand, there are wastewaters which are contaminated with oxyanions such as sulfate and selenate which are often disregarded for AD owing to their adverse effects on the anaerobic digestion bioprocess.

Glycerol is a key constituent in lipid-rich wastewaters, along with long chain fatty acids (Nakasaki et al., 2020). Glycerol can be produced by biological fermentation, chemical synthesis from petrochemicals or hydrogenation of sucrose. It is generated as a waste by-product during the production of bioethanol, soap and biodiesel (Viana et al., 2012). For instance, 100 kg of glycerol is generated as waste for every tonne of biodiesel produced from the transesterification of vegetable or animal oils (Baba et al., 2013). These glycerol waste could be used as substrate for AD, since the latter is inexpensive, has a clearly established metabolic pathway and generates less sludge for disposal (Vasquez et al., 2016). Dehydrogenating glycerol forms dihydroxyacetone which, after phosphorylation, can be converted to succinate and subsequently converted to propionate or pyruvate (Biebl et al., 1999). This in turn leads to simpler compounds such as formate, acetate, hydrogen, carbon dioxide and butyrate. Glycerol is readily available for acidogenic bacteria, but the limiting step is either the acetogenic or methanogenic step. During the AD of glycerol, VFAs accumulation might lead to the collapse of the AD system if they are not consumed by the acetogenic or methanogenic archaea at the same rate they are produced (López et al., 2009). In addition, the organic loading rate of glycerol should be carefully considered to avoid accumulation of metabolites (Vlassis et al., 2013). Realising methane recovery from glycerol is key for promoting a circular economy in industries where it is produced as a waste by-product, e.g. petrochemical, bioethanol and biodiesel production.

Another waste stream of interest are the industrial selenium (Se) rich wastewaters from various anthropogenic activities, such as acid mine drainage from mining, flue gas desulfurization wastewater from coal combustion, petrochemical activities, agricultural drainage and leachate from seleniferous soils (Tan et al., 2019). Due to bioaccumulation of untreated Se released into the environment, a strict discharge limit of 5 µg L^{-1} is set as the effluent regulatory discharge limit (USEPA, 2015). Anaerobic treatment of Se contaminated waste streams offers the possibility to reduce soluble selenium oxyanions (SeO_4^{2-} and SeO_3^{2-}) to insoluble, less toxic elemental selenium (Se^0), and concomitantly covert the organic matter present to energy (Lenz et al., 2008a). Furthermore, the produced biological Se^0 nanoparticles, when recovered, have various commercial applications. However, most Se-laden wastewaters are low in electron donors and require external addition to facilitate the redox process. As such, glycerol wastewater is a sustainable and cost-effective electron donor for anaerobic treatment of Se-laden wastewater (Sinharoy and Lens, 2020).

Unfortunately, most Se-laden wastewaters, typically present in the form of selenate (SeO_4^{2-}) or selenite (SeO_3^{2-}) oxyanions, are rarely considered as a suitable feedstock in biogas plants due to their perceived toxicity (Logan et al., 2022a). Se oxyanions can directly inhibit the microbial groups involved or alter the electron flow in the food web, since Se respirers can compete with methanogens for either electron donor or terminal reductase used for Se oxyanion reduction (Tchobanoglous et al., 2003). Establishing the point of SeO_4^{2-} inhibition on methanogenic systems is critical for the operation of anaerobic digesters, since a decrease in methanogenic activity reduces the bioreactor's ability to degrade the organic matter and recover energy (Lenz et al., 2008). To the best of our knowledge, there have been no studies to establish simultaneous SeO_4^{2-} reduction and methane production during long term operation of Se-laden wastewaters. In contrast, the effect of sulfate on anaerobic digestion, a structural analogon of selenate, has been well studied (Jung et al., 2022). Additionally, there have been no studies that report the co-existence and competition between methane producing archaea and selenium reducing bacteria in a bioreactor operated long term at elevated SeO_4^{2-} concentrations. There is also a lack of research on facilitation of sludge granulation in bioreactors treating selenium wastewaters.

This study aims to demonstrate the long-term continuous methane production and SeO_4^{2-}reduction for the first time using glycerol containing wastewater. The research question also includes whether the SeO_4^{2-} concentration or the COD/SeO_4^{2-} ratio governs the AD of SeO_4^{2-} rich wastewaters. The biogenic Se nanoparticles synthesised were confirmed using X-ray diffraction (XRD), transmission electron microscopy (TEM), scanning electron microscopy (SEM) and energy-dispersive X-ray spectroscopy (EDX). The change in physical characterization of the granules due to selenium exposure was also evaluated. The SeO_4^{2-} concentration that induces a microbial community shift from a methanogenic reactor to an inhibited reactor was established as well.

7.2 Materials and Methods

7.2.1 Inoculum

The characteristics of the anaerobic granular sludge treating dairy wastewater and waste activated sludge treating municipal wastewater used in this study have been described in detail by Logan et al. (2022a). The reactors were inoculated with 50 g VS of mixed sludge (anaerobic granular sludge and waste activated sludge) on a 50:50 VS basis, corresponding to a sludge bed height of about 16 cm.

7.2.2 Synthetic wastewater

A GAL (glucose, acetate and lactate) and glycerol mixture (3000 – 6000 mg/L) was used as the feedstock throughout the experiment. Sodium selenate was purchased from Alfa Aesar (Fisher Scientific, Lancashire, UK) and dissolved in distilled water to obtain 100 mM stock solutions of SeO_4^{2-}. Addition of SeO_4^{2-} concentrations from a range of 10 to 500 µM was introduced to the synthetic wastewater at different operating periods (Table 7.1). A basal nutrient solution was added to the feedstock (mg/L): $MgSO_4 \cdot 7H_2O$ (100), NH_4Cl (280), KH_2PO_4 (40), $Na_2HPO_4 \cdot 2H_2O$ (24), $FeCl_2 \cdot 4H_2O$ (2), H_3BO_3 (0.05), $ZnCl_2$ (0.05), $CuCl_2 \cdot 2H_2O$ (0.03), $MnCl_2 \cdot 4H_2O$ (0.5), $Na_2MoO_4 \cdot 2H_2O$ (0.008), $CoCl_2 \cdot 6H_2O$ (2), $NiCl_2 \cdot 6H_2O$ (0.092), and EDTA (1) (Singh et al., 2020). 2 g/L $NaHCO_3$ was supplemented to the inlet feed.

7.2.3 Up-flow anaerobic sludge bed (UASB) reactor setup and operation

7.2.3.1 Reactor setup

Two identical UASB reactors (acrylic, liquid volume 1.85 L, inner diameter 9 cm, height 81 cm) were operated at 37 °C (Figure 7.1). The digital image of the UASB reactors used is provided in Figure 7.2. The reactor tops were sealed with a rubber stopper. The reactor liquor was recirculated using a peristaltic pump to maintain an upflow velocity of 2 m/h in the reactor. The feed was pumped into the reactor with a peristaltic pump. The effluent from the UASB reactors was received in an effluent collection tank. The biogas produced was collected in 5 L gas bags. Three ports in the side of each reactor allowed pH monitoring (via a pH electrode connected to a transducer), liquid and sludge collection. The reactor was sparged with nitrogen gas (N_2) to ensure anaerobic conditions.

Table 7.1 Operational conditions applied to the two up-flow anaerobic sludge bed (UASB) reactors ($R_{Control}$ and $R_{Selenium}$)

Period	Reactor operation (d)	HRT (h)	Feedstock	COD (mg/l)	OLR (g COD/L·d)	Glycerol fed (g COD/L·d)	Glycerol-COD% in feed (gCOD/L·d)	$R_{Control}$		$R_{Selenium}$	
								Selenate (µM)	COD/Selenate ratio	Selenate (µM)	COD/Selenate ratio
A. First Phase – start-up and acclimatisation											
I	1-7	72	GAL	2400	1.0	0.00	0.0	-	-	-	-
II	8-25	48	GAL	3000	1.5	0.00	0.0	-	-	-	-
III	26-44	48	GAL+Gly	3000	1.5	0.25	16.7	-	-	-	-
IV	45-77	48	GAL+Gly	3000	1.5	0.50	33.3	-	-	-	-
B. Second phase - long term effect of Se concentration											
V	78-85	48	GAL+Gly	3000	1.5	0.50	33.3	-	-	10	2098
VI	86-93	48	GAL+Gly	3000	1.5	0.50	33.3	-	-	25	839
VII	94-105	48	GAL+Gly	3000	1.5	0.50	33.3	-	-	50	420
VIII	106-120	48	GAL+Gly	3000	1.5	0.50	33.3	-	-	100	210
IX	120-131	48	GAL+Gly	3000	1.5	0.50	33.3	-	-	200	105
X	132-136	48	GAL+Gly	3000	1.5	0.50	33.3	-	-	300	70
XI	137-141	48	GAL+Gly	3000	1.5	0.50	33.3	-	-	500	42
XII	142-149	48	GAL+Gly	3000	1.5	0.50	33.3	-	-	500	126
C. Third Phase - effect of COD/Selenate ratio											
XIII	144-149	48	GAL+Gly	6000	3.0	1.0	33.3	-	-	*	*
XIV	150-151	48	GAL+Gly	6000	3.0	1.0	33.3	300	140	*	*
XV	152-155	48	GAL+Gly	6000	3.0	1.0	33.3	400	105	*	*
XVI	156-168	48	GAL+Gly	6000	3.0	1.0	33.3	500	84	*	*
XVII	169-182	48	GAL+Gly	6000	3.0	1.0	33.3	-	-	*	*

* Recovery period for $R_{Selenium}$

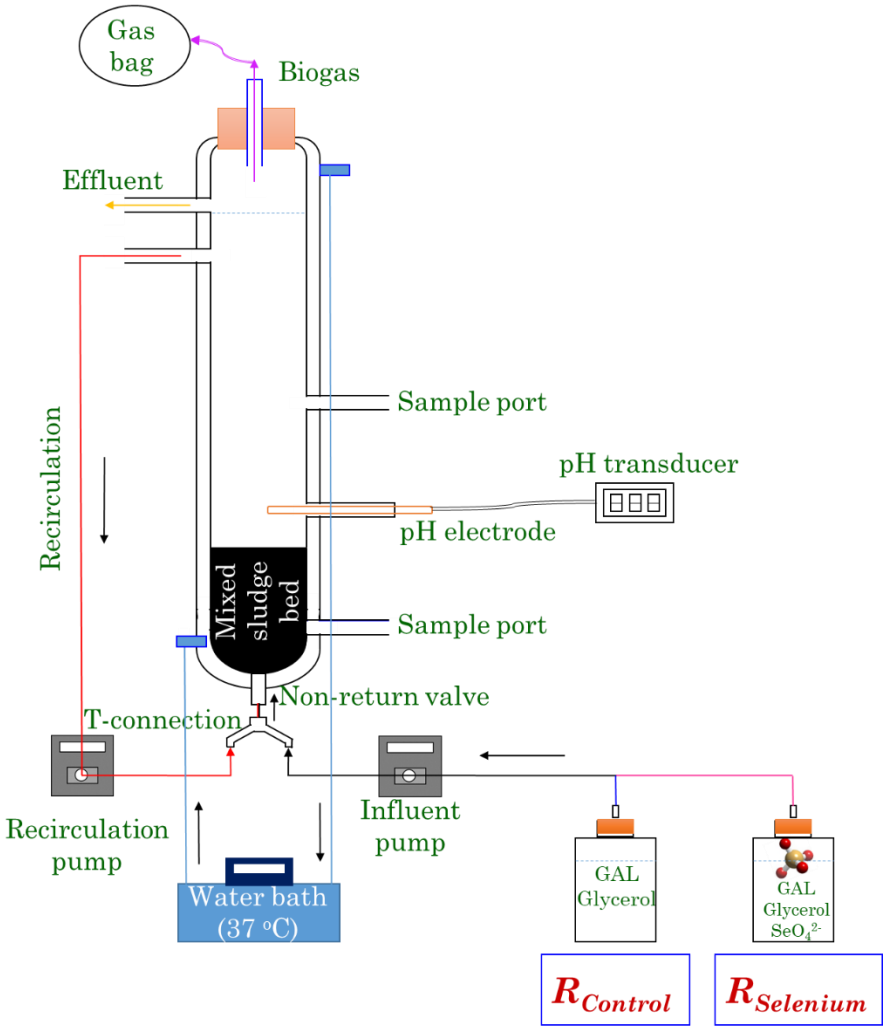

Figure 7.1 Schematic diagram of the up-flow anaerobic sludge bed (UASB) reactor used for the study. Reactors were operated at 37 °C with an upflow velocity of 2 m/h. Both $R_{Control}$ and $R_{Selenium}$ were identical except for the influent (blue line denotes feed for control reactor ($R_{Control}$) and pink line denotes feed for selenium exposed reactor ($R_{Selenium}$))

7.2.3.2 Reactor operation

The operation was ran for 182 days in 3 phases (Table 7.1).

First phase: Startup and acclimatisation. GAL was used as the sole substrate for acclimation in $R_{Control}$ and $R_{Selenium}$ on days 1 – 25 (period I – II). Glycerol was introduced along with the GAL mixture from day 26 onwards (period III). At the end of day 77 (period IV), glycerol contributed for one-third while GAL contributed for two-thirds of the influent COD (COD_i), corresponding to a COD_i of 3000 mg/L, an OLR of 1.5 g COD/L·d and a HRT of 48 h in both $R_{Control}$ and $R_{Selenium}$.

Second phase: Effect of SeO_4^{2-} concentration. From days 78 – 141 (periods V – XI) onwards, SeO_4^{2-} was introduced in a stepwise manner in $R_{Selenium}$ from 10, 25, 50, 100, 200, 300 to 500 µM, resulting in a COD/SeO_4^{2-} ratio of 2098, 839, 420, 210, 105, 70 and 42, respectively. In parallel, $R_{Control}$ was not exposed to SeO_4^{2-} and was kept as the control comparison. $R_{Selenium}$ crashed due to selenium toxicity on days 137 – 141 (period XI), and negligible gas production was observed in this reactor thereafter. Therefore, the reactor was continued in batch operation for period XII.

Third phase: Effect of COD/SeO_4^{2-} ratio. In the third phase of the experiment, $R_{Selenium}$ continued to be operated in batch mode without SeO_4^{2-} addition in an attempt for recovery and revival. This was, however, unsuccessful until the end of the run of the third phase (data not shown). $R_{Control}$ was then used to check whether the COD/SeO_4^{2-} ratio governs the AD process, since it was not yet exposed to Se. The COD in the influent was doubled to 6000 mg COD/L, corresponding to an OLR of 3 g COD/L·d and HRT of 48 h from days 144 – 149 (period XIII). From days 150 – 168 (period XIV-XVI), SeO_4^{2-} was introduced to the influent at 300, 400 and 500 µM, corresponding to a higher COD/SeO_4^{2-} ratio of 140, 105 and 84. A process failure was observed again during Period XVI, and therefore, the system was allowed to 'recover' during days 169 – 182 (Period XVII).

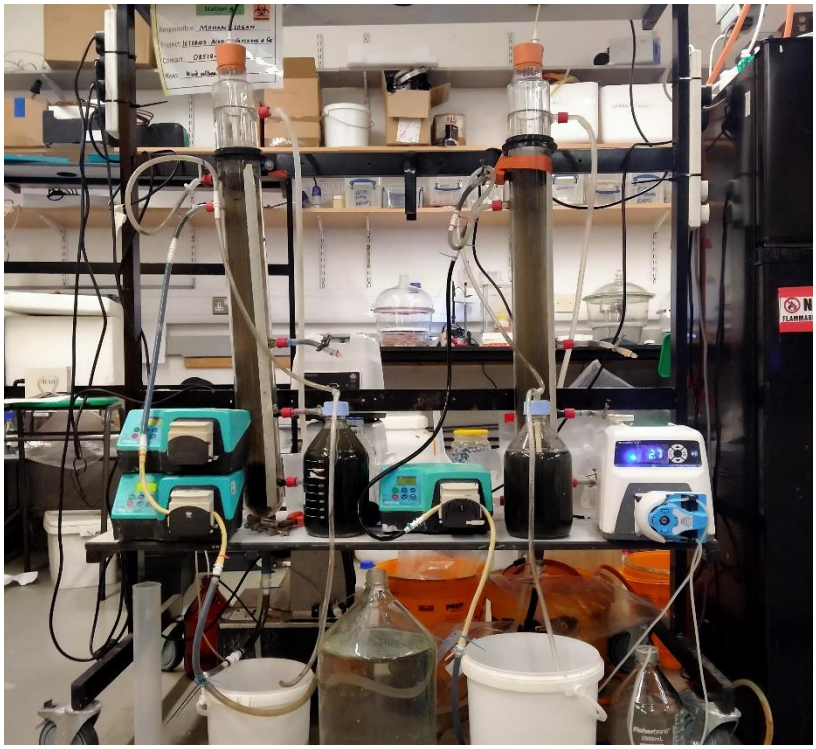

Figure 7.2 Photograph of the UASB reactor setup used in this study

7.2.4 Specific methanogenic activity test

Representative sludge samples from $R_{Selenium}$ (before methanogenic inhibition, period XI) and $R_{Control}$ on day 135 were taken and used to evaluate for their methanogenic activity following the procedure described by Colleran et al. (1992). Acetate and H_2/CO_2 (80:20) were used as the soluble and gaseous direct methanogenic substrates, respectively. The serum reactor configurations were similar to those described in Logan et al. (2022a).

7.2.5 Microbial community analyses

Approximately 2 ml of sludge samples were taken from both reactors during each sampling point where major operational changes were conducted (Figure 7.3) for microbial community analyses (DNA and rRNA). After sampling, the samples were immediately centrifuged at 5,000 rpm for 5 min. The supernatant was discarded and the pellet was flash-frozen using liquid nitrogen before storing at -80 ^{o}C. The pellets were used for RNA and DNA extraction as described by Thorn et al. (2019). RNA purification was carried out using the TURBO DNA-free™ Kit (Ambion by Life Technology) and the complementary deoxyribonucleic acid (cDNA) was generated from DNA-free RNA samples using the superscript reverse transcriptase III kit (Qiagen) (Logan et al., 2022b). Both DNA and cDNA were purified using sodium acetate precipitation (Thermo fisher scientific). The purified DNA and cDNA were sent to an external laboratory (Novogene, Oxford, UK) for *16S rRNA* amplicon sequencing using the MiSeq Illumina platform. The primers used to sequence the V3 – V4 region of the Bacteria *16S rRNA* gene at both DNA and cDNA level were 357wF (CCTACGGGNGGCWGCAG) and 806R (GGACTACHVGGGTWTCTAAT) and 517F (GCYTAAAGSRNCCGTAGC) and 909R (TTTCAGYCTTGCGRCCGTAC) for the V4 – V5 region of the Archaea *16S rRNA* gene.

7.2.6 Analytical techniques

Chemical oxygen demand (COD), total solids (TS) and volatile solids (VS) were determined using standard methods (APHA, 2017). Biogas volume was calculated using the water displacement method. The methane concentration in the biogas was determined using a VARIAN CP-3800 gas chromatograph (Varian, Inc., Walnut Creek, CA, USA). VFAs were measured using a high-performance liquid chromatograph (HPLC) (1260 Infinity II, Agilent, USA) equipped with a Hi-Plex H (300 x 7.7 mm) column, heated at 60 ^{o}C and a refractive

index detector (RID) set at 55 ºC. A 0.005 M H_2SO_4 solution was used as the mobile phase at a flow rate of 0.7 mL/min.

SeO_4^{2-} and SeO_3^{2-} were measured using an ion chromatograph equipped with an electrical conductivity detector (Dionex™ Aquion™, Thermo Scientific, Waltham, USA) as described by Florentino et al. (2020). Samples for Se^0 and total Se analyses were prepared following the protocol described by Mal et al. (2016) and quantified using an inductively coupled plasma – optical emission spectroscopy 5110 synchronous vertical dual view (ICP-OES 5110, Agilent Technologies, Santa Clara, USA). 100 mL biogas was collected weekly in a syringe and scrubbed in 10 mL 65 % HNO_3 acid and then measured by ICP-OES to detect the presence of gaseous selenium components in the biogas.

Sludge samples from $R_{Selenium}$ and $R_{Control}$ taken on day 130 during period IX were analysed for extra polymeric substance (EPS) characterisation and identification of biogenic Se nanoparticles deposited on the sludge surface. The sample from the final day of the experiment was collected and powdered after freeze drying. The powdered sample was analysed for X-ray powder diffraction (XRPD) with an Inel Equinox 6000 (Thermo Scientific, Waltham, USA) using an X-ray source of CuKα radiation (wavelength λ = 1.54056 m) between 2º to 80º (2θ) as described by Duggan et al. (2020). The peak identification in the XRD was performed with a match on the Joint Committee on Powder Diffraction Standards (JCPDS) database. The protocols followed for TEM and SEM preparation, fixation and imaging are described in detail by, respectively, Florentino et al. (2020) and Tan and Lens (2021). Fluorescence emission excitation matrix (FEEM) spectra were recorded on a Shimadzu RF-6000 (Kyoto, Japan) following the method described by Logan et al. (2022b).

7.2.7 Calculations

The COD fraction converted to CH_4 and total VFA were measured, quantified and converted to their COD equivalent at each operational regime. COD accumulated was calculated from subtracting all measured values (CH_4 and total VFA) from the initial COD input. Non-metric multi-dimensional scaling (NMDS) analysis was performed as mentioned by Logan et al. (2022b). Alpha diversity was applied in analyzing complexity of biodiversity for a sample through Observed-species and Shannon indices which were calculated with QIIME (Version 1.7.0) and displayed with R software (Version 2.15.3).

The percent electron flow by the SeRB and MPA can be calculated from the following equations (modified from Hoa et al., 2007):

$$\text{Percent electron flow by MPA} = \left[\frac{A}{(A+B)}\right] \times 100 \qquad \text{Eq. (7.1)}$$

$$\text{Percent electron flow by SeRB} = \left[\frac{B}{(A+B)}\right] \times 100 \qquad \text{Eq. (7.2)}$$

where, A is moles of methane produced and B is moles of selenate reduced.

7.3 Results

7.3.1 Start-up of anaerobic treatment of glycerol containing wastewater

Figure 7.3 shows the average methane yield as well as the Se and sCOD removal efficiency from both $R_{Control}$ and $R_{Selenium}$. During Periods I and II, the daily methane yield fluctuated for both $R_{Selenium}$ and $R_{Control}$ during the initial acclimatization and washout was observed from the sludge bed. The higher methane production rate was possibly due to the conversion of COD from the sludge rather than the substrate provided. The reactor adapted well to the glycerol and a stable performance was achieved in Period III. An average methane production rate of ~200 mL/g COD·d was realised in both reactors until day 56. This stable performance in Period IV was interrupted due to an operational issue. The recirculation pipeline in $R_{Control}$ suffered a leakage on day 57 and was replaced immediately. The replacement of a new recirculation pipeline resulted in the loss of the biofilm that had developed on it and consequently decreased the methane yield to ~ 100 mL/g COD in $R_{Control}$. Around the same time, on day 56, about 15 g of biomass washed out, resulting in a decreased methane yield to ~ 150 mL/g COD in $R_{Selenium}$. Due to this operational issue, $R_{Selenium}$ was continued to be operated at the same operational condition for an extended time period until day 77 to return to a stable performance. An average COD removal efficiency of more than 98% and pH range above 7.5 were observed in both $R_{Selenium}$ and $R_{Control}$ during the start-up phase. More than 90% of the VFAs produced during this phase were acetic and propionic acid (Figure 7.4).

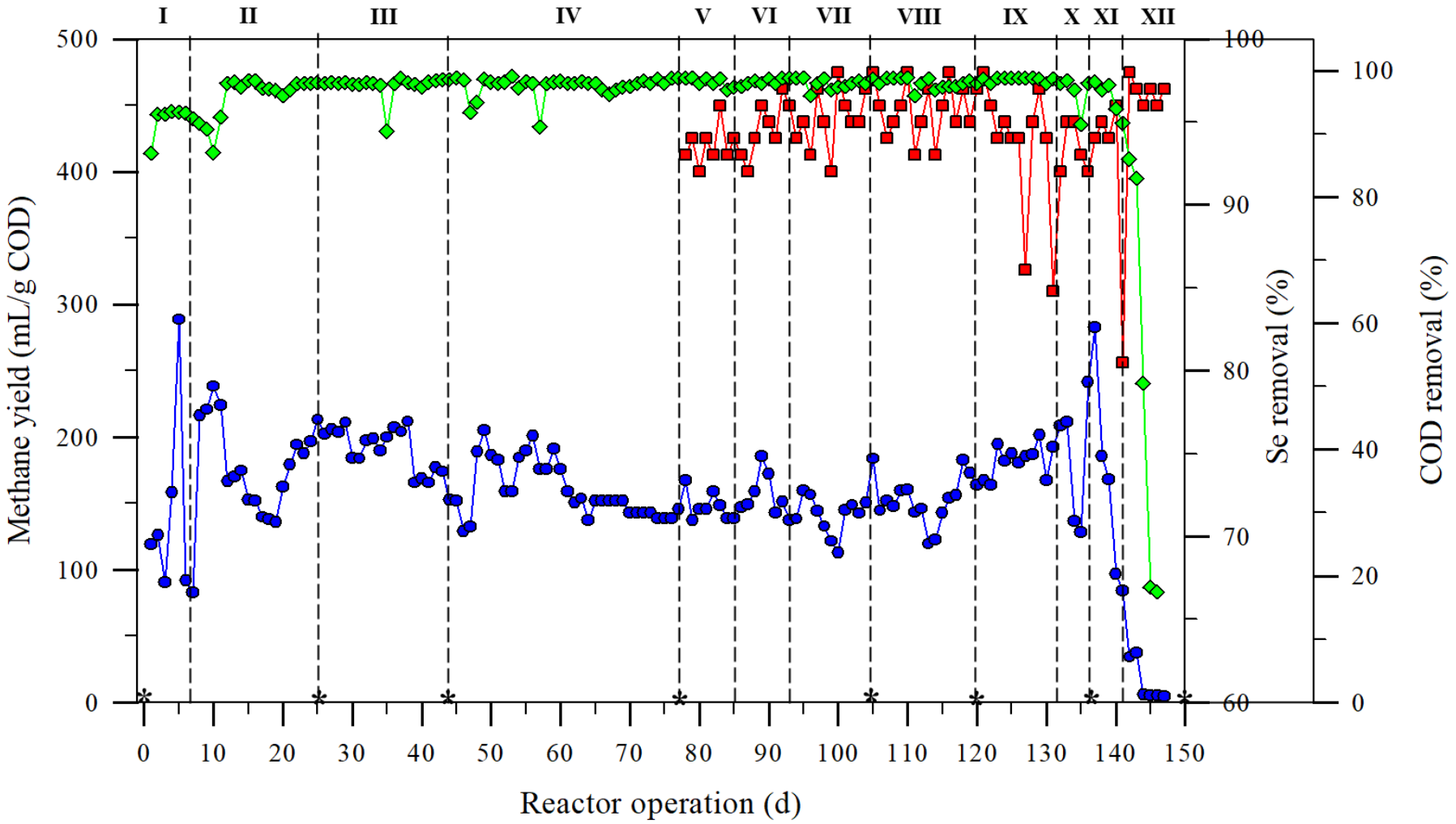
I
II
III
IV
V
VI
VII
VIII
IX
X
XI
XII
Methane yield (mL/g COD)
Se removal (%)
COD removal (%)
Reactor operation (d)
0
100
200
300
400
500
60
70
80
90
100
0
20
40
60
80
100
0
10
20
30
40
50
60
70
80
90
100
110
120
130
140
150

(a)

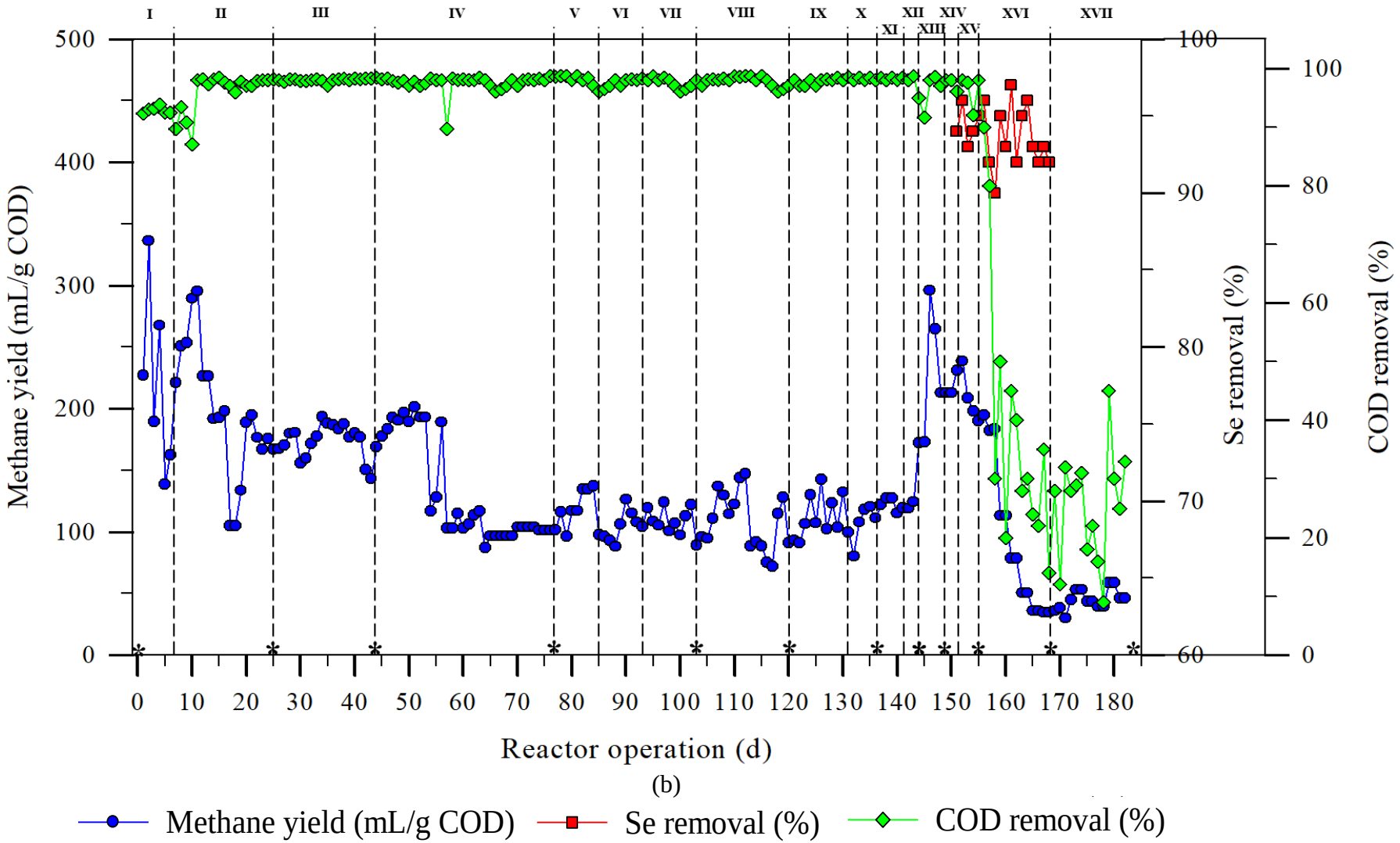

Figure 7.3 Methane yield, Se removal and COD removal in the UASB reactors (A) $R_{Selenium}$ and (B) $R_{Control}$ treating glycerol containing synthetic wastewater. * symbol denotes that sludge samples were taken during the time point for microbial community analysis.

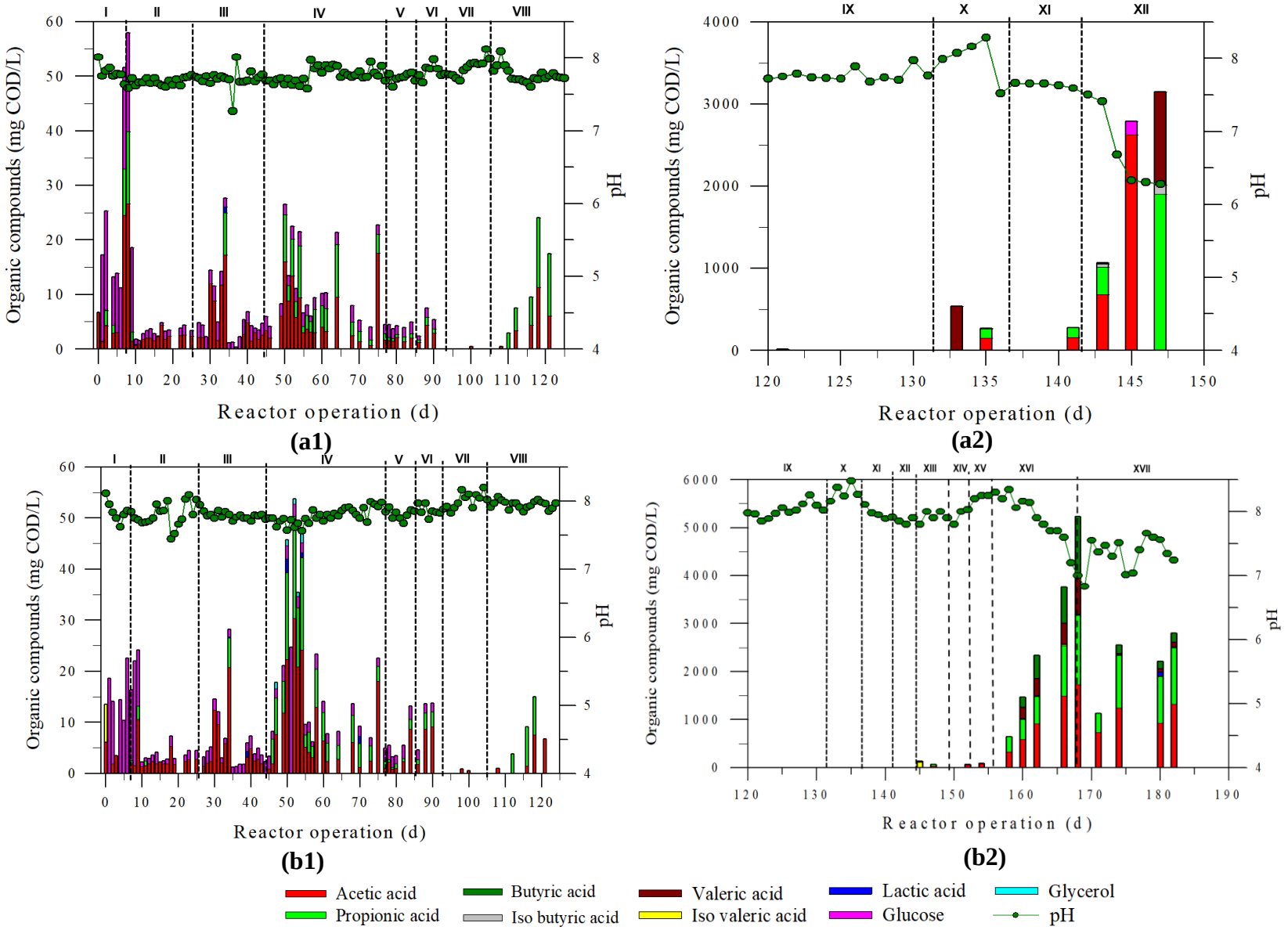

Figure 7.4 Organic compounds profile in $R_{Selenium}$ (a1 and a2) and $R_{Control}$ (b1 and b2) UASB reactors treating glycerol containing synthetic wastewater

7.3.2 Effect of SeO_4^{2-} on methane production from glycerol and GAL containing wastewater

In Period V – X, where the SeO_4^{2-} concentration was increased from 10 to 400 µM, an average daily methane yield of about 150 mL/g COD·d was achieved in $R_{Selenium}$. During this period, the methane concentration in the biogas was found robust between 60-70%. The pH value ranged above 7.5 till as high as 8.5, and the COD removal efficiency was about 98% (Figure 7.3). The COD to methane conversion efficiency was 40 – 55 % until the end of period X. Acetic and propionic acid were the dominant acids produced in Period V – X (Figure 7.4). Simultaneously, more than 90% of soluble selenium removal was accomplished in Periods V – X. An average daily methane yield of about 100 mL/g COD was observed in $R_{Control}$, with a biogas containing 60-70% methane, 98% COD removal efficiency and pH range of 7.5-8.5. Interestingly, selenium was also detected in the biogas, most likely in the form of hydrogen selenide. The average gaseous Se concentration was in the range of 110 to 330 ppb Se_{gas}, when the influent SeO_4^{2-} concentration was increased from 100 to 300 µM.

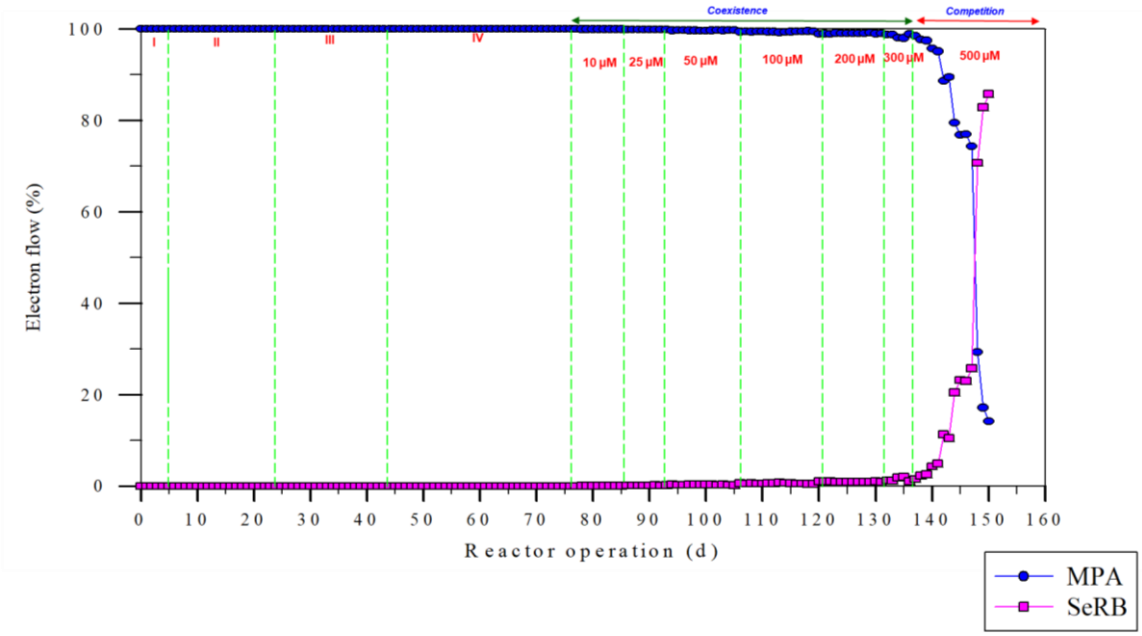

Figure 7.5 Electron flow analysis revealing the flow alteration at 500 µM SeO_4^{2-}

However, methanogenesis rapidly deteriorated in $R_{Selenium}$ at 500 µM SeO_4^{2-} (Period XI – XII). As a result of the elevated SeO_4^{2-}, a negligible daily gas production (< 10 mL/d) was recorded during this time. The methane concentration in the biogas also declined steeply from 70% to less than 10%, clearly showing the Se toxicity on methanogenic archaea. The pH

dropped to 6.5 and the COD removal efficiency was below 20%. Acetic, propionic and valeric acid accumulated in $R_{Selenium}$ during this period (Figure 7.4). At the end of period XI – XII, the COD to methane conversion had drastically reduced from over 40% to around 1%. Figure 7.5 shows the electron flow analysis revealing the flow alteration at 500 µM SeO_4^{2-}. This study also suggests the shift from a methanogenic to a selenium reducing reactor, due to exposure to elevated SeO_4^{2-} concentrations. On the other hand, an average daily methane yield of more than 100 mL/g COD·d was accomplished in $R_{Control}$, with a 98% COD removal efficiency, 60-70% methane concentration in the generated biogas, 7.5-8.5 pH range and without any VFAs accumulation in Periods XI – XII (Figures 7.3 and 7.4).

After $R_{Selenium}$ crashed, a dedicated recovery time period (about a month) was adopted (data not shown). However, the system suffered a permanent methanogenesis process failure, despite several strategies adopted for its recovery, i.e. reduced organic loading rate (OLR < 0.5 g COD/L·d), increased hydraulic retention time (HRT > 72 h), buffer (sodium bicarbonate) addition (2 g COD/L) for pH increment (from 6.5 to 8.0), removing selenate and glycerol from the GAL influent. Though there was negligible methane production, the Se removal efficiency (> 90%) of $R_{Selenium}$ was not hampered in Periods XI – XII.

7.3.3 Influence of COD/SeO_4^{2-} ratio on process performance

The third phase of the experiment addressed the research question of whether the COD/SeO_4^{2-} ratio influences the performance of the AD of selenate containing wastewater (Figure 7.3). This was tested on the $R_{Control}$ as it was not exposed to SeO_4^{2-} until now (Table 7.1). With the COD increment in the influent from 3 g/L to 6 g/L, the average daily methane yield increased from 150 to 200 mL/g COD·d (Period XIII). When SeO_4^{2-} was introduced at 300 and 400 µM in Periods XIV and XV, an average daily methane yield of about 200 mL/g COD·d was realised. However, at 500 µM SeO_4^{2-}, the methane production started to decline again to less than 50 mL/g COD despite the higher COD/SeO_4^{2-} ratio in Period XVI. Correspondingly, the COD to methane conversion reduced from about 52% to 15%.

SeO_4^{2-} was removed from the influent and the system was allowed to recover over a period of nearly a month in Period XVII. The methane production never improved above 50 mL/g COD (Figure 7.3), despite adopting similar strategies stated in the earlier phase (such as reduced OLR, increased HRT, buffer addition and removal of selenate and glycerol from the GAL influent). On the other hand, during this inhibition period (XVI – XVII), the intermediate

compounds especially volatile fatty acids such as acetic, propionic, butyric and valeric acid accumulated in the reactor (Figure 7.4). Figure 7.3 shows more than 90% soluble selenium was removed during concomitant methane production in Periods XIV – XVII. On average, more than 85% total Se was removed both in the second and third phases of the study.

7.3.4 UASB sludge characterisation

7.3.4.1 Methanogenic activity

At the end of phase three, the sludge samples taken from $R_{Selenium}$ and $R_{Control}$ were tested for their specific methanogenic activity after 130 days operation. The SMA value of Se enriched sludge utilizing acetate as the substrate was lower at 940 mL CH_4 g^{-1} VS compared to the control sludge (1690 mL CH_4 g^{-1} VS) (Table 7.2). On the other hand, the sludge enriched with SeRB could utilize gaseous hydrogen as the substrate to reduce SeO_4^{2-} and still resulted in an SMA value of 765 mL CH_4 g^{-1} VS similar to that of the sludge from the control reactor.

The average COD mass balance in $R_{Control}$ during the periods operated without Se exposure as well as at 300 µM SeO_4^{2-} and 500 µM SeO_4^{2-} is shown in Figure 7.6. Though about 50% COD was effectively converted to methane during the periods operated as Control (without Se exposure) and at 300 µM SeO_4^{2-}, only less than 20% COD was converted to methane at 500 µM SeO_4^{2-}, where ~30% COD conversion to VFAs was observed.

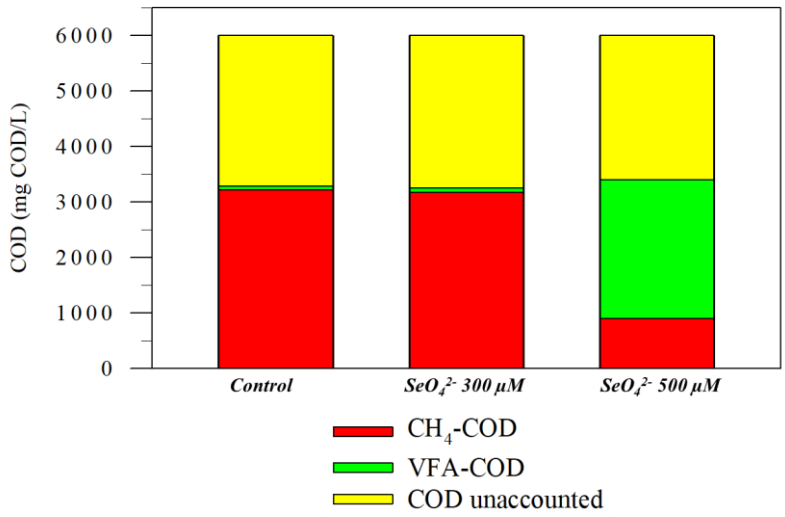

Figure 7.6 COD mass balance for different selenate concentration. COD fraction converted to CH_4 and total VFA were measured, quantified and converted to their COD equivalent. COD

accumulated was calculated from subtracting all measured values (CH_4 and total VFA) from the influent COD.

Table 7.2 Specific methanogenic activity of control and selenium enriched sludge collected on day 130

Substrate	**Specific methanogenic activity (mL CH_4 g^{-1} VS at STP)**		
	Control sludge	**Selenium enriched sludge**	**Selenium enriched sludge spiked with 100 µM SeO_4^{2-}**
Acetate	1693.5 (±224.50)	939.25 (±67.65)	927.84 (±59.93)
H_2/CO_2	720.23 (±55.75)	935.75 (±22.44)	766.18 (±204.86)

7.3.4.2 TEM, SEM and EDX analysis

Red deposits indicating the deposition of biogenic selenium were found in the granules, tubings and sampling ports of the selenium fed UASB reactor (shown in Figure 7.8). Figure 7.7a shows TEM images of the extracellularly synthesised Se nanospheres. SEM-EDX (Figure 7.7c) and XRD (Figure 7.9) measurements supported formation of elemental selenium and metal selenides in the granules. Also the SEM images (Figure 7.7b) showed spherical shaped nanoparticles and the EDX analysis (Figure 7.7c) confirmed the presence of the elemental Se. The XRD peaks (Figure 7.9) are indexed to (100), (101), (102) and (201) lattice planes of Se, being in good agreement with the characteristic peaks in the JCPDS standard card No. 00-065-1876. The interaction of trace metal ions with HSe^- results in the generation of metal selenide minerals. The smaller peaks corresponding to ZnSe (JCPDS card No. 00-037-1463), NiSe (JCPDS card No. 00-018-0888, JCPDS card No. 00-075-0610), MnSe (JCPDS card No. 00-020-0663), FeSe (JCPDS card No. 00-012-0290) and CoSe (JCPDS card No. 00-089-2004) are indicated in Figure 7.9. Notably, XRD spectra showed peak broadening possibly due to a highly amorphous nature of the elemental selenium and metal selenide precipitates.

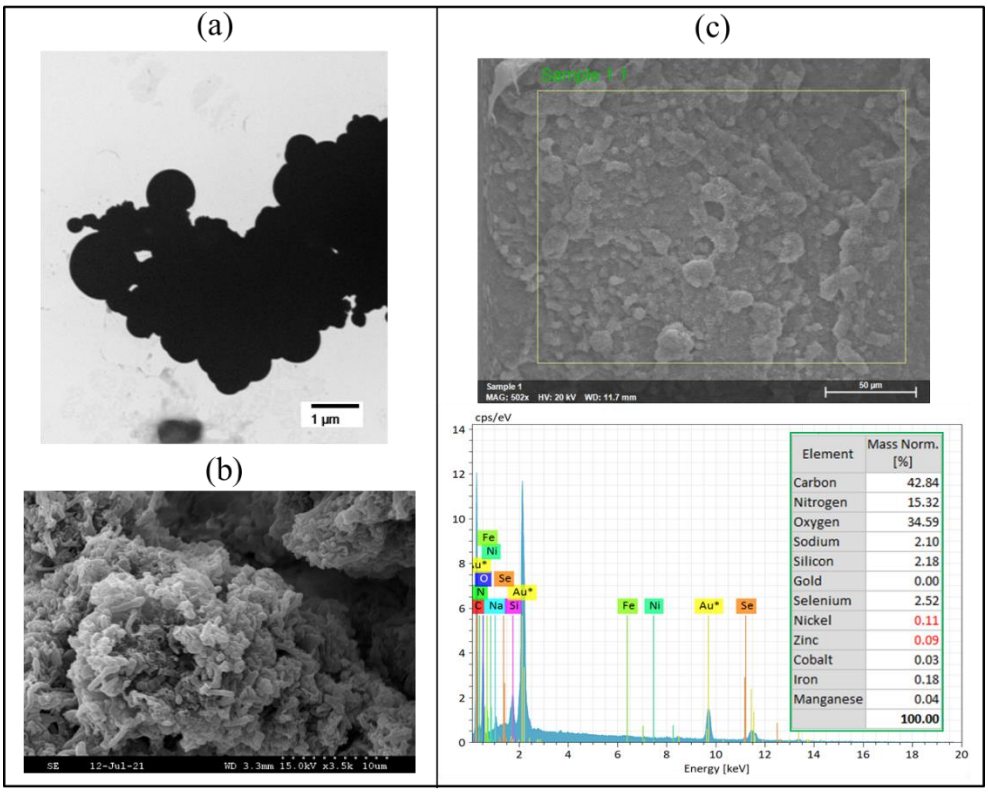

Figure 7.7 Electron microscopic images (a) TEM, (b) SEM, and (c) SEM-EDX of sludge taken from $R_{Selenium}$ on day 140 (Period XI) showing biosynthesis of elemental selenium and metal selenides

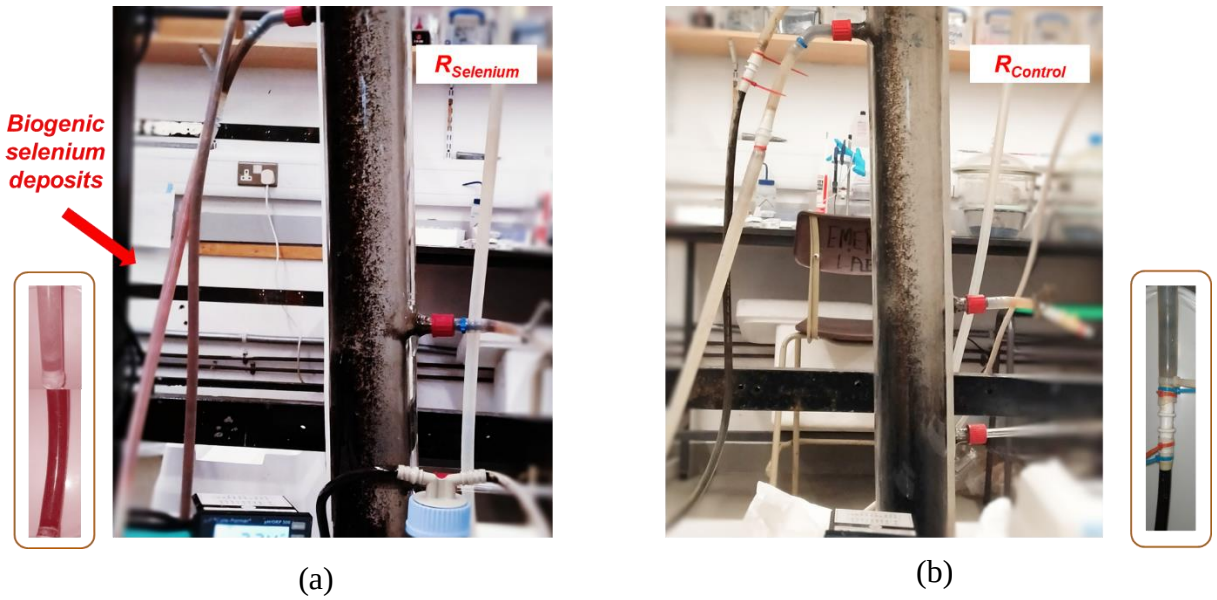

Figure 7.8 Red deposits showing biogenic selenium deposits in $R_{Selenium}$, the UASB reactor fed with selenate (in the left). $R_{Control}$ is shown on the right.

7.3.4.3 Physical and chemical characteristics of the UASB granules

On physical observation, repeated Se exposure led to a more compact and dense sludge bed, when compared to the sludge bed of $R_{Control}$ which was fluffy and more expanded. Figures 7.10a and b shows the solids content (total and fixed) and settling velocity of the $R_{Control}$ and $R_{Selenium}$ sludge at the end of the second phase. About 14 % increase in the total solids and 8.5 % increase in the fixed solids concentration was observed at the end of 150 days of reactor operation. Granules from $R_{Selenium}$ exhibited increased settling velocity by about 33% when compared with $R_{Control}$ granules. Since Se volatilises at 688 ^{o}C and has a density of 4200-4800 kg m^{-3} (McColm, 2013), it is possible that the Se deposition could have contributed to the fixed solids content. The FEEM characterisation analyses of extracellular polymeric substances (EPS) extracted from $R_{Control}$ and $R_{Selenium}$ sludge is presented in Figure 7.11. Relatively lesser humic substances are observed in the EPS extracted from $R_{Selenium}$ sludge.

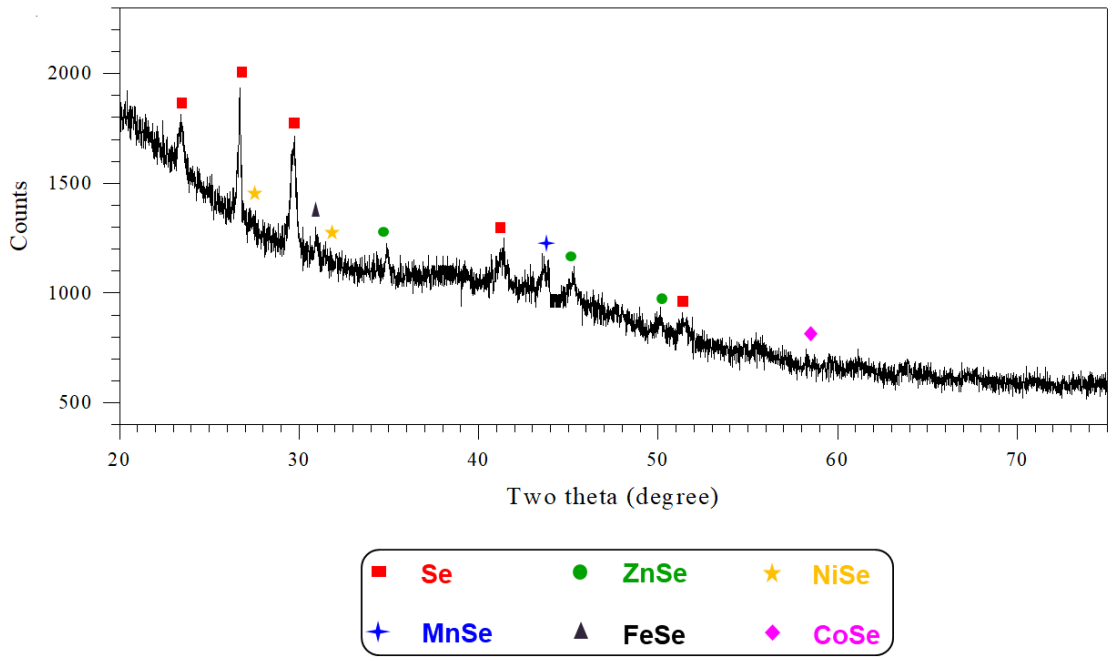

Figure 7.9 X-ray diffraction patterns showing peaks of selenium and trace metal selenides in the sludge from $R_{Selenium}$ on day 140 (Period XI). The identified minerals are marked with the following peak signatures according to the standard database JCPDS: Se (00-065-1876), ZnSe (00-037-1463), NiSe (00-018-0888, 00-075-0610), MnSe (00-020-0663), FeSe (00-012-0290) and CoSe (00-089-2004).

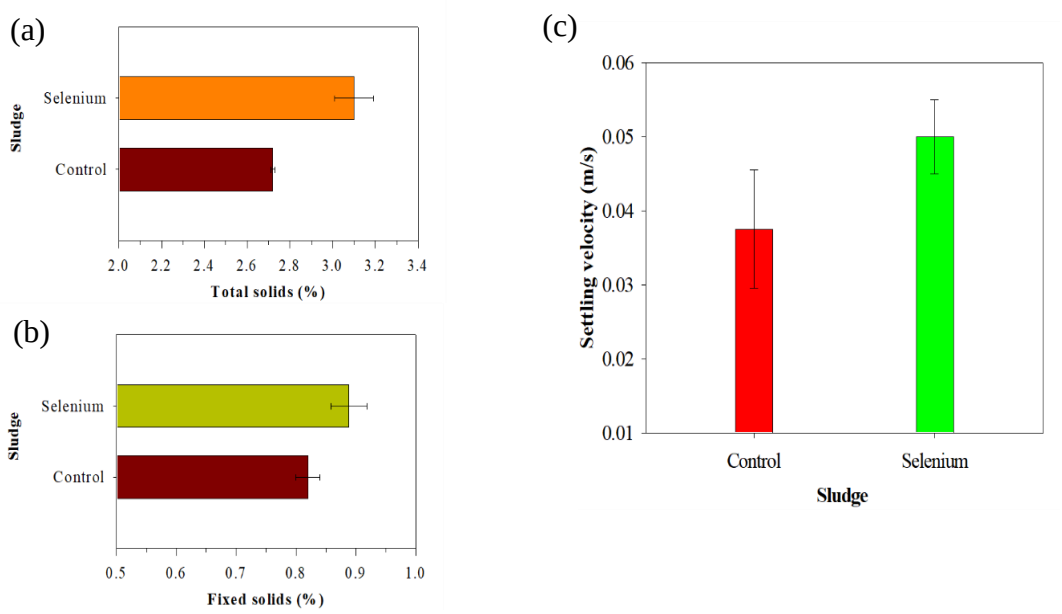

Figure 7.10 (a) Total solids and (b) fixed solids content and (c) settling velocity of sludge from $R_{Control}$ and $R_{Selenium}$ after day 140 of operation (Period XI)

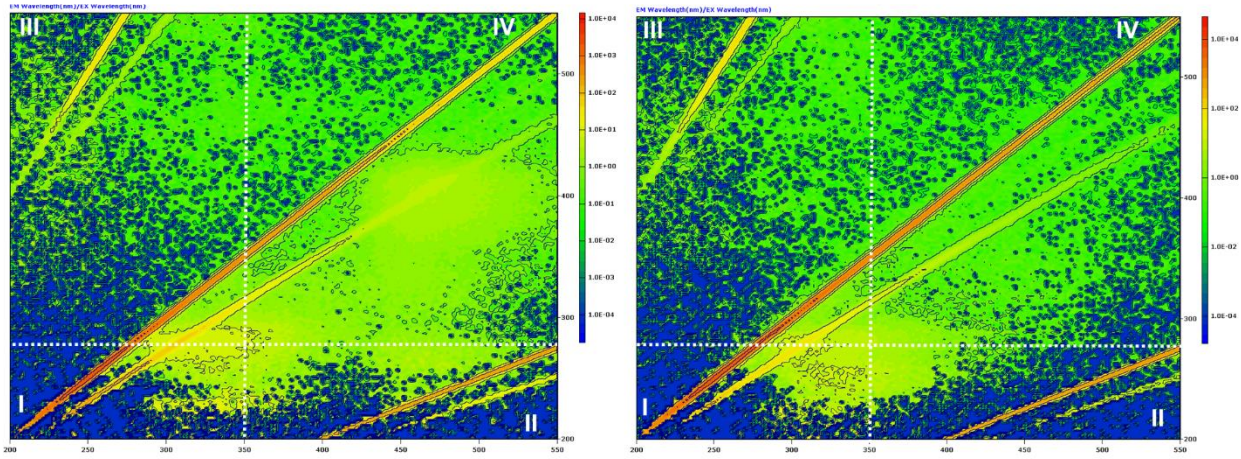

(a) (b)

Figure 7.11 FEEM characterisation analyses of extracellular polymeric substances (EPS) extracted from control (a) and selenium enriched (b) sludge on day 130. Prior to FEEM analyses, the TOC content was normalized to 10 mg/L.

7.3.5 Microbial community dynamics

Figures 7.12a and b show the bacterial communities present in $R_{Selenium}$ and $R_{Control}$ during different periods at DNA and RNA level, respectively. *Lentimicrobium*, *Lactococcus*, *Anaeroarcus*, *Pseudomonas*, *Azovibrio*, *Tolumonas*, *Smithella*, *Cloacimonadales LNR A2-18*, *Syner-01*, *Mesotoga* and *Chthonomonadales* were observed in the total (DNA) bacterial

communities (Figure 7.12a). Higher relative abundance (RA) of *Lentimicrobium, Lactococcus, Pseudomonas, Azovibrio, Acinetobacter, Smithella, Arcobacter* and *Cloacimonadales LNR A2-18, Syner-01* was observed at RNA level (Figure 7.12b).

Figures 7.13a and b present the archaeal communities present in both $R_{Selenium}$ and $R_{Control}$ at the different periods at DNA and RNA level, respectively. The highest RA (~ 80%) of *Methanobacterium* was found in the total (DNA) archaeal communities throughout the operational period. A high RA (< 20%) of *Methanobrevibacter, Candidatus Methanofastidiosum, Methanosphaera,* and *Methanosaeta* was also observed at DNA level (Figure 7.13a). The RA of *Methanosaeta* was the highest amongst the other archaea at RNA level (Figure 7.13b). However, it was quickly replaced by *Methanobacterium* at 500 µM SeO_4^{2-}.

Though the RA of *Methanosaeta* was very low (< 5 %) at DNA level, the RA at RNA level was found very high (~ 80%) at the control and non-inhibitory Se concentration. During periods X-XII, when $R_{Control}$ was not exposed to SeO_4^{2-}, the RA of *Methanosaeta* was about 80%. However, at $R_{Selenium}$ which suffered methanogenic inhibition during this period, the RA of *Methanosaeta* decreased to below 50%. KRONA visually displays the analysis result of taxonomic annotation (Ondov et al., 2011). Circles from inside to outside stand for different taxonomic ranks, and the area of sector means the respective proportion of different OTU annotation results. As shown in the KRONA graphs (Figure 7.14), the RA of *Methanosaeta* was 78% without SeO_4^{2-} exposure and 76% during the operation with 300 µM SeO_4^{2-} at RNA level. At 500 µM SeO_4^{2-}, the RA of *Methanosaeta* decreased to 13%.

The non-metric multi-dimensional scaling (NMDS) plot revealed that a distinct microbial cluster has evolved from the inoculum to the periods treating glycerol and finally at 500 µM SeO_4^{2-} in both $R_{Selenium}$ and $R_{Control}$ (Figure 7.15). Figure 7.17 shows the alpha diversity through observed species and shannon indices. Figure 7.18 presents the flower diagram for $R_{Selenium}$ and $R_{Control}$ at the different operational periods. Each petal in the flower diagram represents a group, with different colours for different groups. The core number in the center is for the number of OTUs present in all groups, while the number in the petals for the unique OTUs only showing in each group. Overall, the richness and diversity of OTUs have reduced over the operational period both in $R_{Selenium}$ and $R_{Control}$. Remarkably, the family Proteobacteria was significantly higher ($p < 0.05$) during Period X (300 µM SeO_4^{2-}) when compared to Period IV (without Se exposure), as shown in the t-test results in Figure 7.16.

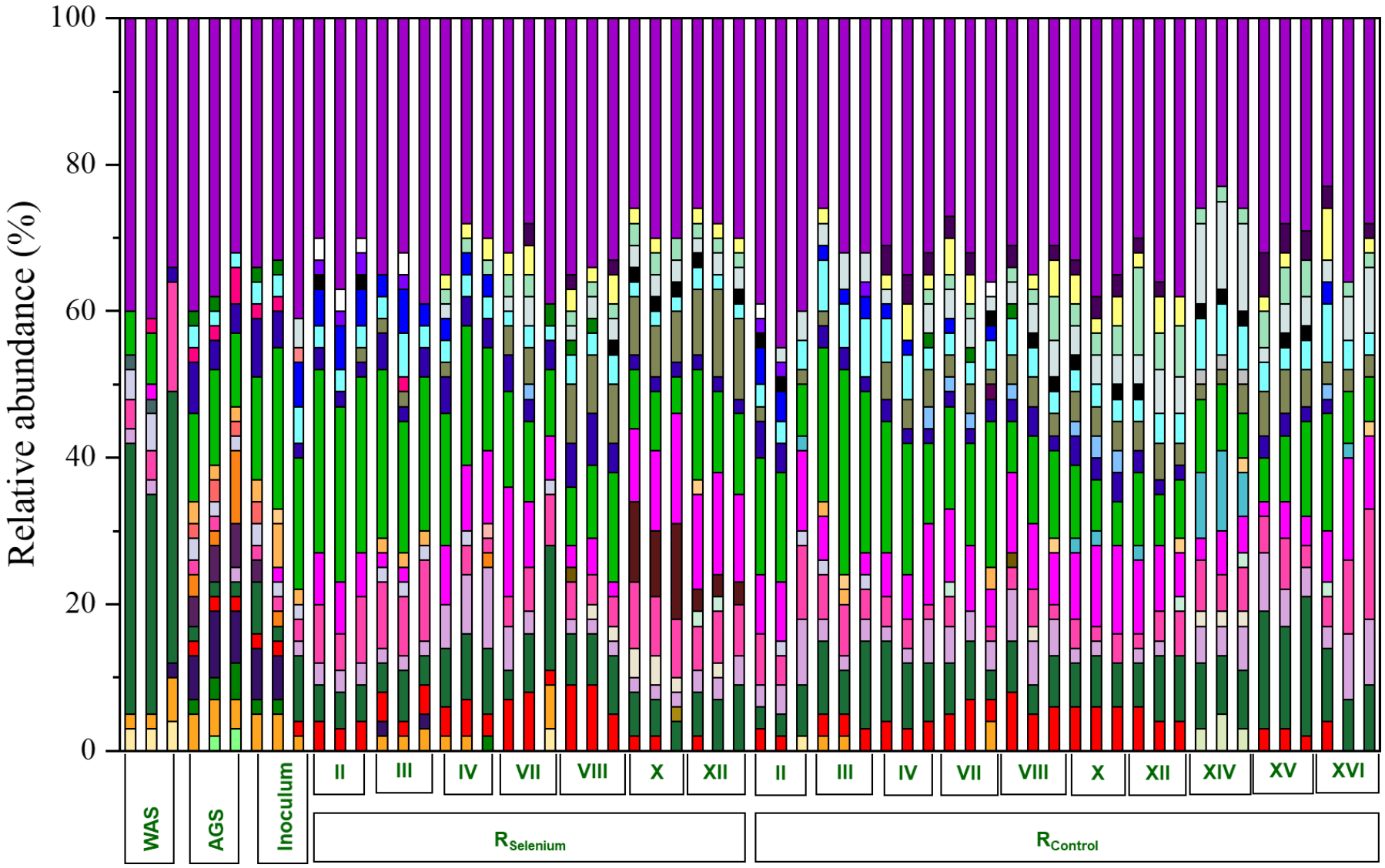
Relative abundance (%)
100
80
60
40
20
0
WAS
AGS
Inoculum
II
III
IV
VII
VIII
X
XII
II
III
IV
VII
VIII
X
XII
XIV
XV
XVI
R Selenium
R Control

(a)

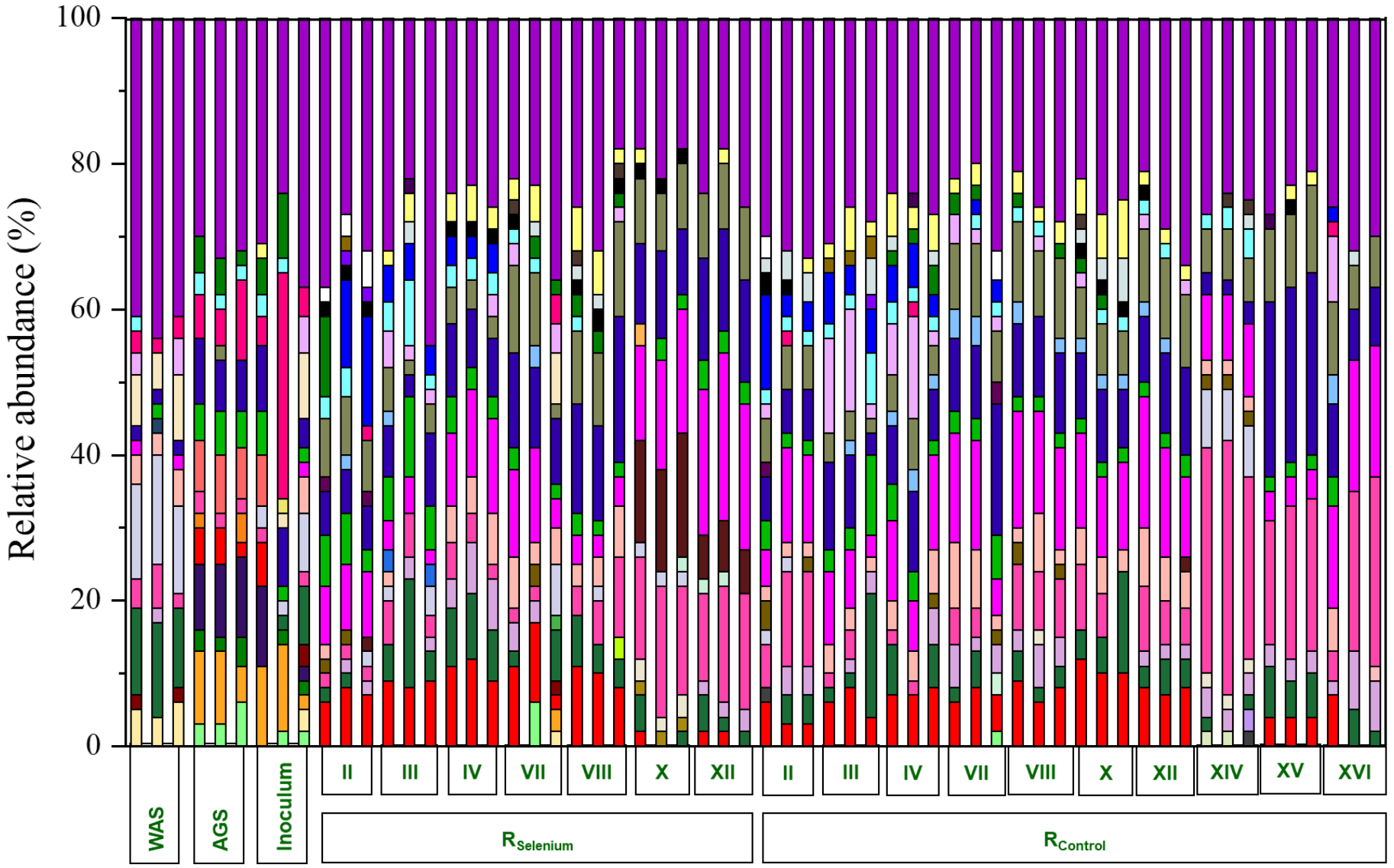
Relative abundance (%)
100
80
60
40
20
0
WAS
AGS
Inoculum
II
III
IV
VII
VIII
X
XII
II
III
IV
VII
VIII
X
XII
XIV
XV
XVI
R Selenium
R Control

(b)

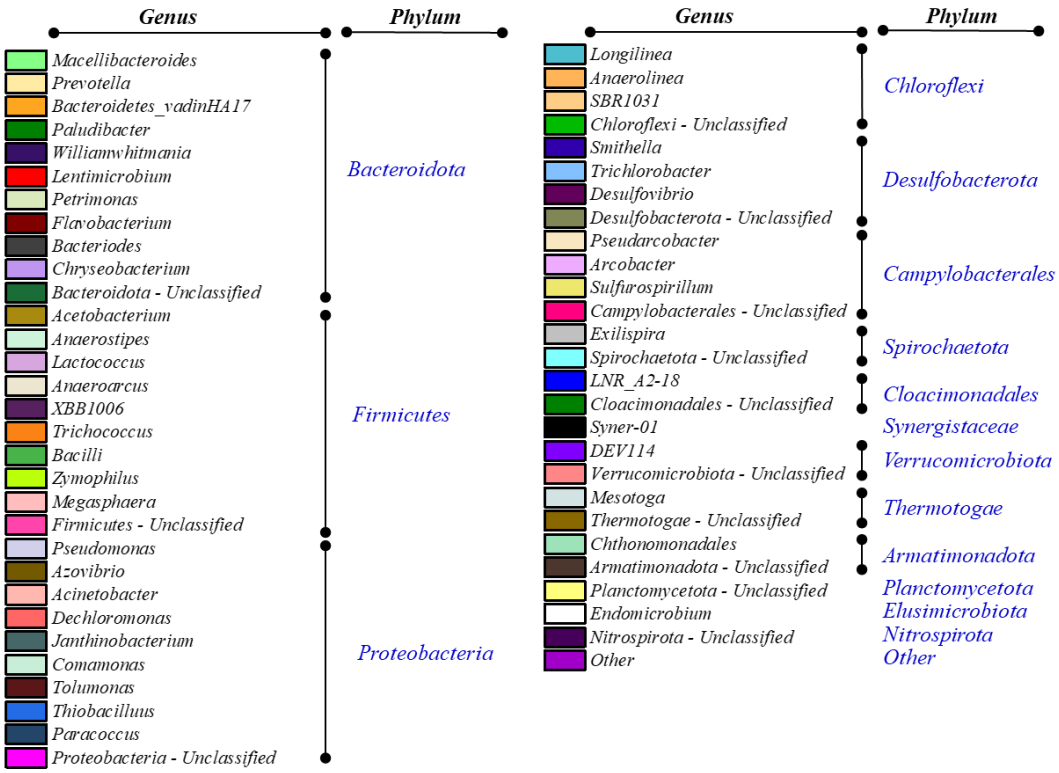

Figure 7.12 Bacterial communities in $R_{Selenium}$ and $R_{Control}$ at different operational periods (RA < 2% at genera rank and unclassified phyla were grouped as 'Other') at (a) DNA level and (b) RNA level

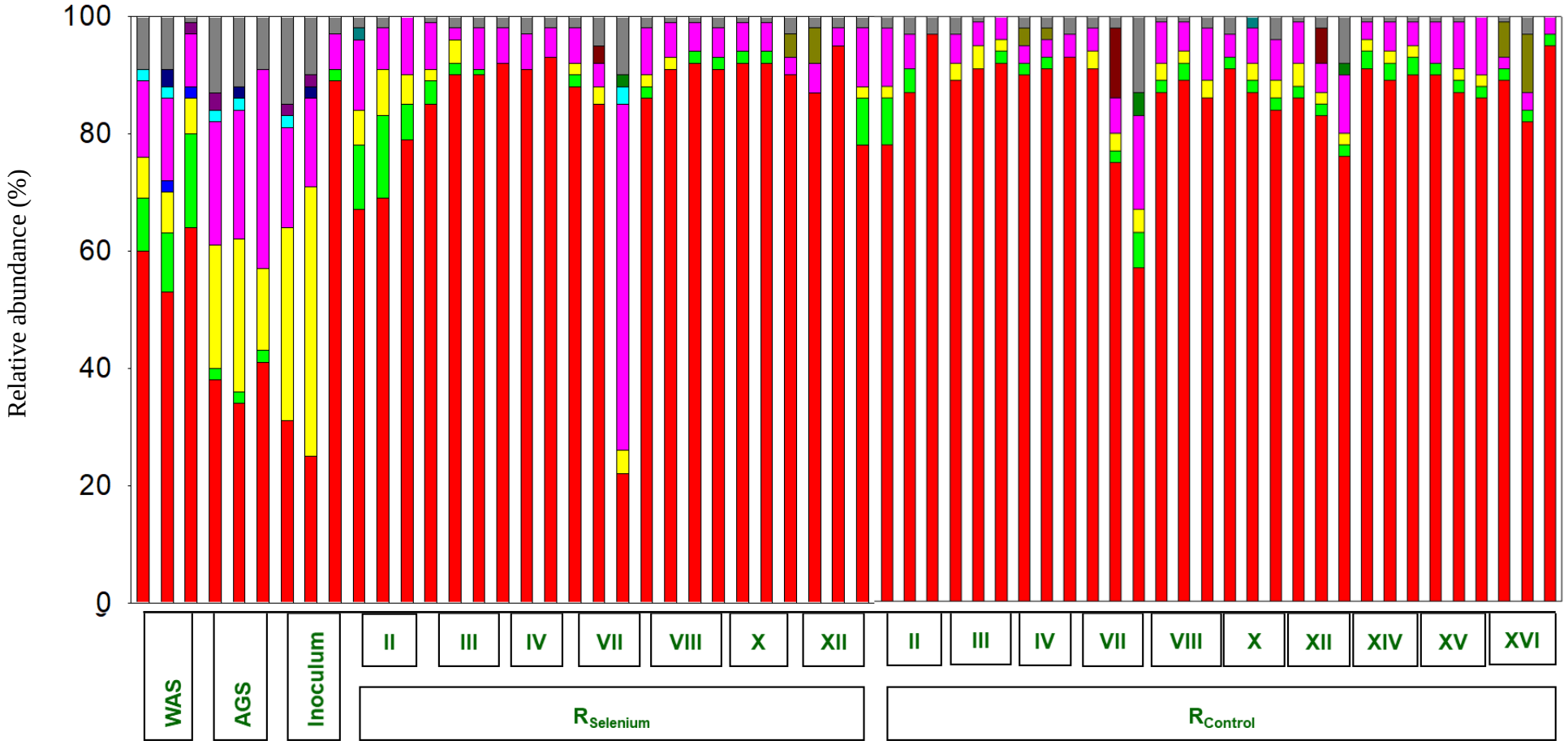
Relative abundance (%)
100
80
60
40
20
0
WAS
AGS
Inoculum
II
III
IV
VII
VIII
X
XII
II
III
IV
VII
VIII
X
XII
XIV
XV
XVI
R Selenium
R Control

(a)

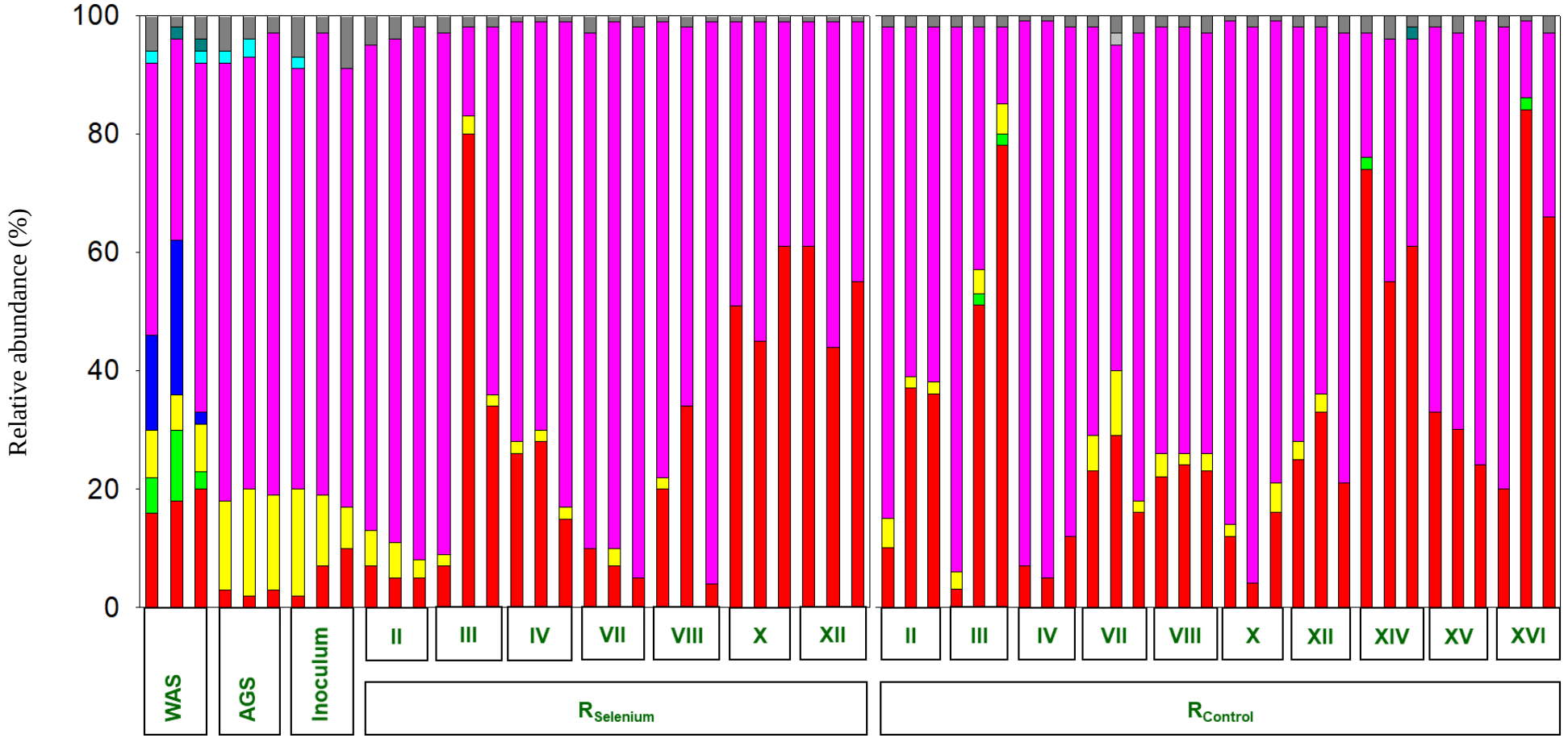
Relative abundance (%)
100
80
60
40
20
0
WAS
AGS
Inoculum
II
III
IV
VII
VIII
X
XII
II
III
IV
VII
VIII
X
XII
XIV
XV
XVI
R Selenium
R Control

(b)

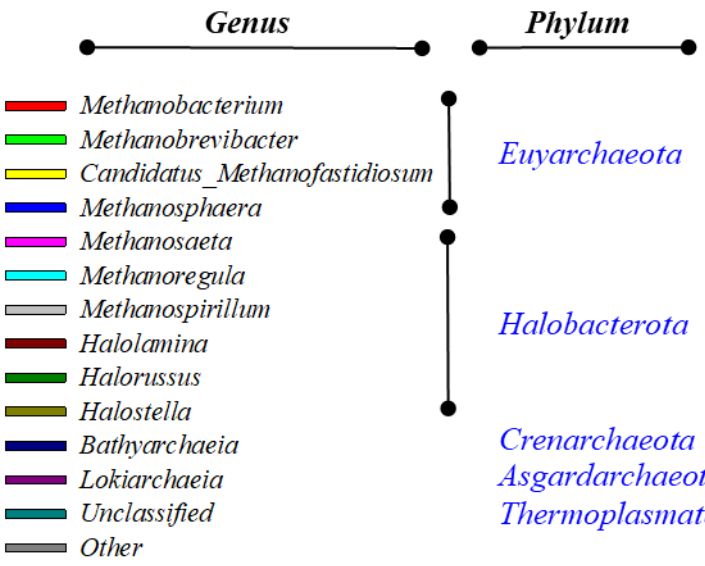

Figure 7.13 Archaeal communities in $R_{Selenium}$ and $R_{Control}$ at different operational periods (RA < 2% at genera rank and unclassified phyla were grouped as 'Other') at a) DNA level and b) RNA level

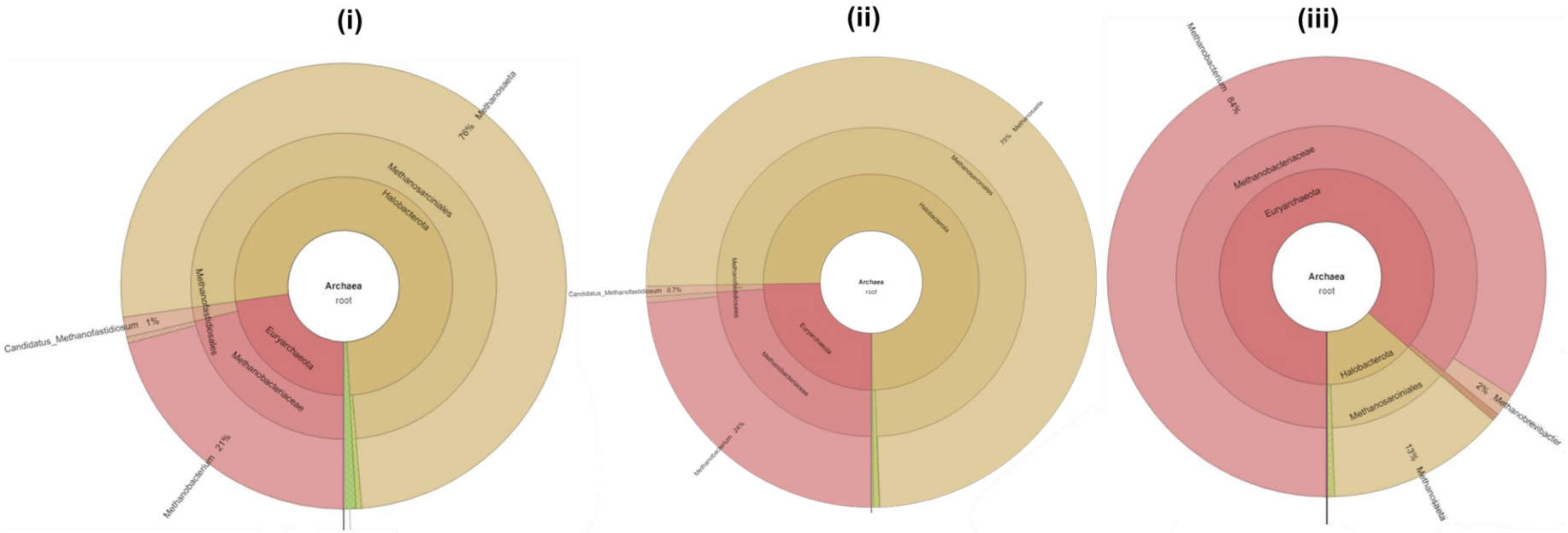

(c)

Figure 7.14 KRONA graph showing RNA based archaeal communities in (i) $R_{Control}$ without Se exposure (day 149, period XII), (ii) $R_{Control}$ at 400 µM SeO_4^{2-} (day 155, period XV) and (iii) $R_{Control}$ at 500 µM SeO_4^{2-} (day 168, period XVI)

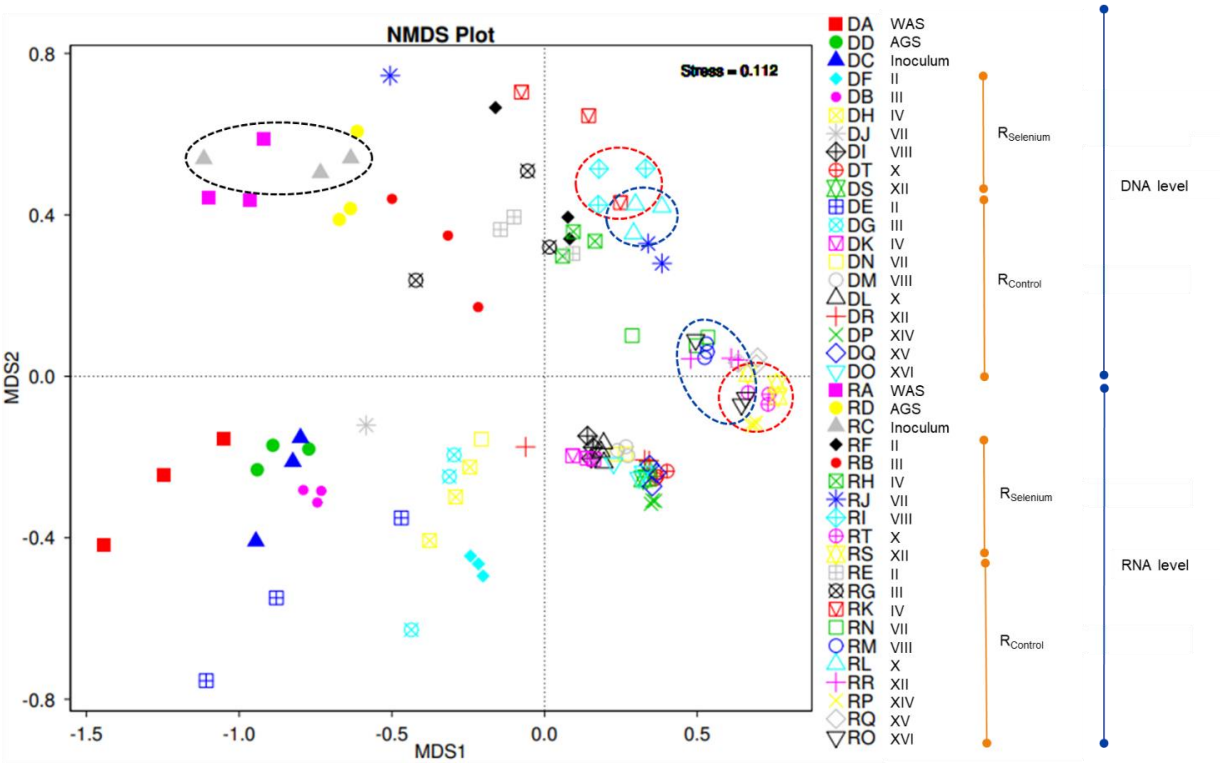

Figure 7.15 Non-metric multi-dimensional scaling (NMDS) ordination of communities at different periods in $R_{Selenium}$ and $R_{Control}$ (stress value < 0.2 is good). Black, red and blue circles denote inoculum, $R_{Selenium}$ (days 120 and 149, periods VIII and XII) and $R_{Control}$ (days 136 and 168, periods X and XVI).

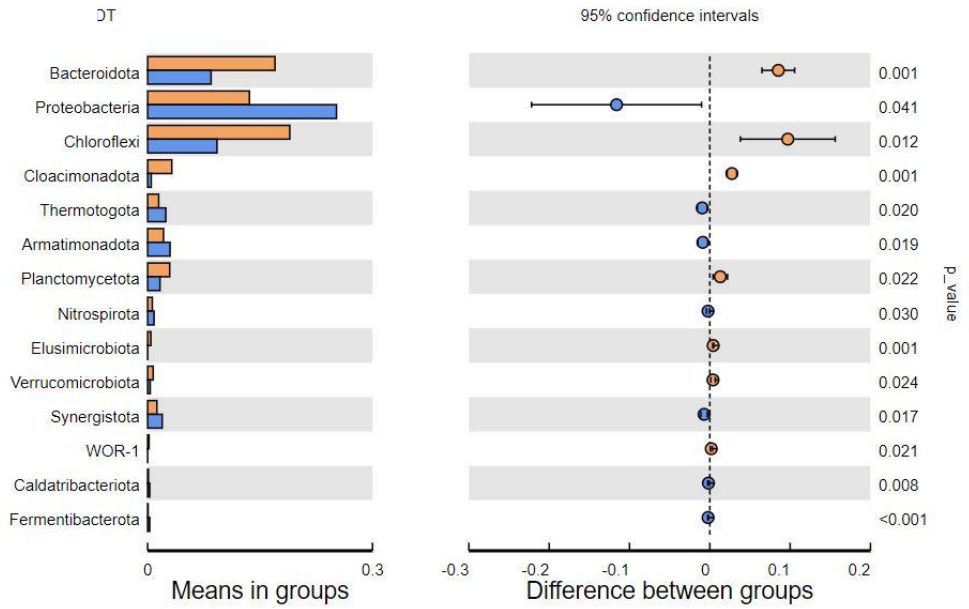

Figure 7.16 T-test performed to determine species with significant variation between groups (p value < 0.05). Orange bar and circle represent period IV, while blue bar and circle represent period X in $R_{Selenium}$

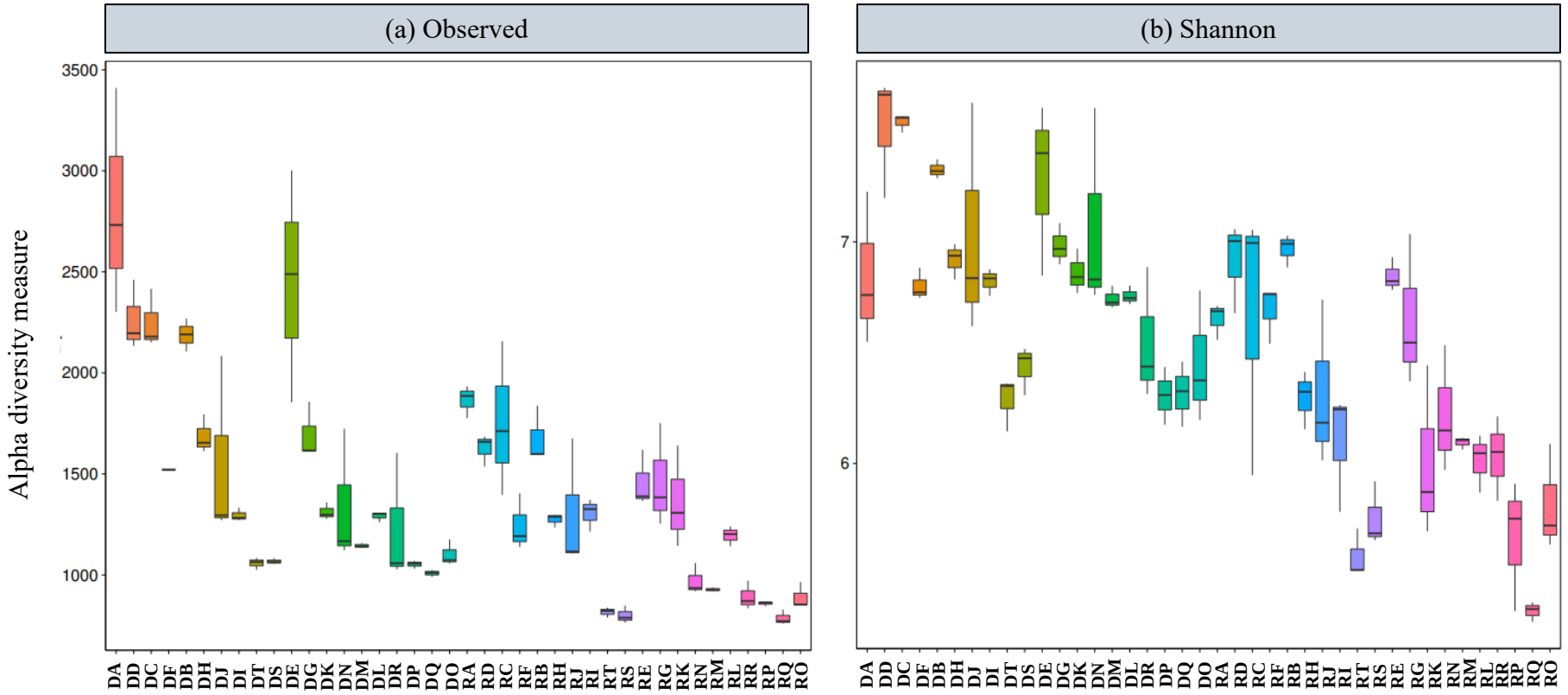

Figure 7.17 Alpha diversity measure of each sample group. Box plots of difference of (a) number of observed species and (b) shannon indices. Legends are same as of Figure 7.15.

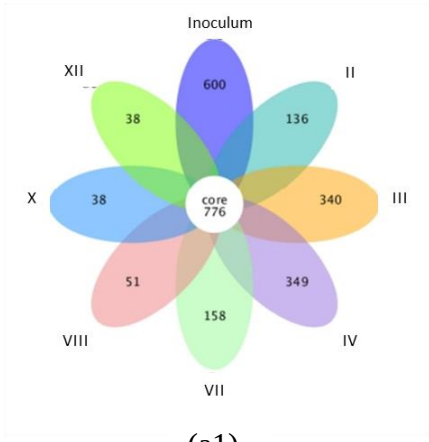

(a1)

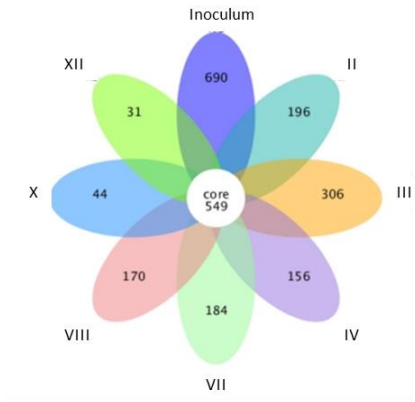

(a2)

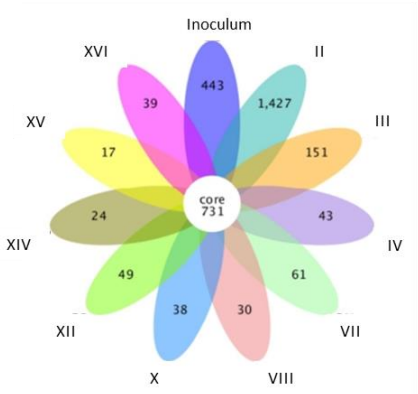

(b1)

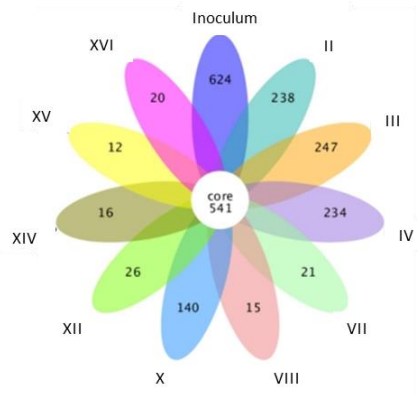

(b2)

Figure 7.18 Flower diagram of (a) $R_{Selenium}$ at different operational periods at DNA level (a1) and RNA level (a2); and (b) $R_{Control}$ at different periods at DNA level (b1) and RNA level (b2)

7.4 Discussion

7.4.1 Concomitant methane production and selenium remediation during the treatment of glycerol based wastewater in UASB reactors

This study for the first time establishes the feasibility of continuous methane production in UASB reactors treating glycerol along with concomitant selenium bioremediation until 400 µM SeO_4^{2-}. Beyond this point, though more than 90% soluble Se was effectively removed, methane production suffered inhibition at an influent concentration of 500 µM SeO_4^{2-}. However, volatile fatty acids could still be produced before complete process failure. Selenate was reduced to precipitate as elemental Se nanoparticles and metal selenides. Such

simultaneous biological processes producing bio-energy, bio-chemicals and bio-products have huge commercial implications when a proper recovery process is designed and implemented within the system.

Furthermore, selenium is a well-established trace element and can stimulate methanogenesis during AD. Ariunbaatar et al. (2016) reported a 30 – 35% increase in methane production from food waste at Se concentrations ranging between 0.32 – 0.63 µM. Above these 'trace levels', the methane production could still be realised (similar to that of Control) until a 'methanogenic threshold' (in this case, 400 µM). After this threshold, acute inhibition of methanogenesis and AD process failure is encountered (at concentrations ≥ 500 µM). Lenz et al. (2008a) reported that the irreversible inhibition of methanogens upon exposure to Se oxyanions ($\geqslant 10^{-3}$ M) might deteriorate the methanogenic treatment capacity of bioreactors treating Se-rich waste streams. Lenz et al. (2008a) also stated that the range between selenium requirement and toxicity in methanogenic anaerobic granular sludge is very small, only a factor of 8–200.

The XRD pattern (Figure 7.9) suggests that the trace metals supplied to the anaerobic digester to support methanogenesis have precipitated as metal selenide. The deficiency of these trace metals could also explain deterioration of the AD process at SeO_4^{2-} concentrations higher than 0.5 mM. Madden et al. (2014) also reported hampered methane generation in AD of sulfate-rich wastewaters due to trace metal sulfide precipitation. Biosynthesis of elemental Se nanoparticles (BioSeNPs) was confirmed with TEM (Figure 7.7a), SEM (Figure 7.7b) and EDX (Figure 7.7c). SeO_4^{2-} treating granules show elemental Se deposits only in the periphery and, over a period of time, realise methanogenesis only through the less affected core of those granules (Lenz et al., 2008a). Synergistic toxicity from additional inhibitors formed from the conversion of Se oxyanions (e.g. H_2Se, which could in turn form selenocysteine and selenomethionine), change in enzyme functionality, accumulation of carboxylic acids, and increased production of reactive oxygen species could also be possible reasons for the process failure due to elevated selenium influent concentrations (Dong et al., 1994; Lenz et al., 2008a).

An average selenate removal efficiency > 90% was achieved by methane producing sludge in the $R_{Selenium}$ UASB reactor (Figure 7.3). Microbial reduction of selenate and selenite by anaerobic sludge has been well documented (Tan et al., 2016). But, there are limited studies on selenate reduction in methanogenic reactors. In both $R_{Control}$ and $R_{Selenium}$, glycerol, glucose or lactate may have been directly used for selenate reduction or may have been fermented to

acetate or hydrogen first, followed by their use by selenate reducing bacteria. This study showed a high Se removal efficiency under long term operation (until 150 days). It is noteworthy that, when the influent COD was 3000 mg/L in the first phase, the Se removal efficiency fell below 80% occasionally. However, in the second phase, when the influent COD was 6000 mg/L, there was consistently above 90% Se removal. A lower COD/selenate ratio has been mainly attributed to lower Se removal rates (Sinharoy et al., 2019). Lenz et al. (2008b) also reported that even in well-functioning selenium reducing bioreactors, temporarily and spatially higher Se concentrations might occur in case of shock loads or due to inhomogeneous mixing of the influent with the reactor liquor.

When the total Se leaving the UASB reactor (~3.5 mg Se/L in this study) exceeds the accepted discharge limit (5 µg Se/L), post-treatment techniques such as slow filtration or dissolved air flotation (DAF) could be used additionally (CH2M HILL, 2010). A two-stage AD reactor, i.e. an acidogenic followed by a methanogenic reactor, could effectively meet the stringent environmental regulation of Se < 5 µg/L (Tan et al., 2016). This could be a cost effective, alternative, and sustainable bioremediation technique, compared with its physical or chemical counterparts. The surplus benefit from biomethane or VFA bioproducts makes AD of Se-rich wastewaters a promising technology compared to bioreactors that are solely employed for selenium removal.

Selenate removal was mainly mediated through dissimilatory microbial reduction as evident from the typical orange-red colour of the elemental Se (Figure 7.8). In addition, trace concentrations of metal selenides precipitated in the sludge bed in the UASB reactor (Figure 7.9). However, the yields and purity of these metal selenides could be lower. Fractions of hydrogen selenide were present in the produced biogas, indicating that H_2Se gas scrubbing might be required during upgrading biogas generated from Se-rich wastewaters. Selenate bioconversion to elemental red selenium during complete inhibition of methanogenesis (Figure 7.3) showed that selenate reduction is not mediated by methanogens. Most of the biogenic elemental Se formed was retained in the mixed sludge bed. Easy recovery of the biomass-associated Se nanoparticles for future reuse is possible with UASB reactors (Piacenza et al., 2017). Se-laden wastewaters often contain co-contaminants such as nitrate and sulfate as well (Tan et al., 2018), and this needs to be taken into consideration for future work. Similarly, the effect of selenite on long term and continuous methane production should also be demonstrated.

7.4.2 Influence of SeO_4^{2-} on the AD process performance

Electron flow governs substrate utilization in AD systems (Hoa et al., 2007). The shift of the electron flow towards selenium reducing bacteria (Figure 7.5) suggests that the methanogenic archaea are deprived of carbon utilisation leading to complete failure of the methanogenic system at higher SeO_4^{2-} concentrations. This was also evident from the COD removal efficiency being reduced to below 20% (Figure 7.3). Volatile fatty acids also accumulated more their consumption rate for methane production (Figure 7.4). Therefore, future studies could explore VFA production from different waste streams with Se oxyanions acting as a chemical inhibitor of the methanogenesis.

This study showed that UASB bioreactors can be employed for the anaerobic treatment of selenate rich wastewater (Figure 7.1). Selenium exposure enhanced sludge granulation (Figure 7.10), a process whereby suspended particles and planktonic cells accumulate, forming small dense biofilm aggregates (Liu et al., 2002). Sludge granulation is also promoted by the prevailing conditions of shear or hydrodynamic stresses (Trego et al., 2020). Ionic supplementation is reported to increase the granulation rate in UASB reactors (Show et al., 2020). Some organisms such *Methanosaeta*, the most active archaea in this study (Figure 7.13), can either aggregate together, attach to suspended particles, or potentially form a bridge between existing microflocs (Hulshoff Pol et al., 2004). In addition to natural granulation, elemental selenium nanoparticles and metal selenide precipitation could have also contributed to increased sludge density and settleability. The rate of biomass and selenium accumulation, their impingement on bioreactor performance as well as requirement to replace biomass are important considerations for biomass management in anaerobic digesters (Trego et al., 2020).

Similar to SRBs, SeRBs might convert organic compounds to VFAs in the absence of SeO_4^{2-} (Plugge et al., 2011). In mesophilic bioreactors treating chalcogen-rich wastewaters, methane is produced from acetate, while hydrogen is consumed by the chalcogen reducing bacteria (Madden et al., 2014). This ‘divergent pathway’ for acetate and hydrogen utilization could have facilitated the co-existence of methanogenic archaea and SeRB which need to be ascertained in future microbial ecology studies. In this study, the sludge enriched with SeRB utilised hydrogen for SeO_4^{2-} reduction and still achieved a similar SMA range as that of the control (Table 7.2).

There is a striking similarity between AD of sulfate and selenate containing wastewater, including alteration in electron flow between methanogenic archaea and SRBs/SeRBs (Wu et

al, 2018), hydrogen chalcogenide (H_2S and H_2Se) toxicity on methanogenic cells (Koster et al., 1986), leading to reduced COD removal efficiency and accumulation of organic compounds (Colleran and Pender, 2002) as well as trace element deficiency at high chalcogenate concentrations due to metal sulfide and metal selenide precipitation (Colleran et al., 1995). However, despite these similarities, the COD/selenate ratio, unlike the COD/sulfate ratio, does not govern the AD process performance or it is too narrow to be detected. SO_4^{2-} induced microbial activity inhibition is related to two mechanisms, viz. substrate competition and toxicity (Costa et al., 2020), whereas SeO_4^{2-} induced inhibition is related solely to toxicity. The Se concentration is thus found to govern the AD processes, or in other words, is enough to cause the inhibitory effect. Similar observations were made in our earlier batch experiments where a DAF slurry with high COD content (~ 40 g/L) was used as the substrate: higher COD/selenate ratios (> 500) could not prevent process failure at 500 µM SeO_4^{2-} (Logan et al., 2022a). The electron flow could not be redirected back to methanogenic archaea despite several strategies to revive the system (Figure 7.5). Selenium could be several times more toxic than sulfur (Spallholz, 1994). According to the US health exposure limits, the exposure limit of H_2S and H_2Se is 10 ppm and 0.05 ppm, respectively, whereas the immediate danger of H_2S and H_2Se is from 100 ppm and 1 ppm, respectively (NIOSH, 2007). The methanogenesis coexistence threshold is 10 mM for SO_4^{2-} (Cetecioglu et al., 2019), whereas it is much lower at 0.4 mM for SeO_4^{2-} (Figure 7.3).

7.4.3 Microbial community evolution during AD of glycerol and selenate rich wastewater

Sulfurospirillum, Arcobacter, Desulfovibrio, Dechloromonas, Acinetobacter and *Pseudomonas,* which are reported to function as selenium reducing genera (Sinharoy and Lens, 2021), were present in the UASB bioreactors (Figure 7.12). Interestingly, the family *Proteobacteria* (which consists of genera such as *Pseudomonas, Acinetobacter, Dechloromonas*) at DNA level was significantly higher ($p < 0.05$) at higher SeO_4^{2-} concentration (300 µM), when compared to the period before Se exposure, as evident from the t-test (Figure 7.16). This suggests that the presence and activity of the selenium reducing bacterial population has increased at increasing SeO_4^{2-} exposure. With no clear inhibition observed at bacterial community level, it is clear that the toxic effect of SeO_4^{2-} is less on fermentative bacteria relative to methanogenic archaea (Figures 7.12 and 7.13).

The distinct clusters in the NMDS plot (Figure 7.15) and decrease in the richness and diversity (Figures 7.17 and 7.18) could be attributed to the long operational period, washout in the initial operational days and the effect of glycerol. Since $R_{Control}$ also showed a decrease in its alpha diversity indices, SeO_4^{2-} exposure is not solely attributed for the reduction in overall richness and diversity.

Few of the bacterial genera found in this study are well-established as fermentative anaerobes in AD. The *Syner-01* genus of the family *Synergistaceae* are syntrophic acetate- and amino-acid-oxidizing bacteria that commonly occur in anaerobic digesters and are capable of metabolizing amino acids (Wang et al., 2021). Similarly, the members of *Lentimicrobium* can ferment carbohydrates, glucose to acetate, malate, propionate, formate and hydrogen (Sun et al., 2016). *Acinetobacter* are well-adapted Gram-negative bacteria that have a high tolerance to toxic substances (Akyol et al., 2016). *Acinetobacter* also quickly degrades cellulose and other organic compounds for providing sufficient metabolic substrates for methanogenic bacteria in the methanogenic phase (Wang et al., 2019). Likewise, *Arcobacter* is a facultative anaerobe that utilizes organic and amino acids as its carbon source (Chen et al., 2020). *Smithella* is a well-known propionate-oxidizing bacterium (Ariesyady et al., 2007).

Though the presence was lower amongst the total archaeal population (Figure 7.13), *Methanosaeta* was the active archaea and could be attributed for the methane production in periods without SeO_4^{2-} exposure ($R_{Control}$) or when operated at non-inhibitory SeO_4^{2-} concentrations ($R_{Selenium}$). *Methanosaeta* is reported as an acetoclastic methanogen (Carr et al., 2017), suggesting acetoclastic methanogenesis being the dominant pathway during this study. However, at 500 µM SeO_4^{2-}, the activity of *Methanosaeta* was severely inhibited (Figures 7.13a and b). The effect of SeO_4^{2-} was evident only on RNA based communities, and not on DNA based communities (Figures 7.12). The close relation between *Lactococcus* (an active fermentative bacteria in Figure 7.12) and *Methanosaeta* (the most active MPA in Figure 7.13) has been shown to be a keystone for stable methane production in UASB treatment of sugar-based wastewaters (Kim et al., 2015).

7.5 Conclusion

Long term and continuous demonstration of simultaneous methane production and selenium (Se) bioremediation by anaerobic digestion was investigated for the first time. SeO_4^{2-} concentration, but not the COD/SeO_4^{2-} ratio, was found to govern the AD process. About 40-50% of the COD was converted to methane, with 80-90% of the soluble and total selenium

were removed. Formation of elemental selenium nanoparticles and trace metal selenides was confirmed with XRD, TEM, SEM and EDX. The SeO_4^{2-} induced methanogenic inhibition caused an electron flow alteration from methanogenic archaea, hampered the COD removal efficiency, induced accumulation of intermediaries (such as VFAs), and gave a loss of EPS components. Microbial community analyses showed co-existence of methanogenic archaea and selenium reducing bacteria, prior to inhibition, until 400 µM SeO_4^{2-}. The activity of *Methanosaeta* was suppressed at 500 µM SeO_4^{2-}. Long-term pilot scale evaluation of AD of Se oxyanion containing wastewaters is required to support further full scale implementation.

7.6 References

Akyol, C., Aydin, S., Ince, O., Ince, B., 2016. A comprehensive microbial insight into single-stage and two-stage anaerobic digestion of oxytetracycline-medicated cattle manure. Chemical Engineering Journal 303, 675-684. https://doi.org/10.1016/j.cej.2016.06.006

APHA, 2017. APHA Standard Methods for the Examination of Water and Wastewater (23rd edition), American Public Health Association, Washington, D.C., USA. ISBN: 9780875532875.

Ariesyady, H.D., Ito, T., Yoshiguchi, K., Okabe, S., 2007. Phylogenetic and functional diversity of propionate-oxidizing bacteria in an anaerobic digester sludge. Applied Microbiology and Biotechnology 75, 673-683. https://doi.org/10.1007/s00253-007-0842-y

Ariunbaatar, J., Esposito, G., Yeh, D.H., Lens, P.N.L., 2016. Enhanced anaerobic digestion of food waste by supplementing trace elements: role of Selenium (VI) and Iron (II). Frontiers in Environmental Science 4(8). https://doi.org/10.3389/fenvs.2016.00008

Atasoy, M., Owusu-Agyeman, I., Plaza, E., Cetecioglu, Z., 2018. Bio-based volatile fatty acid production and recovery from waste streams: Current status and future challenges. Bioresource Technology 268, 773-786. https://doi.org/10.1016/j.biortech.2018.07.042

Baba, Y., Tada, C., Watanabe, R., Fukuda, Y., Chida, N., Nakai. Y., 2013. Anaerobic digestion of crude glycerol from biodiesel manufacturing using a large scale pilot plant: Methane production and application of digested sludge as fertilizer. Bioresource Technology 140, 342-348. http://dx.doi.org/10.1016/j.biortech.2013.04.020

Biebl, H., Menzel, K., Zeng, A.P., Deckwer, W.D., 1999. Microbial production of 1,3-propanediol. Applied Microbiology and Biotechnology 52, 289-297. http://dx.doi.org/10.1007/s002530051523

Cai, Y., Zheng, Z., Zhao, Y., Zhang, Y., Guo, S., Cui, Z., Wang, X., 2018. Effects of molybdenum, selenium and manganese supplementation on the performance of anaerobic digestion and the characteristics of bacterial community in acidogenic stage. Bioresour. Technol. 266, 166-175. https://doi.org/10.1016/j.biortech.2018.06.061

Caporaso, J.G., Lauber, C.L., Walters, W.A., Berg-Lyons, D., Lozupone, C.A., Turnbaugh, P.J., Fierer, N., Knight, R., 2011. Global patterns of 16S rRNA diversity at a depth of millions of sequences per sample. Proceedings of the National Academy of Sciences of the United States of America 108(1), 4516-4522. https://doi.org/10.1073/pnas.1000080107

Carr, S.A., Schubotz, F., Dunbar, R.B., Mills, C.T., Dias, R., Summons, R.E., Mandernack, K.W., 2018. Acetoclastic Methanosaeta are dominant methanogens in organic-rich Antarctic marine sediments. The ISME Journal Multidisciplinary Journal of Microbial ecology 12, 330-342. https://doi.org/10.1038/ismej.2017.150

Cetecioglu, Z., Dolfing, J., Taylor, J., Purdy, K.J., Eyice, Ö., 2019. COD/sulfate ratio does not affect the methane yield and microbial diversity in anaerobic digesters. Water Research 155, 444-454. https://doi.org/10.1016/j.watres.2019.02.038

Chen, Y., Yu, N., Sun, Z., Gou, M., Xia, Z., Tang, Y., Kida, K., 2020. Acclimation Improves Methane Production from Molasses Wastewater with High Salinity in an Upflow Anaerobic Filter Reactor: Performance and Microbial Community Dynamics. Applied Biochemistry and Biotechnology 191, 397-411. https://doi.org/10.1007/s12010-020-03236-7

CH2M HILL, 2010. Review of available technologies for the removal of selenium from water – Final report prepared for North American Metal Council.

Chuenchart, W., Logan, M., Leelayouthayotin, C., Visvanathan, C., 2020. Enhancement of food waste thermophilic anaerobic digestion through synergistic effect with chicken manure. Biomass Bioenergy 136, 105541. https://doi.org/10.1016/j.biombioe.2020.105541

Colleran, E., Finnegan, S., Lens, P., 1995. Anaerobic treatment of sulphate-containing waste streams. Antonie van Leeuwenhoek 67, 29-46. https://doi.org/10.1007/BF00872194

Colleran, S., Pender, S., 2002. Mesophilic and thermophilic anaerobic digestion of sulphate-containing wastewaters. Water Science and Technology 45, 231-235. https://doi.org/10.2166/wst.2002.0339

Costa, R.B., O'Flaherty, V., Lens, P.N.L., 2020. Biological treatment of organic sulfate-rich wastewaters. In book: Environmental Technologies to Treat Sulphur Pollution: Principles and Engineering. IWA Publishing, London, UK. http://dx.doi.org/10.2166/9781789060966_0167

Duggan, A.R., McCabe, B.A., Goggins, J., Clifford, E., 2020. Stabilisation for peat improvement: Extent of carbonation and environmental implications. Journal of Cleaner Production 271, 122540. https://doi.org/10.1016/j.jclepro.2020.122540

European Commission, 2021. Launch by United States, the European Union, and partners of the global methane pledge to keep 1.5C within reach. https://ec.europa.eu/commission/presscorner/detail/en/statement_21_5766

Florentino, A.P., Costa, R.B., Hu, Y., O'Flaherty, V., Lens, P.N.L., 2020. Long chain fatty acid degradation coupled to biological sulfidogenesis: A prospect for enhanced metal recovery. Frontiers in Bioengineering and Biotechnology. https://doi.org/10.3389/fbioe.2020.550253

Hoa, T.T.H., Liamleam, W., Annachhatre, A.P., 2007. Lead removal through biological sulfate reduction process. Bioresource Technology 98(13), 2538-2548. https://doi.org/10.1016/j.biortech.2006.09.060

Hulshogg Pol, L. W., de Castro Lopes, S.I., Lettinga, G., Lens, P.N.L., 2004. Anaerobic sludge granulation. Water Research 38, 1376-1389. https://doi.org/10.1016/j.watres.2003.12.002

Jung, H., Kim, D., Choi, H., Lee, C., 2022. A review of technologies for in-situ sulfide control in anaerobic digestion. Renewable and Sustainable Energy Reviews, 157, 112068. https://doi.org/10.1016/j.rser.2021.112068

Karki, R., Chuenchart, W., Surendra, K.C., Shrestha, S., Raskin, L., Sung, S., Hashimoto, A., Khanal, S.K., 2021. Anaerobic co-digestion: Current status and perspectives. Bioresource Technology 330, 125001. https://doi.org/10.1016/j.biortech.2021.125001

Kim, T.G., Yun, J., Cho, K., 2015. The close relation between *Lactococcus* and *Methanosaeta* is a keystone for stable methane production from molasses wastewater in a UASB reactor. Environmental Biotechnology 99, 8271-8283. https://doi.org/10.1007/s00253-015-6725-8

Lenz, M., Janzen, N., Lens, P.N.L., 2008a. Selenium oxyanion inhibition of hydrogenotrophic and acetoclastic methanogenesis. Chemosphere 73(3), 383-388. https://doi.org/10.1016/j.chemosphere.2008.05.059

Lenz, M., van Hullebusch, E.D., Hommes, G., Corvini, P.F.X., Lens, P.N.L., 2008b. Selenate removal in methanogenic and sulfate-reducing upflow anaerobic sludge bed reactors. Water Research 42(8-9), 2184-2194. https://doi.org/10.1016/j.watres.2007.11.031

Liu, Y., Xu, H.-L., Show, K.-Y., Tay, J.-H., 2002. Anaerobic granulation technology for wastewater treatment. World Journal of Microbiology and Biotechnology 18, 99-113. https://doi.org/10.1023/A:1014459006210

Logan, M., Tan, L.C., Lens, P.N.L., 2022a. Anaerobic co-digestion of dissolved air floatation slurry and selenium rich wastewaters for simultaneous methane production and selenium bioremediation. International Biodeterioration and Biodegradation 172, 105425. https://doi.org/10.1016/j.ibiod.2022.105425

Logan, M., Tan, L.C., Nzeteu, C.O., Lens, P.N.L., 2022b. Enhanced anaerobic digestion of dairy wastewater in a granular activated carbon amended sequential batch reactor. GCB Bioenergy 14(7), 840-857. https://doi.org/10.1111/gcbb.12947

Logan, M., Visvanathan, C., 2019. Management strategies for anaerobic digestate of organic fraction of municipal solid waste: Current status and future prospects. Waste Management and research 37, 27-39. https://doi.org/10.1177/0734242X18816793

López, J.Á.S., Santos, M.Á.M., Pérez, A.F.C., Martín, A.M., 2009. Anaerobic digestion of glycerol derived from biodiesel manufacturing. Bioresource Technology 100(23), 5609-5615. https://doi.org/10.1016/j.biortech.2009.06.017

Madden, P., Al-Raei, A.M., Enright, A.M., Chinalia, F.A., Beer, D., O'Flaherty, V., Collins, G., 2014. Effect of sulfate on low termperature anaerobic digestion. Frontiers in Microbiology 5, 376. https://doi.org/10.3389/fmicb.2014.00376

Mal, J., Nancharaiah, Y.V., van Hullebusch, E.D., Lens, P.N.L., 2016. Effect of heavy metal co contaminants on selenite bioreduction by anaerobic granular sludge. Bioresource Technology 206, 1-8.

McColm, I.J., 2013. Dictionary of Ceramic Science and Engineering. Springer. ISBN 9789400709164.

Nancharaiah, Y.V., Lens, P.N.L., 2015a. Ecology and biotechnology of selenium-respiring bacteria. Microbiol. Mol. Biol. Rev. 79, 61-80. https://doi.org/10.1128/MMBR.00037-14

Nakasaki, K., Nguyen, K.N., Ballesteros Jr., F.C., Maekawa, T., Koyama, M, 2020. Characterizin the microbial community involved in anaerobic digestion of lipid-rich wastewater to produce methane gas. Anaerobe 61, 102082. https://doi.org/10.1016/j.anaerobe.2019.102082

Nancharaiah, Y.V., Lens, P.N.L., 2015b. Selenium biomineralization for biotechnological applications. Trends Biotechnol. 33(6), 323-330. https://doi.org/10.1016/j.tibtech.2015.03.004

NIOSH, 2017. NIOSH Pocket Guide to Chemical Hazards. Department of Health and Human Services, Centers for Disease Control and Prevention, National Institute for Occupational Safety and Health. https://www.cdc.gov/niosh/docs/2005-149/pdfs/2005-149.pdf

O'Flaherty, V., Lens, P., Leahy, B., Colleran, E., 1998. Long-term competition between sulphate-reducing and methane-producing bacteria during full-scale anaerobic treatment of citric acid production wastewater. Water Research 32, 815-825. https://doi.org/10.1016/S0043-1354(97)00270-4

Ondov, Brian D., Nicholas H. Bergman, and Adam M. Phillippy. Interactive metagenomic visualization in a Web browser. BMC bioinformatics 12, 385. https://doi.org/10.1186/1471-2105-12-385

Sela-Adler, M., Ronen, Z., Herut, B., Antler, G., Vigderovich, H., Eckert, W., Sivan, O., 2017. Co-existence of methanogenesis and sulfate reduction with common substrates in sulfate-rich estuarine sediments. Front. Microbiol. 8, 766. https://dx.doi.org/10.3389%2Ffmicb.2017.00766

Show, K., Yan, Y., Yao, H., Guo, H., Li, T., Show, D., Chang, J., Lee, D., 2020. Anaerobic granulation: A review of granulation hypotheses, bioreactor designs and emerging green applications. Bioresource Technology 300, 122751. https://doi.org/10.1016/j.biortech.2020.122751

Sinharoy, A., Saikia, S., Pakshirajan, K., 2019. Biological removal of selenite from wastewater and recovery as selenium nanoparticles using inverse fluidized bed bioreactor. Journal of Water Process Engineering 32, 100988. https://doi.org/10.1016/j.jwpe.2019.100988

Spallholz, J.E., 1994. On the nature of selenium toxicity and carcinostatic activity. Free Radical Biology and Medicine, 17(1), 45-64. https://doi.org/10.1016/0891-5849(94)90007-8

Sun, L., Toyonaga, M., Ohashi, A., Tourlousse, D.M., Matsuura, N., Meng, X.Y., Tamaki, H., Hanada, S., Cruz, R., Yamaguchi, T., Sekiguchi, Y., 2016. *Lentimicrobium saccharophilum* gen. nov., sp. nov., a strictly anaerobic bacterium representing a new family in the phylum Bacteroidetes, and proposal of *Lentimicrobiaceae* fam. Nov. International Journal of Systematic and Evolutionary Microbiology 66, 7. https://doi.org/10.1099/ijsem.0.001103

Tan, L.C., Mal, J., Lens, P.N.L., 2019. Selenium remediation using granular and biofilm systems. In. Microbial biofilms in bioremediation and wastewater treatment 103, CRC Press, Boca Raton, USA.

Tan, L.C., Nancharaiah, Y.V., van Hullebusch, E.D., Lens, P.N.L., 2016. Selenium: Environmental significance, pollution, and biological treatment technologies. Biotechnol. Adv. 34(5), 886-907. https://doi.org/10.1016/j.biotechadv.2016.05.005

Tchobanoglous, G., Burton, F.L., Stensel, H.D., 2003. Wastewater engineering treatment and reuse. Boston, US. McGraw-Hill Higher Education.

Trego, A.C., O'Sullivan, S., Mills, S., Porca, E., Quince, C., Ijaz, U.Z., Collins, G., 2020. Methanogenic granules are replicated, whole microbial communities with reproducible responses to environmental cues. Preprint available at Research Square. https://doi.org/10.21203/rs.3.rs-16883/v1.

USEPA, 2015. Draft aquatic life ambient water quality criterion for selenium – Freshwater 2015. United States Environmental Agency EPA 822-P-15-001. https://nepis.epa.gov/Exe/ZyPDF.cgi/P100MZGX.PDF?Dockey=P100MZGX.PDF

van Lier, J.B., van der Zee F.P., Frijters, C.T.M.J., Ersahin, M.E., 2015. Celebrating 40 years anaerobic sludge bed reactors for industrial wastewater treatment. Reviews in Environmental Science and Bio/Technology 14, 681-702. https://doi.org/10.1007/s11157-015-9375-5

Vasquez, J., Nakasaki, K., 2016. Effects of shock loading versus stepwise acclimation on microbial consortia during the anaerobic digestion of glycerol. Biomass and Bioenergy 86, 129-135. https://doi.org/10.1016/j.biombioe.2016.02.001

Viana, M.B., Freitas, A.V., Leitão, R.C., Pinto, G.A.S., Santaella, S.T., 2012. Anaerobic digestion of crude glycerol: a review. Environmental Technology Reviews 1, 81-92. https://doi.org/10.1080/09593330.2012.692723

Vlassis, T., Stamatelatou, K., Antonopoulou, G., Lyberatos, G., 2013. Methane production via anaerobic digestion of glycerol: a comparison of conventional (CSTR) and high-rate (PABR) digesters. Journal of Chemical Technology and Biotechnology 88, 2000-2006. https://doi.org/10.1002/jctb.4059

Wang, J., Xu, L., Huang, B., Li, J., Jin, R., 2021. Multiple electron acceptor-mediated sulfur autotrophic denitrification: Nitrogen source competition, long-term performance and microbial community evolution. Bioresource Technology 329, 124918. https://doi.org/10.1016/j.biortech.2021.124918

Wang, S., Ma, F., Ma, W., Wang, P., Zhao, G., Lu, X., 2019. Influence of Temperature on Biogas Production Efficiency and Microbial Community in a Two-Phase Anaerobic Digestion System. MDPI Water 11(1), 133. https://doi.org/10.3390/w11010133

Wu, J., Niu, Q., Li, L., Hu, Y., Mribet, C., Hojo, T., Li, Y., 2018. A gradual change between methanogenesis and sulfidogenesis during a long-term UASB treatment of sulfate-rich chemical wastewater. Science of the Total Environment 636, 168-176. https://doi.org/10.1016/j.scitotenv.2018.04.172

Chapter 8 General Discussion and Future Perspectives

8.1 General discussion

8.1.1 Unravelling anaerobic digestion of lipid- and selenium-rich substrates

Methane production and sulfate reduction during anaerobic digestion (AD) of sulfate-rich wastewater were demonstrated in the early 1980s, with the objective to evaluate the optimal COD/sulfate ratio that governed the process performance (Colleran et al., 1995). Similarly, bioremediation of selenium (Se), from the same chalcogen group, has gained attention in the past three decades. Though Se is a well-known trace metal to stimulate methanogenesis in AD (Ariunbaatar et al., 2016), at elevated concentrations it is often perceived as not suitable owing to toxicity (Lenz et al., 2008). Considering these challenges and limitations, this PhD research bridged this gap to demonstrate simultaneous methane production and Se bioremediation during AD of Se oxyanion containing wastewater.

On the other hand, lipid-rich wastewaters such as dairy wastewater are often treated using a dissolved air floatation (DAF) unit before AD. The process parameters for AD of DAF slurries are not well established. With this background, this research considered dairy wastewater based DAF slurry as the substrate for batch assays. The challenge due to impaired methane production from lipid-rich wastewaters was overcome directly through supplementation of cost-effective conductive materials. This research evaluated the potential of granular activated carbon amendment for enhanced methane production.

The state-of-the art review (**chapter 2**) presents current approaches and proposes future prospects for AD of DAF slurry, sulfate- and selenate-rich wastewaters. The effect of initial pH and substrate concentration on the biomethane potential of dairy wastewater based DAF slurry was evaluated in **chapter 3**. Thereafter, sequential batch reactors were operated for enhanced anaerobic dairy wastewater degradation by the addition of conductive materials in **chapter 4.** Methanogenesis from Se supplemented DAF slurry (derived from dairy wastewater) was obtained in **chapter 5**. Concomitant volatile fatty acids (VFA) production and Se bioremediation was demonstrated with food waste as the electron donor in **chapter 6.** Based on the previous two chapters, long term and continuous anaerobic treatment of selenate and glycerol containing wastewater in up-flow anaerobic sludge bed (UASB) reactors was conducted in **chapter 7.** The major findings from the individual chapters of this PhD are shown in Figures 8.1 and 8.2. Figure 8.3 outlines the link of these findings from chapter 3 to chapter 7.

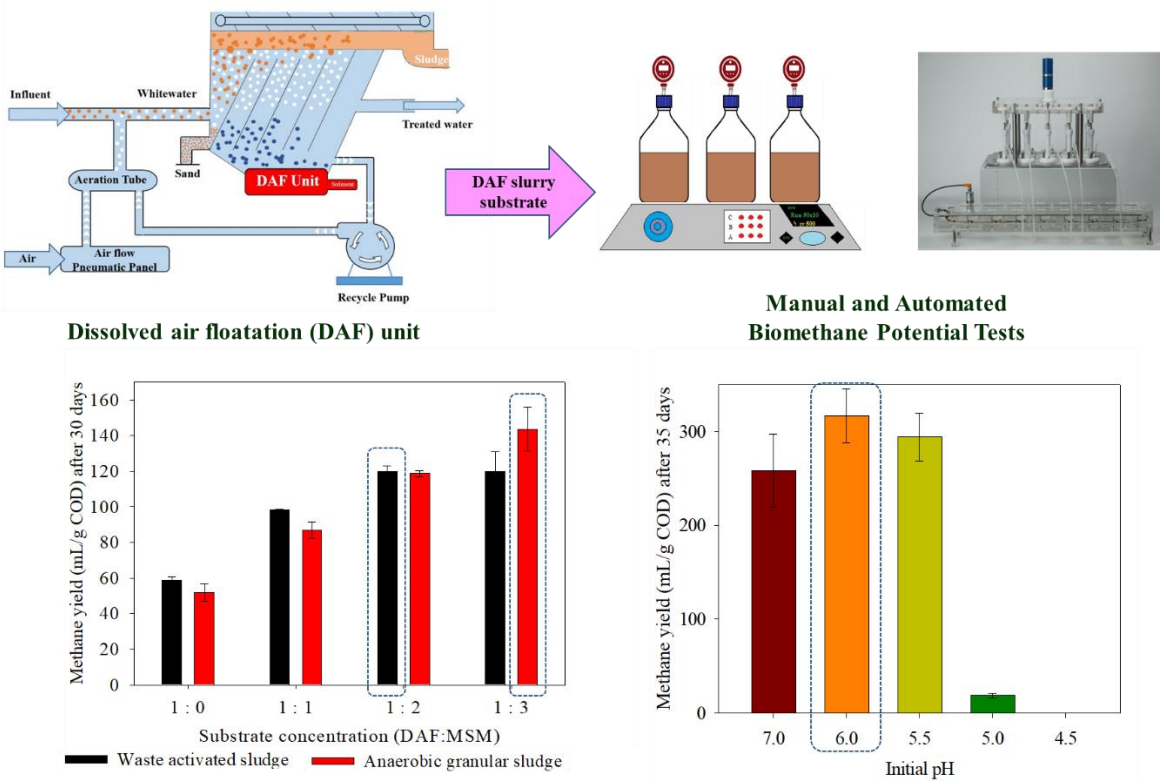

(a)

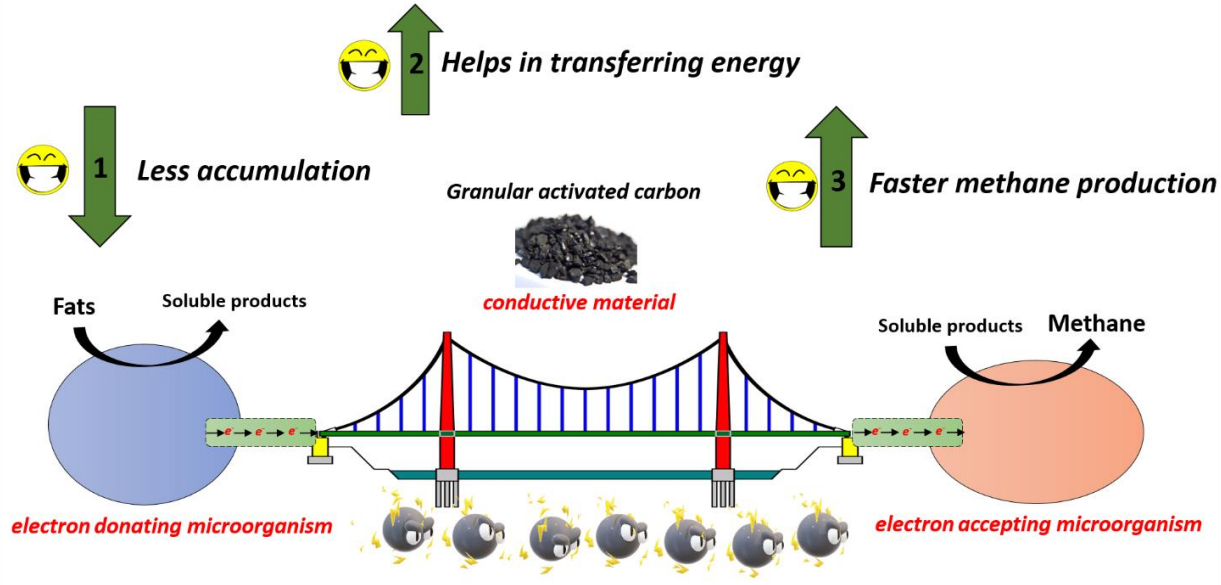

(b)

Figure 8.1 Enhanced anaerobic degradation of lipid-rich wastewaters in a) manual and automated biomethane potential tests (**Chapter 3**) and b) conductive material amended sequential batch reactor (**Chapter 4**)

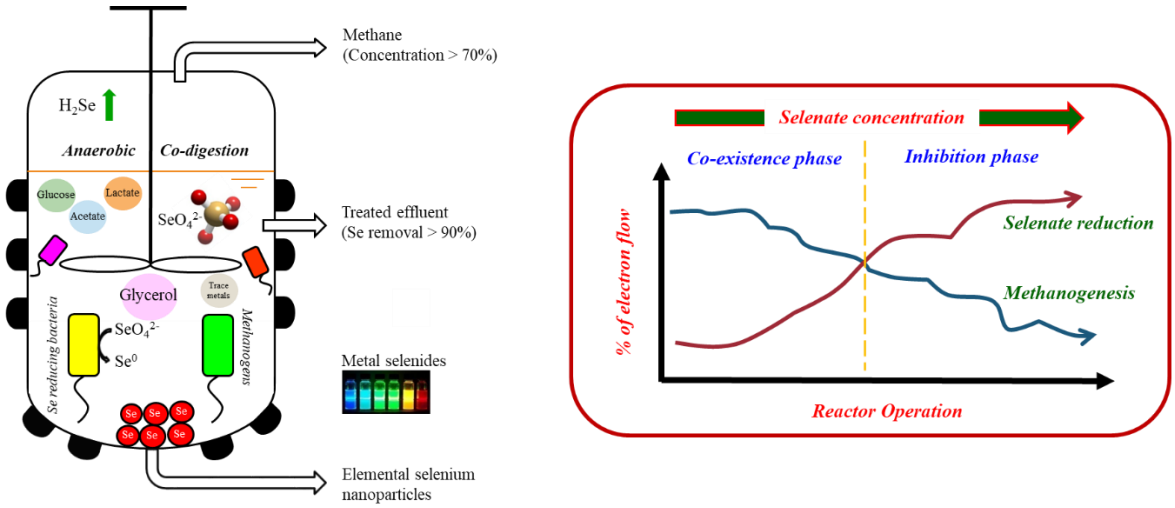

(a)

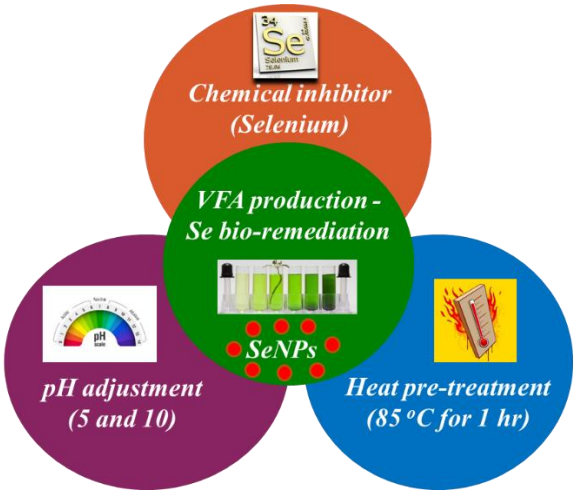

(b)

Figure 8.2 Anaerobic digestion of selenium rich wastewater for selenium bioremediation and a) simultaneous methane production with dissolved air floatation slurry or glycerol as electron donors in batch and upflow anaerobic sludge bed reactors (**Chapters 5 and 7**) and b) concomitant volatile fatty acids production using food waste in batch reactors (**Chapter 6**)

8.1.2 Enhanced anaerobic degradation of lipid-rich wastewater

In **chapters 3 and 4,** lipid-rich wastewaters from the dairy industry and a DAF slurry derived from it were used as the substrates (Figures 8.1a and b). **Chapter 3** focused on a preliminary study to enhance the biomethane potential of a DAF slurry through adjustment of substrate concentration and initial pH. Three-fold dilution increased the methane production with

granular sludge (Figure 3.1). An optimal inoculum to substrate ratio of at least 1.5 and 2.0 was recommended for WAS and AGS, respectively. The improvement due to substrate dilution were attributed to a higher inoculum to substrate ratio and nutrient availability from the mineral medium, but reduced LCFA toxicity and VFA accumulation. The methane yield was enhanced by 23% upon adjustment of the initial pH of the DAF slurry from pH 7 to pH 6 with HCl addition (Figure 3.3), which could be due to improved hydrolysis of the DAF slurry to LCFAs for acidogenic and methanogenic bacteria. GAC supplementation was found to enhance the methanogenesis of dairy wastewater in a sequential batch reactor in **chapter 4**. The reduction in lag phase was observed at all four cycles in the GAC-amended reactor (Table 4.2). The organic compounds, especially lipids, accumulated in the absence of conductive material (Figure 4.3). E-pili like structures that could aid long-distance electron shuttling were observed due to the presence of GAC (Figure 4.5). Improved methane production was likely due to the activity of potentially syntrophic and electroactive microorganisms such as *Geobacter, Synergistes, Methonolinea* and *Methanosaeta* (Figures 4.6 and 4.7).

8.1.3 Anaerobic digestion of selenium-rich wastewater for bioenergy and bioproducts and selenium remediation

The influence of selenium oxyanions on anaerobic digestion of model substrates (glycerol, as well as a glucose, acetate and lactate (GAL) mixture) as well as real waste (food waste) and wastewaters (DAF slurry) were evaluated in **chapters 5, 6 and 7** (Figures 8.2a and b). **Chapter 5** assessed the biomethane potential from DAF slurry supplemented with Se oxyanions. The inhibition test found that the half-maximal inhibitory concentration (IC_{50}) for methane production using waste activated sludge was 0.08 mM for SeO_4^{2-} and 0.07 mM for SeO_3^{2-}, compared to 2.10 mM for SeO_4^{2-} and 0.08 mM for SeO_3^{2-} using anaerobic granular sludge, respectively (Figure 5.2 and Table 5.3). During the degradation test, the methane yield (180 mL/g COD) was unaffected when supplemented with 0.10 mM SeO_4^{2-} or SeO_3^{2-}, after 65 days of incubation (Figure 5.2). However, the lag phase duration was prolonged by 50 % at 0.05 mM Se and by 90 % at 0.10 mM Se, respectively (Table 5.5).

Chapter 6 investigated enhanced VFA production from food waste via three different strategies, viz. (i) pH adjustment (to acid pH 5.0 and alkaline pH 10.0), (ii) heat treatment of the inoculum (at 85 ^{o}C for an hour) and (iii) supplementation of Se oxyanions (up to 500 µM). The highest VFA yield (0.516 g COD/g VS) was achieved at pH 10, which was 45% higher than the maximum VFA yield at pH 5 (Figure 6.1). Heat treatment improved VFA

accumulation in alkaline conditions, but was detrimental for selenate reduction at acidic pH. The VFA composition was dominated by acetic and propionic acids at pH 10 with the heat treated inoculum, which diversified at other test conditions (Figure 6.4). More than 95% Se removal was observed at acidic (with non-heat treated inoculum) and alkaline (with and without heat treated inoculum) pH (Figure 6.6). Se oxyanions acted as a chemical inhibitor in methanogenic alkaline conditions with non-heat treated inoculum (Figure 6.2).

Chapter 7 evaluated AD of selenate rich wastewaters in a continuous UASB setup. Glycerol was used as the electron donor, in addition to a glucose, acetate and lactate (GAL) mixture. An average daily methane yield of 150 mL/g COD was achieved from Se-laden wastewater (<400 µM), which was similar and comparable to the Se free control (Figure 7.3). 100% glycerol was removed, despite the presence of SeO_4^{2-}. Methanogenic archaea and selenium reducing bacteria were both active in the UASB reactors until 400 µM SeO_4^{2-} (Figures 7.12 and 7.13). Methanogenesis was inhibited at a 500 µM Se influent concentration, which was attributed to several reasons including electron flow alteration, VFAs accumulation, and COD removal efficiency reduction. The inhibition was due to reduced activity of the acetoclastic methanogenic archaea *Methanosaeta* (Figure 7.14). Interestingly, selenium facilitated sludge granulation, evident from a clear increase in solids content and settling velocity of Se enriched granules when compared to the control (Figure 7.10). SeO_4^{2-} concentration, but not the COD/SeO_4^{2-} ratio, governed the AD process performance (Figure 7.3a vs Figure 7.3b).

More than 90% Se removal was achieved with electron donors such as DAF slurry, glycerol and food waste in **chapters 5, 6 and 7**. Biosynthesis of extracellular Se nanoparticles and metal selenides was observed, supported by XRD, SEM, TEM and SEM-EDX. Overall, anaerobic granular sludge was efficient for methanogenesis of lipid-rich wastewater, but waste activated sludge was better in Se oxyanion reduction, especially to overcome selenite toxicity (**chapters 3 – 7**).

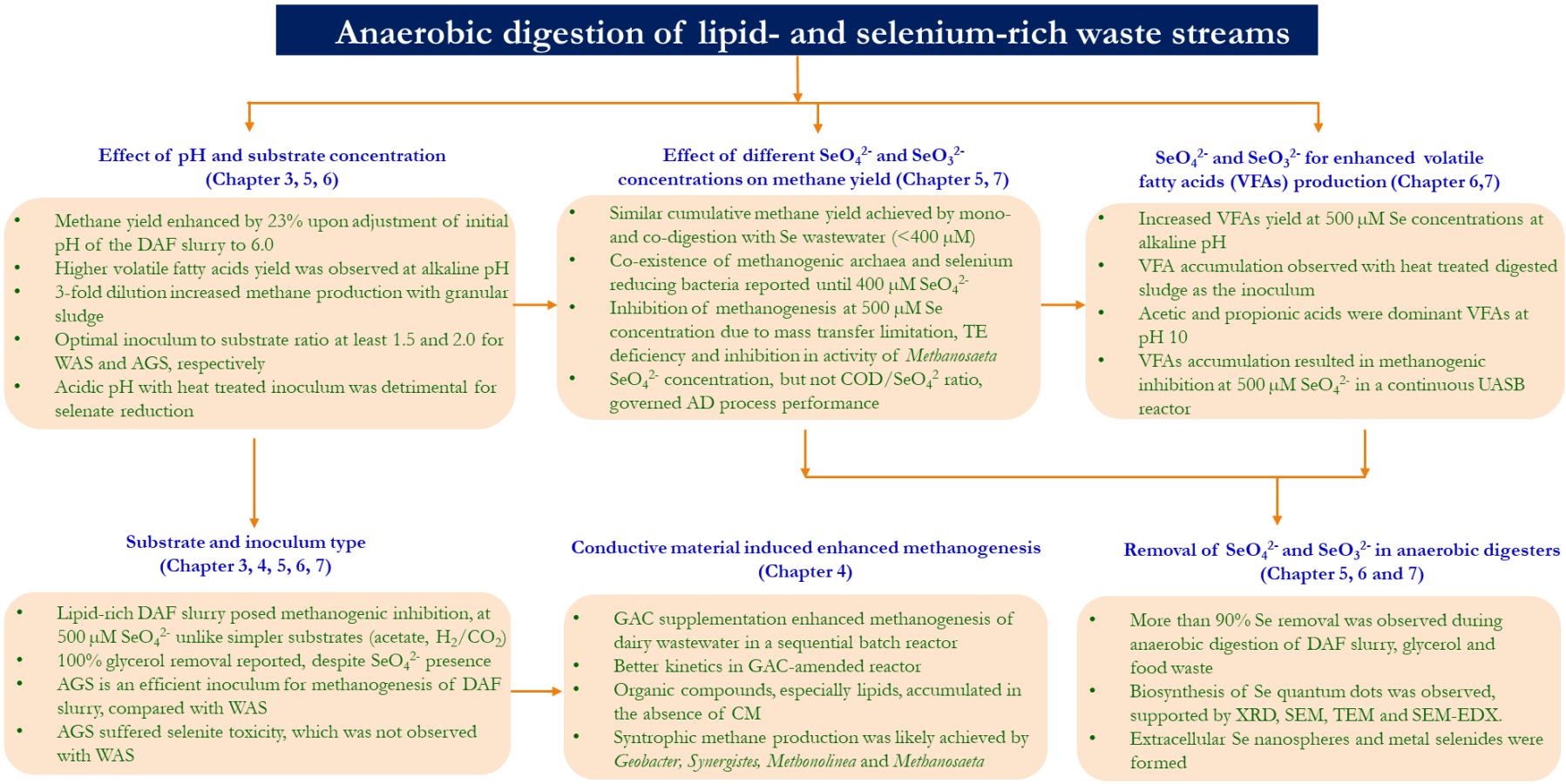

Figure 8.3 Summary of the major findings of this PhD research

8.2 Future perspectives

8.2.1 Approaches for anaerobic digestion of wastewaters with high inorganic content

Bioenergy and bioproduct recovery from Se laden wastewaters have so far not been investigated in detail. Though methane production from sulfate-rich wastewaters has been widely studied in the past three decades, selenate or selenite rich wastewaters have received little attention in the past two decades. The fundamental aspects of AD of Se oxyanions containing wastewaters have many undiscovered aspects. The optimization of the operational parameters, viz. pH, temperature, loading rate, retention time, and solid content for anaerobic treatment of Se rich wastewater is required in future research. With the successful demonstration of AD of selenate rich wastewater in this thesis, long term and continuous impact of selenite during AD can also be evaluated. Se-laden wastewaters are often accompanied by co-contaminants such as nitrate and sulfate, and thus need also to be taken into consideration for future research (Tan et al., 2018). With this PhD thesis focused solely on selenium, the effect of tellurium oxyanions on methanogenesis can be carried out in future research as well.

8.2.2 Anaerobic digestion bioprocess operation

8.2.2.1 Biogas upgradation

The raw biogas generated in the AD process contains undesired constituents such as H_2S, CO_2, NH_3, siloxanes and VOCs. These can be removed through physio-chemical or biological methods (Das et al., 2022). The existing upgrading technologies include absorption, adsorption and membrane separation, whereas the emerging technologies include cryogenic technology, in-situ methane enrichment and supersonic separation (Sahota et al., 2018). In addition to these well-known impurities, H_2Se could also be present when treating Se rich wastewaters as shown in this PhD thesis (Chapter 7). Therefore, technologies to remove H_2Se need to be developed, owing to the toxic and corrosive nature of H_2Se (Nkuissi et al., 2020). The purified and upgraded biogas can meet high-end applications such as vehicular fuel or direct-grid injection.

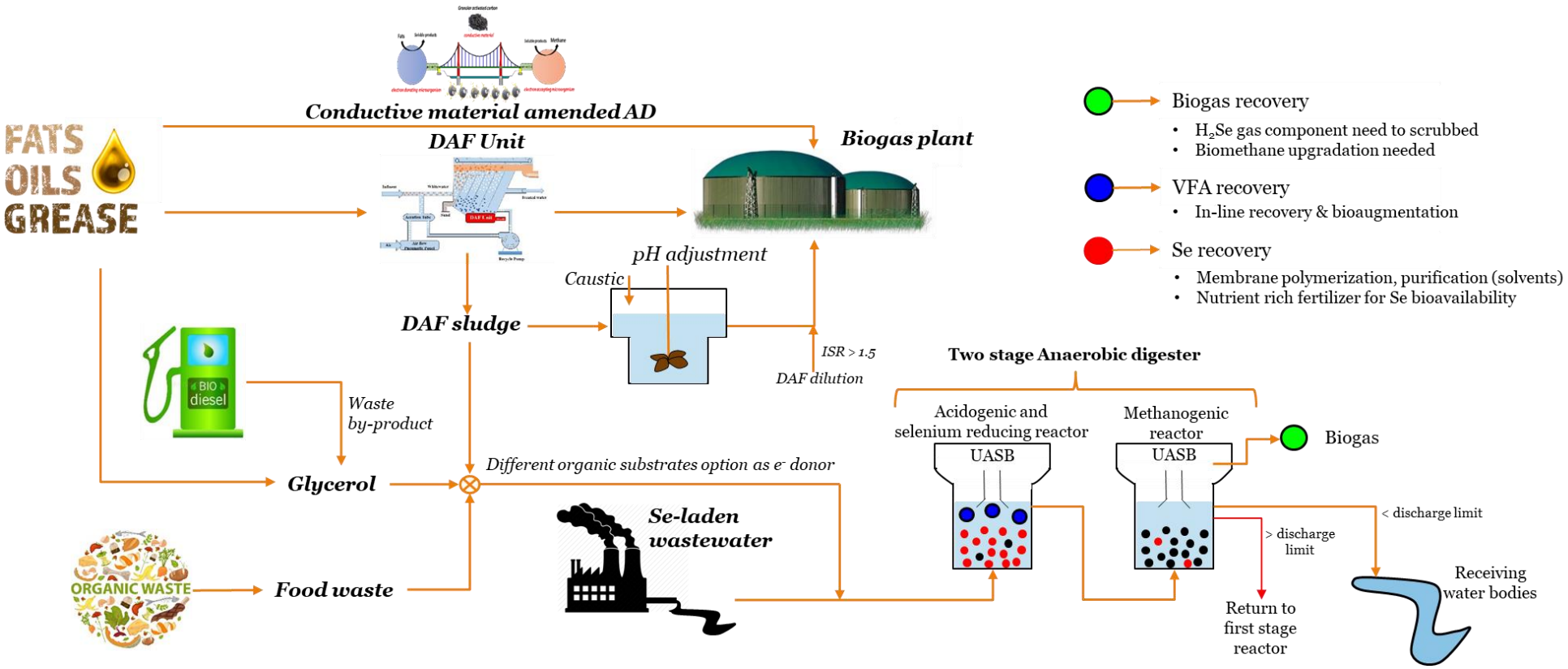

Figure 8.4 Future prospects for bioenergy and bioproducts recovery from lipid-rich and selenium-laden waste streams. DAF: dissolved air floatation; Se: Selenium; UASB: upflow anaerobic sludge bed reactor and VFA: volatile fatty acids.

8.2.2.2 Conductive material supplementation for enhanced process performance

Though it is clear that there could be a significant improvement in the conductive material induced AD process (Chapter 4), the underlying mechanism is still not clearly established. For instance, there is no common unified protocol to confirm associated processes such as direct interspecies electron transfer (DIET). Microbial (fluorescence in situ hybridization (Zhao et al., 2015), meta-omic methods for detecting genes (Shrestha et al., 2013), transcripts (Rotaru et al., 2014) and proteins (Wang et al., 2018)), electrochemical (cyclic voltammetry measurements (Yin et al., 2018)) and metabolic (carbon isotope analysis (Rotaru et al., 2018) and inhibitor tests (van Steendam et al., 2019)) characterisation methods could confirm DIET during AD. Metagenomics and transcriptomic analyses to study e-pili gene expression (Holmes et al., 2017) is also needed to conclude their promotion induced by the conductive material. Integrating the findings from this PhD thesis, a long term study on conductive material supplementation to overcome toxicity during the anaerobic treatment of Se rich wastewater can be carried in the future which might allow reactor operation at elevated Se concentrations.

8.2.2.3 Anaerobic digestion in the era of Industry 4.0

Industry 4.0 has already made its advent in the water and wastewater sector which is marked by digitalisation and automation (Fernando et al., 2022). For example, the internet of things (IoT) allows the online monitoring of the process performance such as pH, temperature, oxidation-reduction potential, quantity and quality of biogas produced through employing sensors (Logan et al., 2019). The real-time data generated eases operation and maintenance and avoids complex analytical laboratory procedures which may not be viable at a decentralised level due to their cost and lead times. The off-site monitoring allows the central station to track the performance (Matheri et al., 2022), make precautionary measures to prevent process failures (Trubetskaya et al., 2021) and direct onsite remedial intervention in decentralised community-scale plants (Cruz et al., 2021). Pilot-scale studies are needed on ‘Biogas Plants 4.0’ to enable retrofitting full-scale plants with sensor technology to realise the aforementioned benefits.

8.2.3 Reactor configurations for anaerobic treatment of lipid- and selenium-rich substrates

8.2.3.1 Two-stage anaerobic digestion

In a two-stage AD, the initial hydrolysis phase of the substrate degradation and the production of a rich organic acid reactor liquor occur in the first stage, followed by metabolization of these organic acids by a methanogenic consortium in the second stage (Rajendran et al., 2020). Two-stage anaerobic sulfate-rich wastewater treatment was proposed very early with the objective to reduce most of the sulfate in the first stage (Genschow et al., 1996). Since this study found that the toxicity of Se on fermentative bacteria was relatively less when compared with the methanogenic archaea (Figures 7.12 and 7.13), the first stage is envisaged to serve as an acidogenic and selenium reducing reactor (Figure 8.4). This could meet higher productivity, stability and efficiency in two-stage AD. Demonstration of pilot-scale two-stage anaerobic digesters, which may be operated with further elevated Se concentrations, is required before commercial implementation. Conversely, research on dark fermentative hydrogen generation from Se rich wastewater can also be explored. It should be noted that a two-stage AD is more suitable for wastewaters abundant in lipids (relative to carbohydrates or proteins), due to their initial rapid hydrolysis followed by slow acidification via β-oxidation (Alves et al., 2009).

8.2.3.2 Anaerobic membrane bioreactor

An anaerobic membrane bioreactor (AnMBR) is an advanced reactor configuration compared to the conventional continuously stirred tank reactors or up-flow anaerobic sludge bed reactors (Aslam et al., 2022). The retention of biomass in this technology leads to operation at even higher organic loading rates (Hanvajanawong et al., 2022). The AnMBR has achieved popularity in treating lipid-rich wastewaters due to its high treatability and biogas generation (Yee et al., 2019). There is huge potential for utilizing a submerged anaerobic membrane bioreactor (Giménez et al., 2012) for the treatment of Se-laden wastewater which has so far not been demonstrated.

The main concern of using membrane technology in an anaerobic system is biofouling (Cheng et al., 2018), which could be mitigated by using a high flow rate and biogas recirculation as a means for membrane scouring (Wang et al., 2020). Membranes fabricated with either covalent Se or colloidal Se^0 can be utilized to reduce biofouling (Tan et al., 2018).

Reduction in biofilm formation and flux loss was reported when organo-Se was covalently attached to the membrane surface (Vercellino et al, 2013).

8.2.3.3 Bioelectrochemical treatment

The microbial fuel cell (MFC) technology allows several bio-based processes, including removal of chemical oxygen demand, nitrification, denitrification, selenate and heavy metals, to be carried out in the same bioreactor via bioelectrochemical remediation mediated by electroactive microbes (Kumar et al., 2019). Treatment of lipid-rich wastewater for power production via (algal-based) MFCs has been developed (Elakkiya and Niju, 2020). The research on Se remediation in MFCs has only recently gained attention (Holmes and Gu, 2016). Bioelectrochemical system for bioenergy and remediation of Se-laden wastewater has not yet been reported.

8.2.4 Strategies for product valorization

8.2.4.1 Carboxylic acids production and recovery

Bioaugmentation is an effective strategy by adding microorganisms externally to the indigenous mixed microbial community to enhance the microbial activity for improving the VFA production efficiency (Zhang et al., 2017). There is a wide scope to explore tailor-made bio-based VFA production by bioaugmentation that could provide market competitiveness for petrochemical-based VFAs. Chapter 6 showed selenium oxyanions can be used as a chemical methanogenic inhibitor to enhance VFAs. This can be demonstrated on a continuous and pilot scale for possible commercial implementation. The biologically produced and recovered VFAs can meet end-use applications such as bioplastics, biodiesel, biological nutrients recovery and electricity generation (Khatami et al., 2021).

Research on chain elongation is still in its infancy which is a new emerging open-culture anaerobic biotechnological process that converts these VFAs (and an electron donor) to the more valuable medium-chain fatty acids (MCFAs) through pathways such as the reverse β–oxidation pathway (Angenent et al., 2016). Studies that demonstrate in-line recovery of these acids produced through methods such as gas stripping with absorption, adsorption, solvent extraction, electrodialysis, reverse osmosis, nanofiltration and membrane contractor are required (Atasoy et al., 2018).

8.2.4.2 Selenium remediation and recovery

Se remediation by biological treatment using different groups of microorganisms, reactor configurations, operation strategies, and co-contaminants are becoming well established (Sinharoy and Lens, 2020). The new and emerging technologies are phytoremediation and phycoremediation. In phytoremediation, aquatic plants such as *Azolla* and *Lemna minor* (common duckweeds) take up and accumulate Se (Golob et al., 2021, Miranda et al., 2020). Recently, valorization of Se-enriched duckweed generated from wastewater as micronutrient biofertilizer was reported by Li et al. (2021). Similarly, algae are being explored at a pilot scale for Se remediation (Zou et al., 2020). Therefore, aquatic plants or algae could be employed in constructed wetland based Se bioremediation. Subsequently, Se enriched crops above biofortified levels could be effectively managed through AD.

Though research on Se bioremediation has progressed, a simple process for recovery and purification of Se nanoparticles has not yet been established. A series of centrifugation, sonication followed by hexane separation steps recovered Se nanoparticles from biomass (Jain et al., 2015). The recovered biogenic selenium nanoparticles have antibacterial and anticancer properties and find applications in semiconductors, nanobiosensors and environmental remediation as well (Wadhwani et al., 2016). Biogranules can be simply dried and then used as a fertilizer for soil augmentation of Se deficit regions to increase the Se bioavailability (Wang et al. 2017). However, the biomass produced while treating industrial wastewater can also contain various other contaminants that can be harmful to the environment. Therefore, apprehensions on the toxic effect and health ramifications of using Se-rich biomass as fertilizer for biofortification should be addressed (Tan et al., 2016).

8.3 Conclusion

Anaerobic digestion of lipid-rich wastewater (dairy wastewater and DAF slurry derived from it) and selenium-containing wastewater has been comprehensively investigated. Cost-effective conductive material (granular activated carbon) supplementation enhanced anaerobic degradation of complex industrial wastewaters. The selenate concentration threshold for the realisation of methanogenesis was established. More significant is the selenium remediation that could be achieved simultaneously during methane or VFA production. This PhD dissertation advanced knowledge in bioenergy and bioproducts from selenium and lipid-rich wastewater management.

8.4 References

Alves, M.M., Pereira, M.A., Sousa, D.Z., Cavaleiro, A.J., Picavet, M., Smidt, H., Stams, A.J.M., 2009. Waste Lipids to energy: how to optimize methane production from long-chain fatty acids (LCFA). Microbial Biotechnology 5, 538-550. https://doi.org/10.1111/j.1751-7915.2009.00100.x

Angenent, L. T., Richter, H., Buckel, W., Spirito, C. M., Steinbusch, K. J. J., Plugge, C. M., et al. 2016. Chain elongation with reactor microbiomes: open-culture biotechnology to produce biochemicals. Environmental Science and Technology 50, 2796–2810. https://doi.org/10.1021/acs.est.5b04847

Ariunbaatar, J., Esposito, G., Yeh, D.H., Lens, P.N.L., 2016. Enhanced anaerobic digestion of food waste by supplementing trace elements: role of Selenium (VI) and Iron (II). Frontiers in Environmental Science and Engineering 4(8). https://doi.org/10.3389/fenvs.2016.00008

Aslam, A., Khan, S.J., Shahzad, H.M.A., 2022. Anaerobic membrane bioreactors (AnMBRs) for municipal wastewater treatment-potential benefits, constraints, and future perspectives: An updated review. Science of The Total Environment 802, 149612. https://doi.org/10.1016/j.scitotenv.2021.149612

Atasoy, M., Owusu-Agyeman, I.O., Plaza, E., Cetecioglu, Z., 2018. Bio-based volatile fatty acid production and recovery from waste streams: Current status and future challenges. Bioresource Technology 268, 773-786. https://doi.org/10.1016/j.biortech.2018.07.042

Cheng, D., Ngo, H.H., Guo, W., Liu, Y., Chang, S.W., Nguyen, D.D., Nghiem, L.D., Zhou, J., Ni, B., 2018. Anaerobic membrane bioreactors for antibiotic wastewater treatment: performance and membrane fouling issues. Bioresource technology 267, 714-724. https://doi.org/10.1016/j.biortech.2018.07.133

Colleran, E., Finnegan, S., Lens, P., 1995. Anaerobic treatment of sulphate-containing waste streams. Antonie van Leeuwenhoek 67, 29-46. https://doi.org/10.1007/BF00872194

Das, J., Ravishankar, H., Lens, P.N.L., 2022. Biological biogas purification: Recent developments, challenges and future prospects. Journal of Environmental Management 304, 114198. https://doi.org/10.1016/j.jenvman.2021.114198

Cruz, I.A., Andrade, L.R., Bharagava, R.N., Nadda, A.K., Bilal, M., Figueiredo, R.T., Ferreira, L.F., 2021. An overview of process monitoring for anaerobic digestion. Biosystems Engineering 207, 106-119. https://doi.org/10.1016/j.biosystemseng.2021.04.008

Elakkiya, E., Niju, S., 2020. Simultaneous treatment of lipid rich ghee industry wastewater and power production in algal biocathode based microbial fuel cell. Energy Sources, Part A: Recovery, Utilization, and Environmental Effects. https://doi.org/10.1080/15567036.2020.1823529

Fernando, W.A.M., Khadaroo, S.N.B.A., Poh, P.E., 2022. Artificial Intelligence in Wastewater Treatment Systems in the Era of Industry 4.0: A Holistic Review. In: Ong, H.L., Doong, Ra., Naguib, R., Lim, C.P., Nagar, A.K. (Eds.) Artificial Intelligence and Environmental Sustainability. Algorithms for Intelligent Systems. Springer, Singapore. https://doi.org/10.1007/978-981-19-1434-8_3

Genschow, E., Hegemann, W., Maschke, C., 1996. Biological sulfate removal from tannery wastewater in a two-stage anaerobic treatment. Water Research 30, 2072-2078. https://doi.org/10.1016/0043-1354(96)00332-6

Giménez, J.B., Martí, N., Ferrer, J., Seco, A., 2012. Methane recovery efficiency in a submerged anaerobic membrane bioreactor (SAnMBR) treating sulphate-rich urban wastewater: Evaluation of methane losses with the effluent. Bioresource Technology 118, 67-72. https://doi.org/10.1016/j.biortech.2012.05.019.

Golob, A., Vogel-Mikuš, K., Brudar, N., Germ, M., 2021. Duckweed (*Lemna minor* L.) successfully accumulates selenium from selenium-impacted water. Sustainability 13, 13423. https://doi.org/10.3390/su132313423

Hanvajanawong, K., Suyamud, B., Suwannasilp, B.B., Lohwacharin, J., Visvanathan, C., 2022. Unravelling capability of two-stage thermophilic anaerobic membrane bioreactors for high organic loading wastewater: Effect of support media addition and irreversible fouling. Bioresource Technology 348, 126725. https://doi.org/10.1016/j.biortech.2022.126725

Holmes, A.B., Gu, F.X., 2016. Emerging nanomaterial for the applications of selenium removal for wastewater treatment. Environmental Science: Nano 3, 982–996. https://doi.org/10.1039/C6EN00144K

Holmes, D., Shrestha, P.M., Walker, D.J.F., Dang, Y., Nevin, K.P., Woodard, T.L., Lovley, D.R., 2017. Metatranscriptomic evidence for direct interspecies electron transfer between *Geobacter* and *Methanothrix* species in methanogenic rice paddy soils. Applied and Environmental Microbiology 83, 9. https://doi.org/10.1128/AEM.00223-17

Jain, R., Jordan, N., Weiss, S., Foerstendorf, H., Heim, K., Kacker, R., Hübner, R., Kramer, H., van Hullebusch, E.D., Farges, F., Lens, P.N., 2015. Extracellular polymeric substances govern the surface charge of biogenic elemental selenium nanoparticles. Environmental Science & Technology 49, 1713-1720. https://doi.org/10.1021/es5043063

Khatami, K., Atasoy, M., Ludtke, M., Baresel, C., Euice, O., Cetecioglu, Z., 2021. Bioconversion of food waste to volatile fatty acids: Impact of microbial community, pH and retention time. Chemosphere 275, 129981. https://doi.org/10.1016/j.chemosphere. 2021.129981

Kumar, S.S., Kumar, V., Malyan, S.K., Sharma, J., Mathimani, T., Maskarenj, M.S., Ghosh, P.C., Pugazhendhi, A., 2019. Microbial fuel cells (MFCs) for Bioelectrochemical treatment of different wastewater streams. Fuel 254, 115526. https://doi.org/10.1016/j.fuel.2019.05.109

Lenz, M., Janzen, N., Lens, P.N.L., 2008. Selenium oxyanion inhibition of hydrogenotrophic and acetoclastic methanogenesis. Chemosphere 73(3), 383-388. https://doi.org/10.1016/ j.chemosphere.2008.05.059

Logan, M., Safi, M., Lens, P., Visvanathan, C., 2019. Investigating the performance of internet of things based anaerobic digestion of food waste. Process Safety and Environmental Protection 127, 277-287. https://doi.org/10.1016/j.psep.2019.05.025

Li, J., Otero-Gonzalez, L., Parao, A., Tack, P., Folens, K., Ferrer, I., Lens, P.N.L., Laing, G.D., 2021. Valorization of selenium-enriched sludge and duckweed generated from wastewater as micronutrient biofertilizer. Chemosphere 281, 130767. https://doi.org/10.1016/j.chemosphere. 2021.130767

Matheri, A.N., Belaid, M., Njenga, C.K., Ngila, J.C., 2022. Water and wastewater digital surveillance for monitoring and early detection of the COVID-19 hotspot: industry 4.0. International Journal of Environmental Science and Technology, 1-18. https://doi.org/10.1007/ s13762-022-03982-7

Miranda, A.F., Kumar, N.R., Spangenberg, G., Subudhi, S., Lal, B., Mouradov, A., 2020. Aquatic plants, *Landoltia punctata*, and *Azolla filiculoides* as bio-converters of wastewater to biofuel. Plants 9, 437. https://doi.org/10.3390/plants9040437

Nkuissi, H.J.T., Konan, F.K., Hartiti, B. and Ndjaka, J.M., 2020. Toxic materials used in thin film photovoltaics and their impacts on environment. In Reliability and Ecological Aspects of Photovoltaic Modules. IntechOpen. http://dx.doi.org/10.5772/intechopen.88326

Rajendran, K., Mahapatra, D., Venkatraman, A.V., Muthuswamy, S., Pugazhendhi, A., 2020. Advancing anaerobic digestion through two-stage processes: Current developments and future trends. Renewable and Sustainable Energy Reviews 123, 109746. https://doi.org/10.1016/j.rser.2020.109746

Rotaru, A.E., Shrestha, P.M., Liu, F., Markovaite, B., Chen, S., Nevin, K.P., Lovley, D.R., 2014. Direct interspecies electron transfer between *Geobacter metallireducens* and *Methanosarcina barkeri*. Applied and Environmental Microbiology 80(15), 4599-4605. https://doi.org/10.1128/AEM.00895-14

Rotaru, A.E., Calabrese, F., Stryhanyuk, H., Musat, F., Shrestha, P.M., Weber, H.S., Snoeyenbos-West, O.L., Hall, P.O., Richnow, H.H., Musat, N. and Thamdrup, B., 2018. Conductive particles enable syntrophic acetate oxidation between *Geobacter* and *Methanosarcina* from coastal sediments. mBio, 9(3), e00226-18. https://doi.org/10.1128/mBio.00226-18

Sahota, S., Shah, G., Ghosh, P., Kapoor, R., Sengupta, S., Singh, P., Vijay, V., Sahay, A., Vijay, V.K., Thakur, I.S., 2018. Review of trends in biogas upgradation technologies and future perspectives. Bioresource Technology Reports 1, 79-88. https://doi.org/10.1016/j.biteb.2018.01.002

Shrestha, P.M., Rotaru, A.E., Summers, Z.M., Shrestha, M., Liu, F., Lovley, D.R., 2013. Transcriptomic and genetic analysis of direct interspecies electron transfer. Applied and Environmental Microbiology 79(7), 2397-2404. https://doi.org/10.1128/AEM.03837-12

Tan, L.C., Nancharaiah, Y.V., van Hullebusch, E.D., Lens, P.N.L., 2016. Selenium: Environmental significance, pollution, and biological treatment technologies. Biotechnol. Adv. 34(5), 886-907. https://doi.org/10.1016/j.biotechadv.2016.05.005

Tan, L.C., Calix, E.M., Rene, E.R., Nancharaiah, Y.V., van Hullebusch, E.D., Lens, P.N., 2018. Amberlite IRA-900 ion exchange resin for the sorption of selenate and sulfate: equilibrium, kinetic, and regeneration studies. Journal of Environmental Engineering 144(11), 04018110. https://doi.org/10.1061/(ASCE)EE.1943-7870.0001453

Trubetskaya, A., Horan, W., Conheady, P., Stockil, K., Merritt, S., Moore, S., 2021. A methodology for assessing and monitoring risk in the industrial wastewater sector. Water Resources and Industry, 25, 100146. https://doi.org/10.1016/j.wri.2021.100146

Van Steendam, C., Smets, I., Skerlos, S., Raskin, L., 2019. Improving anaerobic digestion via direct interspecies electron transfer requires development of suitable characterization methods. Current Opinion in Biotechnology 57, 183-190. https://doi.org/10.1016 /j.copbio.2019.03.018

Vercellino, T., Morse, A., Tran, P., Song, L., Hamood, A., Reid, T., Moseley, T., 2013. Attachment of organo-selenium to polyamide composite reverse osmosis membranes to inhibit biofilm formation of S. aureus and E. coli. Desalination 309, 291-295. https://doi.org/10.1016/j.desal.2012.10.020

Wadhwani, S.A., Shedbalkar, U.U., Singh, R., Chopade, B.A., 2016. Biogenic selenium nanoparticles: current status and future prospects. Applied Microbiology and Biotechnology 100, 2555–2566. https://doi.org/10.1007/s00253-016-7300-7

Wang, J., Cahyadi, A., Wu, B., Pee, W., Fane, A.G., Chew, J.W., 2020. The roles of particles in enhancing membrane filtration: A review. Journal of Membrane Science 595, 117570. https://doi.org/10.1016/j.memsci.2019.117570

Wang, T., Zhang, D., Dai, L., Dong, B., Dai, X., 2018. Magnetite triggering enhanced direct interspecies electron transfer: a scavenger for the blockage of electron transfer in anaerobic digestion of high-solids sewage sludge. Environmental Science and Technology 52(12), 7160-7169. https://doi.org/10.1021/acs.est.8b00891

Yee, T.L., Rathnayake, T., Visvanathan, C., 2019. Performance evaluation of a thermophilic anaerobic membrane bioreactor for palm oil wastewater treatment. Membranes 9, 55. https://doi.org/10.3390/membranes9040055

Yin, Q., Yang, S., Wang, Z., Xing, L., Wu, G., 2018. Clarifying electron transfer and metagenomic analysis of microbial community in the methane production process with the

addition of ferroferric oxide. Chemical Engineering Journal 333, 216-225. https://doi.org/10.1016/j.cej.2017.09.160

Zhang, Q.Q., Yang, G.F., Zhang, L., Zhang, Z.Z., Tian, G.M., Jin, R.C., 2017. Bioaugmentation as a useful strategy for performance enhancement in biological wastewater treatment undergoing different stresses: application and mechanisms. Critical Reviews in Environmental Science and Technology 47, 1877-1899, https://doi.org/10.1080/10643389.2017.1400851

Zhao, Z., Zhang, Y., Wang, L., Quan, X., 2015. Potential for direct interspecies electron transfer in an electric-anaerobic system to increase methane production from sludge digestion. Scientific reports 5(1), 1-12. https://doi.org/10.1038/srep11094

Zou, H., Huang, J.C., Zhou, C., He, S., Zhou, W., 2020. Mutual effects of selenium and chromium on their removal by *Chlorella vulgaris* and associated toxicity. Science of The Total Environment 724, 138219. https://doi.org/10.1016/j.scitotenv.2020.138219

Author information

Biography

Mohanakrishnan Logan was born on 11th May 1992 in Chengalpattu (Tamil Nadu, India). Mohan completed his bachelors in Civil Engineering at Jerusalem College of Engineering (Chennai, India) in 2013 and obtained his masters in Environmental Management at Anna University (Chennai, India) in 2016. He researched an algal-based biogas purification process in his master's dissertation. He served as a lecturer in Civil Engineering at the Polytechnic and Engineering Colleges in Chennai (India) and worked as a project management consultant at the Indian Leather Industry Foundation, Chennai (India). In 2017, he moved to Bangkok (Thailand) as a research associate at the Asian Institute of Technology where he worked on a Newton Fund project on IoT-based centralised monitoring of community scale anaerobic digestion. He started as a PhD research fellow at National University of Ireland Galway (Ireland) in June 2019. He obtained a COST action fellowship to carry out a short term scientific mission at the KTH Royal Institute of Technology (Stockholm, Sweden). His research area of interest is on conductive material induced enhanced anaerobic digestion, methane and volatile fatty acids production from selenium rich wastewater, and simultaneous selenium bioremediation.

Publications

Logan, M., Tan, L.C., Nzeteu, C.O., Lens, P.N.L., 2022. Enhanced anaerobic digestion of dairy wastewater in a granular activated carbon amended sequential batch reactor. GCB Bioenergy 14(7), 840-857. https://doi.org/10.1111/gcbb.12947

Logan, M., Tan, L.C., Lens, P.N.L., 2022. Anaerobic co-digestion of dissolved air floatation slurry and selenium rich wastewater for simultaneous methane production and selenium

bioremediation. International Biodeterioration and Biodegradation 172, 105425. https://doi.org/10.1016/j.ibiod.2022.105425

Logan, M., Ravishankar, H., Tan, L.C., Lawrence, J., Fitzgerald, D., Lens, P.N.L., 2021. Anaerobic digestion of dissolved air floatation slurries: Effect of substrate concentration and pH. Environmental Technology and Innovation 21, 101352. https://doi.org/10.1016/j.eti.2020.101352

Logan, M., Safi, M., Lens, P.N.L., Visvanathan, C., 2019. Investigating the performance of IoT based anaerobic digestion of food waste. Process Safety and Environmental Protection 127, 277-287. https://doi.org/10.1016/j.psep.2019.05.025

Conferences

Logan, M., Lens, P.N.L., 2021. Anaerobic digestion of selenate rich wastewater for simultaneous production of methane and removal of selenium. 14th International Conference on Challenges in Environmental Science and Engineering, 6 - 7, Nov. 2021, Online.

Logan, M., Lens, P.N.L., 2021. Effect of selenium on methanogenic treatment of glycerol containing wastewater. EPRI Selenium Summit, 26 - 28, Oct. 2021, Online.

Logan, M., Tan. L.C., Lens, P.N.L., 2020. A novel integrated approach for simultaneous methane production and selenium remediation through anaerobic co-digestion of lipid- and selenium-rich wastewaters. 7th International Conference on Research Frontiers in Chalcogen Cycle Science and Technology, 10 - 11, Dec. 2020, Online.

Logan, M., Tan. L.C., Lens, P.N.L., 2020. Anaerobic co-digestion of lipid- and selenium-rich wastewaters for methane production and selenium remediation. MaREI symposium - Climate Action Session, 23 - 27, Nov. 2020, Online.

Logan, M., Safi, M., Lens, P.N.L., Visvanathan, C., 2020. Performance investigation of internet of things based anaerobic digestion. MaREI Biofuels Symposium, 29 Apr. 2020, Online.

Courses and modules

Modules		ECTS	Status	Remark
Registered in 2019				
GS508	Formulating a Research Project Proposal	5	Completed	Pass
Registered in 2020				
GS526	Oral/poster communications	5	Completed	Pass
GS509	Participation in Workshops/Courses	5	Completed	Pass
Registered in 2021				
GS5103	Conference Organisation	5	Completed	Pass
GS511	Research Placement	5	Completed	Pass
GS502	Journal Club Programme	5	Completed	Pass